

Asian PhD School on Advanced Power Electronics, 2021

Advanced Digital Current Regulation Strategies for Grid Connected Inverters

Professor Grahame Holmes

Professor Brendan McGrath

Part 1: Fundamentals of Current Regulation

- Principles of Pulse Width Modulation
- Ideal and Practical Current Regulators, Maximum Possible Regulator Gains
- Improving Current Regulator Performance
- Single Phase and Three Phase Systems
- z-domain Sampled Digital Current Regulators
- Discrete Time State Space Realisations, Overmodulation and Antiwindup

Part 2: Current Regulation for Grid Connected Inverters

- Current Regulation with LCL Filters, Reduction in Maximum Possible Gains
- Current Regulation with Common Mode EMI Filtering

Part 3: Advanced Current Regulation

- Regulation with Unbalanced and Harmonically Distorted Grid Voltages
- Self Synchronising Regulation, Startup and Fault-Ride-Through Management

Part 1: Fundamentals of Current Regulation

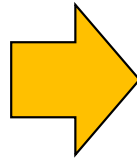
Primary Objectives of a Current Regulation System

- Minimize steady state magnitude (and phase for an AC system) output variable error, preferably achieving zero steady state error.
- Accurately track the commanded reference variable during transient changes. This requires a regulation system to have as high a bandwidth as possible, to achieve the best possible dynamic response.
- Limit the peak value of the output variable, to avoid overload conditions.
- Minimize low order harmonics in the load variable, and compensate for DC-link voltage ripple, deadtime delays, semiconductor device voltage drops, load parameter variation and other practical second order effects associated with the operation of the electrical conversion system.

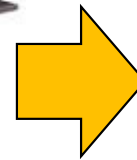
Structure of Current Regulators



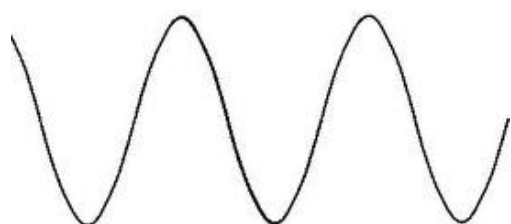
Electrical Source



Switched Power Converter



Load Motor



Target Current Reference



Controller

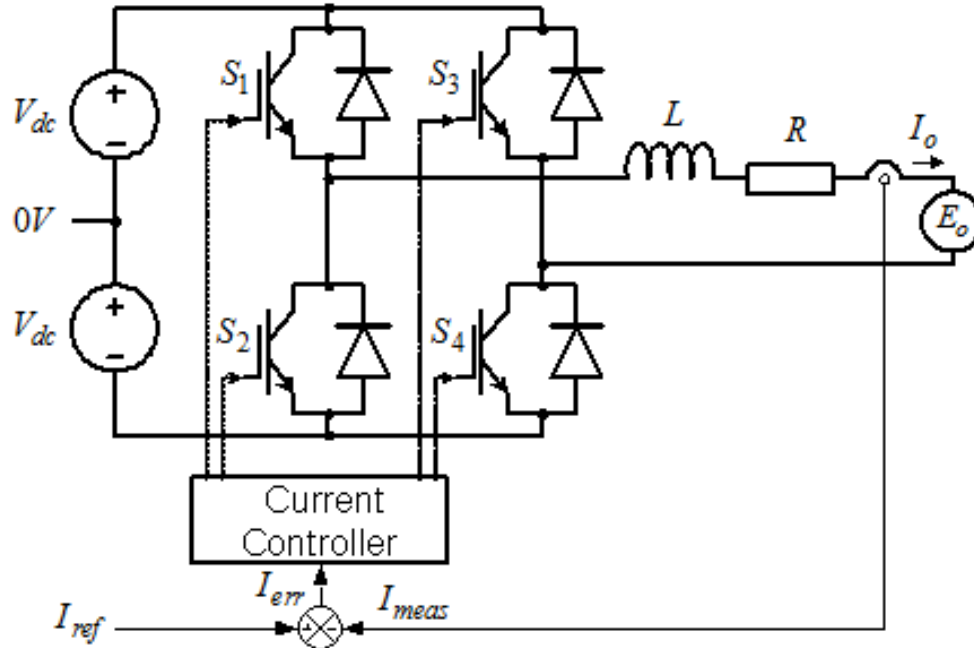


Current Measurement

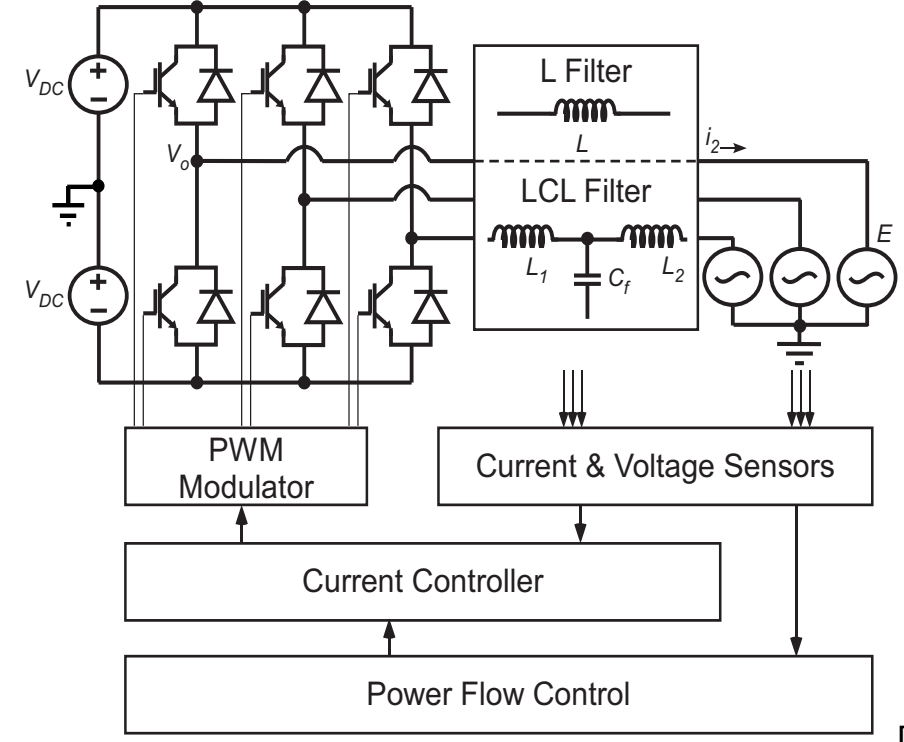


General Arrangement of Current Regulation for an Electrical Motor Drive System

Structure of Current Regulators



Single Phase Current
Regulated System



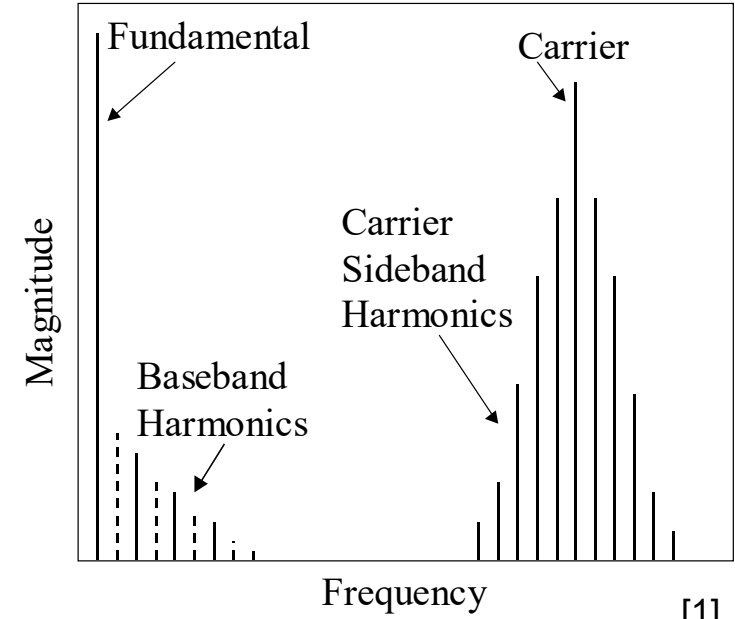
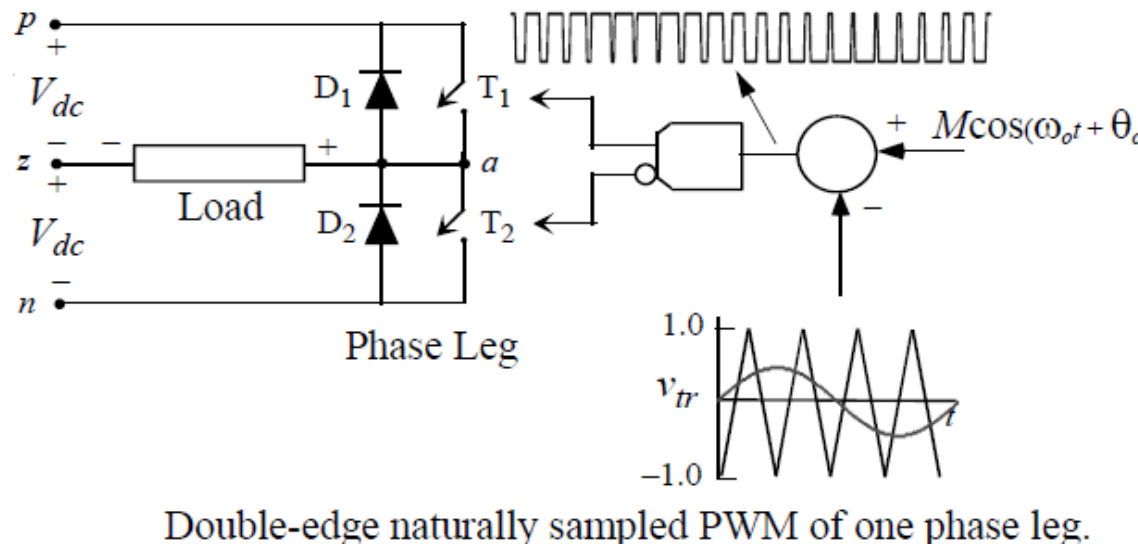
Three Phase Current Regulated
System (L or LCL Filter)

Requirements of Current Regulation

- Power electronic AC conversion systems require precise current regulation with high bandwidth
- Traditional wisdom:
 - Stationary Frame PI regulator gains can never be set high enough to get acceptably small steady state error
 - Synchronous Frame (P+Resonant) control is mandatory
- Unresolved question:

What are the stationary frame PI gain limits? - simple theory says they can be arbitrarily large without regulator instability
- Answering this question allows best possible PI regulator performance to be determined for any particular application

Pulse Width Modulation of Voltage Source Inverter [1]



[1]

$$f(t) = \frac{A_{00}}{2} + \sum_{n=1}^{\infty} [A_{0n} \cos(n[\omega_o t + \theta_o]) + B_{0n} \sin(n[\omega_o t + \theta_o])] \quad \boxed{\text{DC Offset}}$$

Fundamental Component & Baseband Harmonics

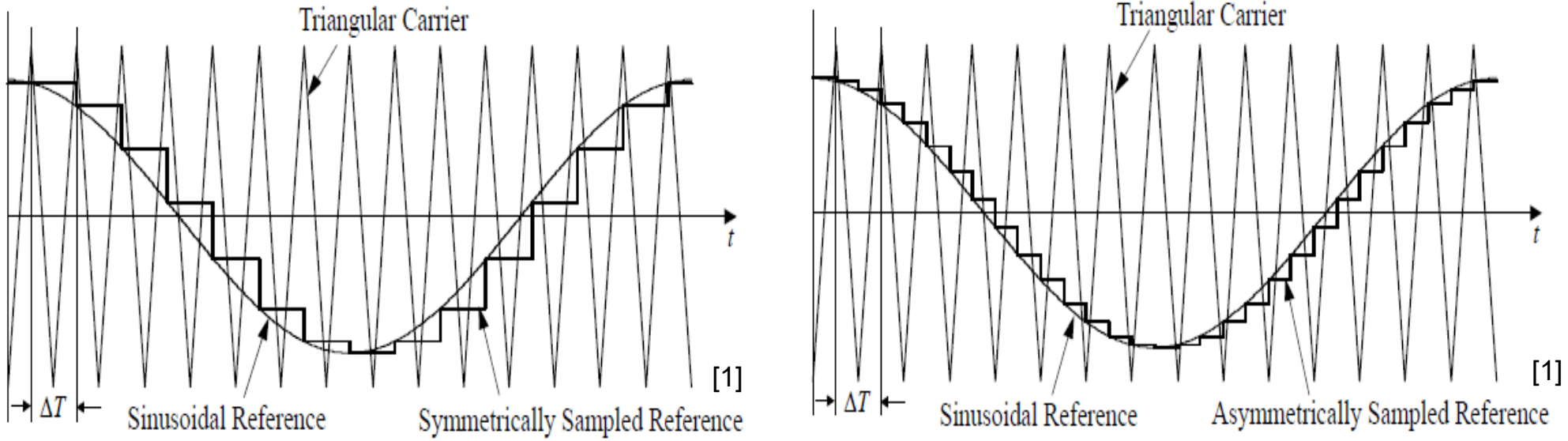
$$+ \sum_{m=1}^{\infty} [A_{m0} \cos(m[\omega_c t + \theta_c]) + B_{m0} \sin(m[\omega_c t + \theta_c])] \quad \boxed{\text{Carrier Harmonics}}$$

$$+ \sum_{m=1}^{\infty} \sum_{n=-\infty}^{\infty} \left[A_{mn} \cos(m[\omega_c t + \theta_c] + n[\omega_o t + \theta_o]) + B_{mn} \sin(m[\omega_c t + \theta_c] + n[\omega_o t + \theta_o]) \right] \quad \boxed{\text{Sideband Harmonics}}$$

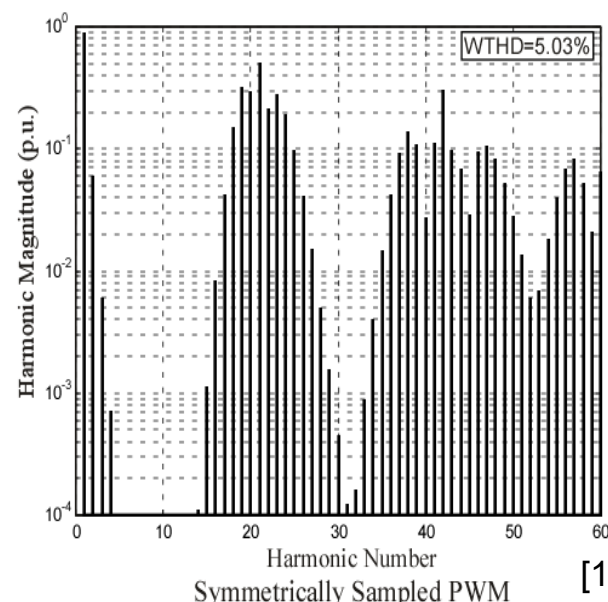
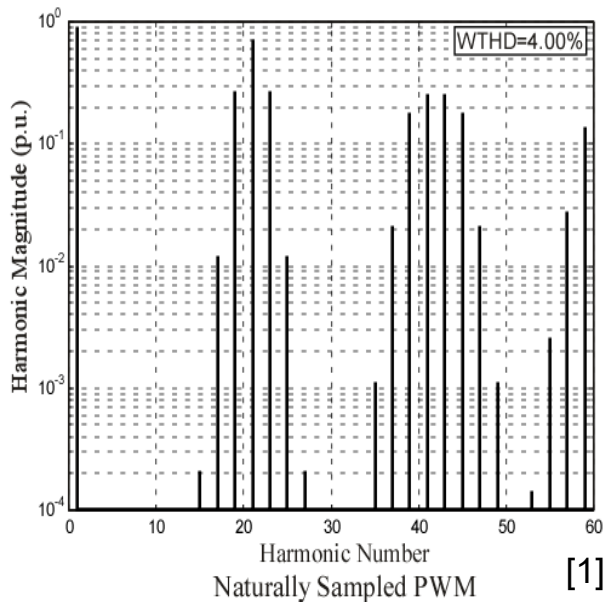
[1]

Fundamental and
Baseband Harmonics
are the relevant
harmonics for current
regulation.

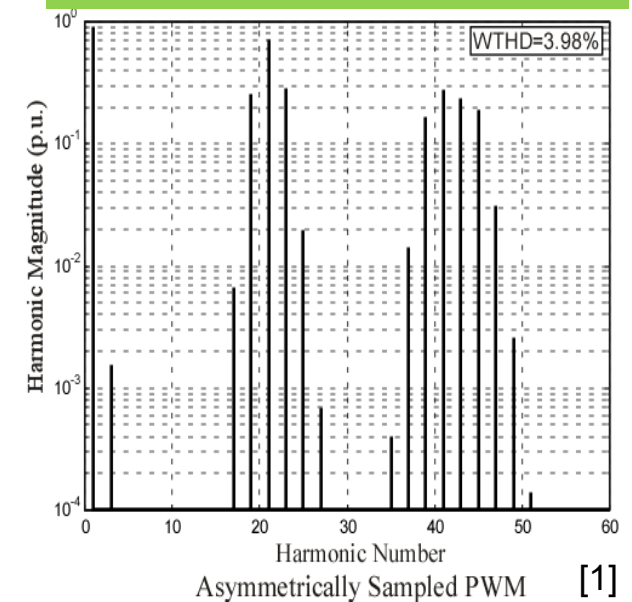
Sampled PWM of Inverter Phase Leg



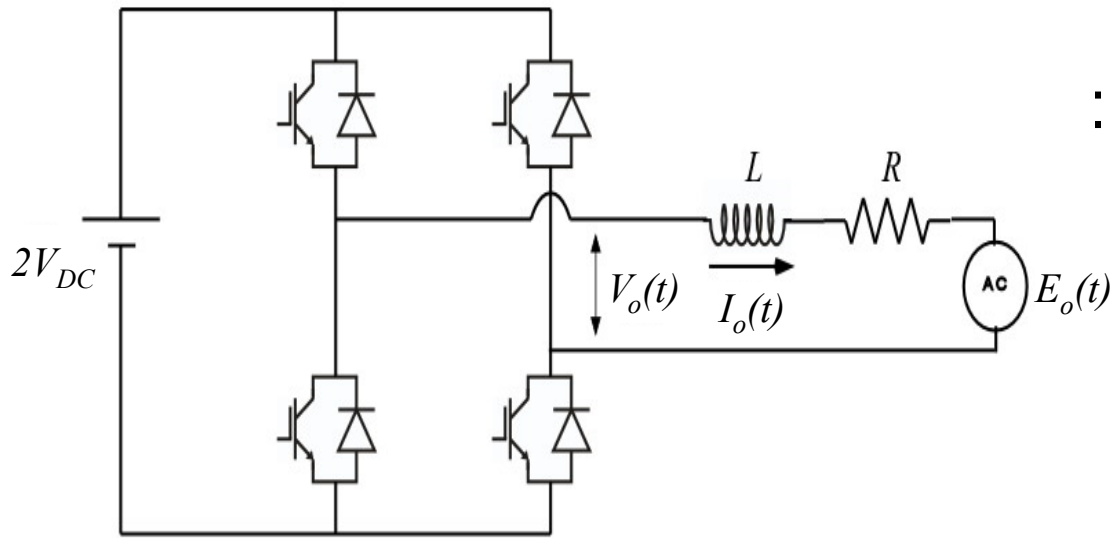
NOTE: Sampled references are delayed wrt their sinusoidal sources.



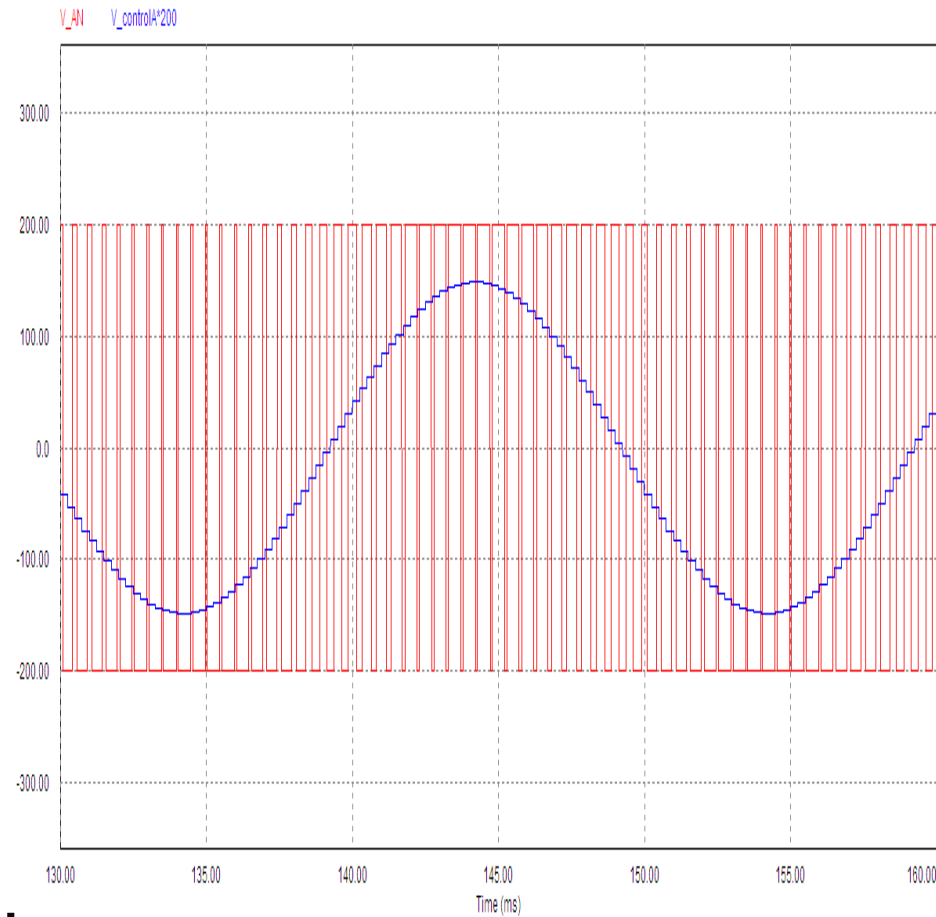
ALWAYS USE THIS APPROACH



Ideal “Average” Model of Single Phase VSI



$$V_o(t) - E_o(t) = RI_o(t) + L \frac{dI_o(t)}{dt}$$



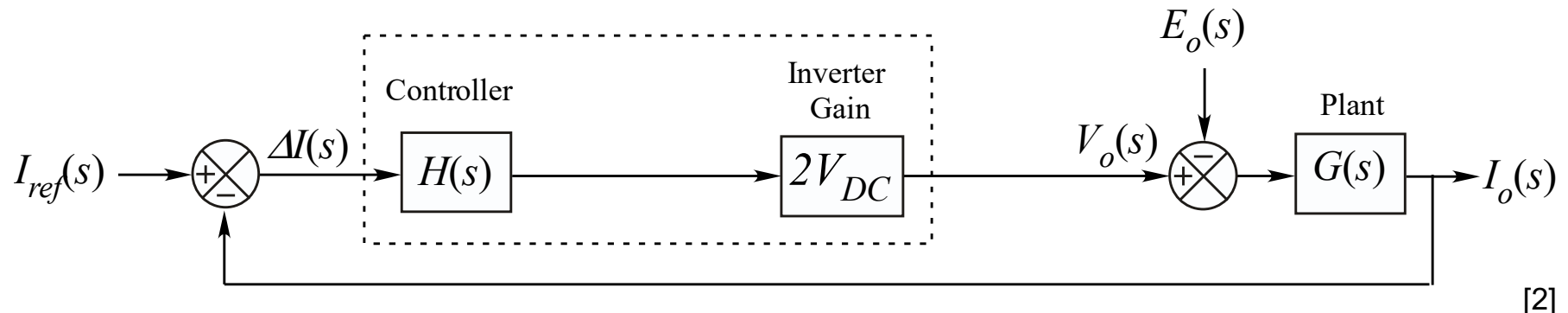
- Averaged model in Laplace form:

$$I_o(s) = \frac{V_o(s) - E_o(s)}{R + sL}$$

$$V_o(t) = M(t)2V_{DC}$$

Ideal Linear AC Current Regulated System

The ideal system reduces (in control terms) to the s-domain form of:



[2]

under the simplifications of

- The Modulator/VSI reduces to a linear gain ($2V_{DC}$), ignoring switching harmonics (which cannot be controlled anyway)
- The input disturbance (E_o) represents the motor back-emf
- Plant block is defined by:

$$G(s) = \frac{1}{R + sL} = \frac{1}{R} \cdot \frac{1}{1 + sT_p}$$

$$T_p = \frac{L}{R}$$

Ideal Linear AC Current Regulated System

- Analysis of the system block diagram:

$$\begin{aligned}I_o(s) &= G(s)[V_o(s) - E_o(s)] \\&= G(s)H(s)2V_{DC}[I_{ref}(s) - I_o(s)] - G(s)E_o(s)\end{aligned}$$

$$I_o(s)[1 + G(s)H(s)2V_{DC}] = G(s)H(s)2V_{DC}I_{ref}(s) - G(s)E_o(s)$$

- Solving for $I_o(s)$ gives the closed loop transfer function of:

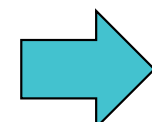
$$I_o(s) = I_{ref}(s) \frac{H(s)2V_{DC}G(s)}{1 + H(s)2V_{DC}G(s)} - E_o(s) \frac{G(s)}{1 + H(s)2V_{DC}G(s)}$$

Reference tracking Disturbance rejection

- Primary performance objectives are

$$\frac{I_o(s)}{I_{ref}(s)} \approx 1$$

$$\frac{I_o(s)}{E_o(s)} \leq \varepsilon$$



Make $H(s)$ as
large as possible

Ideal Linear AC Current Regulated System

- Try a simple PI regulator:

$$H(s) = K_P \left(1 + \frac{1}{s\tau_i} \right) = K_P \left(\frac{1 + s\tau_i}{s\tau_i} \right)$$

- Open Loop Forward Path Gain:

$$H(s)V_{DC}G(s) = \frac{2V_{DC}K_P}{R\tau_i} \cdot \frac{1 + s\tau_i}{s(1 + sT_p)}$$

- Classical control theory states system is stable provided:

$$\angle 2V_{DC}H(j\omega_c)G(j\omega_c) > -180^\circ \quad \text{when} \quad |2V_{DC}H(j\omega_c)G(j\omega_c)| = 1$$

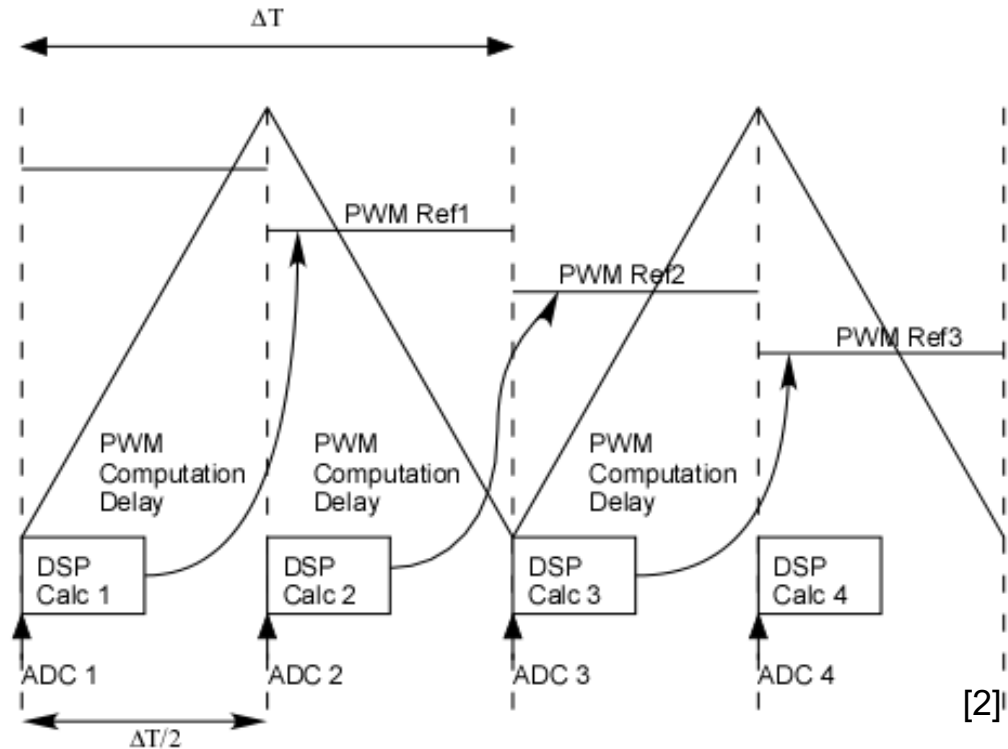
- Simple PI forward path phase response asymptotes to -90° at high frequencies. Hence system is unconditionally stable irrespective of PI gain K_p and integrator time constant τ_i .

THIS CLEARLY DOES NOT MATCH REALITY – WHY?

Sampling and Transport Delay

THE OBVIOUS CANDIDATE

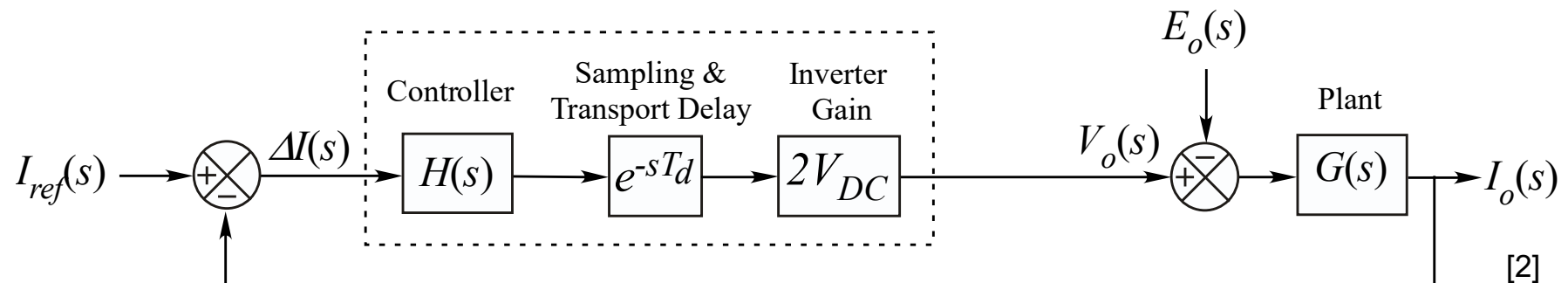
- Asymmetrical regular sampled PWM introduces a quarter carrier-period sampling delay (ZOH) into the control process.
- Computation delay and synchronous sampling cause a further half-carrier transport delay (Z^1).
- Overall delay of 0.75 of the carrier period is introduced into the forward path of the control loop.



*Sampling and Transport Delay
caused by PWM process and digital
controller sampling/computation.*

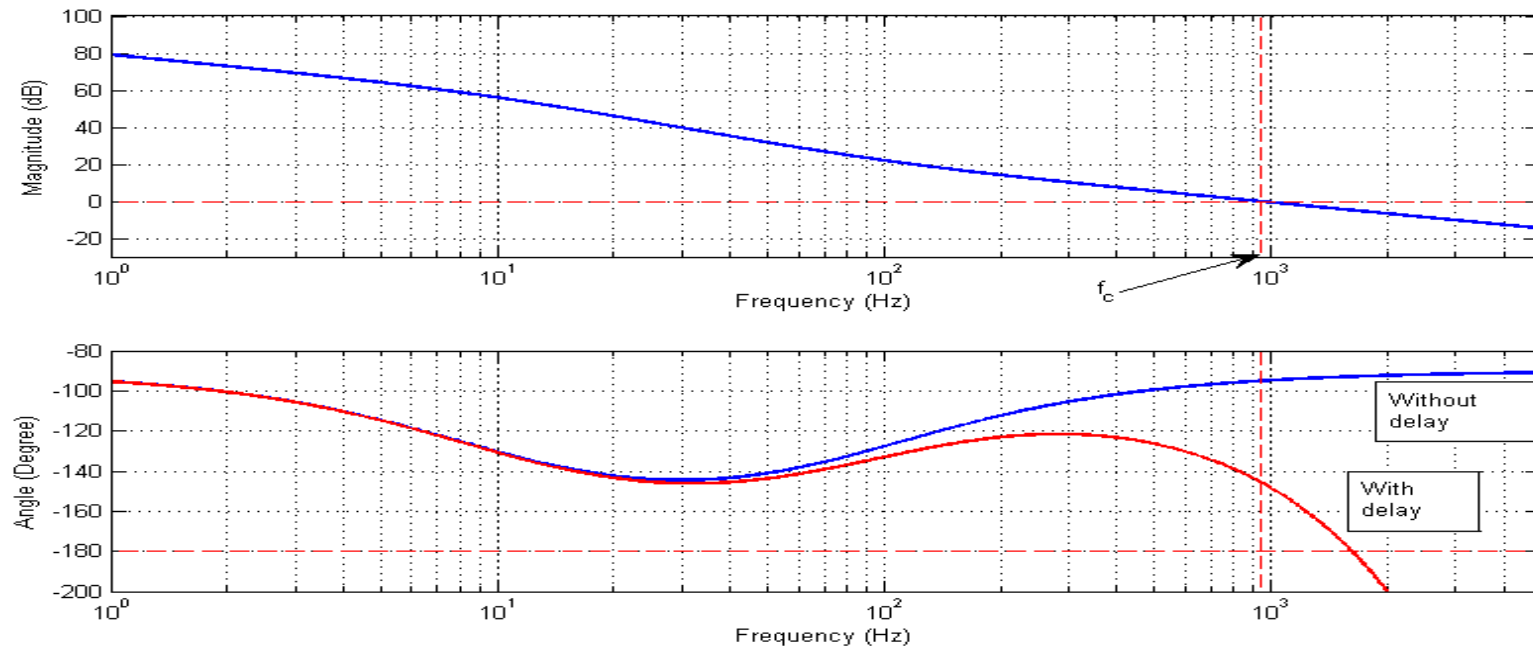
$$T_d = 0.75\Delta T = 0.75/f_s$$

Effect of Regulator Delay on Frequency Response



[2]

Stationary frame PI Regulator with sampling and transport delay



[2]

Bode plot of open loop forward path gain for ideal and regulators with transport delay

The gain limitation is now clear – forward path phase goes below 180° as frequency increases. Forward loop gain magnitude must fall less than 1.0 before this occurs.

Stationary Frame PI Regulator Maximum Gains [2]

- Forward path transfer function with regulator delay T_d

$$H(s)e^{-sT_d} 2V_{DC}G(s) = \frac{K_p 2V_{DC}}{R} \left(\frac{1 + s\tau_i}{s\tau_i} \right) e^{-sT_d} \left(\frac{1}{1 + sT_p} \right)$$

- Transfer function phase angle at cross over frequency $s = j\omega_c$

$$\angle\{H(j\omega_c)2V_{DC}G(j\omega_c)\} = \tan^{-1}(\omega_c\tau_i) - \pi/2 - \omega_c T_d - \tan^{-1}(\omega_c T_p) = -\pi + \phi_m$$

$$\omega_c \gg \frac{1}{T_p} \rightarrow \tan^{-1}(\omega_c T_p) \approx \pi/2 \rightarrow \omega_c = \frac{\tan^{-1}(\omega_c\tau_i) - \phi_m}{T_d} \approx \frac{\pi/2 - \phi_m}{T_d}$$

Hence for a given regulator delay, ω_c is the system bandwidth at ϕ_m = selected phase margin

Stationary Frame PI Regulator Maximum Gains

- Maximum possible K_p is for a given ω_c is:

$$K_p = \frac{R}{2V_{DC}} \omega_c \tau_i \sqrt{\frac{(1 + \omega_c^2 T_p^2)}{(1 + \omega_c^2 \tau_i^2)}}$$



$$K_p \approx \frac{\omega_c L}{2V_{DC}}$$

assuming

$$\omega_c^2 T_p^2 \gg 1$$

$$\omega_c^2 \tau_i^2 \gg 1$$

- Integral time constant τ_i can be determined by making

$$\tan^{-1}(\omega_c \tau_i) \approx \pi / 2$$



$$\tau_i \approx \frac{10}{\omega_c}$$

- These gains are independent of the plant time constant, and are determined only by ϕ_m T_d V_{DC} and L

For any given system with regulator delay T_d , these are the maximum possible PI gains for a phase margin of ϕ_m

Example Grid Inverter: Calculations & Results

Circuit Parameter	Value
Resistive load (R) (Ω)	1.2
Inductive load (L) (mH)	10.0
Switching Freq. (f _s) (Hz)	5000
DC Bus volt. (2V _{DC}) (V)	400
Back EMF volt. (V _{EMF}) (V _{RMS})	220
Back EMF freq. (Hz)	50
Sampling period (T) (sec)	10 ⁻⁴

Circuit parameters

$$T_d = 0.75 / 5e^3 = 1.5e^{-4} \text{ sec}$$

$$\phi_m = 40^\circ = 0.698 \text{ rad}$$

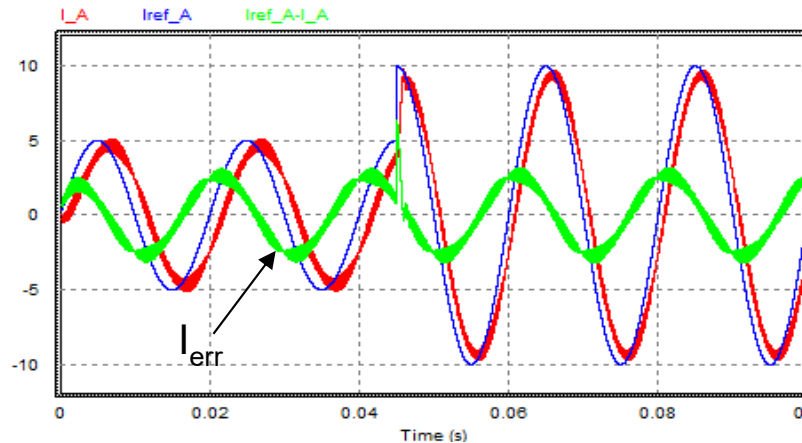
$$\omega_c = \frac{\pi/2 - \phi_m}{T_d} = \frac{1.56 - 0.698}{1.5e^{-4}} = 5.81 \text{ krad/s}$$

$$K_p = \frac{\omega_c L}{2V_{DC}} = \frac{5.81e^3 * 10e^{-3}}{400} = 0.145 \text{ A}^{-1}$$

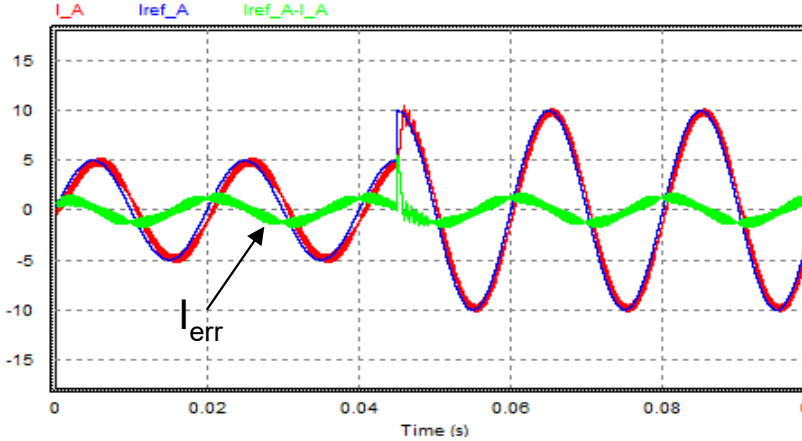
$$\tau_i = \frac{10}{\omega_c} = \frac{10}{5.82e^3} = 1.72 \text{ msec}$$

Practical Linear AC Current Regulated System

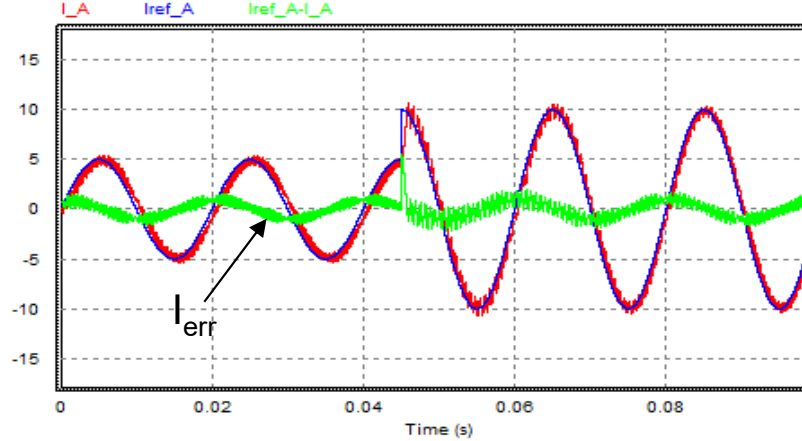
Circuit Parameter	Value
Resistive load (R) (Ω)	1.2
Inductive load (L) (mH)	10.0
Switching Freq. (f_s) (Hz)	5000
DC Bus volt. ($2V_{DC}$) (V)	400
Back EMF volt. (V_{EMF}) (V_{RMS})	220
Back EMF freq. (Hz)	50
Sampling period (T) (sec)	10^{-4}



$K_p = 0.145$
Steady state error,
damped transient



$K_p = 0.218$
Reducing steady
state error,
underdamped
transient



$K_p = 0.247$
Less steady state
error, very
underdamped
transient

- Clearly gain cannot be arbitrarily increased despite prediction of ideal theory.

Practical PI Regulator Performance Evaluation

- The current error $\Delta I(s)$ as a function of control inputs is :

$$\Delta I(s) = I_{ref}(s) \frac{1}{1 + H(s)e^{-sT_d} 2V_{DC}G(s)} + E_o(s) \frac{G(s)}{1 + H(s)e^{-sT_d} 2V_{DC}G(s)} = \Delta I_I(s) + \Delta I_D(s)$$

- It has two elements: Closed Loop Tracking Error - the ability of regulation system to follow current reference:

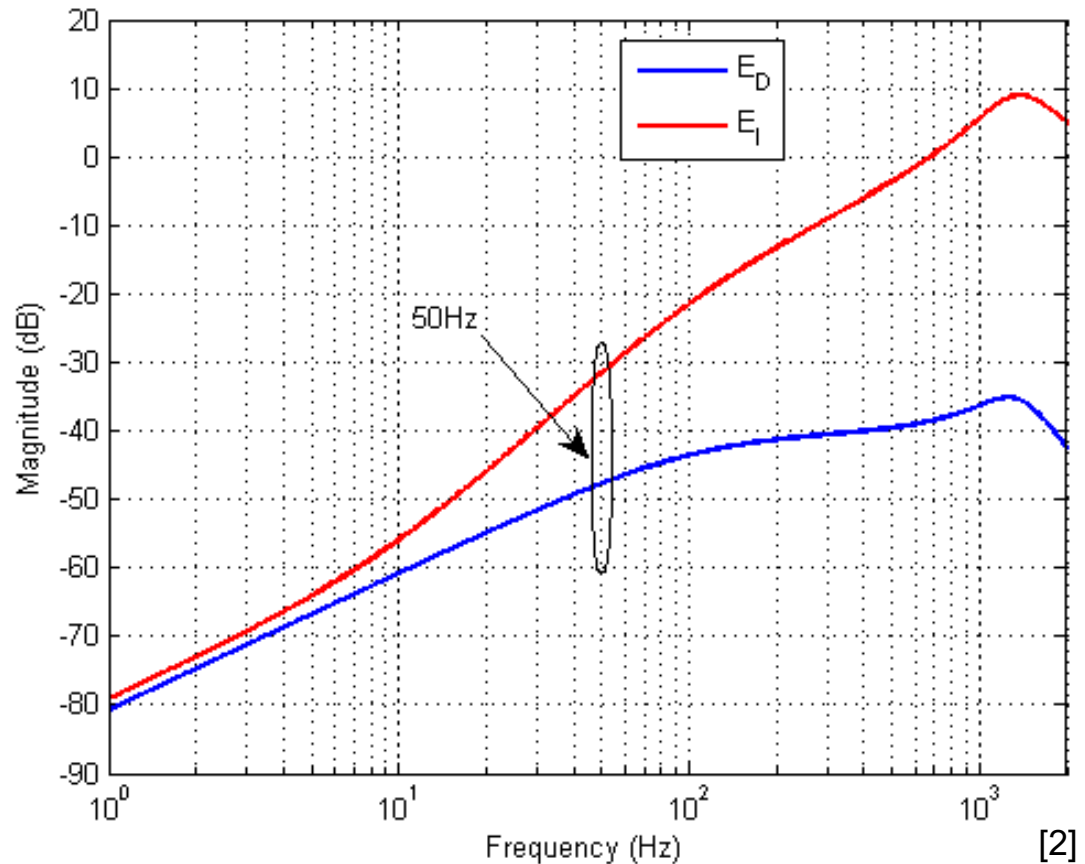
$$E_I(s) = \frac{\Delta I_I(s)}{I_{ref}(s)} = \frac{1}{1 + H(s)e^{-sT_d} 2V_{DC}G(s)}$$

- Closed Loop Disturbance Rejection Error – regulation system sensitivity to backemf disturbance:

$$E_D(s) = \frac{\Delta I_D(s)}{E_o(s)} = \frac{G(s)}{1 + H(s)e^{-sT_d} 2V_{DC}G(s)}$$

Practical PI Regulator Performance Evaluation

- Both tracking error and disturbance rejection error increase with frequency (controller gain reduces)
- Disturbance error increases more slowly because of plant pole
- BUT, magnitude of disturbance injection (emf) is usually larger → still creates more error

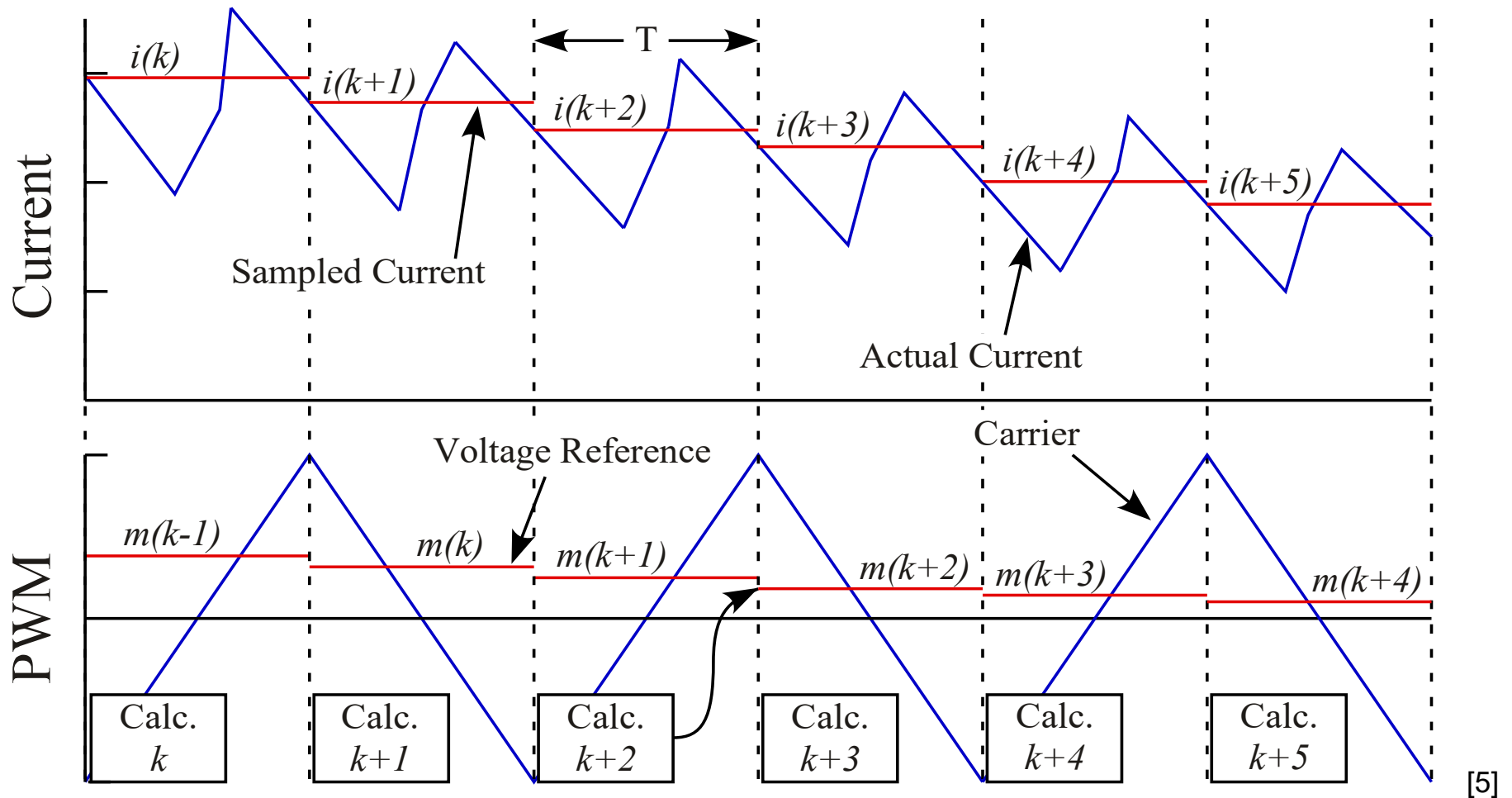


Irrespective of the contribution, the error at AC fundamental frequency is usually unacceptably large with PI controller even with maximum possible gains.

Stationary Frame Regulator Enhancements

- Maximised gains are often insufficient to achieve acceptable regulator performance, especially when error caused by back EMF is considered
- The following enhancements can be considered
 - **Minimise regulator delay** to achieve the maximum possible gains. Use asymmetrical regulator sampled PWM and synchronous sampling of current (avoids a Low Pass Filter) as a matter of course.
 - Reduce the **back EMF disturbance** effect with feed forward compensation
 - Increase the **regulator gain** at the fundamental target frequency (Proportional-Resonant Controller)
- Lets see how these ideas work

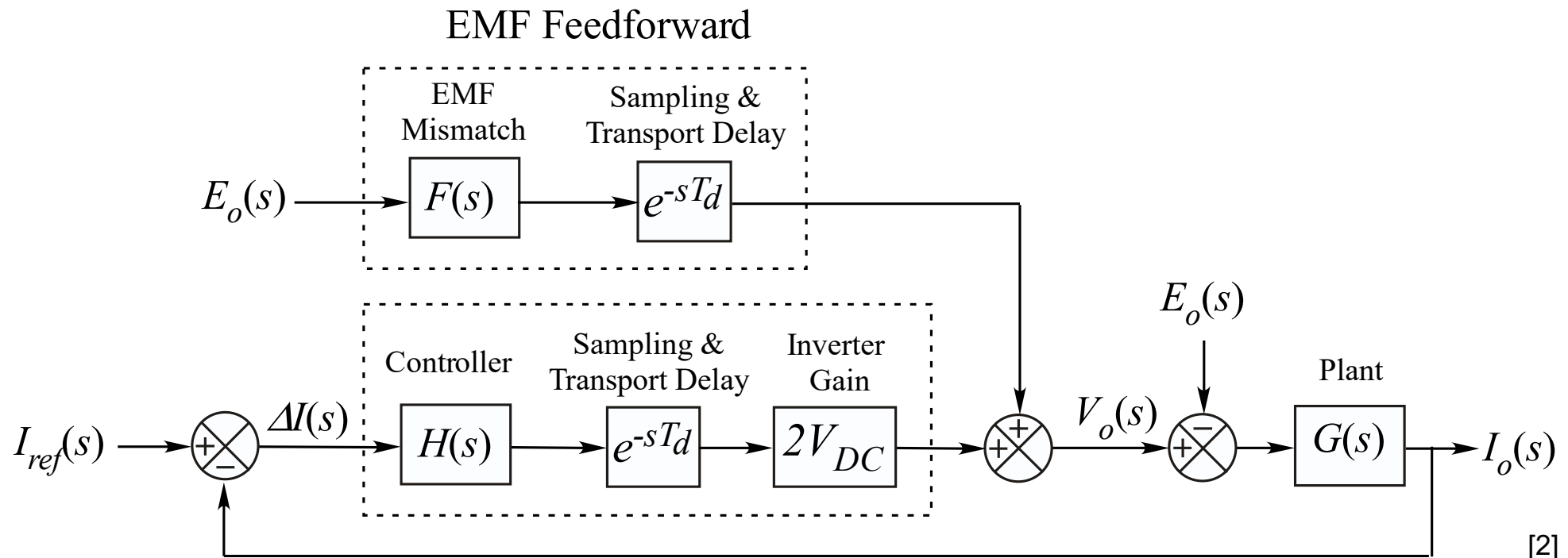
Minimise delay - synchronously sample the current



- Sample at top and bottom of (implied) carrier for asymmetrical modulation
- Sampled current corresponds to average current without the phase delay of a LP filter (HF switched volt-seconds == LF commanded volt-seconds)
- Still has $\frac{1}{2}$ carrier interval transport delay due to finite calculation time

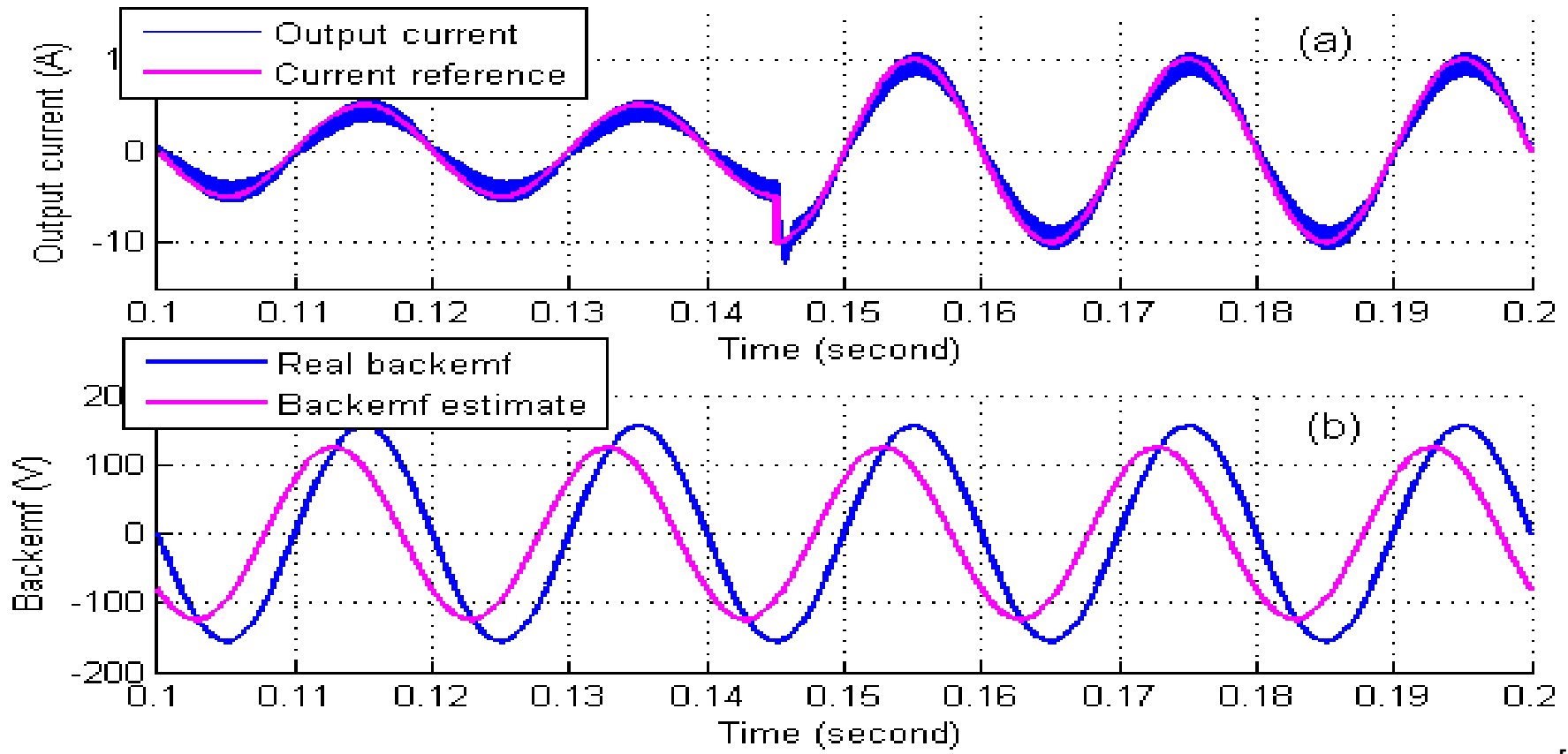
Feedforward Compensation of Backemf Disturbance [3]

- Back EMF is predictable, and so its effect can be reduced by feedforwarding the measured (or estimated) value



Average model AC current regulation system with back EMF feedforward

Accuracy of Back EMF Estimation



[16]

(a) Performance of PI regulator with backemf feedforward

(b) Miss estimated back EMF estimation (80% magnitude, 40° phase lead)

Increase Fundamental Gain with PR Regulator

- Key limitation of PI regulator is high $E_D(s)$ at fundamental reference frequency (ω_0)
- An alternative approach is to increase controller gain at ω_0 without affecting high frequency gain determined by K_p
- This is the strategy of the P+Resonant (PR) controller, with a resonant gain peak at ω_0 :

$$H_{PR}(s) = K_p \left(1 + \frac{1}{\tau_i} \frac{s}{s^2 + \omega_0^2} \right)$$

Controller provides near infinite gain at the target AC frequency → Reference tracking error and disturbance error are near zero at the AC frequency

Note : PR regulator is sensitive to mismatch between the resonant term and AC fundamental frequency.

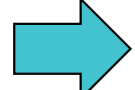
Maximum Gains with PR Regulator

- Forward Path Gain:

$$H_{PR}(s)e^{-sT_d} 2V_{DC}G(s) = \frac{K_p 2V_{DC}}{R} \left(1 + \frac{1}{\tau_i} \frac{s}{s^2 + \omega_o^2} \right) e^{-sT_d} \left(\frac{1}{1 + sT_p} \right)$$

$$T_p = \frac{L}{R}$$

- At the cross-over frequency: $s = j\omega_c$


$$H_{PR}(j\omega_c)e^{-j\omega_c T_d} 2V_{DC}G(j\omega_c) = \frac{K_p 2V_{DC}}{R} \left(1 + \frac{1}{\tau_i} \frac{j\omega_c}{\omega_o^2 - \omega_c^2} \right) e^{-j\omega_c T_d} \left(\frac{1}{1 + j\omega_c T_p} \right)$$

- If $\omega_c \gg \omega_o$, then:

FORWARD PATH GAIN ≈

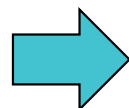
$$\frac{K_p 2V_{DC}}{R} \left(1 + \frac{1}{j\omega_c \tau_i} \right) e^{-j\omega_c T_d} \left(\frac{1}{1 + j\omega_c T_p} \right) = \frac{K_p 2V_{DC}}{R} \left(\frac{1 + j\omega_c \tau_i}{j\omega_c \tau_i} \right) e^{-j\omega_c T_d} \left(\frac{1}{1 + j\omega_c T_p} \right)$$

- This is identical to the PI expression, viz:

$$H(j\omega_c)e^{-j\omega_c T_d} 2V_{DC}G(j\omega_c) = \frac{K_p 2V_{DC}}{R} \left(\frac{1 + j\omega_c \tau_i}{j\omega_c \tau_i} \right) e^{-j\omega_c T_d} \left(\frac{1}{1 + j\omega_c T_p} \right)$$

Maximum Gains with PR Regulator

- Therefore the maximum gains for the PR controller are the same as for the PI controller, and are defined by:
 - Target Phase Margin ϕ_m
 - DC link voltage $2V_{DC}$
 - Load Inductance L
 - PWM/Current regulator transport delay T_d

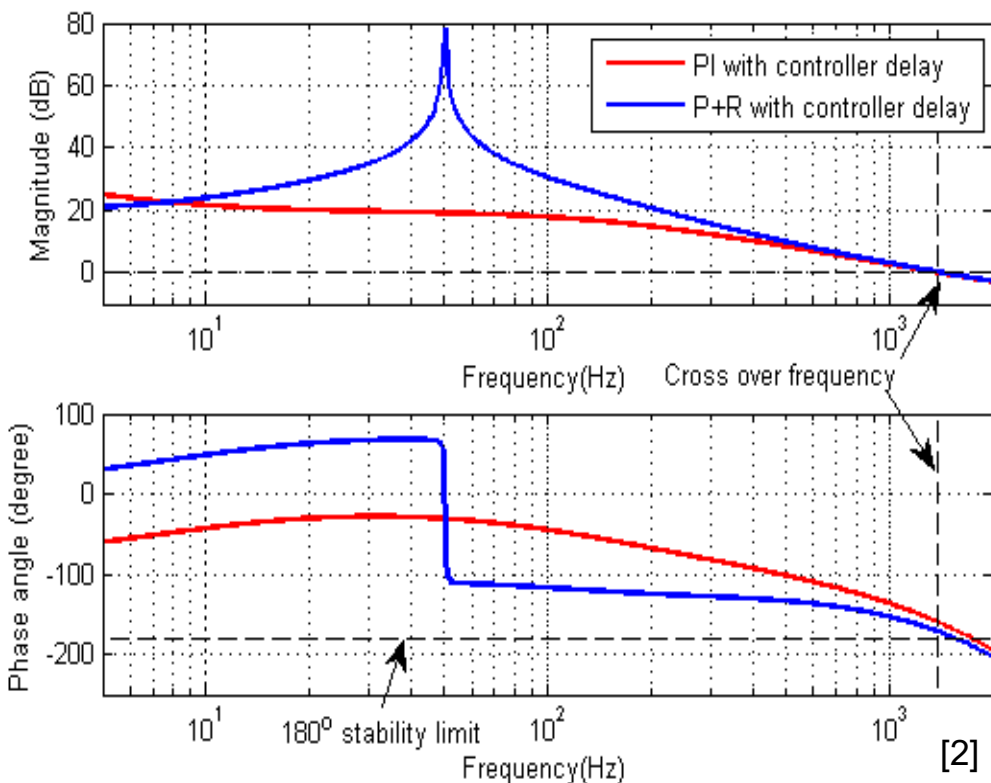


$$\omega_c = \frac{\pi/2 - \phi_m}{T_d}$$

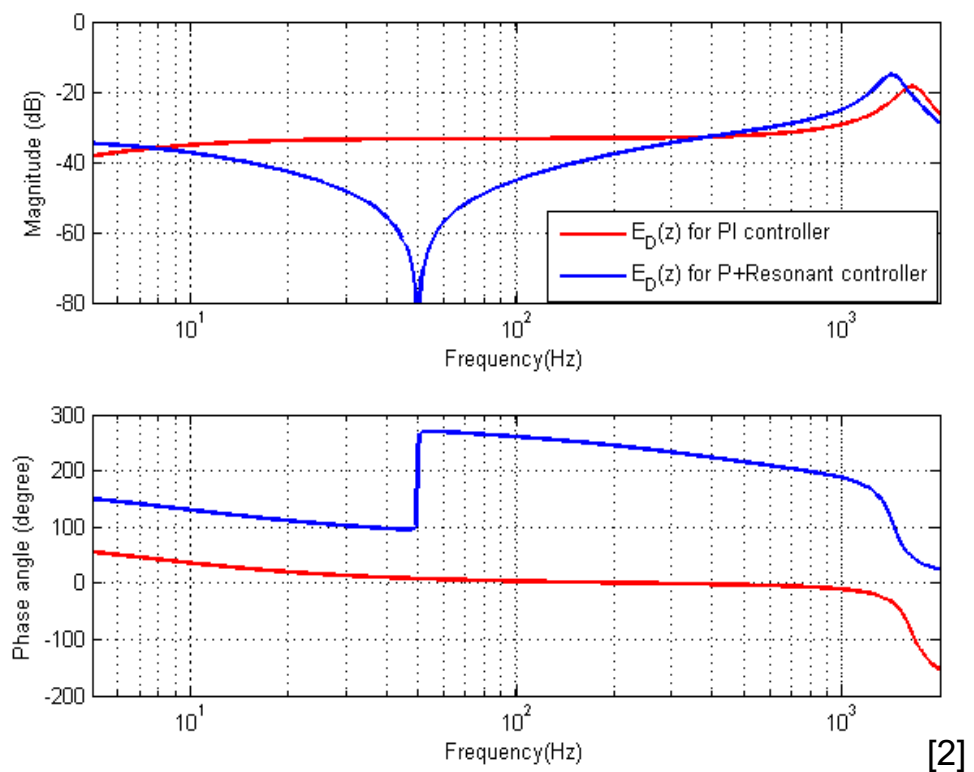
$$K_p = \frac{\omega_c L}{2V_{DC}}$$

$$\tau_i = \frac{10}{\omega_c}$$

Maximum Gains with PR Regulator



Bode plot of $GH(s)$ for PI and PR regulators with transport delays

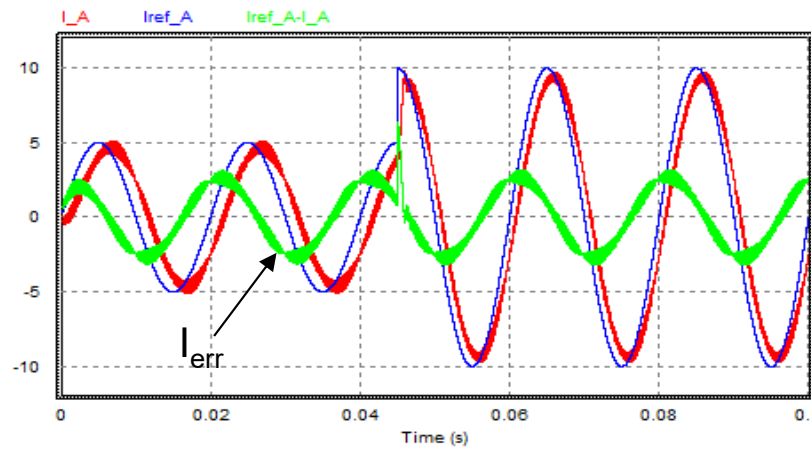


Closed Loop Disturbance Rejection Error $E_D(s)$ for PI and PR controllers

- Resonant gain peak improves backemf disturbance rejection at ω_0
- Also reduce $E_l(s)$ at ω_0 , leading to better tracking

Practical Linear AC Current Regulated System

Circuit Parameter	Value
Resistive load (R) (Ω)	1.2
Inductive load (L) (mH)	10
Switching Freq. (f_s) (Hz)	5000
DC Bus volt. ($2V_{DC}$) (V)	400
Back EMF volt. (V_{EMF}) (V_{RMS})	220
Back EMF freq. (Hz)	50
Sampling period (T) (sec)	10^{-4}

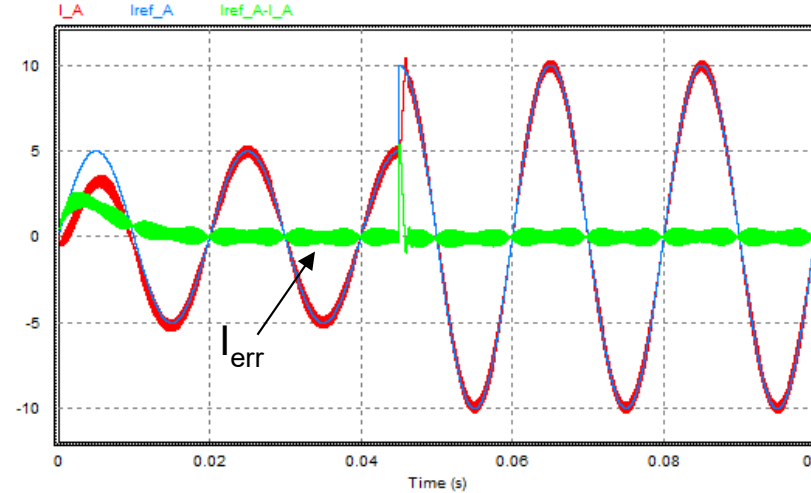


PI controller:

$$K_p = 0.145$$

$$\phi = 40^\circ$$

Steady state error,
damped transient



PR controller:

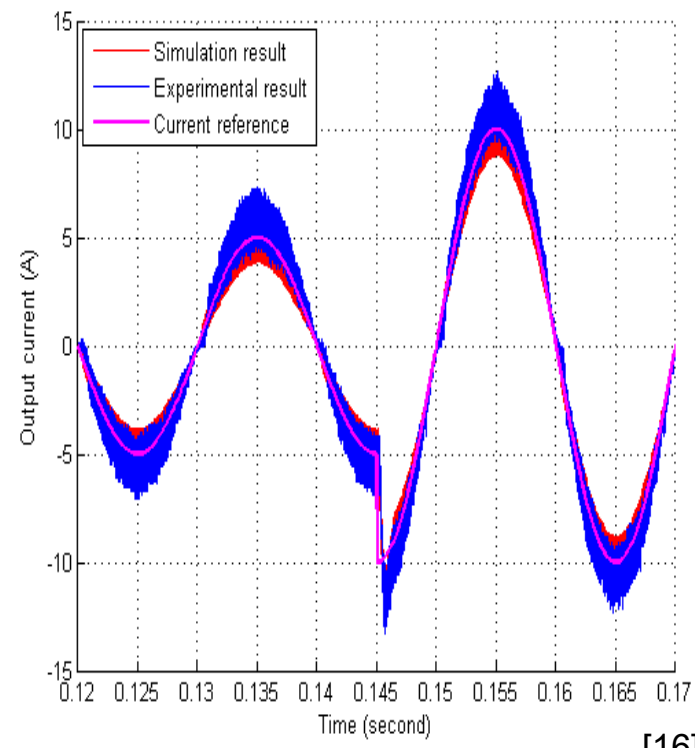
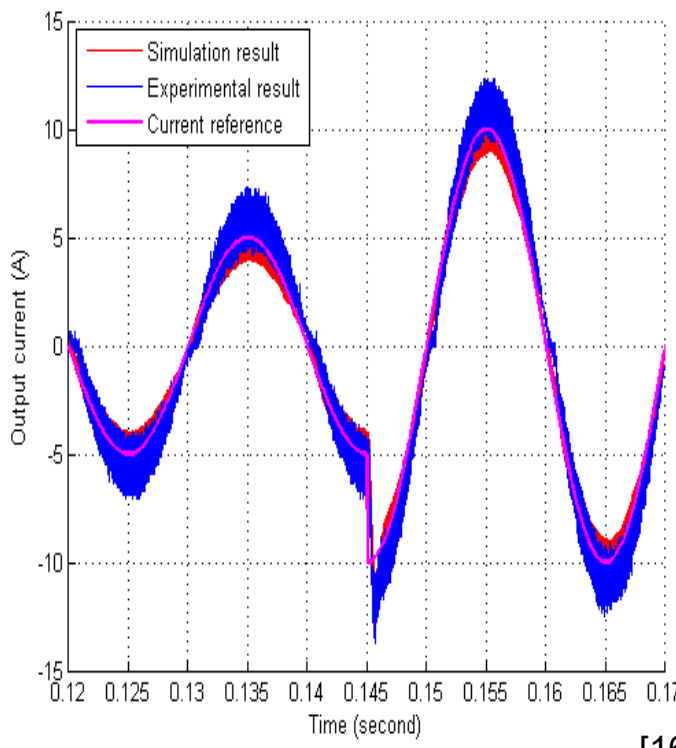
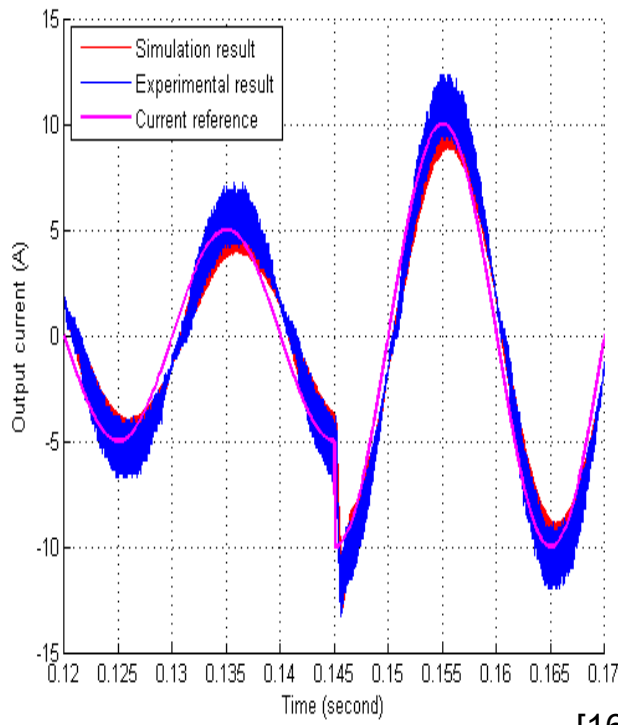
$$K_p = 0.145$$

$$\phi = 40^\circ$$

Negligible steady
state error,
damped transient

**PI verses PR controller
response with same gains.**

Experimental Confirmation: Comparison Results



PI controller without
backemf feed forward

[16]

PI controller with
backemf feed forward

[16]

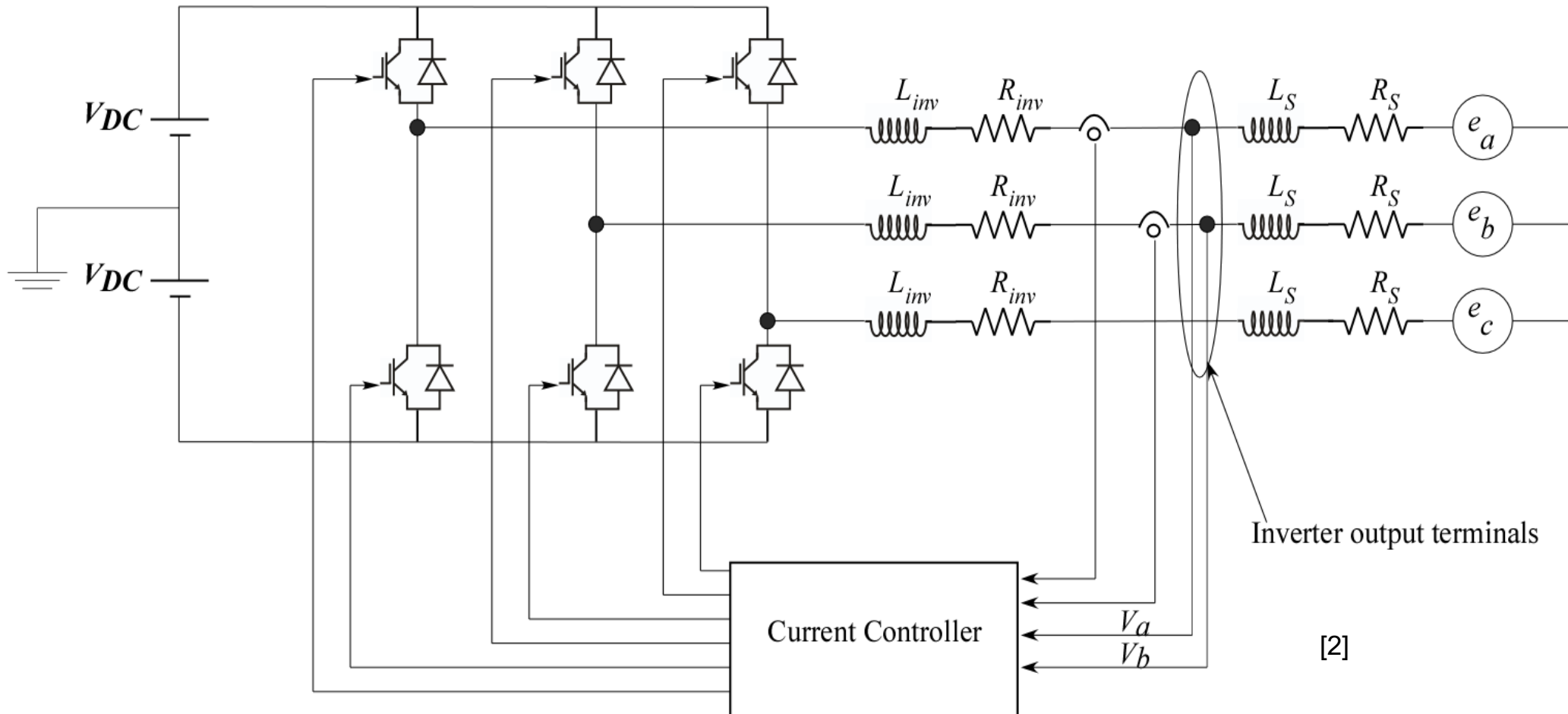
PR controller

[16]

**Simulated and Experimental system response with
110Vrms backemf**

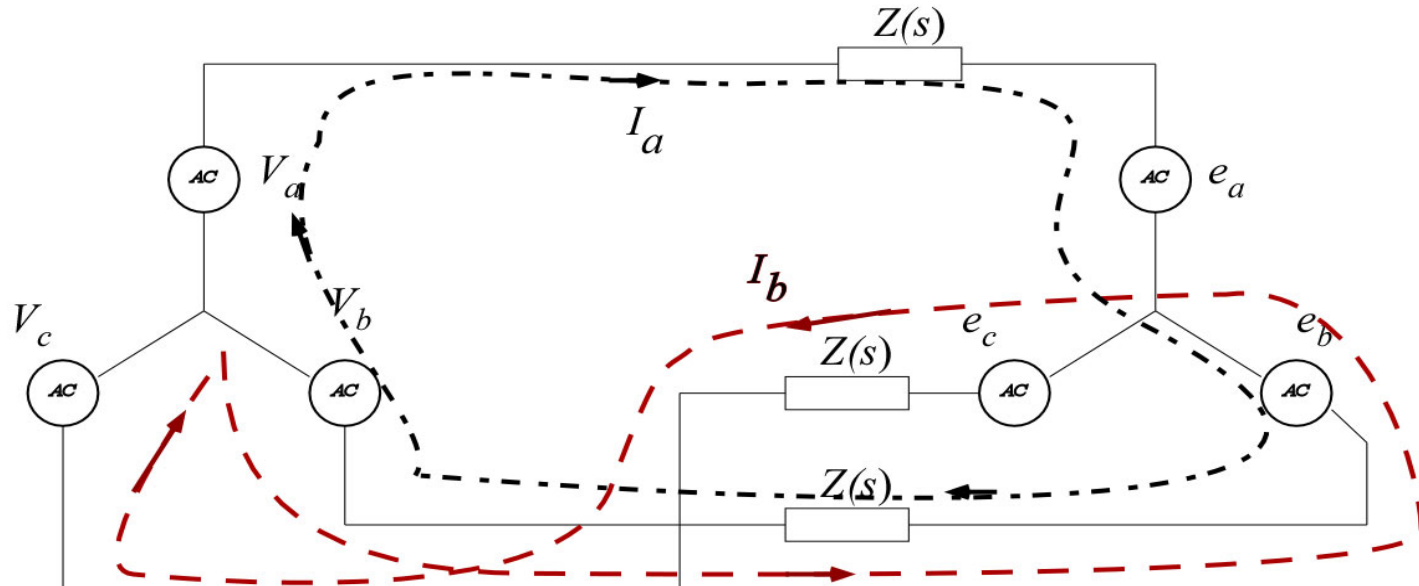
Same transient response for all three alternatives

Three Phase AC Current Regulated VSI



Three phase Voltage Source Inverter (VSI) connected to a back EMF load through a series R-L impedance

Three Phase AC Current Regulated VSI



- KVL loops:

$$V_a(s) = 2I_a(s)Z(s) - I_b(s)Z(s) + E_a(s) - E_b(s) + V_b(s)$$

$$V_b(s) = 2I_b(s)Z(s) - I_a(s)Z(s) + E_b(s) - E_c(s) + V_c(s)$$

- For balanced system:

$$V_a(s) + V_b(s) + V_c(s) = 0$$

$$E_a(s) + E_b(s) + E_c(s) = 0$$

$$\rightarrow V_c(s) = -V_a(s) - V_b(s)$$

$$\rightarrow E_c(s) = -E_a(s) - E_b(s)$$

Three Phase AC Current Regulated VSI

- For an isolated three phase system

$$i_a(s) + i_b(s) + i_c(s) = 0$$

- Substituting voltage and current constraints into KVL loops gives

$$i_a(s) = \frac{V_a(s) - E_a(s)}{R + sL}$$

$$i_b(s) = \frac{V_b(s) - E_b(s)}{R + sL}$$

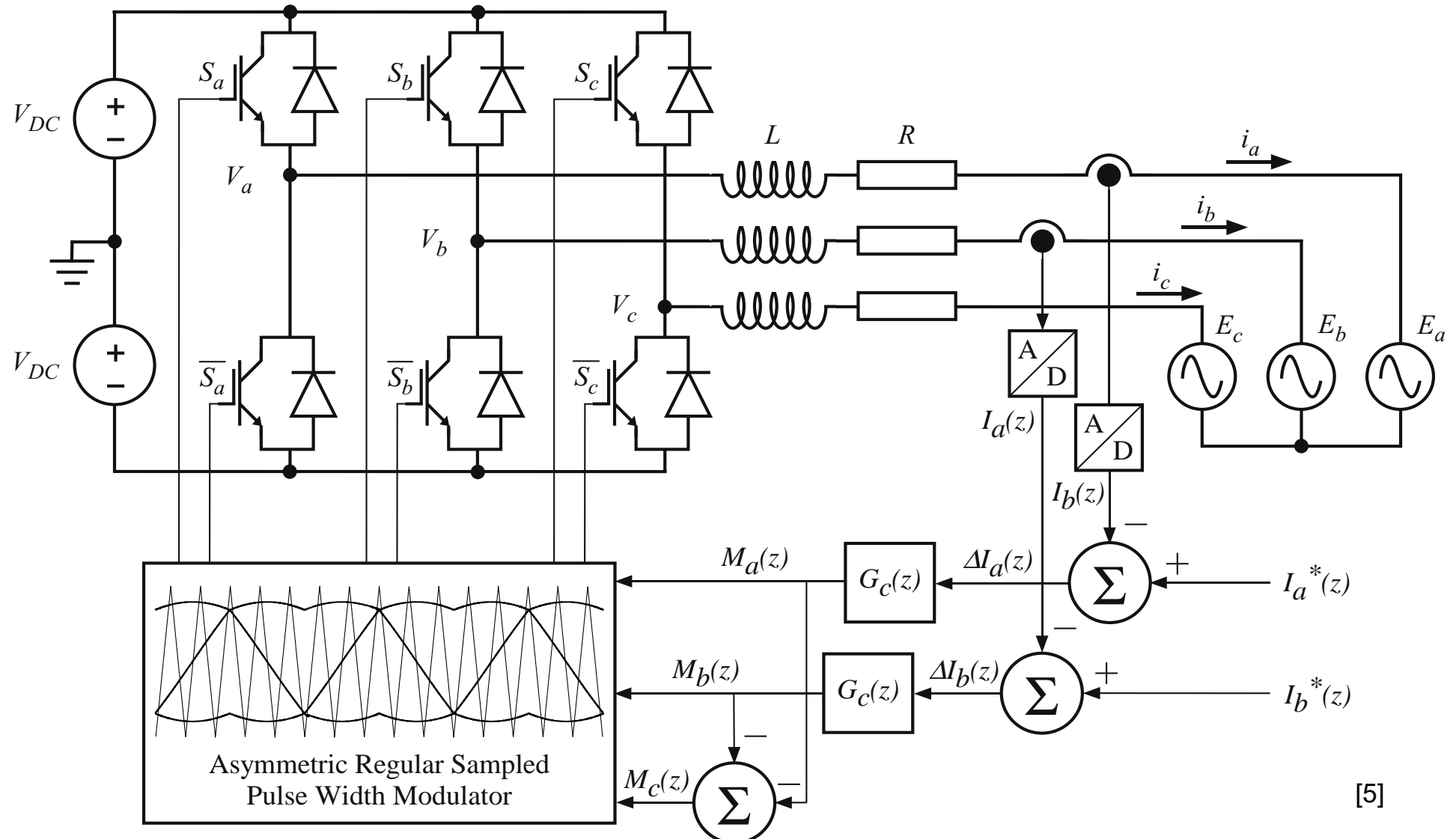
$$i_c(s) = \frac{V_c(s) - E_c(s)}{R + sL}$$

Thus only two currents need to be controlled for a three phase system, each regulated only by their individual phase voltages using previous single phase theory

- Modulate third phase to achieve balanced system using:

$$V_c(s) = -V_a(s) - V_b(s)$$

Three Phase AC Current Regulated VSI



[5]

Topology of a three phase AC current regulated voltage source inverter

Three Phase AC Current Regulated VSI

- 2 out of 3 AC currents sampled each $\frac{1}{2}$ carrier interval:

$$T = 1/(2f_c)$$

- Current errors feed through high gain controllers $G_C(z)$ to produce modulation commands $M_a(z)$ and $M_b(z)$
- Phase C PWM signal derived from phases A and B:

$$M_c(z) = -M_a(z) - M_b(z)$$

- Space vector common mode offset added viz.:

$$v_{off} = -\frac{1}{2} [\max(M_a(z), M_b(z), M_c(z)) + \min(M_a(z), M_b(z), M_c(z))]$$

$$M_k'(z) = M_k(z) + v_{off}(z) \quad k \in \{a, b, c\}$$

Example Grid Inverter: Calculations & Results

Circuit Parameter	Value
Resistive load (R) (Ω)	1.2
Inductive load (L) (mH)	20
Switching Freq. (f_s) (kHz)	5.0
DC Bus volt. ($2V_{DC}$) (V)	400
Back EMF volt. (V_{EMF}) (V_{RMS})	80
Back EMF freq. (Hz)	50
Sampling period (T) (sec)	10^{-4}

Circuit parameters

$$T_d = 0.75 / 5e^3 = 1.5e^{-4} \text{ sec}$$

$$\phi_m = 40^\circ = 0.698 \text{ rad}$$

$$\omega_c = \frac{\pi/2 - \phi_m}{T_d} = \frac{1.56 - 0.698}{1.5e^{-4}} = 5.81 \text{ krad/s}$$

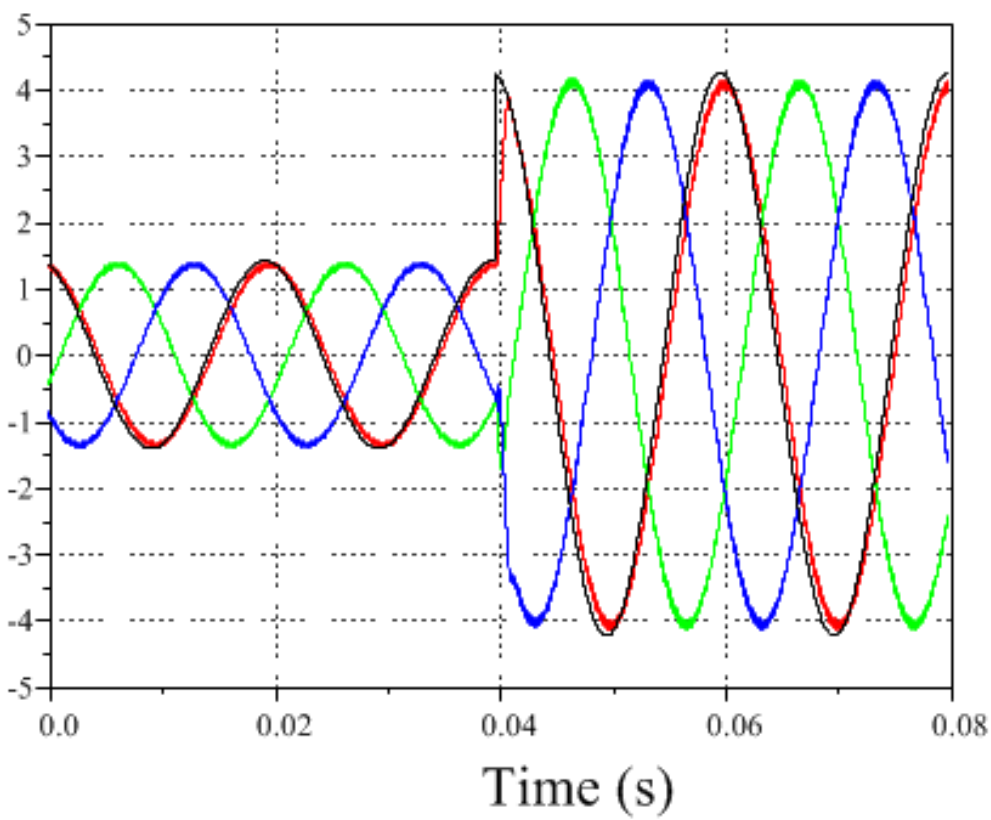
$$K_p = \frac{\omega_c L}{V_{DC}} = \frac{5.81e^3 * 20e^{-3}}{200} = 0.582 \text{ A}^{-1}$$

$$\tau_i = \frac{10}{\omega_c} = \frac{10}{5.82e^3} = 1.73 \text{ msec}$$

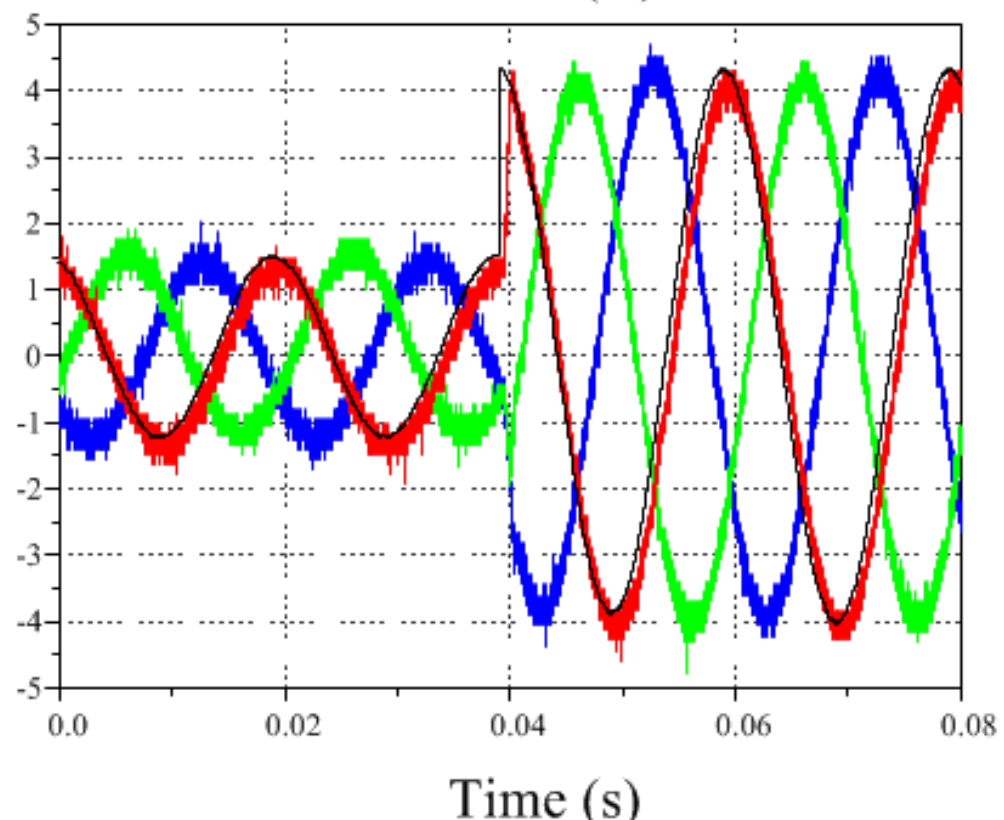
Note - effective DC source voltage for K_p gain calculation changes from $2V_{DC}$ for single phase system to V_{DC} for three phase system

Simulated and Experimental PI Current Responses

PI Regulator - Simulation
Three Phase Currents (A)

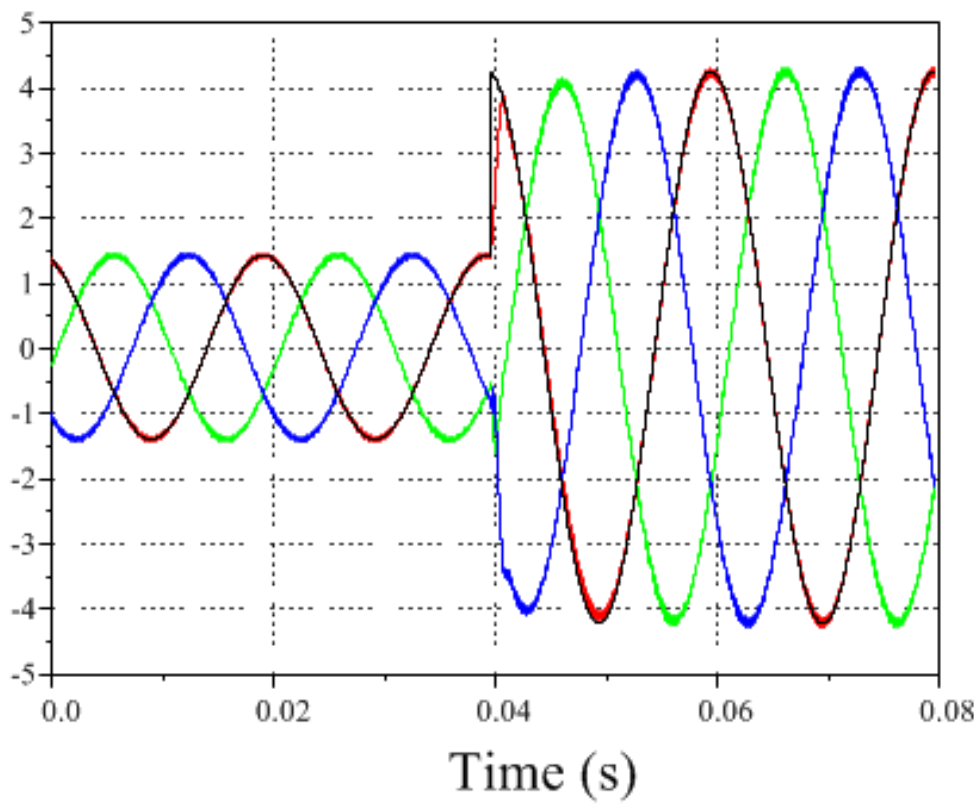


PI Regulator - Experimental
Three Phase Currents (A)

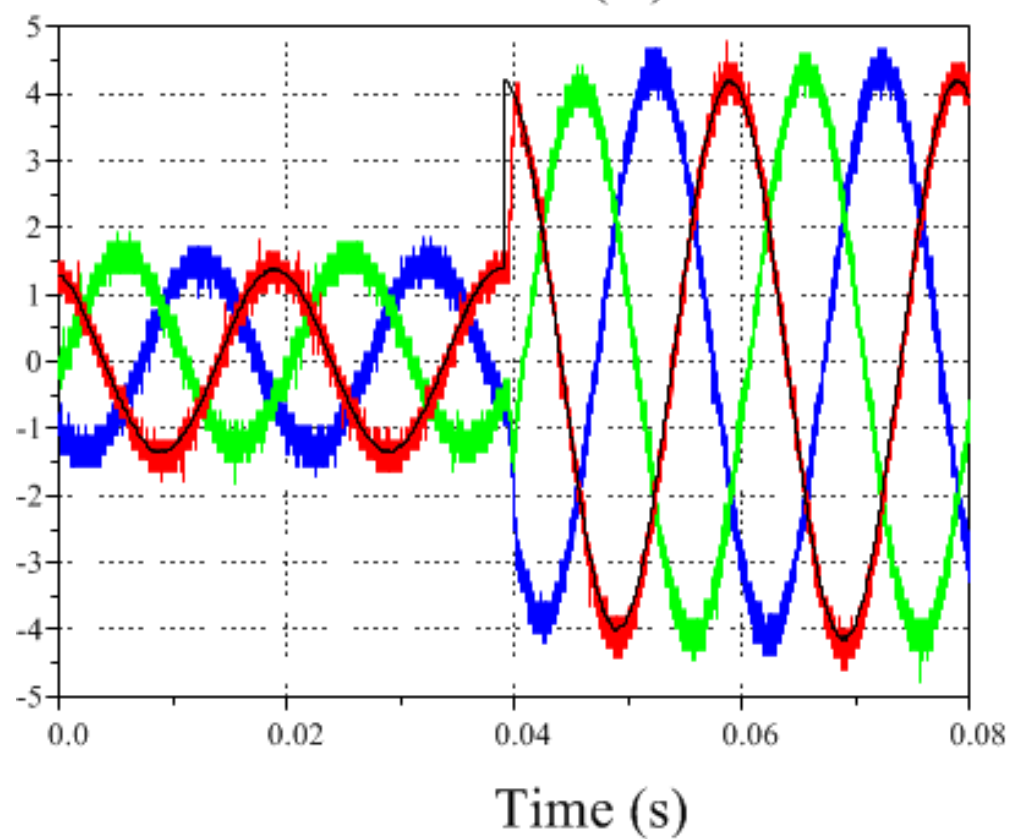


Simulated and Experimental PR Current Responses

PR Regulator - Simulation
Three Phase Currents (A)



PR Regulator - Experimental
Three Phase Currents (A)



Orthogonal Reference Frames: $\alpha\beta$ stationary frame

- ABC frame : Three non-orthogonal variables with two degrees of freedom
- $\alpha\beta$ frame: Two orthogonal variables
- Clarke (alpha-beta) transform:

$$\begin{bmatrix} i_\alpha \\ i_\beta \end{bmatrix} = T_{\alpha\beta} \begin{bmatrix} i_a \\ i_b \\ i_c \end{bmatrix} = \sqrt{\frac{2}{3}} \begin{bmatrix} 1 & -1/2 & -1/2 \\ 0 & \sqrt{3}/2 & -\sqrt{3}/2 \end{bmatrix} \begin{bmatrix} i_a \\ i_b \\ i_c \end{bmatrix}$$

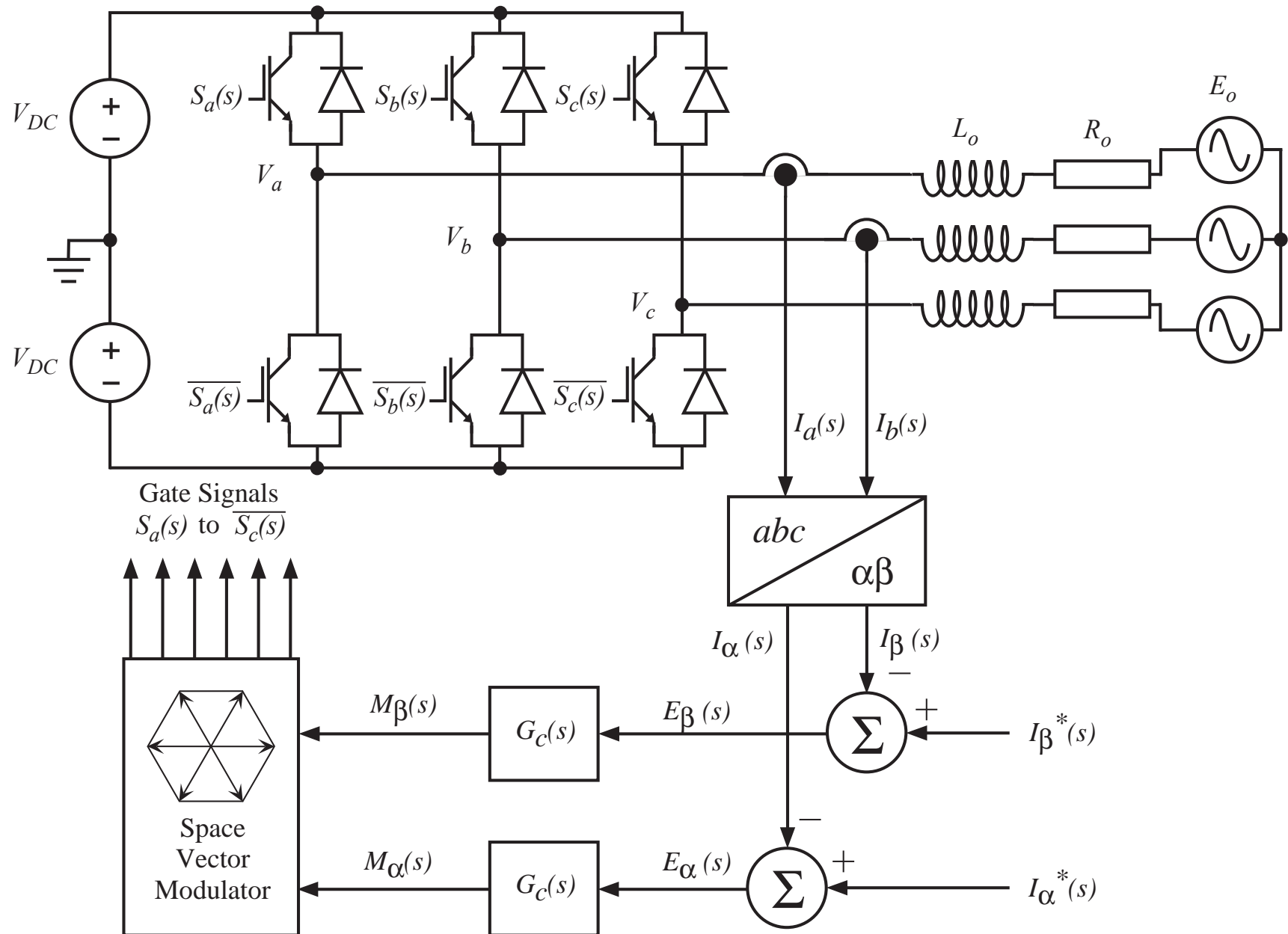
- Inverse Clarke transform:

$$\begin{bmatrix} i_a \\ i_b \\ i_c \end{bmatrix} = T_{\alpha\beta}^T \begin{bmatrix} i_\alpha \\ i_\beta \end{bmatrix} = \sqrt{\frac{2}{3}} \begin{bmatrix} 1 & 0 \\ -1/2 & \sqrt{3}/2 \\ -1/2 & -\sqrt{3}/2 \end{bmatrix} \begin{bmatrix} i_\alpha \\ i_\beta \end{bmatrix}$$

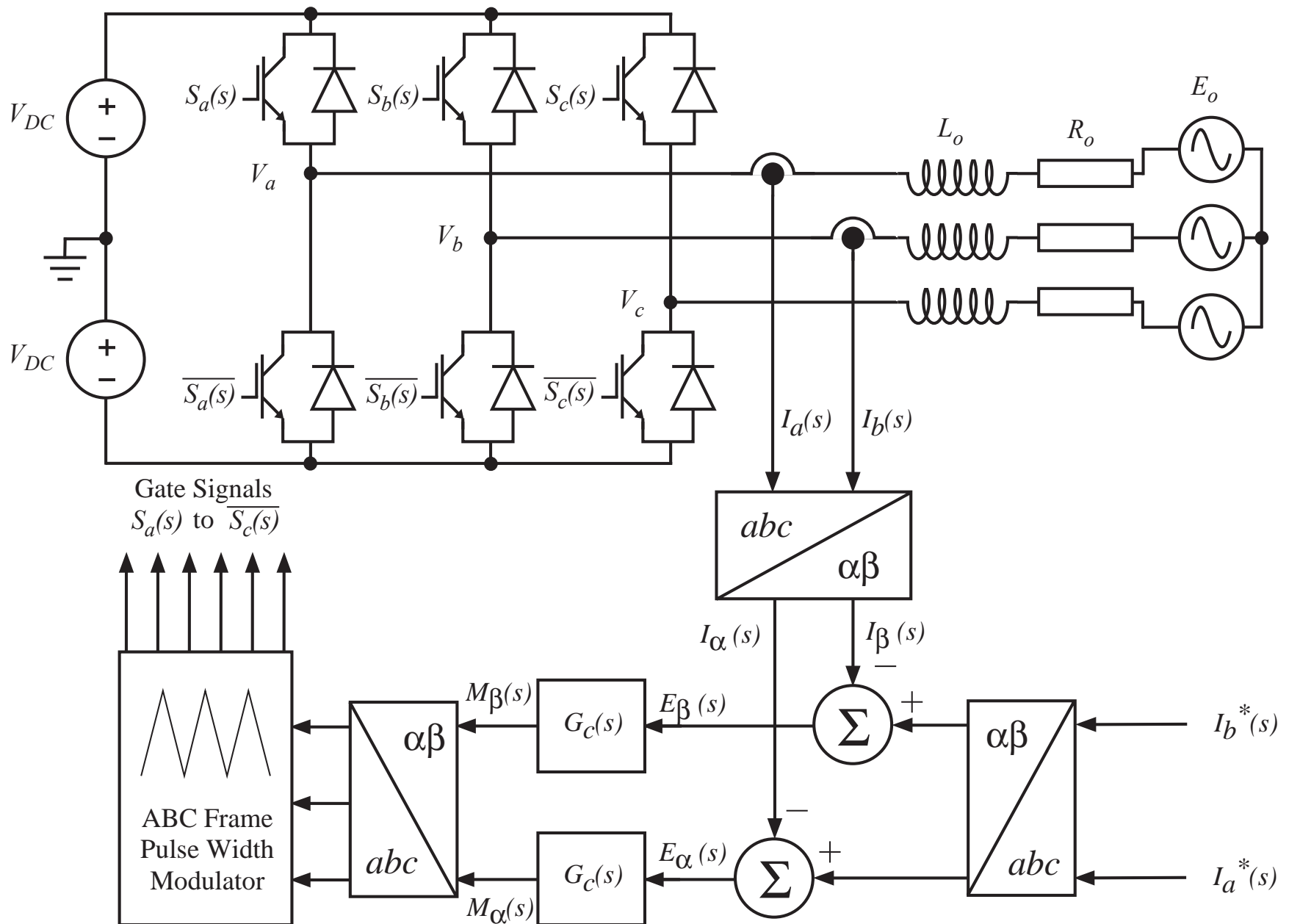
Orthogonal Reference Frames: $\alpha\beta$ stationary frame

- The $(\alpha\beta)$ quantities are sinusoidal
- Hence gain maximisation approach is identical to the (abc) frame current regulator
- The regulator output is compatible with a direct space vector modulator – no need to indirectly calculate the phase C PWM command for SV implementation (but still need to decode SV output to phase leg switching commands)
- References can be defined in either the (abc) or the $(\alpha\beta)$ frames as suits application

Orthogonal Reference Frames: $\alpha\beta$ stationary frame



Orthogonal Reference Frames: $\alpha\beta$ stationary frame



Orthogonal Reference Frames: dq rotating frame

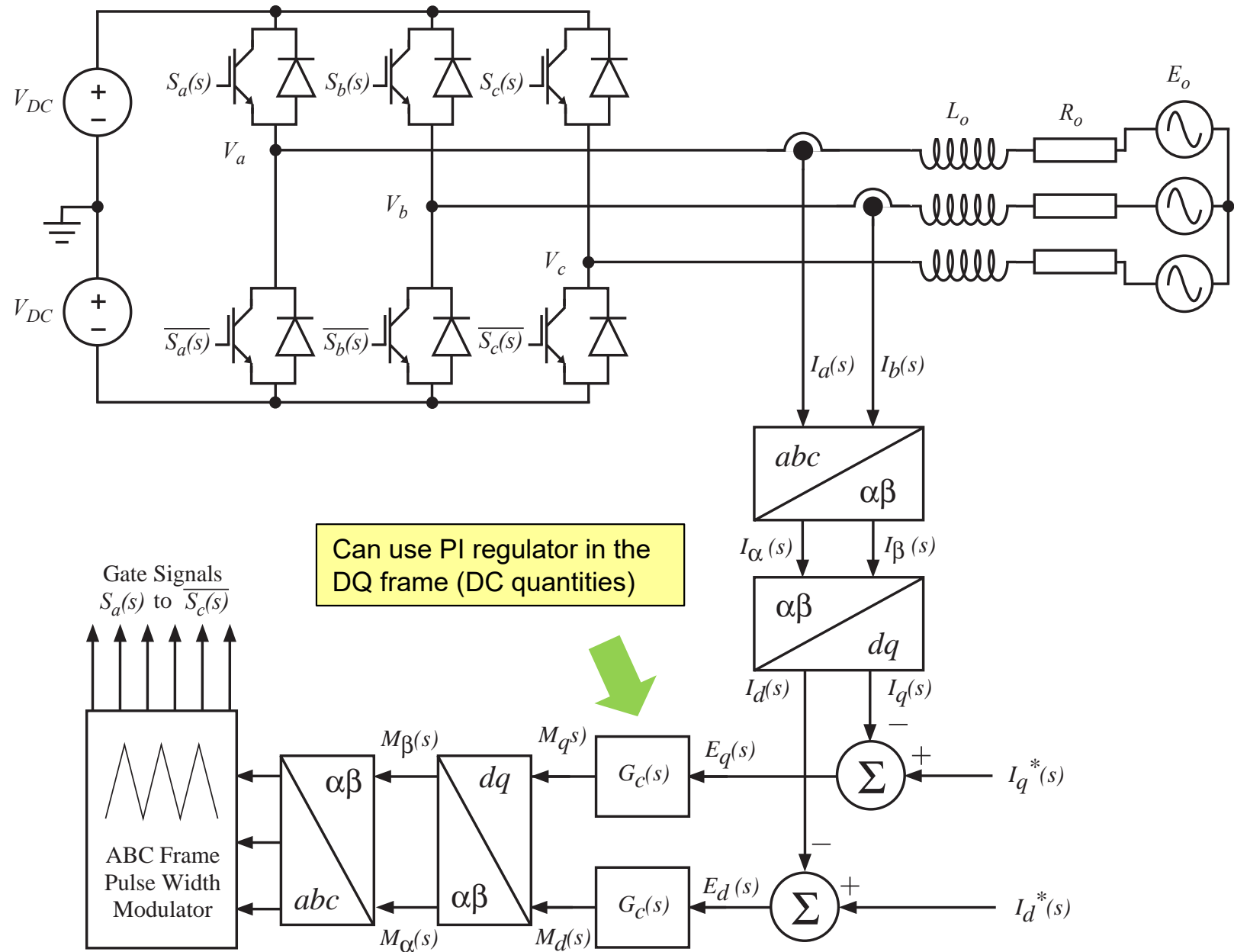
- Synchronous frame – AC quantities are transformed to equivalent DC quantities
- Park transform – $(\alpha\beta)$ to (dq)

$$\begin{bmatrix} i_d \\ i_q \end{bmatrix} = T_{dq} \begin{bmatrix} i_\alpha \\ i_\beta \end{bmatrix} = \begin{bmatrix} \cos \theta & \sin \theta \\ -\sin \theta & \cos \theta \end{bmatrix} \begin{bmatrix} i_\alpha \\ i_\beta \end{bmatrix} \quad \theta = \omega t$$

- Inverse Park transform:

$$\begin{bmatrix} i_\alpha \\ i_\beta \end{bmatrix} = T_{dq}^T \begin{bmatrix} i_d \\ i_q \end{bmatrix} = \begin{bmatrix} \cos \theta & -\sin \theta \\ \sin \theta & \cos \theta \end{bmatrix} \begin{bmatrix} i_d \\ i_q \end{bmatrix} \quad \theta = \omega t$$

Orthogonal Reference Frames: dq rotating frame



Reference Frames: regulator transformation [4]

Stationary frame $\alpha\beta$ controller

$$\begin{bmatrix} K_P \left(1 + \frac{1}{s\tau_i} \right) & 0 \\ 0 & K_P \left(1 + \frac{1}{s\tau_i} \right) \end{bmatrix}$$

Rotating frame DQ controller

$$\begin{bmatrix} K_P \left(1 + \frac{1}{\tau_i} \frac{s}{s^2 + \omega_o^2} \right) & \frac{1}{\tau_i} \frac{\omega_o}{s^2 + \omega_o^2} \\ -\frac{1}{\tau_i} \frac{\omega_o}{s^2 + \omega_o^2} & K_P \left(1 + \frac{1}{\tau_i} \frac{s}{s^2 + \omega_o^2} \right) \end{bmatrix}$$

Stationary Frame PI regulator transforms to Synchronous Frame Resonant [3]

$$\begin{bmatrix} K_P \left(1 + \frac{1}{\tau_i} \frac{s}{s^2 + \omega_o^2} \right) & \frac{1}{\tau_i} \frac{\omega_o}{s^2 + \omega_o^2} \\ -\frac{1}{\tau_i} \frac{\omega_o}{s^2 + \omega_o^2} & K_P \left(1 + \frac{1}{\tau_i} \frac{s}{s^2 + \omega_o^2} \right) \end{bmatrix}$$

$$\begin{bmatrix} K_P \left(1 + \frac{1}{s\tau_i} \right) & 0 \\ 0 & K_P \left(1 + \frac{1}{s\tau_i} \right) \end{bmatrix}$$

Synchronous Frame PI regulator transforms to Stationary Frame Resonant [3]

Gains are the same in both frames of reference and
hence can be calculated as before

SOGI Discrete Time State Space Realisations [5]

Resonant Controllers:

- Eliminate AC steady state error without requiring frame of reference transformation
- Provide equivalent dynamics to dq frame PI regulators
- Applicable to single phase systems (generate quadrature voltage set)
- Facilitate harmonic compensation for active filters, LCL filters, etc.

Often implemented using Second Order Generalised Integrator (SOGI)

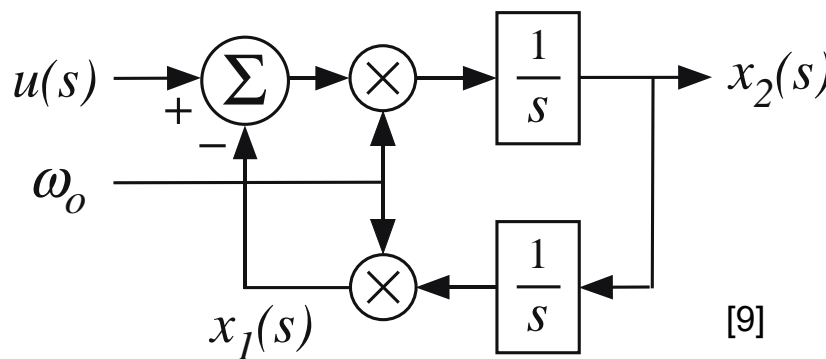
- Structure uses dual integrators with target frequency as an input
- Allows for online frequency adaptation (sine and cosine lookup tables)
- Facilitates frequency tracking for drive, wind turbine, grid applns.

SOGI must be discretized (s-domain to z-domain) to form difference equations for digital implementation in a microprocessor

- Of 8 possible z-domain transforms, only Tustin (pre-warp), pole-zero matched, impulse invariant, and first- and zero-order-hold avoid errors for resonators [6]
- SOGIs are typically implemented using integral approximations, which create errors compared to their s-domain counterpart [6]

SOGI Resonator Fundamentals

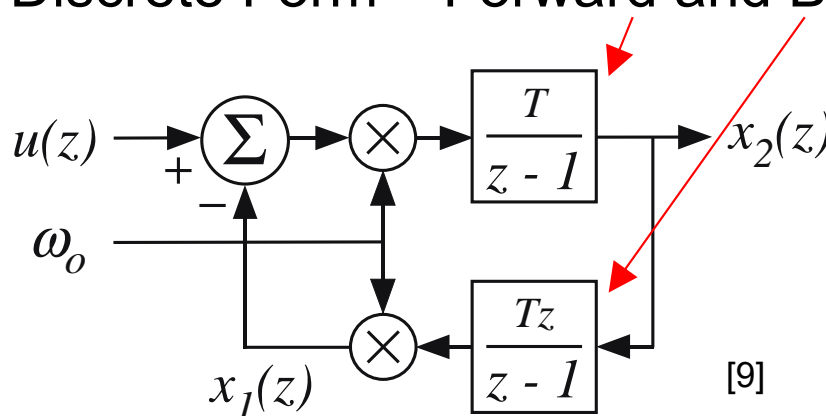
- Conventional SOGI architecture – $x_2(s)$ output used for current control:



$$\frac{x_1(s)}{u(s)} = D(s) = \frac{\omega_o^2}{s^2 + \omega_o^2}$$

$$\frac{x_2(s)}{u(s)} = Q(s) = \frac{\omega_o s}{s^2 + \omega_o^2}$$

- Discrete Form – Forward and Backward Euler integral approximations:



$$\frac{x_1(z)}{u(z)} = D(z) = \frac{\omega_o^2 T^2 z}{z^2 - 2z(1 - \omega_o^2 T^2 / 2) + 1}$$

$$\frac{x_2(z)}{u(z)} = Q(z) = \frac{\omega_o T (z-1)}{z^2 - 2z(1 - \omega_o^2 T^2 / 2)z + 1}$$

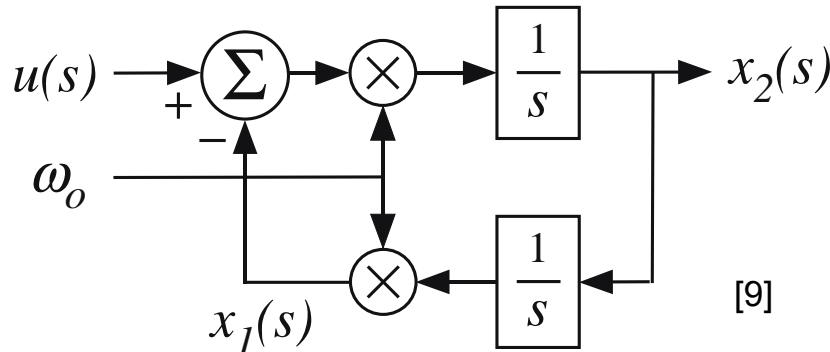
- For accuracy, the denominator should be [6]:

$$z^2 - 2 \cos(\omega_o T)z + 1$$

- Euler based SOGI's use a Taylor series approximation to this target polynomial which results in resonance errors.

State Space SOGI Formulation [6]

- Continuous time state space definition of the SOGI:



$$\begin{aligned}\dot{\mathbf{x}}(t) &= \mathbf{A}\mathbf{x}(t) + \mathbf{B}u(t) \\ y(t) &= \mathbf{C}\mathbf{x}(t) + \mathbf{D}u(t)\end{aligned}$$

[9]

where:

$$\mathbf{A} = \begin{bmatrix} 0 & \omega_o \\ -\omega_o & 0 \end{bmatrix}$$

$$\mathbf{B} = \begin{bmatrix} 0 \\ \omega_o \end{bmatrix}$$

$$\mathbf{C} = \begin{bmatrix} 1 & 0 \\ 0 & 1 \end{bmatrix}$$

$$\mathbf{D} = \begin{bmatrix} 0 \\ 0 \end{bmatrix}$$

- Equivalent discrete time formulation:

$$\begin{aligned}\mathbf{x}(k+1) &= \mathbf{A}_d \mathbf{x}(k) + \mathbf{B}_d u(k) \\ y(k) &= \mathbf{C}_d \mathbf{x}(k) + \mathbf{D}_d u(k)\end{aligned}$$

- The A_d , B_d , C_d and D_d matrices are set by the discretisation strategy
- The most viable error free discretization forms for state space are Zero order hold (ZOH), First order hold (FOH) and Tustin (prewarp),

Zero Order Hold (ZOH) Realisation

- State space equivalent ZOH transformation:

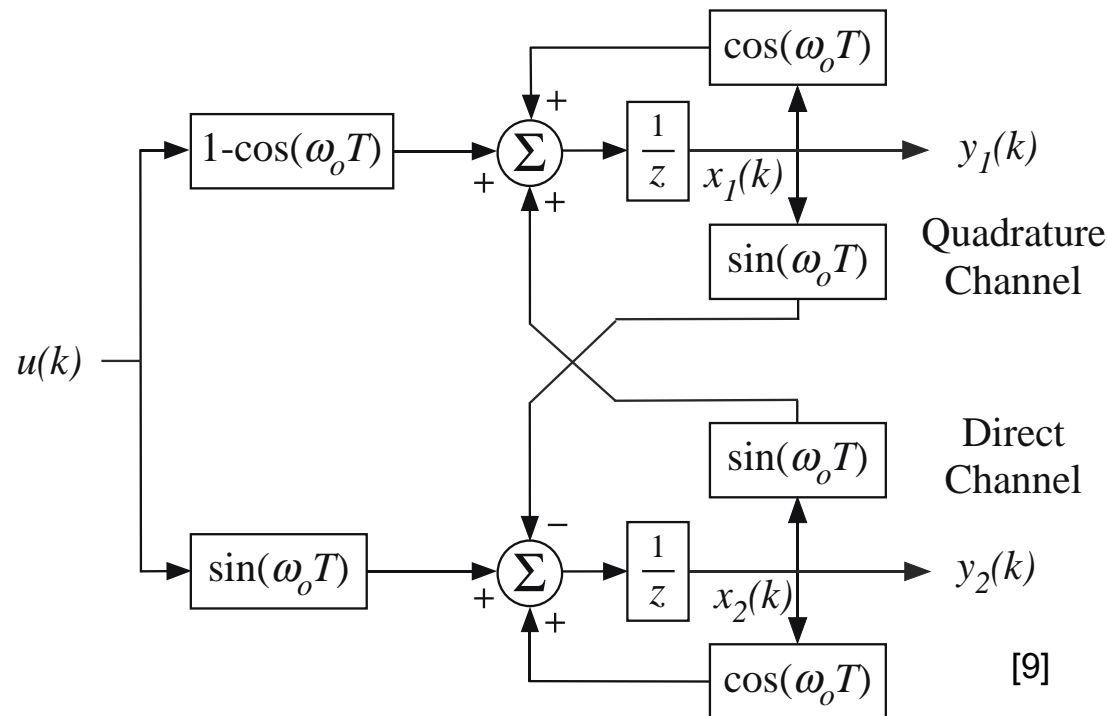
$$\mathbf{A}_d = e^{\mathbf{A}T} = \mathcal{L}^{-1}\left\{[s\mathbf{I} - \mathbf{A}]^{-1}\right\}_{t=T} = \begin{bmatrix} \cos(\omega_o T) & \sin(\omega_o T) \\ -\sin(\omega_o T) & \cos(\omega_o T) \end{bmatrix}$$

$$\mathbf{C}_d = \mathbf{C} = \begin{bmatrix} 1 & 0 \\ 0 & 1 \end{bmatrix}$$

$$\mathbf{B}_d = \left\{ \int_0^T e^{\mathbf{A}\tau} d\tau \right\} \mathbf{B} = \mathbf{A}^{-1} [\mathbf{A}_d - \mathbf{I}] \mathbf{B} = \begin{bmatrix} 1 - \cos(\omega_o T) \\ \sin(\omega_o T) \end{bmatrix}$$

$$\mathbf{D}_d = \mathbf{D} = \begin{bmatrix} 0 \\ 0 \end{bmatrix}$$

- Equivalent Block Diagram:



No resonance error since:

$$\det[z\mathbf{I} - \mathbf{A}_d] = z^2 - 2\cos(\omega_o T)z + 1$$

First Order Hold (FOH) Realisation

- FOH realisation first requires formation of :

$$\begin{bmatrix} \Phi & \Gamma_1 & \Gamma_2 \\ 0 & 1 & 0 \\ 0 & 0 & 1 \end{bmatrix} = e^{\mathbf{A}_c T} = \mathcal{L}^{-1} \left\{ s\mathbf{I} - \begin{bmatrix} \mathbf{A} & \mathbf{B} & 0 \\ 0 & 0 & 1/T \\ 0 & 0 & 0 \end{bmatrix} \right\}_{t=T}$$

- Then the Ad, Bd, Cd and Dd matrices are defined as :

$$\mathbf{A}_d = \Phi = \begin{bmatrix} \cos(\omega_o T) & \sin(\omega_o T) \\ -\sin(\omega_o T) & \cos(\omega_o T) \end{bmatrix}$$

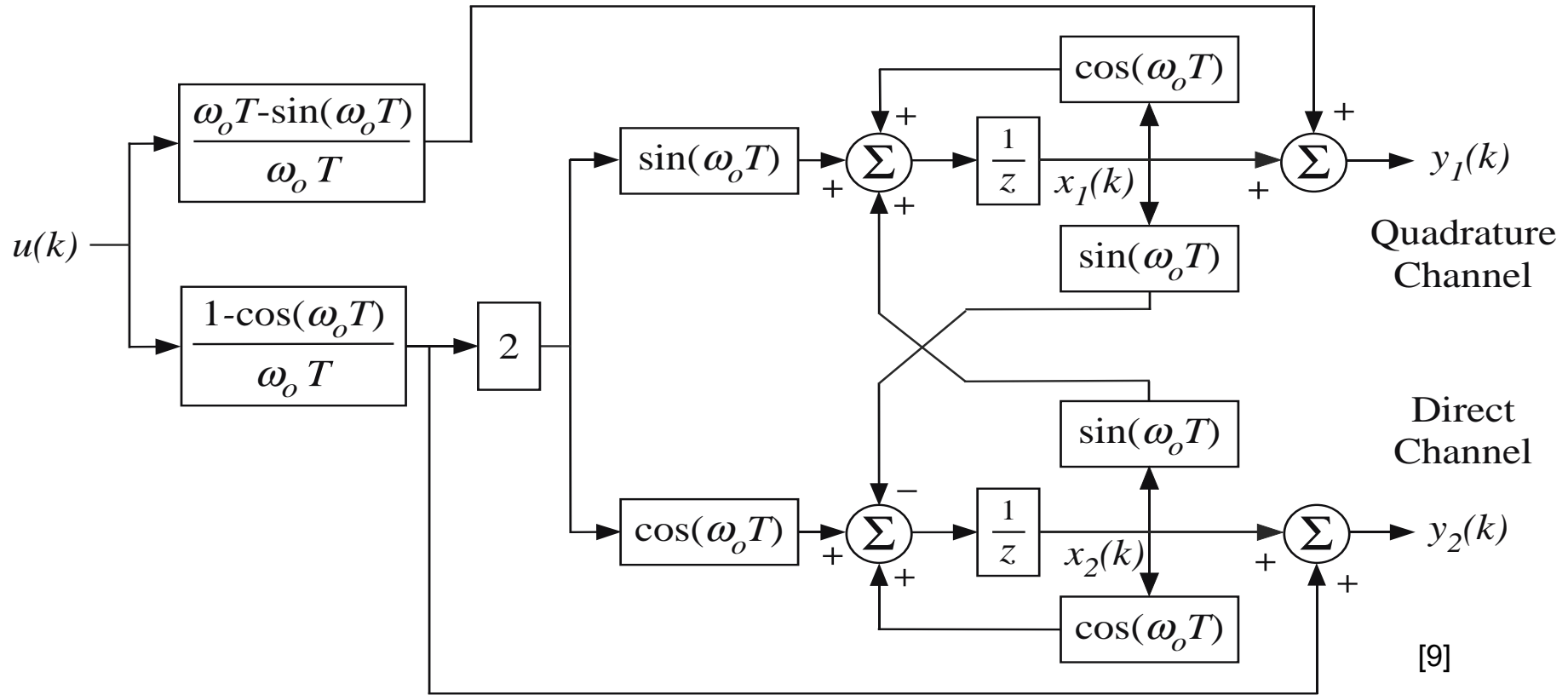
$$\mathbf{B}_d = \Gamma_1 + [\Phi - \mathbf{I}] \Gamma_2 = \frac{2(1 - \cos(\omega_o T))}{\omega_o T} \begin{bmatrix} \sin(\omega_o T) \\ \cos(\omega_o T) \end{bmatrix}$$

$$\mathbf{C}_d = \mathbf{C} = \begin{bmatrix} 1 & 0 \\ 0 & 1 \end{bmatrix}$$

$$\mathbf{D}_d = \mathbf{D} + \mathbf{C} \Gamma_2 = \frac{1}{\omega_o T} \begin{bmatrix} \omega_o T - \sin(\omega_o T) \\ 1 - \cos(\omega_o T) \end{bmatrix}$$

First Order Hold (FOH) Realisation

- Block Diagram Realisation:



- Similar to ZOH, but with direct feed-through action and pre-filtering
- Again no resonance error since:
$$\det[z\mathbf{I} - \mathbf{A}_d] = z^2 - 2\cos(\omega_o T)z + 1$$

Tustin with Pre-warping Realisation

- Take the Laplace Transform of the SOGI SSE:

$$\begin{aligned}s\mathbf{X}(s) &= \mathbf{AX}(s) + \mathbf{BU}(s) \\ \mathbf{Y}(s) &= \mathbf{CX}(s) + \mathbf{DU}(s)\end{aligned}$$

- Then recall the Tustin (pre-warp) transform:

$$s \rightarrow \left\{ \frac{\omega_o}{\tan(\omega_o T/2)} \frac{z-1}{z+1} \right\}$$

- Applying the transform yields the discrete SSE:

$$\begin{aligned}\left\{ \frac{\omega_o}{\tan(\omega_o T/2)} \frac{z-1}{z+1} \right\} \mathbf{X}(z) &= \mathbf{AX}(z) + \mathbf{BU}(z) \\ \mathbf{Y}(z) &= \mathbf{CX}(z) + \mathbf{DU}(z)\end{aligned}$$

- Converting back to time domain produces the difference eqn:

$$\begin{aligned}\left[\mathbf{I} - \frac{\tan(\omega_o T/2)}{\omega_o} \mathbf{A} \right] \mathbf{x}(k+1) - \left[\frac{\tan(\omega_o T/2)}{\omega_o} \mathbf{B} \right] u(k+1) \\ = \left[\mathbf{I} + \frac{\tan(\omega_o T/2)}{\omega_o} \mathbf{A} \right] \mathbf{x}(k) + \left[\frac{\tan(\omega_o T/2)}{\omega_o} \mathbf{B} \right] u(k)\end{aligned}$$

Tustin with Pre-warping Realisation

- Collecting terms generates the discrete SSE matrices:

$$\mathbf{A}_d = \left[\mathbf{I} + \frac{\tan(\omega_o T/2)}{\omega_o} \mathbf{A} \right] \left[\mathbf{I} - \frac{\tan(\omega_o T/2)}{\omega_o} \mathbf{A} \right]^{-1}$$

$$\mathbf{B}_d = 2 \left[\mathbf{I} - \frac{\tan(\omega_o T/2)}{\omega_o} \mathbf{A} \right]^{-1} \frac{\tan(\omega_o T/2)}{\omega_o} \mathbf{B}$$

$$\mathbf{C}_d = \mathbf{C} \left[\mathbf{I} - \frac{\tan(\omega_o T/2)}{\omega_o} \mathbf{A} \right]^{-1}$$

$$\mathbf{D}_d = \left\{ \mathbf{D} + \mathbf{C} \left[\mathbf{I} - \frac{\tan(\omega_o T/2)}{\omega_o} \mathbf{A} \right]^{-1} \frac{\tan(\omega_o T/2)}{\omega_o} \mathbf{B} \right\}$$

- Substituting the SOGI matrices gives:

$$\mathbf{A}_d = \begin{bmatrix} \cos(\omega_o T) & \sin(\omega_o T) \\ -\sin(\omega_o T) & \cos(\omega_o T) \end{bmatrix}$$

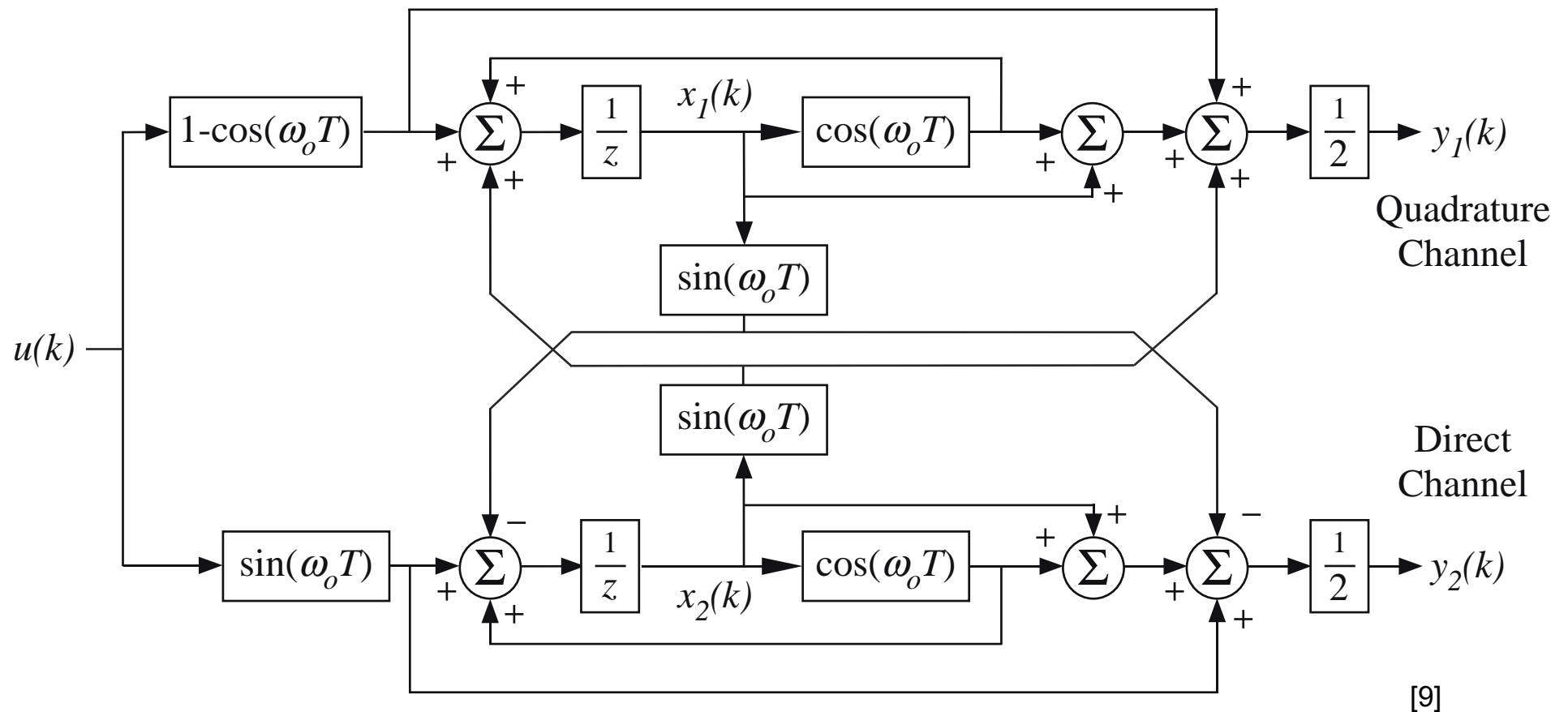
$$\mathbf{B}_d = \begin{bmatrix} 1 - \cos(\omega_o T) \\ \sin(\omega_o T) \end{bmatrix}$$

$$\mathbf{C}_d = \frac{1}{2} \begin{bmatrix} 1 + \cos(\omega_o T) & \sin(\omega_o T) \\ -\sin(\omega_o T) & 1 + \cos(\omega_o T) \end{bmatrix}$$

$$\mathbf{D}_d = \frac{1}{2} \begin{bmatrix} 1 - \cos(\omega_o T) \\ \sin(\omega_o T) \end{bmatrix}$$

Tustin with Pre-warping Realisation

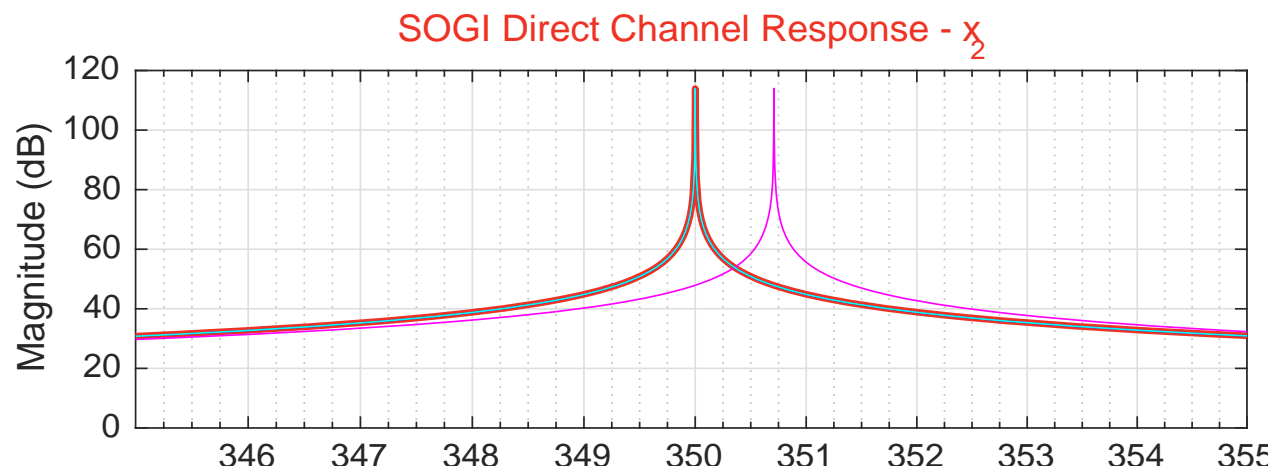
- Block Diagram realisation:



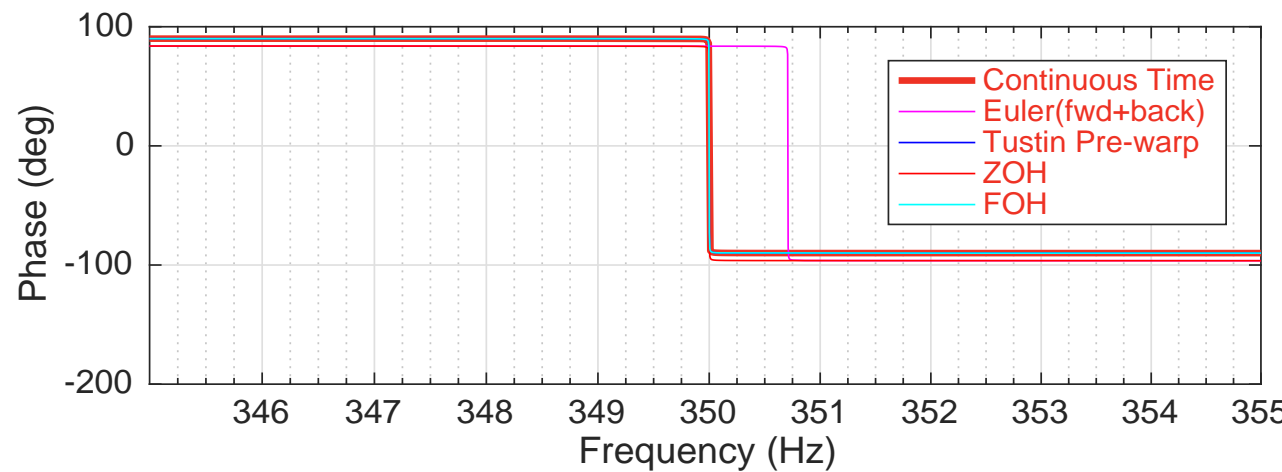
- As with FOH, there is direct feed-through of the input
- Again no resonance error since -
$$\det[z\mathbf{I} - \mathbf{A}_d] = z^2 - 2 \cos(\omega_o T)z + 1$$

Conventional vs. State Space SOGI

- Euler based SOGI has error that gets worse as resonance → Nyquist freq.
- In contrast – each State Space SOGI matches the continuous time SOGI response



[9]



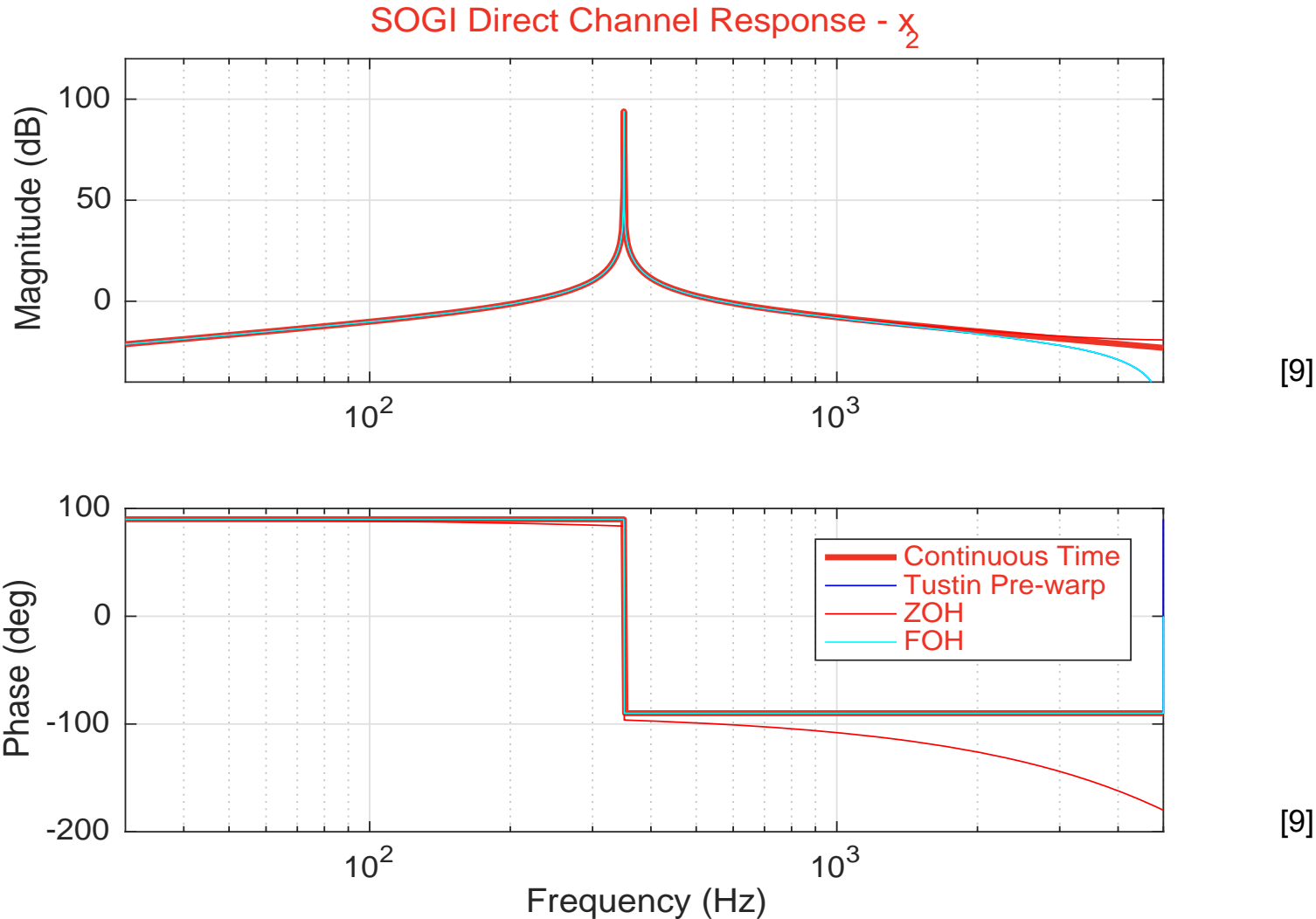
[9]

- Direct SOGI chan. - 7th harm. (i.e. a 350Hz) for a sample freq. 10kHz.

Conventional vs. State Space SOGI

Tustin (prewarp) and FOH also have different zeros to ZOH

- Leads to a better phase roll-off characteristic:



- This effect can improve the stability margin of a current controller

Overmodulation and Controller Windup [7]

AC current regulators are susceptible to controller wind-up

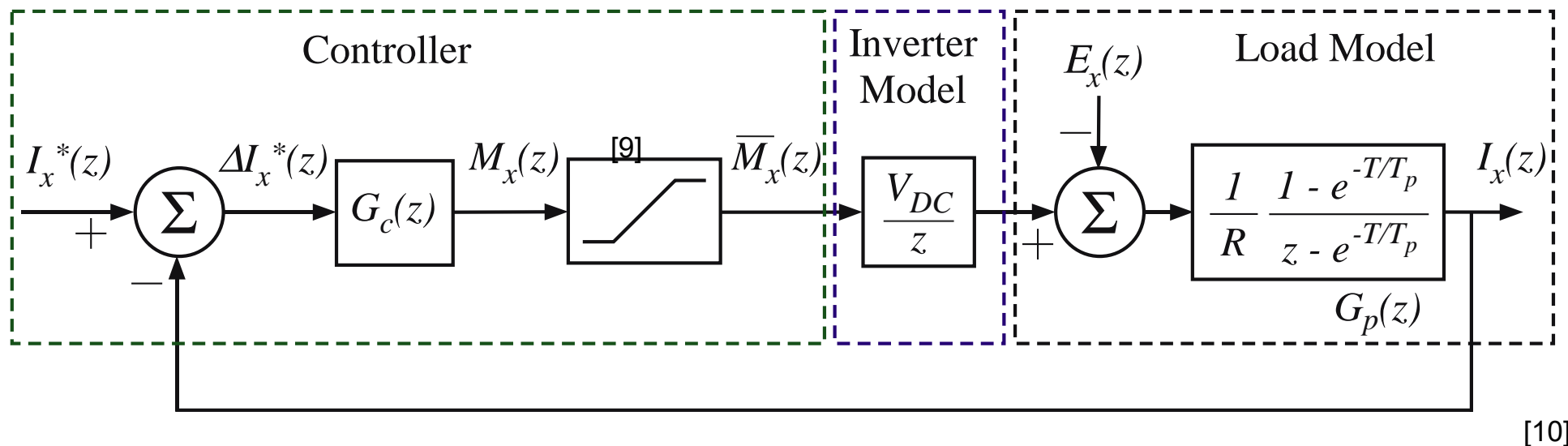
- Occurs when the regulator commands max. Volts with non-zero error
- Marginally stable Integrators/Resonators wind-up to large values
- Leads to long recovery times and can de-stabilize the regulator

Strategies include

- Integrator freeze – Not suitable for PR controllers (no integrator)
- Back-calculation – Takes effect when saturation occurs. Includes
 - Damping modes in the saturated state
 - Phase matching of compensation signal
- Feedback restructure where controller dynamics feed from output
 - Simple concept – has been shown to fix wind-up induced instability
 - BUT – Requires algebraic re-formulation of controller transfer function
- Signal Conditioning Concepts (recommended here)
 - Controller dynamics are still fed by the saturated controller output
 - Advantage – No re-formulation of the controller transfer function

Discrete Time Model of the Regulation System

- VSI modeled in z-domain as a single phase equivalent feedback loop:



- Load model : The LR filter between the VSI and back-emf
- Inverter model : The DC bus gain and PWM transport delay
- Controller : PR type regulator which generates the modulation command, and includes a saturation non-linearity
- PWM Limits set to: $\pm 2/\sqrt{3} = \pm 1.15$

Conditioning the Current Error Signal

- Define the physically realizable current error as : $\overline{\Delta I}_x(z)$
- This produces the constrained PWM command $\overline{M}_x(z)$ without saturating:

$$\overline{M}_x(z) = \text{sat}\left\langle G_c(z)\overline{\Delta I}_x(z) \right\rangle = \text{sat}\left\langle g_\infty \overline{\Delta I}_x(z) + \overline{G}_c(z)\overline{\Delta I}_x(z) \right\rangle = g_\infty \overline{\Delta I}_x(z) + \overline{G}_c(z)\overline{\Delta I}_x(z)$$

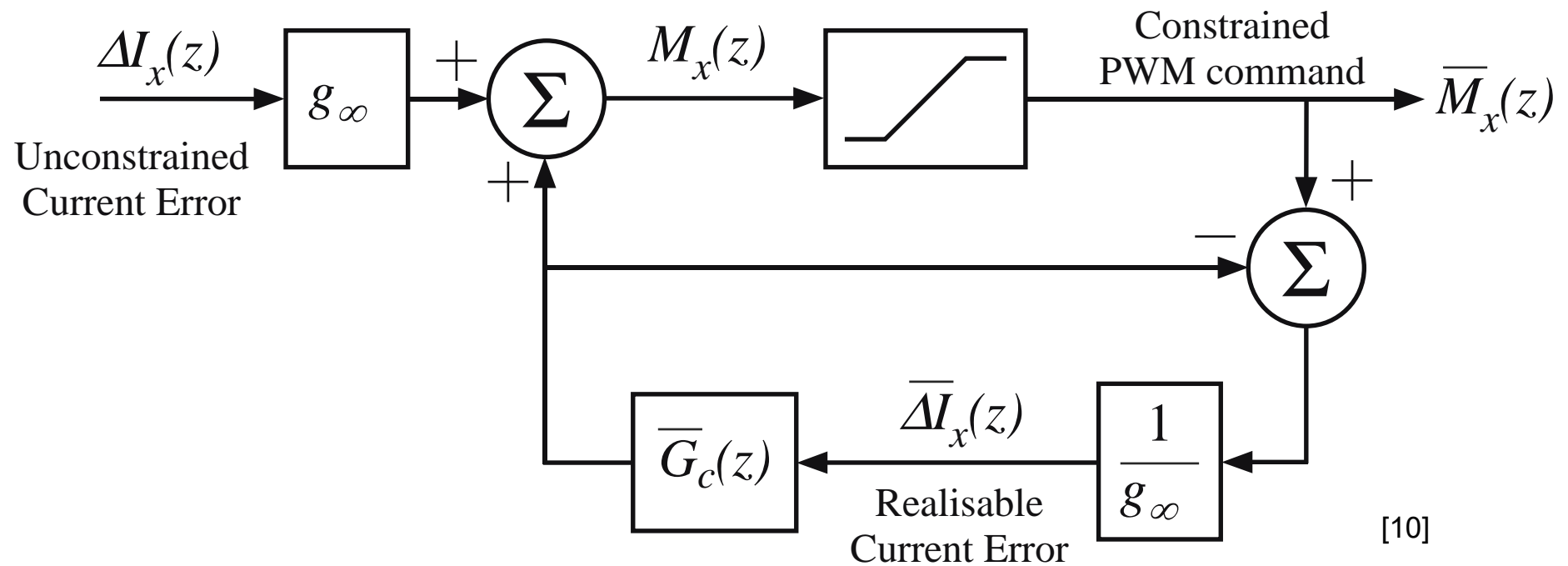
- Recognize the following equivalence due to the saturation function:
- Hence solving for the physically realizable current error gives:

$$\overline{\Delta I}_x(z) = \frac{\overline{M}_x(z) - \overline{G}_c(z)\overline{\Delta I}_x(z)}{g_\infty}$$

where: $\overline{M}_x(z) = \text{sat}\left\langle g_\infty \Delta I_x(z) + \overline{G}_c(z)\overline{\Delta I}_x(z) \right\rangle$

Conditioned Anti-Windup Controller Architecture

- This defines a conditioned (i.e. anti-windup) controller architecture of:



- Important Features:
 - The controller dynamics are fed from the constrained PWM signal
 - The controller dynamic transfer function is the same as the strictly proper formulation – no additional algebraic manipulation required

Discrete Time Controller Prototypes

- PR controller transfer function:

$$G_c(z) = K_p \left(1 + \sum_{h=1}^N \frac{1}{T_{r,h}} R_h(z) \right)$$

- Five type of discrete $R(z)$:

- Impulse Invariant
- Pole-Zero Matched
- Tustin with Pre-warping
- Zero Order Hold (ZOH)
- First Order Hold (FOH)

Form	$R_h(z)$
Impulse Invariant	$T \frac{z^2 - \cos(h\omega_o T)z}{z^2 - 2\cos(h\omega_o T)z + 1}$
P.Z. Matched	$\frac{2(1+T)[1-\cos(h\omega_o T)]}{(h\omega_o)^2 T} \frac{z-1}{z^2 - 2\cos(h\omega_o T)z + 1}$
Tustin (pre)	$\frac{\sin(h\omega_o T)}{2h\omega_o} \frac{z^2 - 1}{z^2 - 2\cos(h\omega_o T)z + 1}$
ZOH	$\frac{\sin(h\omega_o T)}{h\omega_o} \frac{z-1}{z^2 - 2\cos(h\omega_o T)z + 1}$
FOH	$\frac{[1-\cos(h\omega_o T)]}{(h\omega_o)^2 T} \frac{z^2 - 1}{z^2 - 2\cos(h\omega_o T)z + 1}$

- Controller Gains set to achieve Target phase margin ϕ_m :

h = harmonic order (1 for now)

$$\omega_{c(\max)} = \frac{\pi/2 - \phi_m}{1.5T}$$

$$K_p = \frac{\omega_{c(\max)} L}{V_{DC}}$$

$$T_{r,1} = \frac{10}{\omega_{c(\max)}}$$

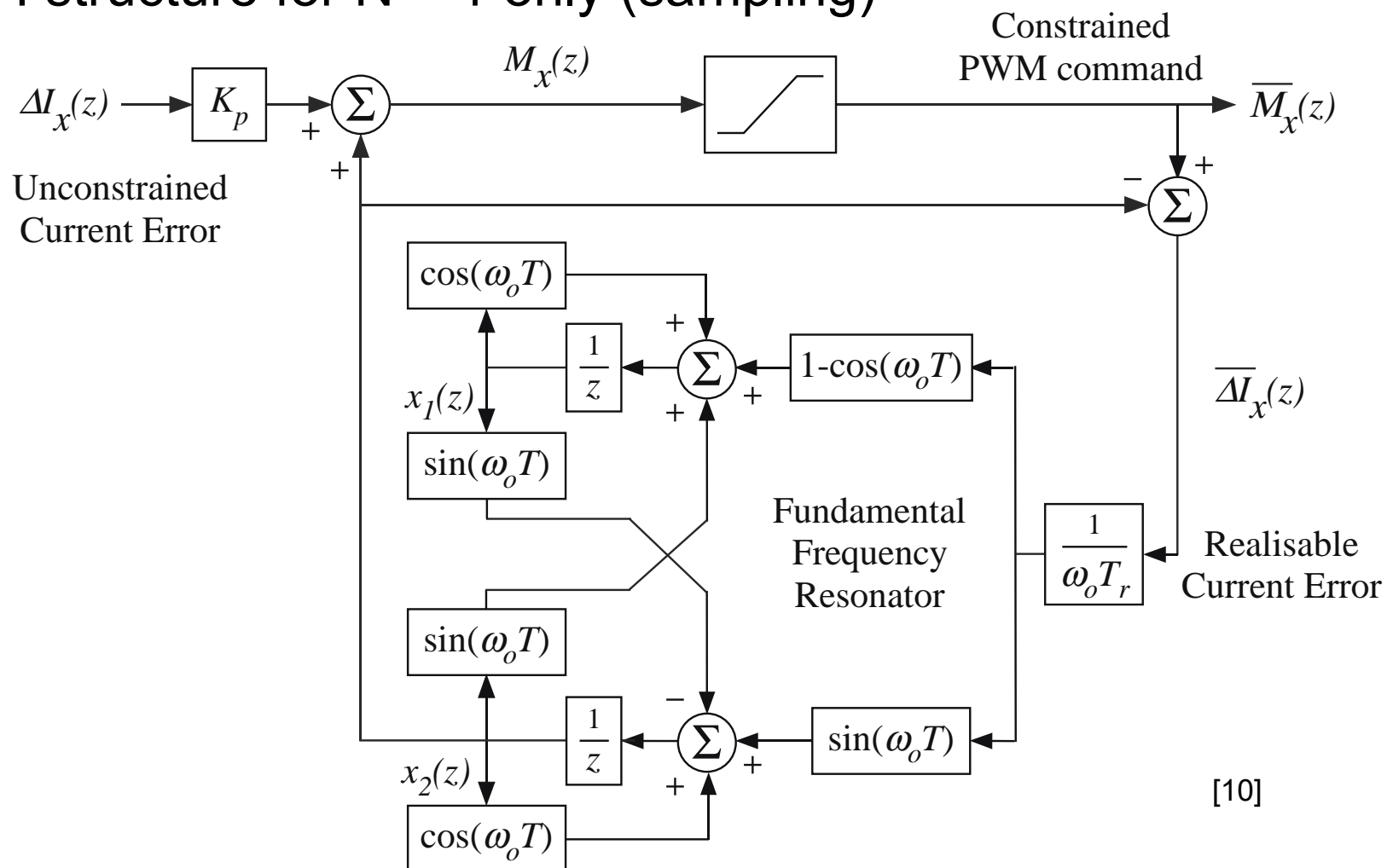
Strictly Proper Controller Prototype Definitions

- Signal conditioning requires that the controller be expressed in a strictly proper formulation (to avoid algebraic loops), viz: $G_c(z) = g_\infty + \bar{G}_c(z)$

Form	g_∞	$\bar{G}_c(z)$
Impulse Invariant	$K_p \left(1 + \sum_{h=1}^N \frac{T}{T_{r,h}} \right)$	$K_p \sum_{h=1}^N \left[\frac{T}{T_{r,h}} \frac{\cos(h\omega_o T)z - 1}{z^2 - 2\cos(h\omega_o T)z + 1} \right]$
P.Z. Matched	K_p	$K_p \sum_{h=1}^N \left[\frac{1}{T_{r,h}} \frac{2(1+T)[1-\cos(h\omega_o T)]}{(h\omega_o)^2 T} \frac{z-1}{z^2 - 2\cos(h\omega_o T)z + 1} \right]$
Tustin (pre)	$K_p \left(1 + \sum_{h=1}^N \frac{1}{T_{r,h}} \frac{\sin(h\omega_o T)}{2h\omega_o} \right)$	$K_p \sum_{h=1}^N \left[\frac{1}{T_{r,h}} \frac{\sin(h\omega_o T)}{2h\omega_o} \frac{2(\cos(h\omega_o T)z - 1)}{z^2 - 2\cos(h\omega_o T)z + 1} \right]$
ZOH	K_p	$K_p \sum_{h=1}^N \left[\frac{1}{T_{r,h}} \frac{\sin(h\omega_o T)}{h\omega_o} \frac{z-1}{z^2 - 2\cos(h\omega_o T)z + 1} \right]$
FOH	$K_p \left(1 + \sum_{h=1}^N \frac{1}{T_{r,h}} \frac{[1-\cos(h\omega_o T)]}{(h\omega_o)^2 T} \right)$	$K_p \sum_{h=1}^N \left[\frac{1}{T_{r,h}} \frac{[1-\cos(h\omega_o T)]}{(h\omega_o)^2 T} \frac{2(\cos(h\omega_o T)z - 1)}{z^2 - 2\cos(h\omega_o T)z + 1} \right]$

SS Discrete Time Regulator with Antiwindup

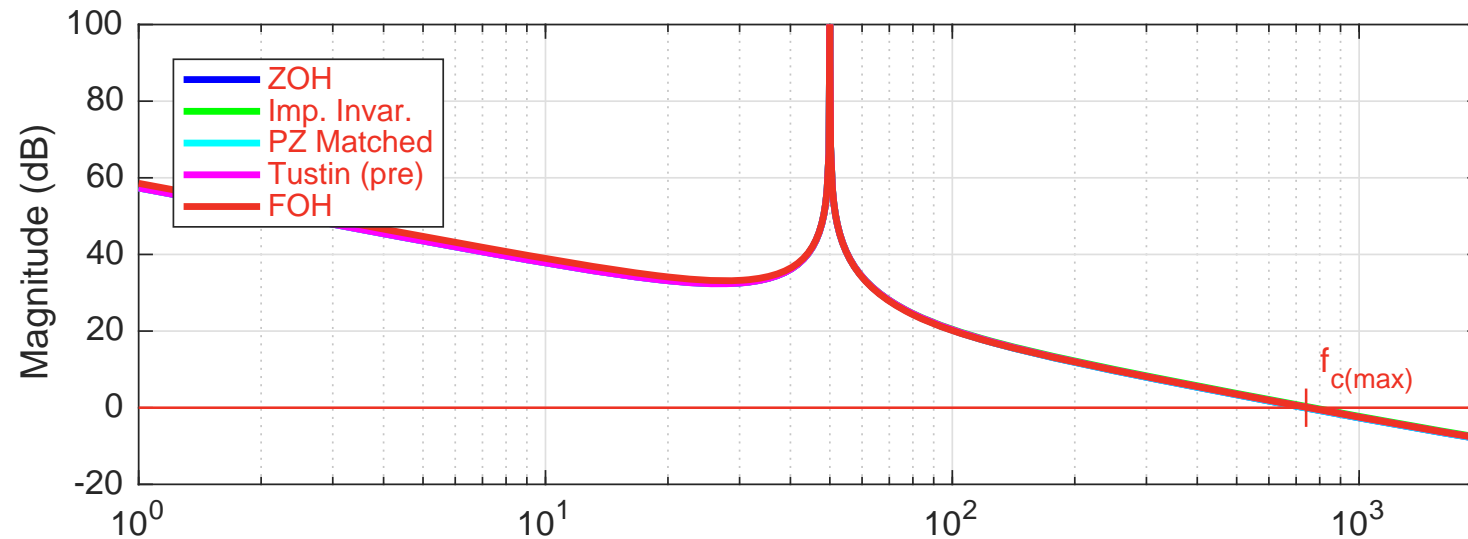
- Current regulator implemented using state space form
- Minimal realization requiring only 2 shift operations per resonator
- ZOH structure for N = 1 only (sampling)



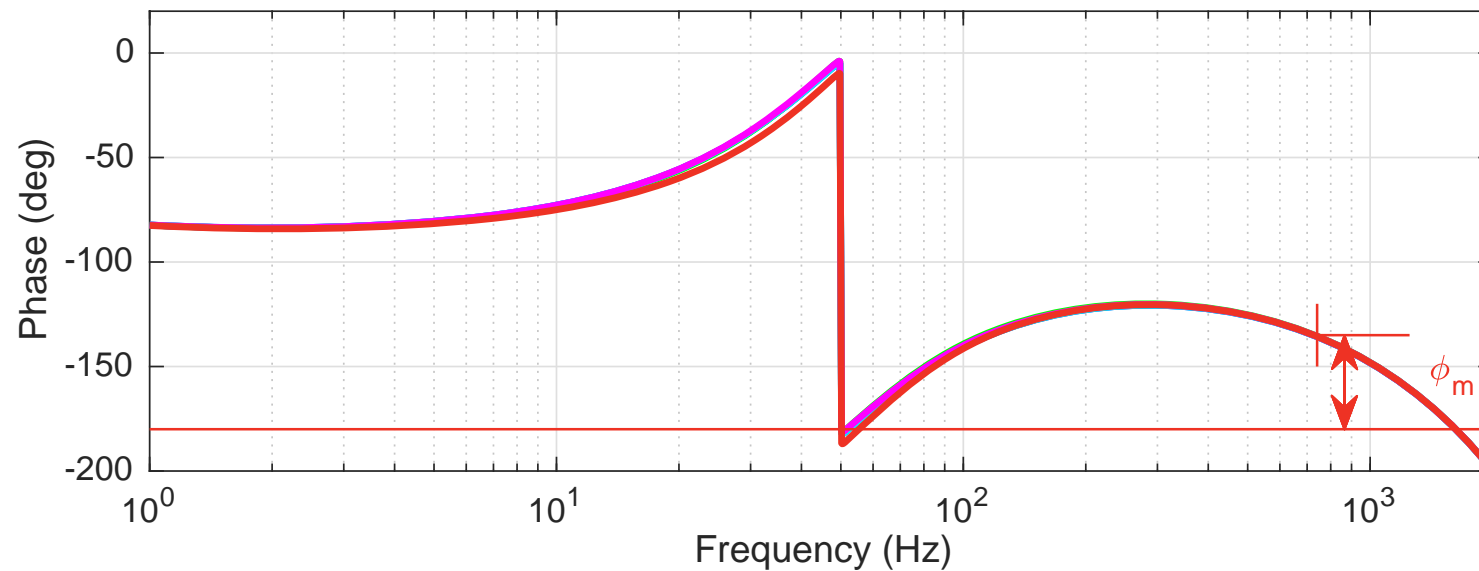
Current Regulator Frequency Response

- F_C

or



[10]

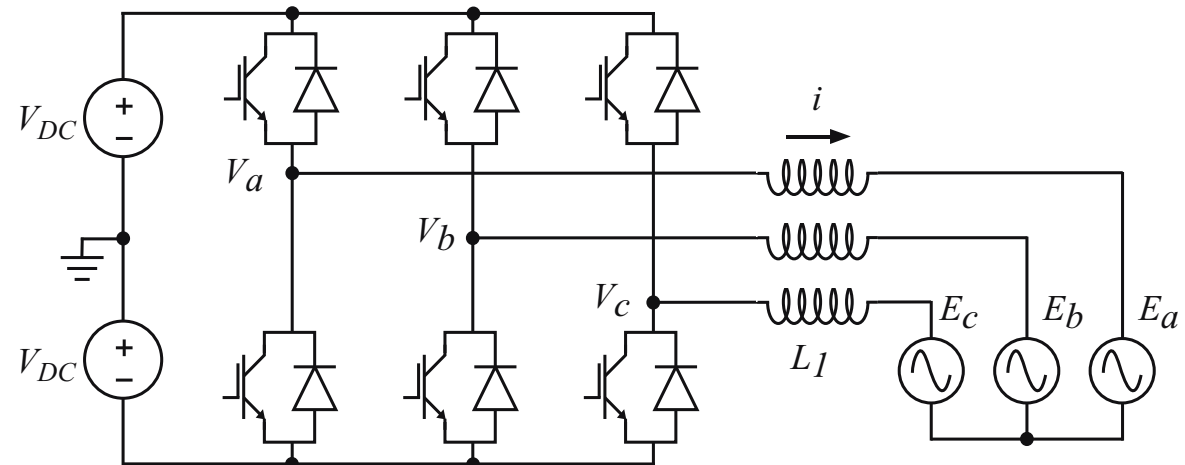


[10]

Simulation and Experimental Scenario

- SS SOGI and conditioning antiwindup architecture tested using PSIM / MATLAB simulations, and matching experiment, for a three-phase, current regulated, grid-connected inverter (TMS320F2812)

- Grid emulated using MX30 programmable AC source:
 - Clean 50 Hz Grid voltage
 - 160V(pk) output magnitude requires 92% mod depth



[9]

Inverter Parameters

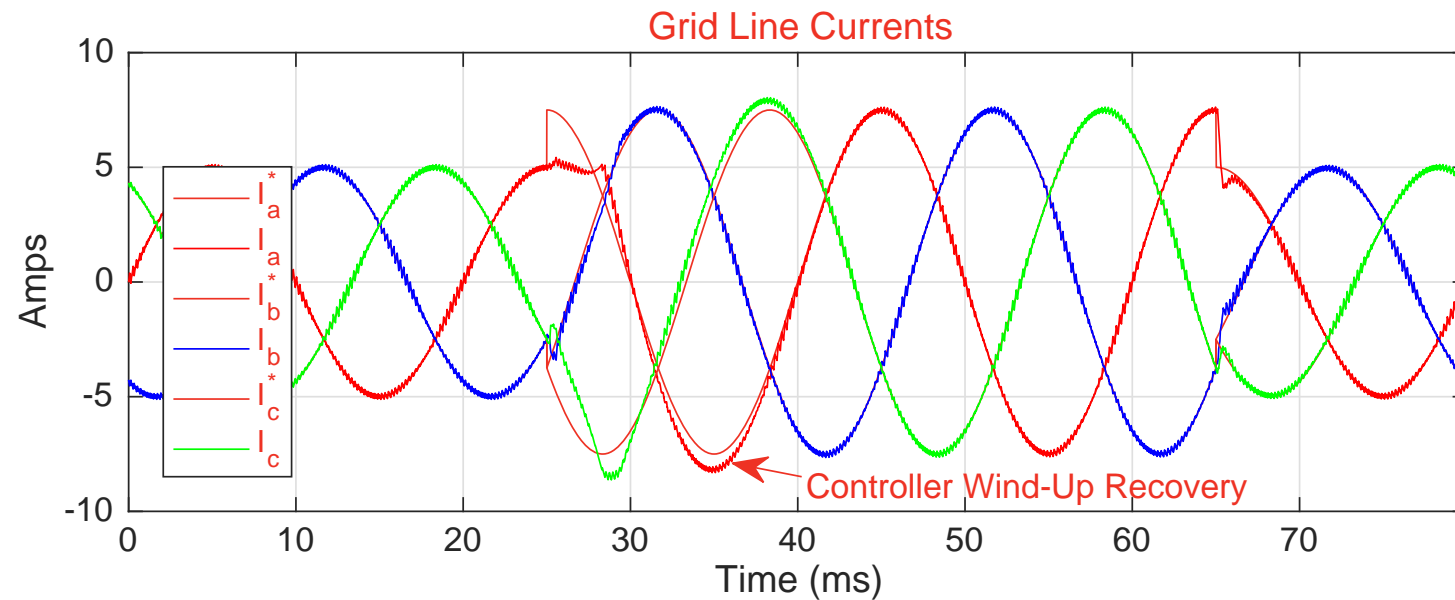
$2V_{DC} = 300V$	$L = 15mH$	$R = 0.1\Omega$
$f_o = 50Hz$	$f_c = 5kHz$	$T = 100\mu s$

Controller Gains

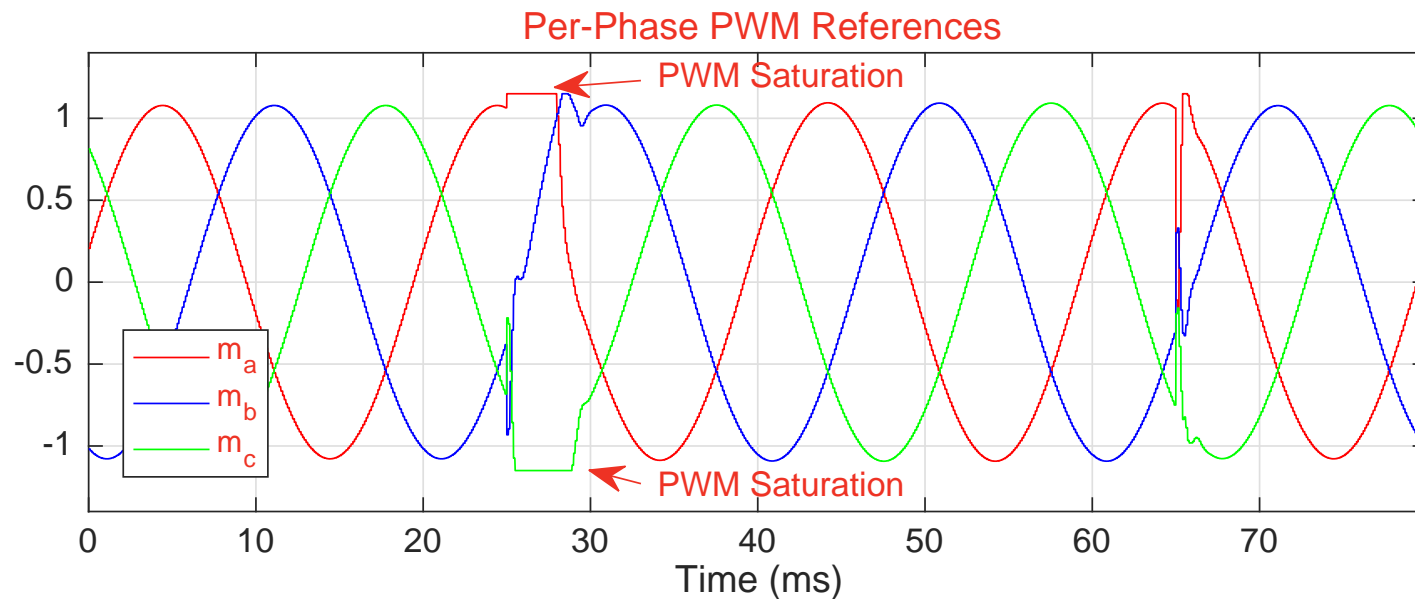
$\phi_m = 50^\circ$	$\omega_{c(\max)} = 4,655\text{rad/s}$	
$K_p = 0.466A^{-1}$	$T_{r1} = 2.1ms$	
$T_{r5} = 11ms$	$T_{r7} = 21ms$	$T_{r11} = 43ms$

Simulated Performance – Undistorted 50 Hz Grid

- ZOH PR current regulator (without anti-wind-up)



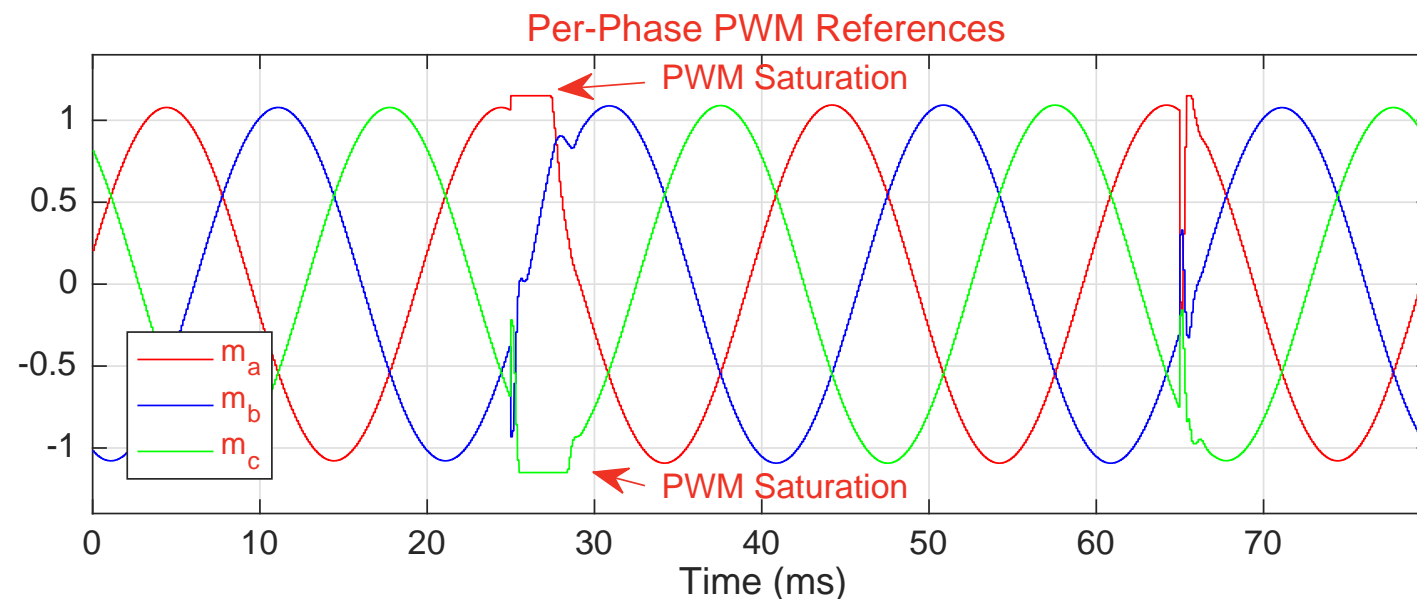
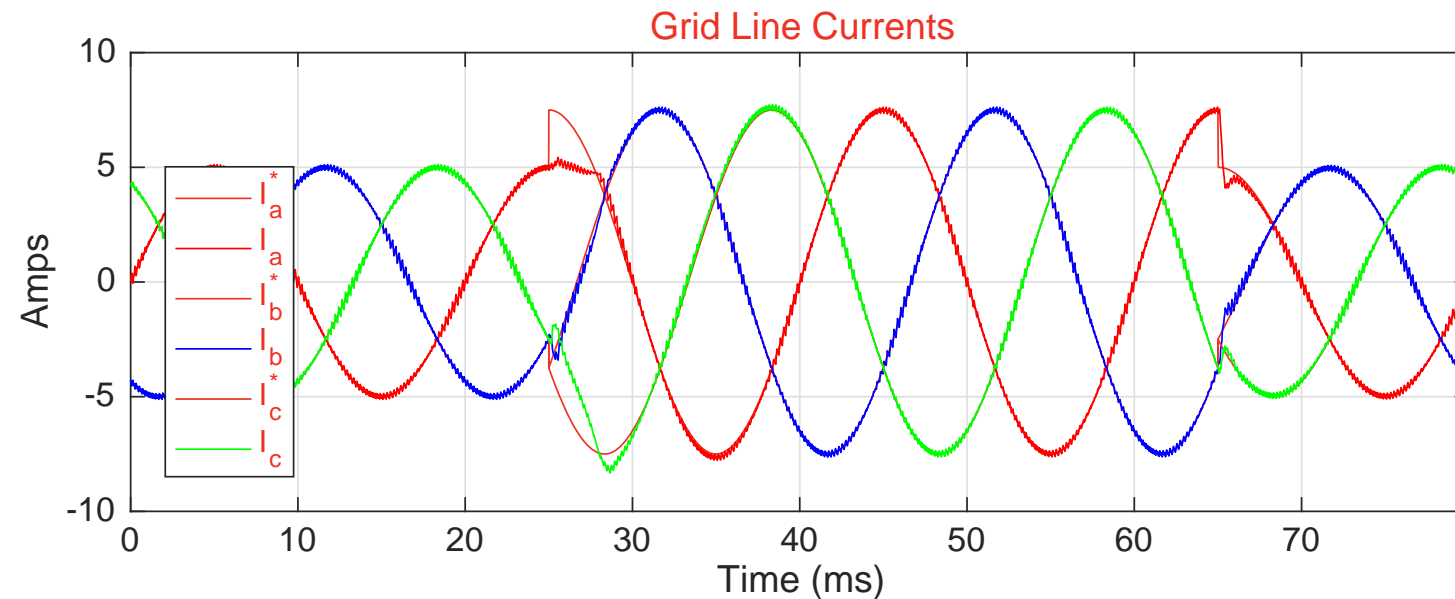
[10]



[10]

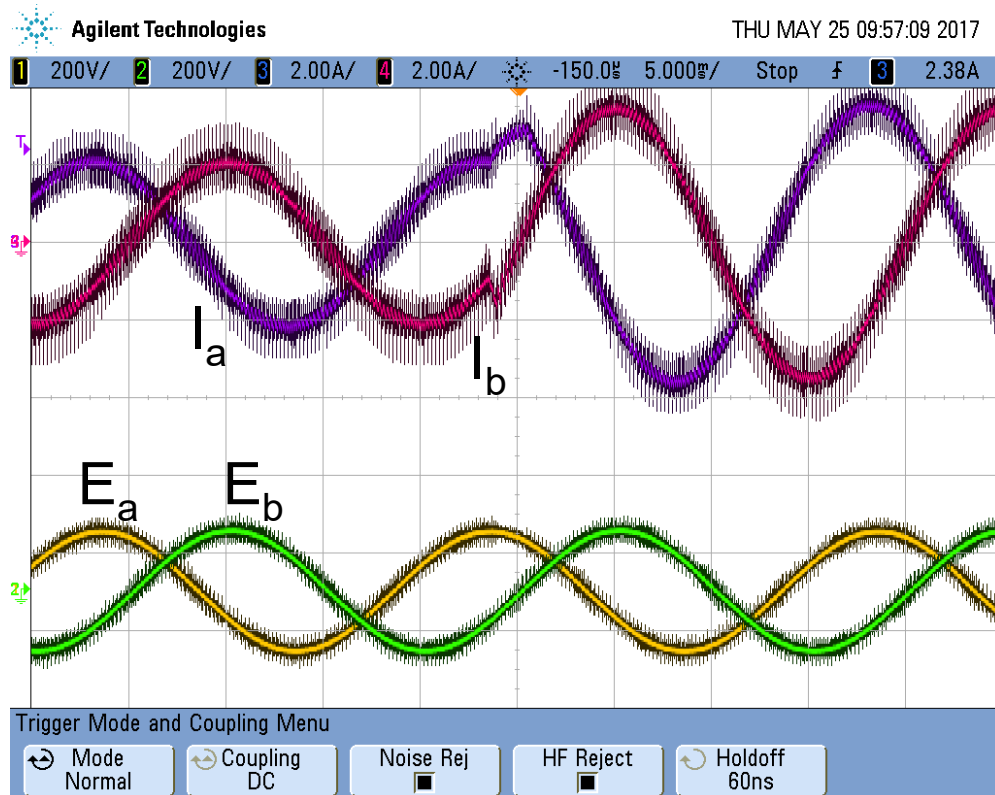
Simulated Performance – Undistorted 50 Hz Grid

ZOH PR current regulator (with anti-wind-up)



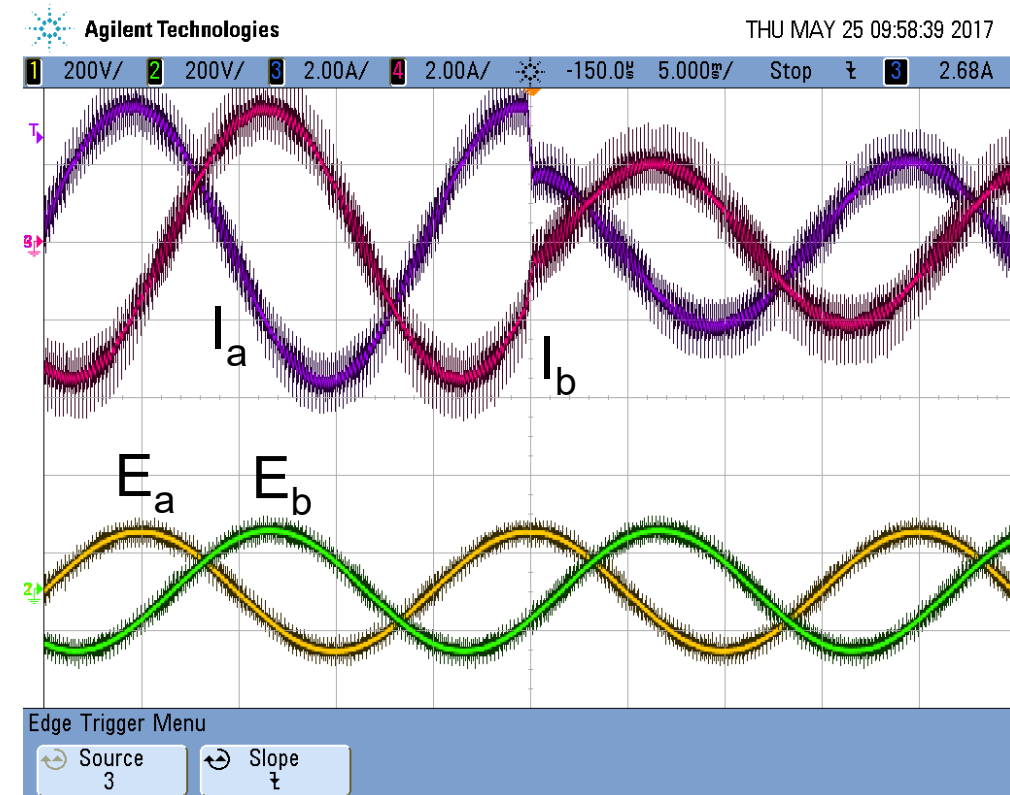
Experimental Performance – Undistorted 50 Hz Grid

ZOH PR current regulator (with anti-wind-up)



[10]

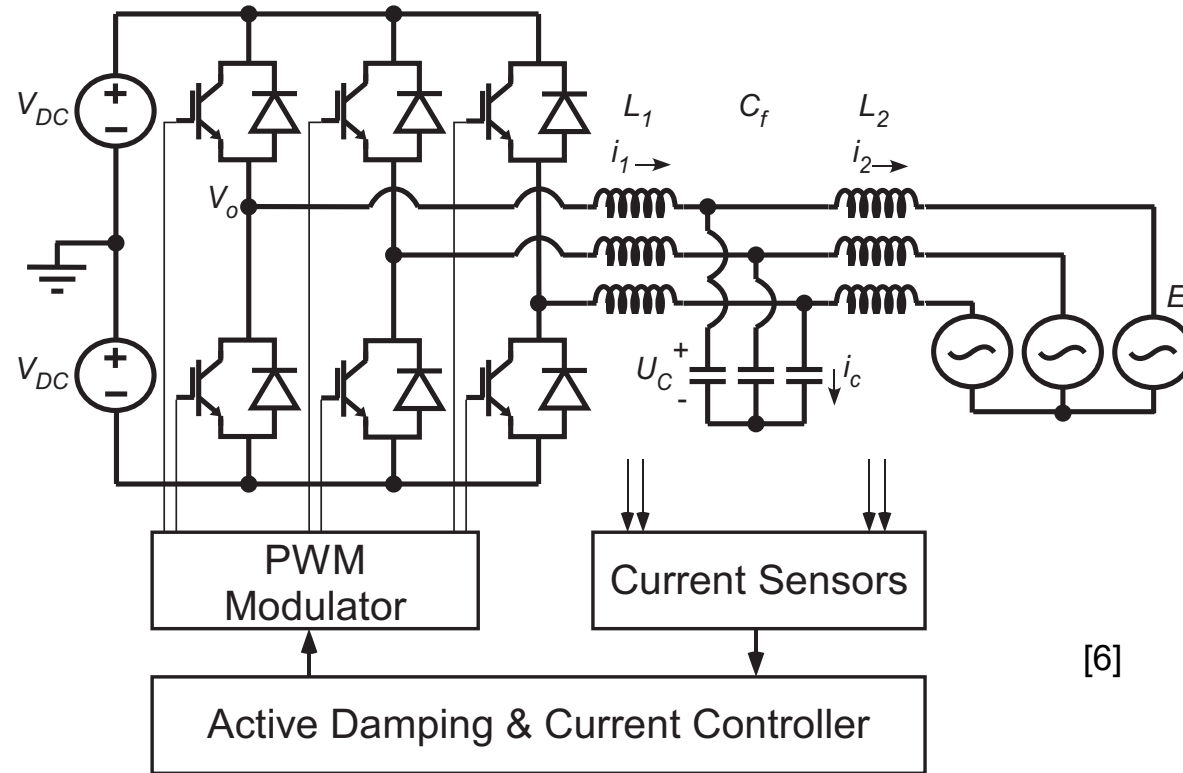
Step-up transient



[10]

Step-down transient

Part 2: Current Regulation for Grid Inverters



- LCL filter → Third order line filter for grid connected inverters
- Benefits of LCL filters (over L filters)
 - Greater attenuation, less size, less cost
- Major design challenges
 - LC network resonance, low harmonic impedance

Comparable L and LCL Filters [9]

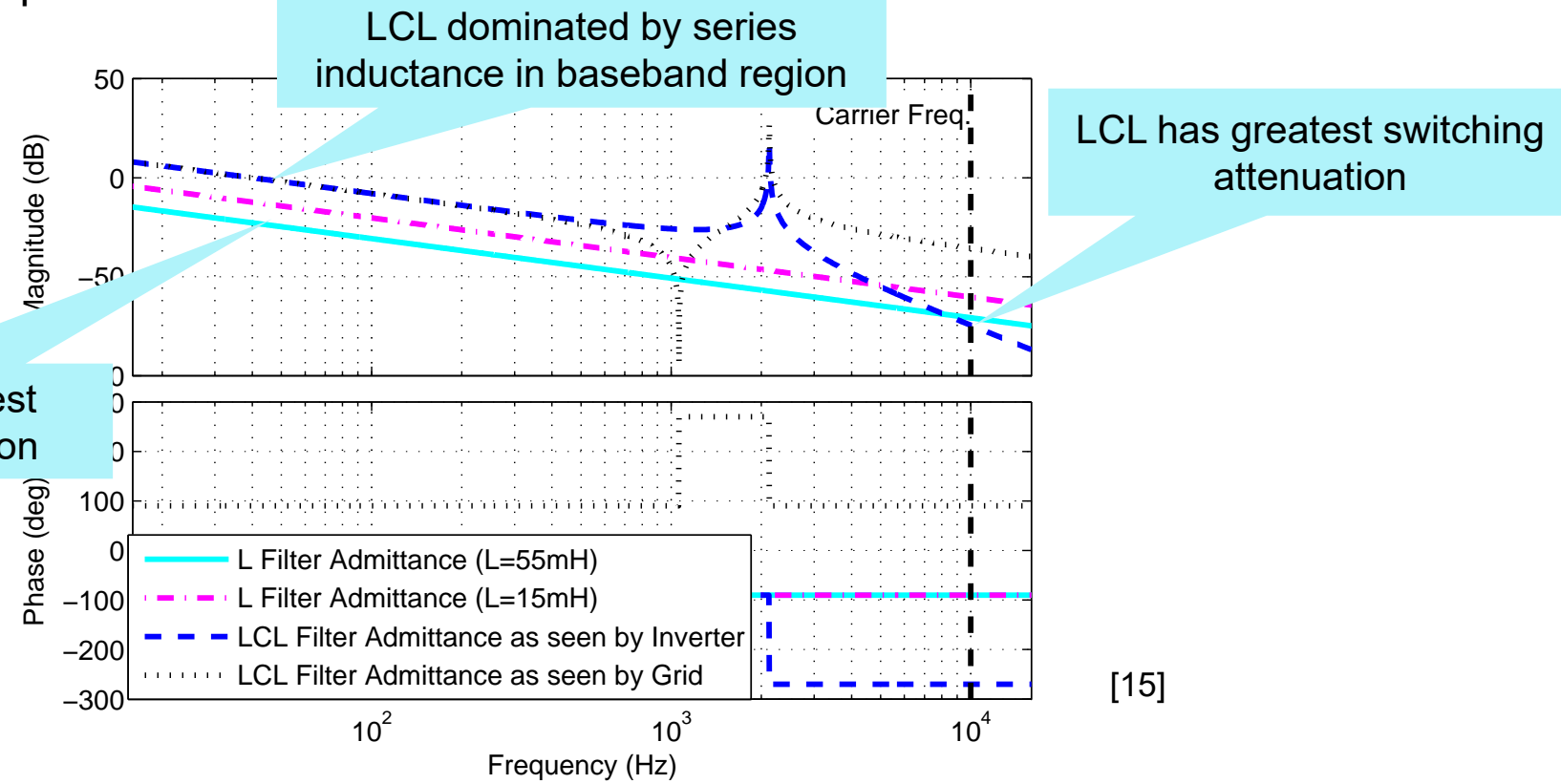
To meet IEEE519 requires impedance >100pu @ 10kHz

	@ 50Hz	@ 10kHz
$L = 55\text{mH}$	0.5pu	100pu
$L = 16.5\text{mH}$	0.15pu	30pu

$L_1 = 3\text{mH}$	@ 50Hz	@ 10kHz
$C_f = 7.5\mu\text{F}$	0.036pu	154pu
$L_2 = 1\text{mH}$		

L filter impedance

LCL filter impedance



LCL filter cannot achieve the same baseband filtering as L filter, with matching switching frequency

Control Loop Synthesis and Analysis

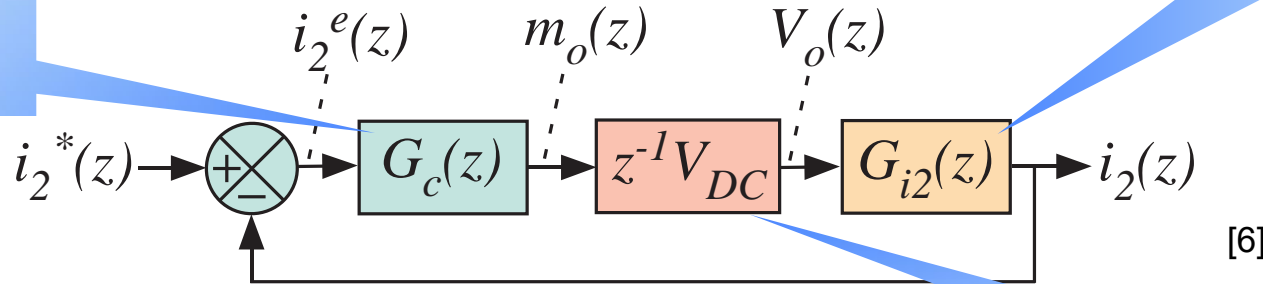
- LCL resonance damping:
 - Passively using series or shunt resistances
 - Actively using an additional state variable in the control law
- How to synthesise the current controller?
 - Analyse using discrete time models (i.e. state space or z -domain)
 - Sampling delay accounted for using a ZOH transformation of the LCL filter s -domain transfer function(s)
 - Transport delay accounted for using a z^{-1} shift operator
- Active damping is proposed in multiple forms:
 - Capacitor current feedback is the most commonly accepted
- Damping may not be required under some circumstances

LCL Filter Controller Options [10]

- **Single loop**

- Difficult to manage LCL resonance

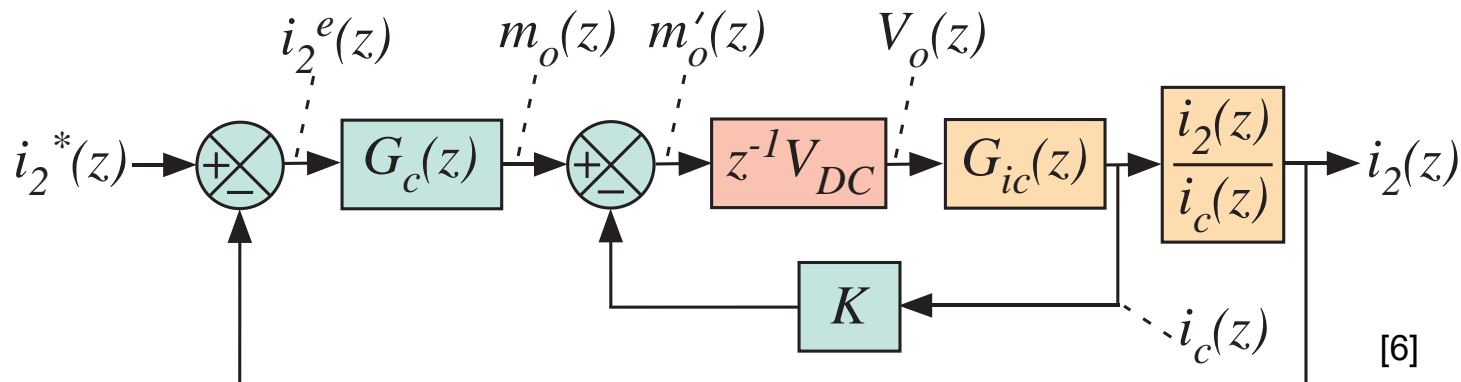
Controller



Plant (LCL)

- **Active damping (dual loop)**

- Commonly feedback of i_c (or variant) for damping, through gain K



Inverter

Which controller is suitable and when? → use Bode analysis

L and LCL Filter Equations

- L Filter

$$i_2(s) = \frac{1}{sL} [V_o(s) - E(s)] = Y_L(s) [V_o(s) - E(s)]$$

$Y_L(s)$ is the filter admittance seen by the grid and converter for an L filter

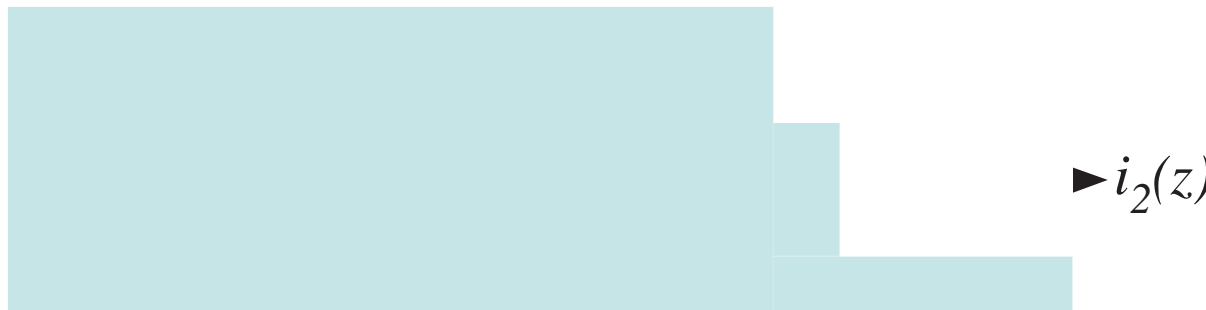
- LCL Filter

$$\begin{aligned} i_2(s) &= \frac{1}{sL_1L_2C_f} \frac{1}{(s^2 + \omega_{res}^2)} V_o(s) - \frac{1}{sL_1L_2C_f} \frac{(L_1C_f s^2 + 1)}{(s^2 + \omega_{res}^2)} E(s) \\ &= Y_v(s) V_o(s) + Y_G(s) E(s) \end{aligned}$$

$Y_v(s)$ and $Y_G(s)$ are the filter admittances seen by the converter and grid for an LCL filter, where $\omega_{res}^2 = (L_1 + L_2)/(L_1L_2C_f)$

- NOTE : filter resistance neglected to model worst case undamped filter characteristic

Discrete Time Model – Single Loop Controller



- Plant transfer function (grid current from inverter output)

$$G_{i2}(s) = \frac{i_2(s)}{V_o(s)} = \frac{1}{sL_1L_2C_f} \frac{1}{(s^2 + \omega_{res}^2)}$$

where

$$\omega_{res} = \sqrt{\frac{L_1 + L_2}{L_1L_2C_f}}$$

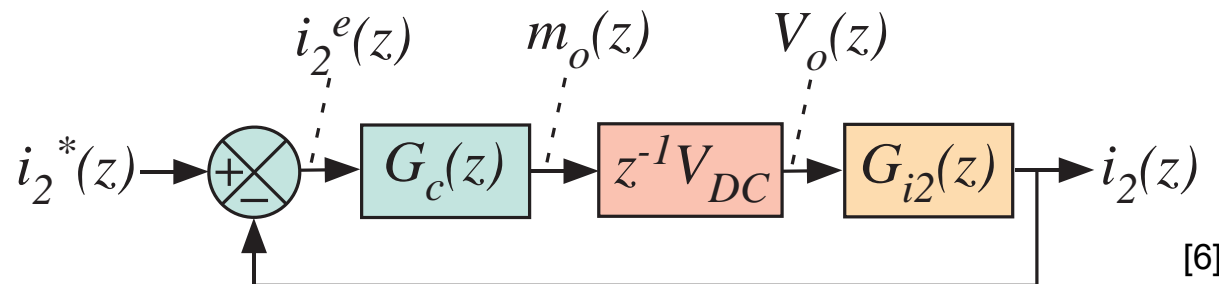
- Using ZOH discretization (for a sampled system) of

$$\frac{z-1}{z} Z \left\{ \frac{G(s)}{s} \right\}$$

gives

$$G_{i2}(z) = \frac{i_2(z)}{V_o(z)} = \frac{T}{(L_1 + L_2)(z - 1)} - \frac{\sin(\omega_{res}T)}{(L_1 + L_2)\omega_{res}} \times \frac{z - 1}{z^2 - 2z \cos(\omega_{res}T) + 1}$$

Discrete Time Model – Single Loop Controller



- PR fundamental controller (Tustin with prewarping)

$$G_c(s) = K_p \left(1 + \frac{1}{T_r} \frac{s}{s^2 + \omega_0^2} \right) \quad \xrightarrow{\text{blue arrow}} \quad G_c(z) = K_p \left(1 + \frac{1}{T_r} \frac{\sin(\omega_0 T)}{2\omega_0} \frac{z^2 - 1}{(z^2 - 2z \cos(\omega_0 T) + 1)} \right)$$

- Inverter model with PWM transport delay

$$V_o(z) = z^{-1} V_{DC} m_o(z)$$

- Open loop forward path equation (without active damping)

$$\frac{i_2(z)}{i_2^e(z)} = z^{-1} V_{DC} G_c(z) G_{i2}(z)$$

Discrete Time Model – Dual Loop Controller

- Inner loop plant transfer function (capacitor current)

- Active damping

$$G_{ic}(s) = \frac{i_c(s)}{V_o(s)} = \frac{1}{sL_1} \frac{s^2}{(s^2 + \omega_{res}^2)}$$

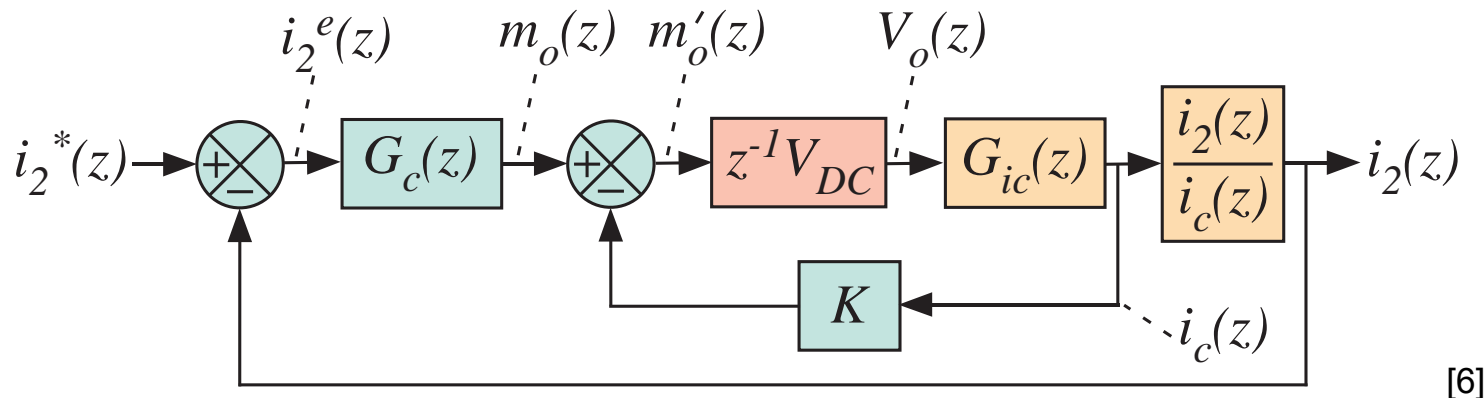
- Using ZOH discretization (for a sampled system)

$$G_{ic}(z) = \frac{i_c(z)}{V_o(z)} = \frac{\sin(\omega_{res}T)}{\omega_{res}L_1} \times \frac{z-1}{z^2 - 2z \cos(\omega_{res}T) + 1}$$

- Closed inner loop with gain K (including inverter model)

$$\frac{i_c(z)}{m_o(z)} = \frac{V_{DC}G_{ic}(z)}{z + KV_{DC}G_{ic}(z)}$$

Discrete Time Model – Dual Loop Controller



- Equation relating i_2 to i_c
 - Impulse invariant discretization (sampling delay already in model)

$$\frac{i_2(s)}{i_c(s)} = \frac{G_{i2}(s)}{G_{ic}(s)} = \frac{1}{s^2 L_2 C}$$

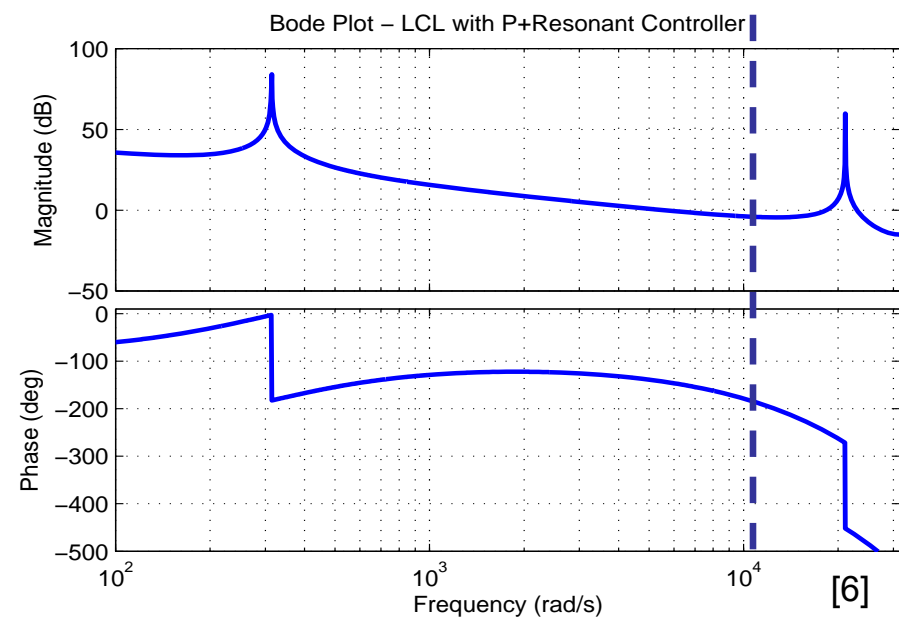
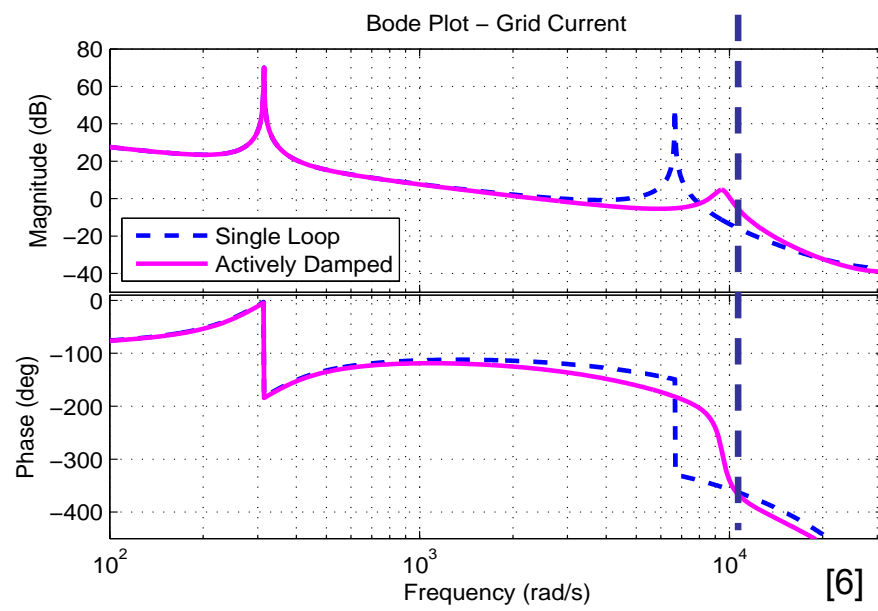
Zimp

$$\frac{i_2(z)}{i_c(z)} = \frac{z T^2}{(z - 1)^2 L_2 C}$$

- Overall open loop forward path equation with active damping

$$\begin{aligned} \frac{i_2(z)}{i_2^e(z)} &= G_c(z) \times \frac{i_c(z)}{m_o(z)} \times \frac{i_2(z)}{i_c(z)} \\ &= G_c(z) \times \frac{V_{DC} G_{ic}(z) [i_2(z)/i_c(z)]}{z + KV_{DC} G_{ic}(z)} \end{aligned}$$

LCL Filter Active Damping Regions [10]



- Low LCL resonant frequency
 - -180ϵ phase jump with unbounded gain
 - Unstable without damping
 - Stabilised with active damping
- High LCL resonant frequency
 - -180ϵ phase jump occurs after phase crosses -180ϵ due to delay roll-off
 - Stable without damping
- Critical LCL frequency (ω_{crit}) → forward path phase reaches -180ϵ

Critical LCL Resonant Frequency

- To find ω_{crit}

$$\angle \frac{i_2}{i_e} (z = e^{j\omega T}) = \angle e^{-j\omega T} V_{DC} G_c(e^{j\omega T}) G_{i2}(e^{j\omega T}) = -\pi$$

- PR controller response well below crossover frequency

- Phase contribution of controller is negligible: $\angle G_c(e^{j\omega T}) \approx 0$

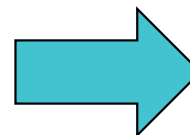
- LCL resonance \rightarrow no phase contribution until the resonant frequency is reached

- Hence plant phase reduces to

$$\angle G_{i2}(e^{j\omega T}) = \angle \frac{1}{e^{j\omega T} - 1}$$

- with substitution and manipulation

$$\angle \frac{i_2}{i_e} (z = e^{j\omega T}) = -\omega T - \frac{\pi}{2} - \frac{\omega T}{2} = -\pi$$



$$\omega_{crit} = \frac{\pi}{3T}$$

- Below ω_{crit} damping is required
- Above ω_{crit} single control loop is sufficient

Exploring the Active Damping Regions

- Closed loop poles → Required for root loci
- Using conventional $1+G(z)=0$, from forward path $G(z)$
 - Single loop controller

$$z + V_{DC} K_p G_{i2}(z) = 0$$

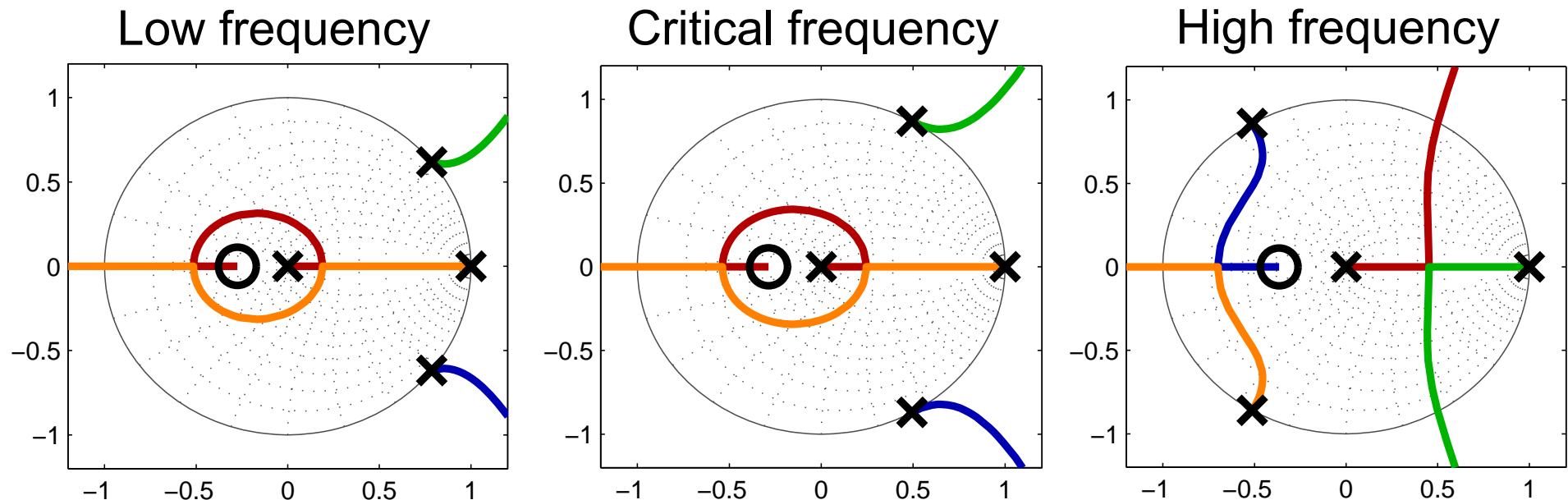
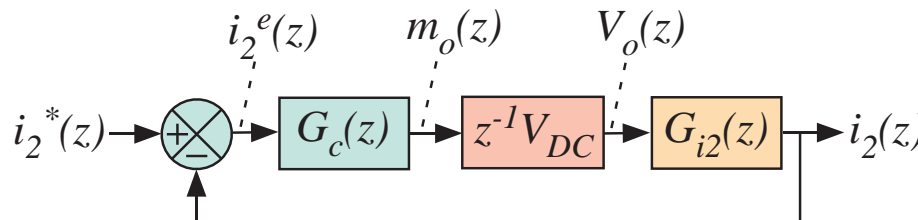
- Inner loop of dual loop controller

$$z + V_{DC} K G_{ic}(z) = 0$$

- Overall dual loop controller

$$z + V_{DC} K G_{ic}(z) + V_{DC} K_P G_{ic}(z) \left[i_2(z)/i_c(z) \right] = 0$$

Single Loop (i_2) Controller Root Loci

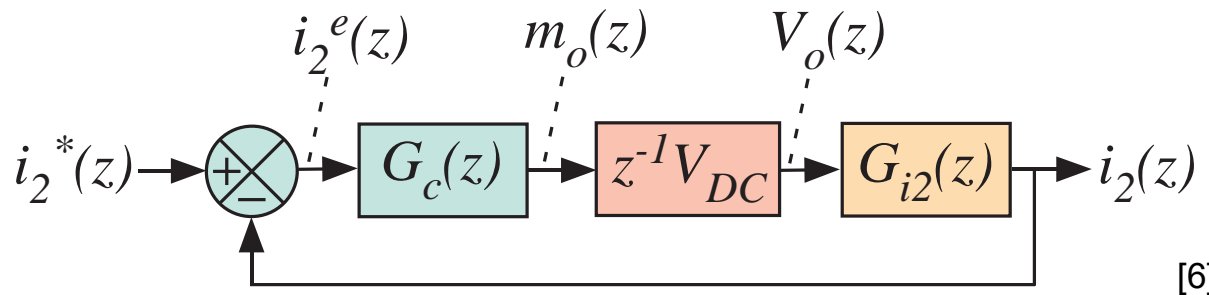


- No damping capability at critical or low frequencies
- Provides damping of poles at high frequency
 - No active damping required → agree with Bode
- All systems have loci which track unstable through

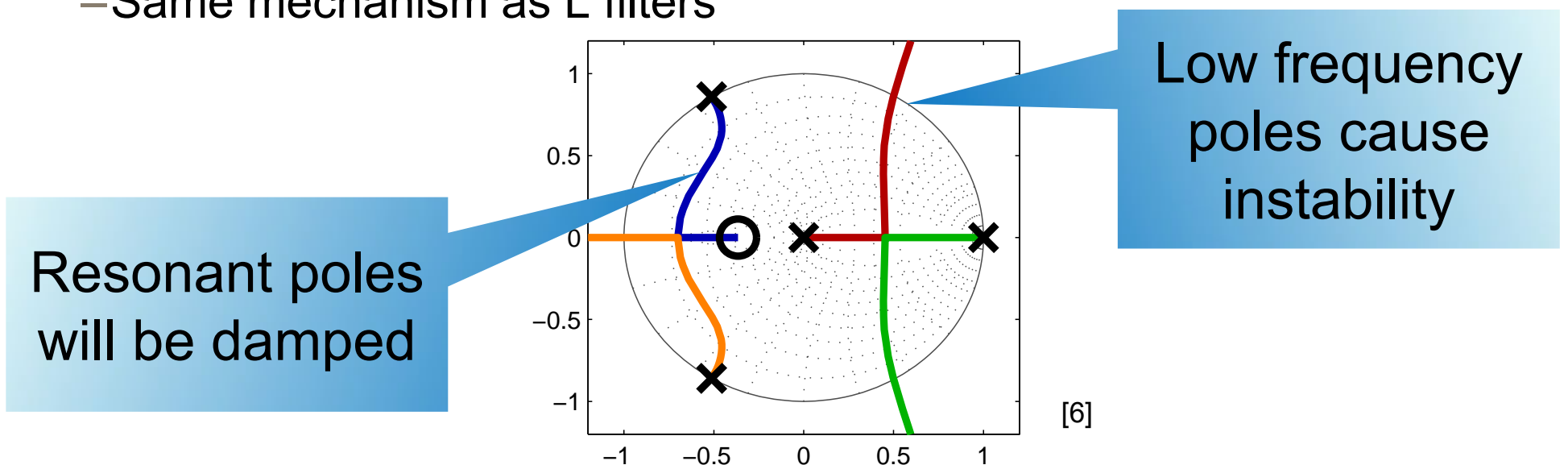
$$z = 0.5 \pm j\sqrt{3}/2$$

Controller when Resonance Above ω_{crit}

- Single loop controller is suitable
 - Stable, active damping unnecessary



- Gain limitation → Low frequency poles, not resonance
 - Same mechanism as L filters



Gain Selection when Resonance Above ω_{crit}

- Using the same method as for standard L filters [2]
 - Resonance and controller → minimal magnitude and phase contribution at crossover frequency
 - Only low frequency model required → series inductance plant

$$\frac{i_2(z)}{i_2^e(z)} = z^{-1} V_{DC} K_p \frac{T}{(z-1)(L_1 + L_2)}$$

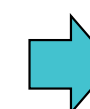
- Calculate crossover ω_c frequency for a desired phase margin φ_m

$$\begin{aligned}\angle \frac{i_2}{i_2^e}(z = e^{j\omega_c T}) &= \angle \frac{V_{DC} K_p T}{(L_1 + L_2)} \frac{1}{e^{j\omega_c T} (e^{j\omega_c T} - 1)} \\ &= -\frac{\pi}{2} - \frac{\omega_c T}{2} - \omega_c T = -\frac{\pi}{2} - \frac{3}{2} \omega_c T\end{aligned}$$

$$\varphi_m = \pi + \angle \frac{i_2}{i_2^e}(z = e^{j\omega_c T}) = \frac{\pi}{2} - \frac{3}{2} \omega_c T$$



$$\omega_c = \frac{\pi/2 - \varphi_m}{3T/2}$$

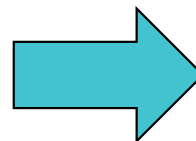


$$\omega_c = \frac{\pi/2 - \varphi_m}{T_d}$$

Gain Selection when Resonance Above ω_{crit}

- Proportional gain is set to achieve unity gain at desired crossover frequency ω_c

$$K_p = \left| \frac{(L_1 + L_2)(e^{j\omega_c T} - 1)}{V_{DC}T} \right|$$

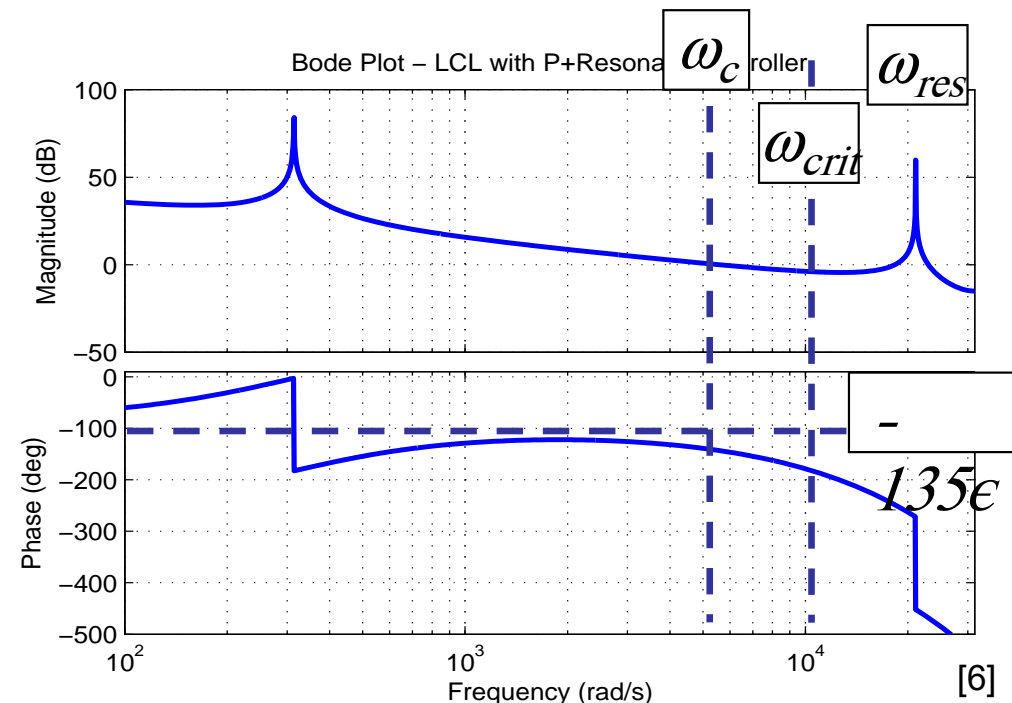


$$K_p \approx \frac{\omega_c (L_1 + L_2)}{V_{DC}}$$

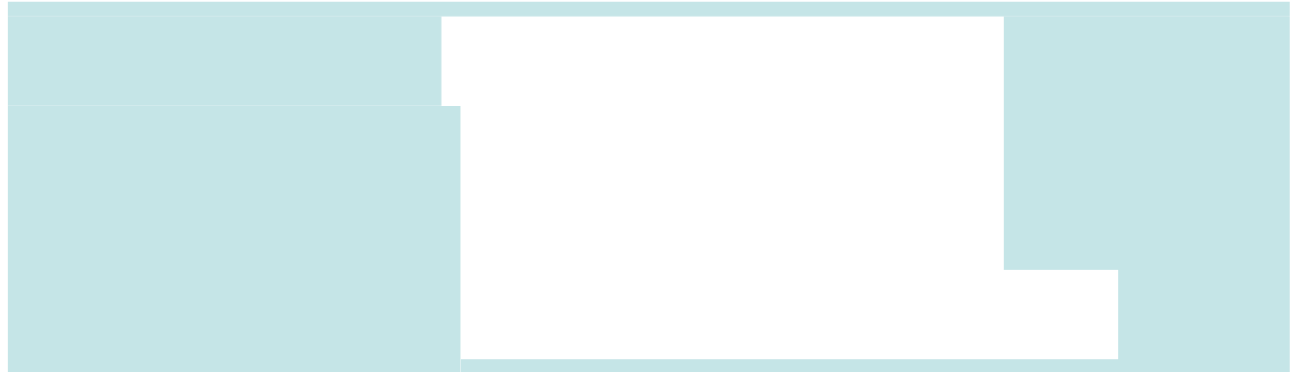
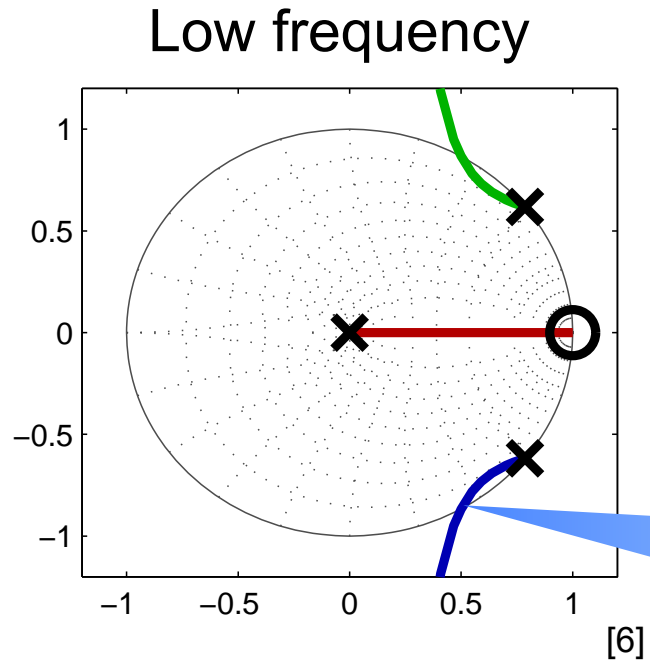
- Design PR controller time constant (T_r)
 - Phase contribution minimal at ω_c

$$T_r \approx 10/\omega_c$$

High Frequency System	
$L_1 = 6mH$	$L_2 = 2mH$
$C_f = 1.5\mu F$	$L_{eq} = 1.5mH$
$2V_{DC} = 650V$	$f_s = 5kHz$
$\omega_{res} = 21.1krads^{-1}$	$T = 0.1msec$
$\omega_{crit} = 10.5krads^{-1}$	$T_d = 0.15msec$
$\varphi_m = 45\epsilon$	$\omega_c = 5.24krads^{-1}$
$K_p = 0.129A^{-1}$	$T_r = 1.9msec$



Dual Loop Controller: Inner Loop (i_c) Root Loci

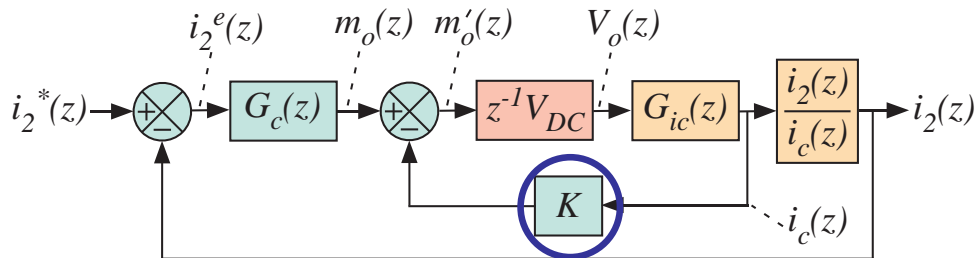


$$z = 0.5 \pm j\sqrt{3}/2$$

Critical frequency

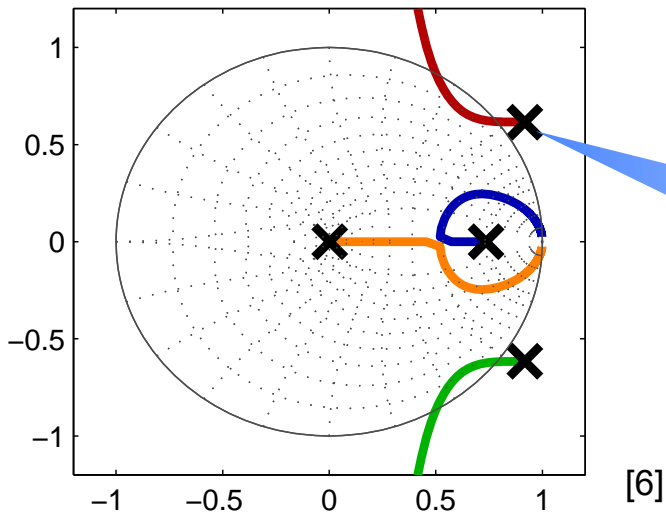
- Only low frequency region examined
 - High frequency → not required
 - Critical frequency → not effective (next slide)
- Provides damping of poles – Limited range of K

Dual Loop Controller Root Loci



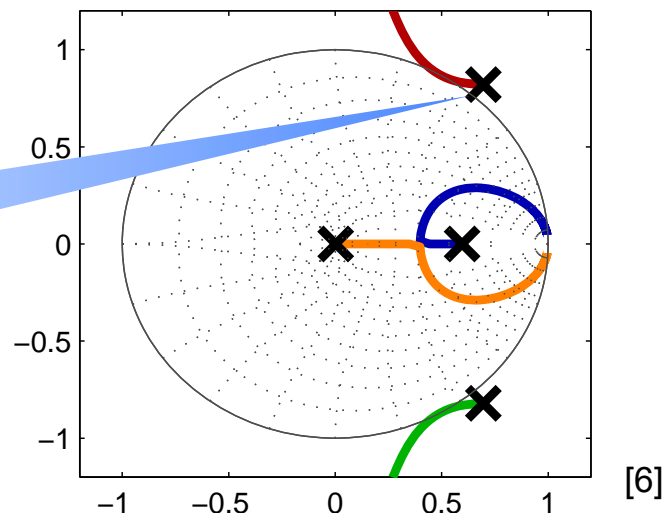
Varying K
(active damping)

Low frequency



Poles start
unstable

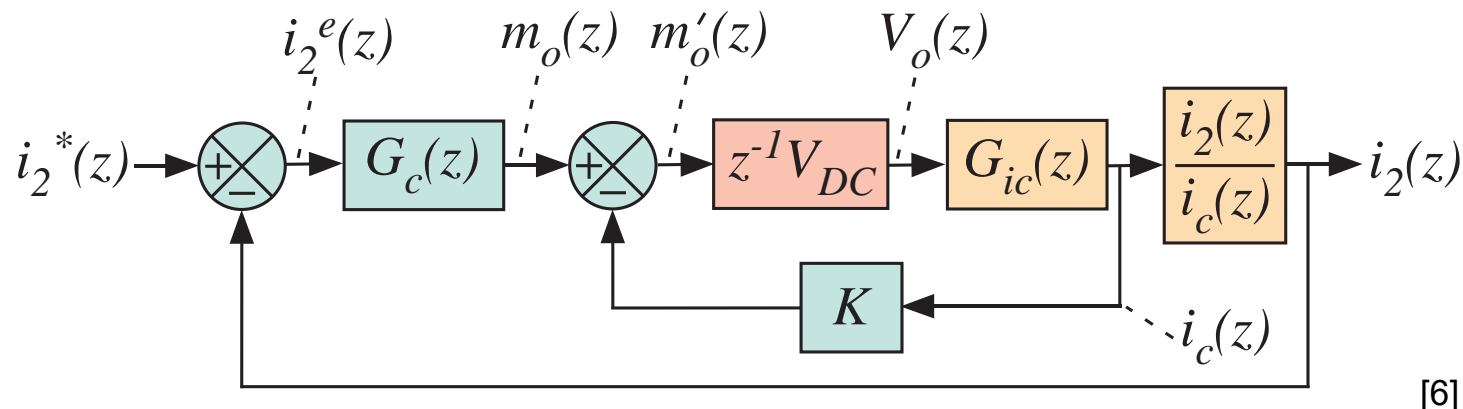
Critical frequency



- At low frequency
 - Poles are moved inside unit circle by active damping
 - Limitation to damping gain K before instability
- At critical frequency – never enter unit circle

Dual Loop Controller when Resonance Below ω_{crit}

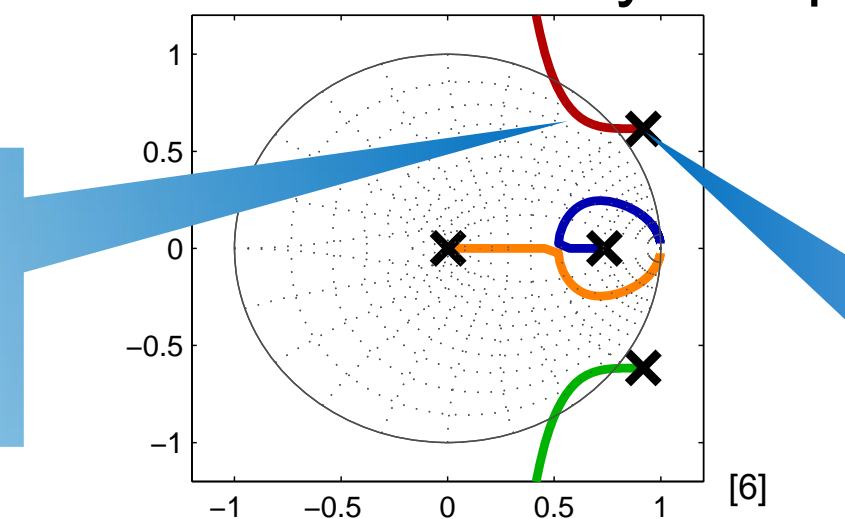
- Dual loop controller (active damping) required
 - Capacitor current feedback selected



[6]

- Gain selection will ensure maximally damped poles

Active damping
draws poles
into stability



Poles originate
outside unit
circle

[6]

Gain Selection when Resonance Below ω_{crit}

- Low frequency still dominated by series filter inductance
- Phase margin must consider phase contribution of resonance
 - Crossover frequency ratio of resonant frequency [Tang et. al. 2012]

$$\omega_c \approx 0.3\omega_{res}$$

- Proportional gain and PR time constant → Same manner as earlier

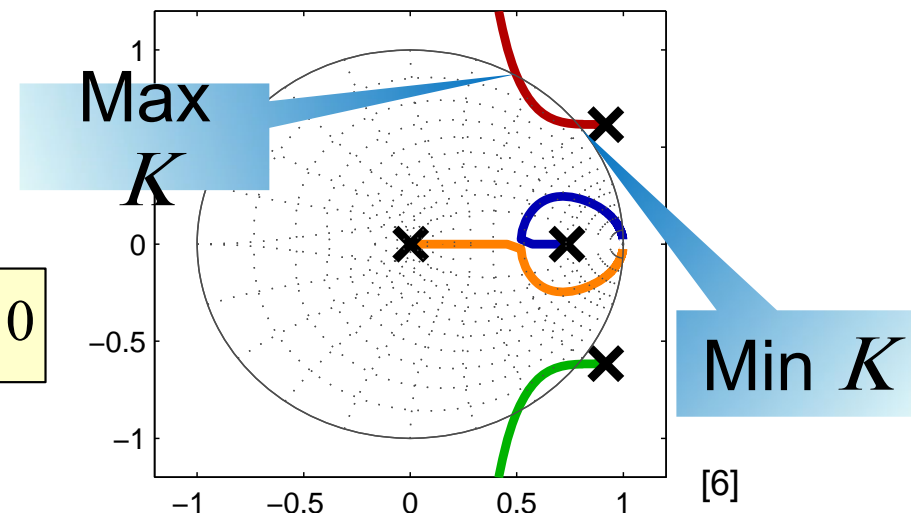
$$K_p \approx \frac{\omega_c (L_1 + L_2)}{V_{DC}}$$

$$T_r \approx 10/\omega_c$$

- Best possible damping gain
 - Maximally damped poles
 - Closed loop characteristic equation

$$z + V_{DC}KG_{ic}(z) + V_{DC}K_PG_{ic}(z)\left[i_2(z)/i_c(z)\right] = 0$$

- Bounded range for K



Bounded Range for K (Resonance Below ω_{crit})

- **Maximum value (K_{max})**

- Magnitude of characteristic equation → adapted to equal 1

$$\left| \frac{V_{DC} \sin(\omega_{res} T)}{\omega_{res} L_1} \times \frac{K(z-1)^2 + K_p \gamma_{LC}^2 T^2 z}{z(z-1)(z^2 - 2z \cos(\omega_{res} T) + 1)} \right| = 1$$

- Substitute in critical point

$$z_0 = 0.5 + j\sqrt{3}/2$$

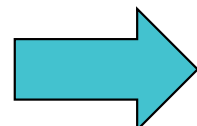
- Solve for K_{max}

$$K_{max} = \frac{\omega_{res} L_1}{V_{DC} \sin(\omega_{res} T)} |1 - 2 \cos(\omega_{res} T)| + K_p \gamma_{LC}^2 T^2$$

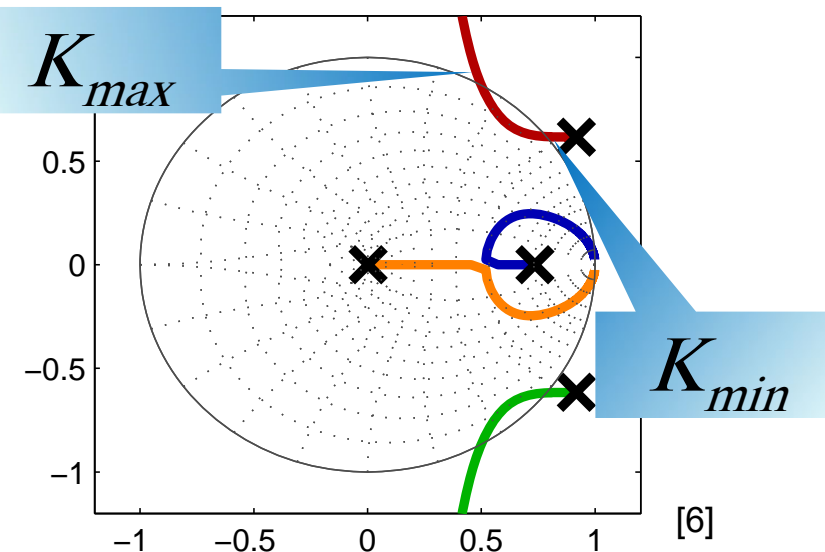
- **Minimum value (K_{min})**

- Ratio of K to K_p identified using
 - Routh's Stability Criterion [Liu et. al. 2012]
 - Rearranged as limitation

$$\frac{K_p}{K} \leq \frac{L_1 + L_2}{L_1}$$



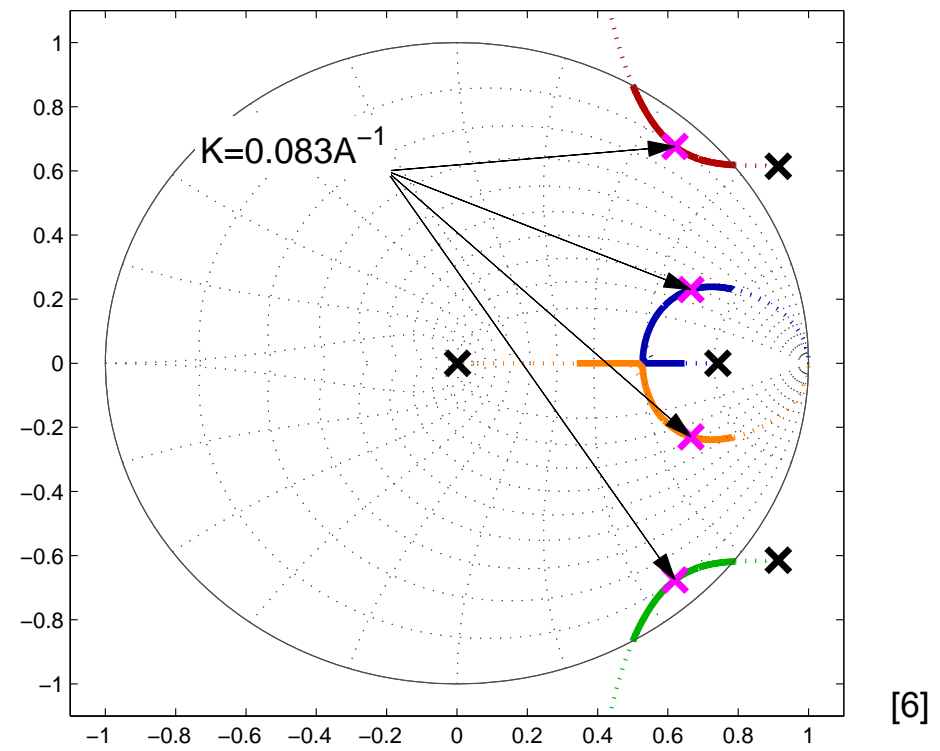
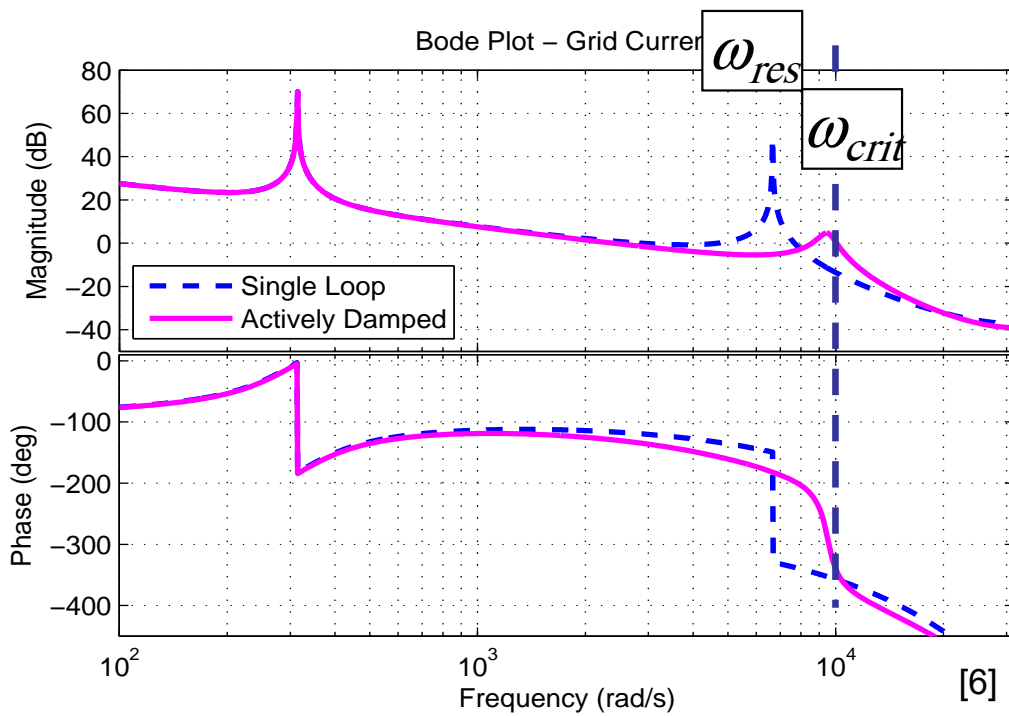
$$K_{min} = \frac{K_p L_1}{L_1 + L_2}$$



[6]

Final Gain Selection (Resonance Below ω_{crit})

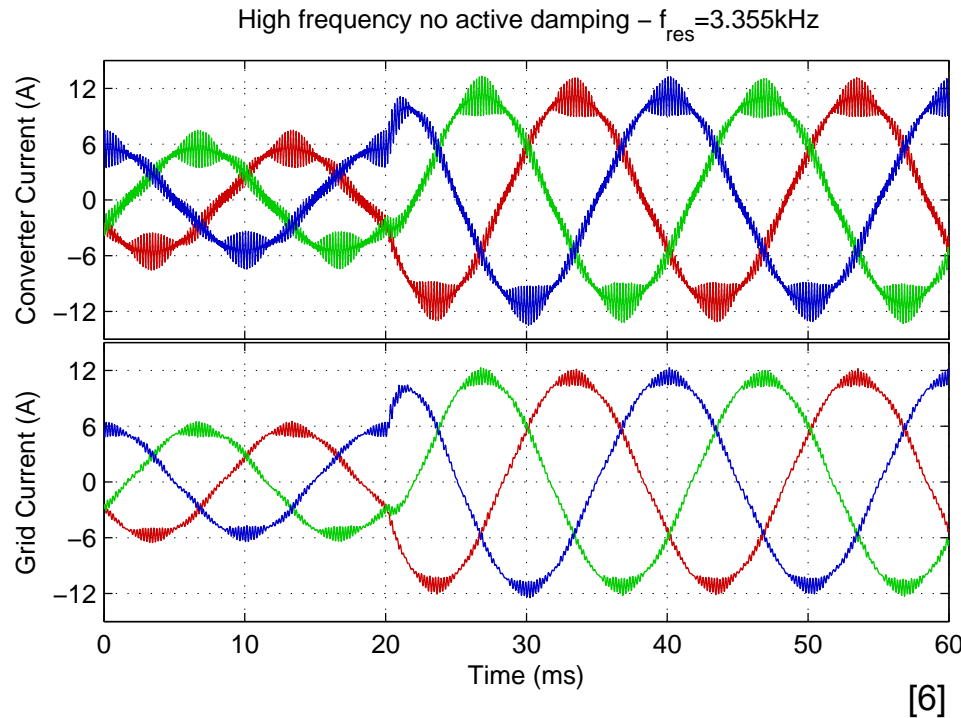
- Bounded range → Solid line
 - $K_{min} = 0.044A^{-1}$
 - $K_{max} = 0.124A^{-1}$
- Maximum damping $K=0.083A^{-1}$



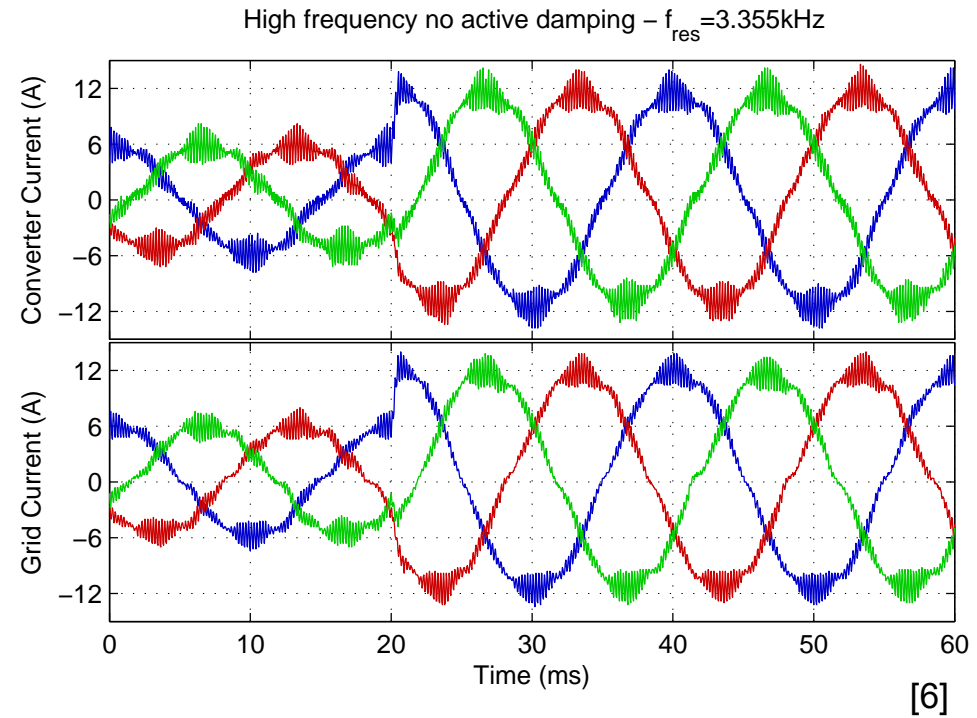
Low Frequency System	
$L_1 = 6mH$	$L_2 = 2mH$
$C_f = 15\mu F$	$f_s = 5kHz$
$\omega_{res} = 6.67krads^{-1}$	$\omega_c = 0.36\omega_{res}$
$\omega_{crit} = 10.5krads^{-1}$	$\omega_c = 2.4krads^{-1}$
$K_p = 0.059A$	$T_r = 4.2mse$
c	$K = 0.083A^{-1}$

High Resonant Frequency System Results

- Simulation (PSIM)



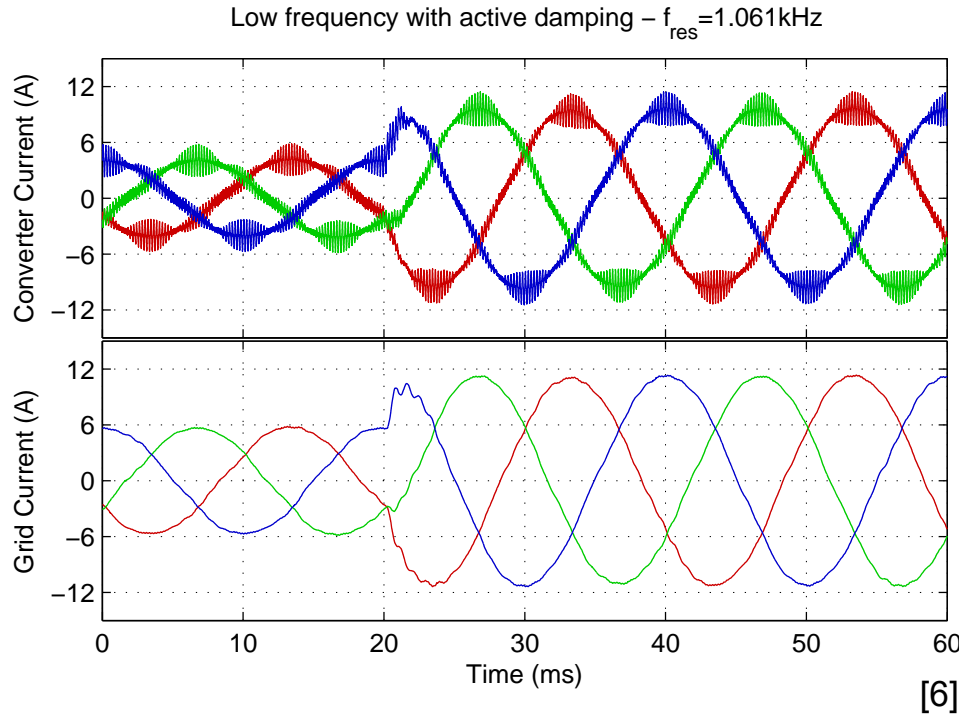
- Experimental



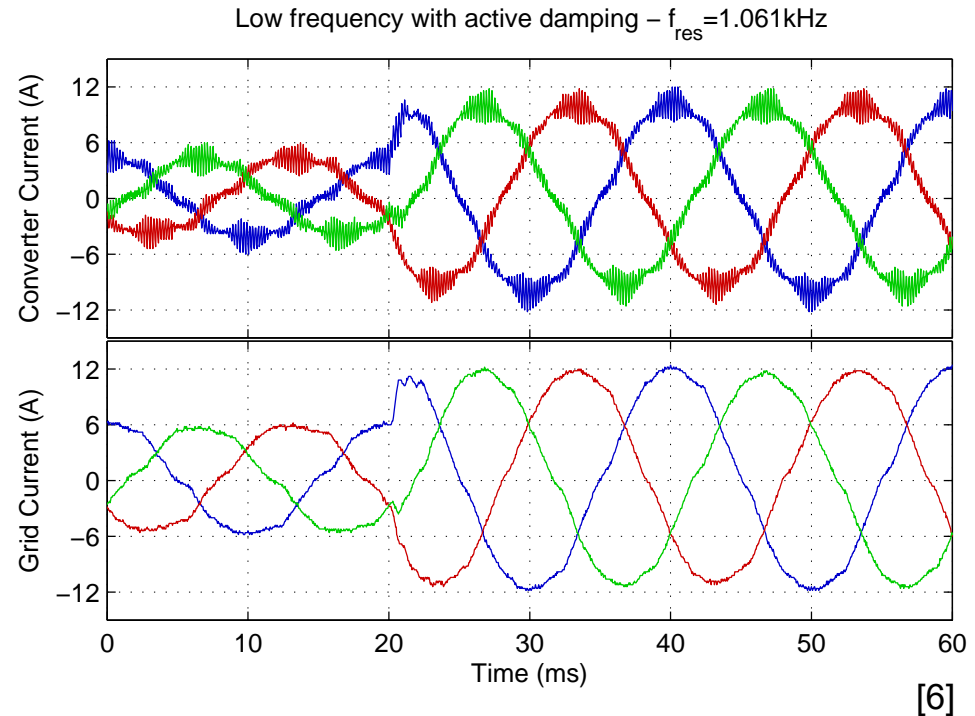
- No visible oscillation
- Rapid transient response → maximised gains
- Similar to single L filter system
- High ripple → poor filtering

Low Resonant Frequency System Results

- Simulation (PSIM)



- Experimental



- Transient damped in 3 to 4 oscillations
 - Agreement with root locus design → underdamped poles
- Minor dynamic performance reduction
 - Limited bandwidth despite maximised gains

Current Regulation with DC bus Common Mode [11]

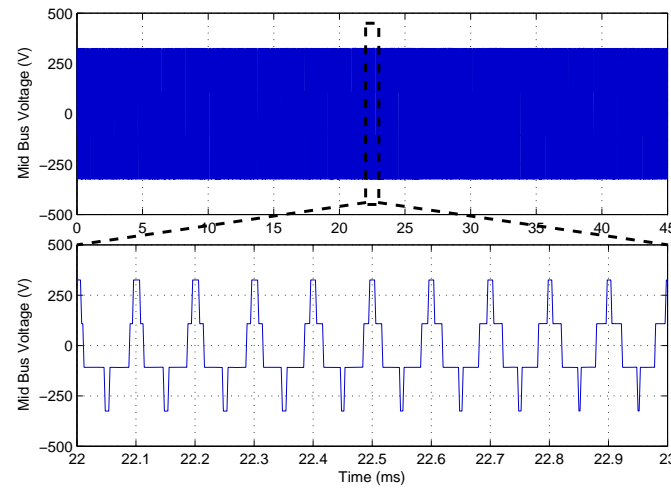
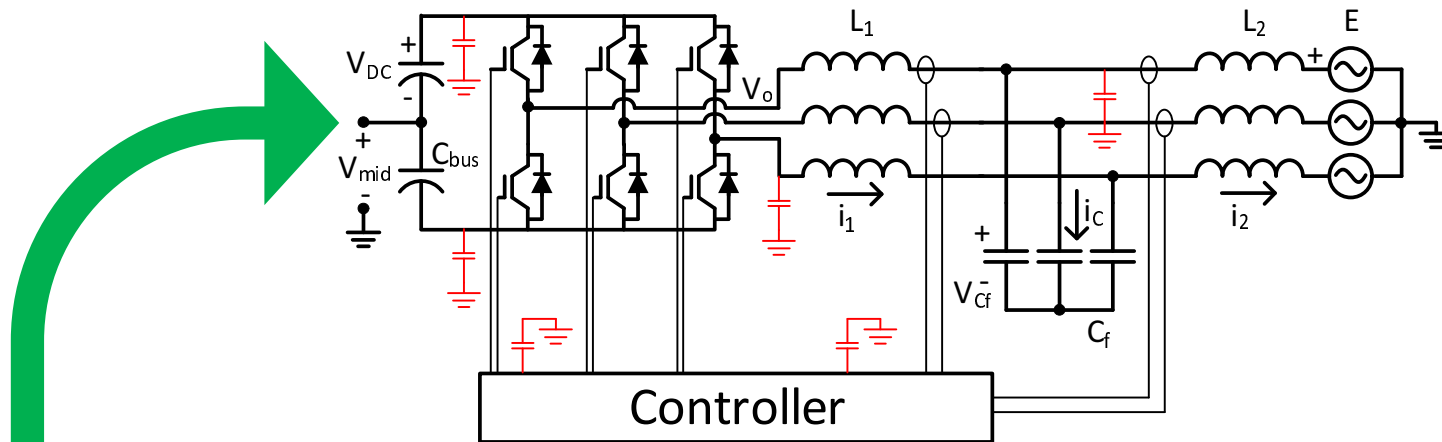
The Challenge:

- VSIs produce 6 step common mode voltage on DC bus
 - Large high frequency CM current through parasitic capacitances
- Common mode EMI can cause malfunction or catastrophic failure of a converter
- Analogues to CM problem in motor drives
- Virtual Neutral filter and similar topologies (reported in literature and used commercially) mitigate common mode voltage on DC bus

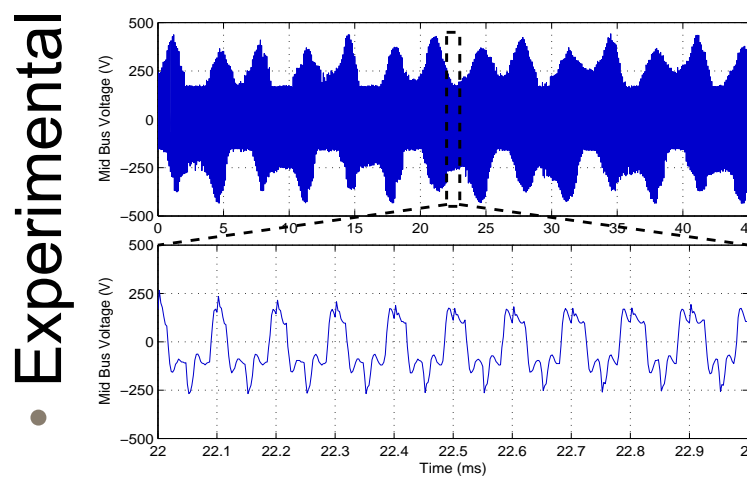
Difficulties:

- No clear design method when using LCL filter

DC Bus Common Mode Midpoint Voltage



• Simulation (Ideal)
[7]

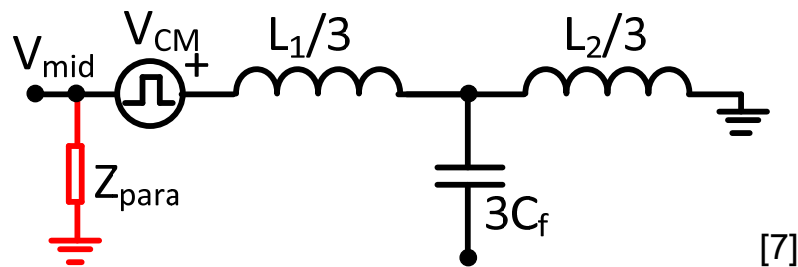


• Experimental
[7]

- CM voltage seen at V_{mid} (with respect to ground)
 - Large currents flow through parasitic capacitances
 - Disrupts loads connected to DC bus or current controller

CM: Harmonic model & Parasitic Impedance

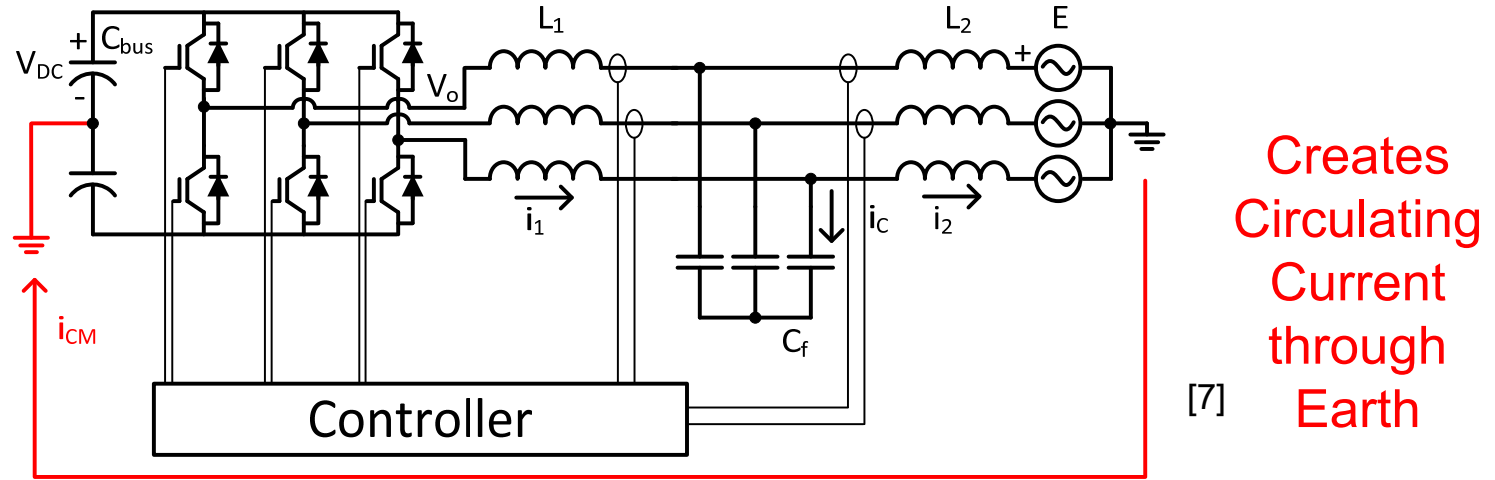
- CM harmonics represented as combined voltage source connected DC mid point to grid earth through LCL filter



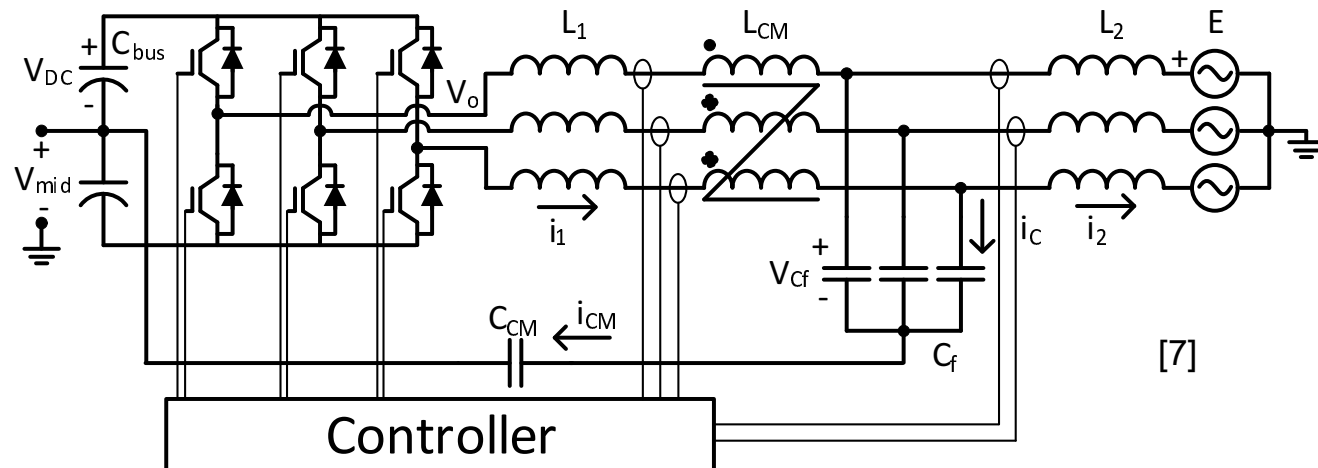
- No parasitic DC bus connection to earth means $V_{\text{mid}} = V_{\text{CM}}$
- Parasitic impedance between DC bus and earth creates impedance divider with LCL filter $\rightarrow V_{\text{CM}}$ reduces somewhat and RINGS at impedance resonance frequency.

CM: Virtual Neutral Filter

- Tie V_{mid} to neutral/earth to stop DC bus fluctuating wrt earth



- OR, tie V_{mid} to virtual neutral at capacitor star point [12]



- Needs additional L_{CM} and C_{CM} to limit CM current

CM: Equivalent Common Mode Circuit

- Common mode equations

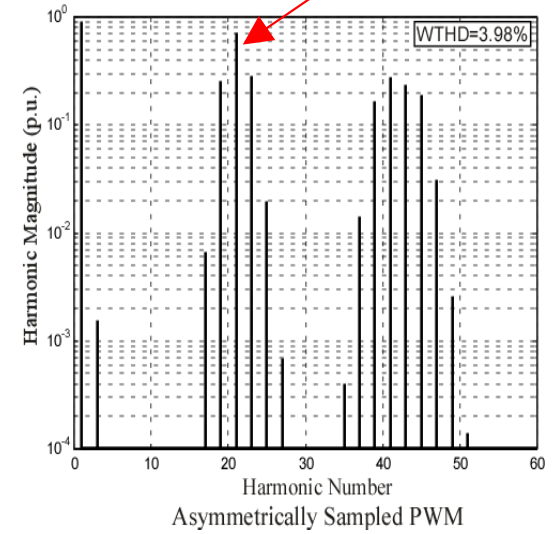
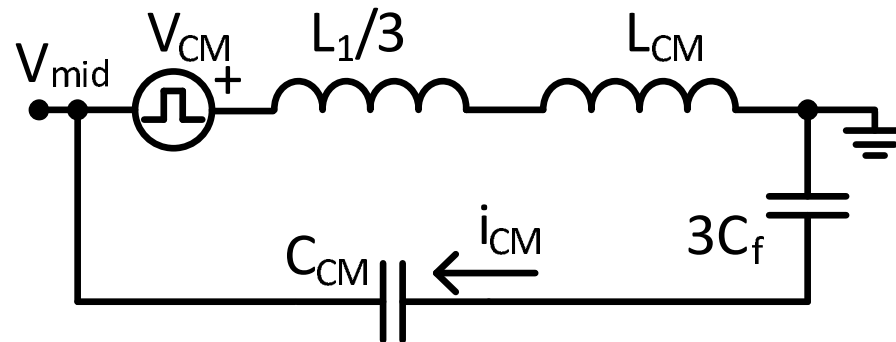
$$V_{mid}(s) + V_{CM}(s) = s \left(\frac{L_1}{3} + L_{CM} \right) i_{CM}(s)$$

$$V_{DC} S_{CM}(s) = V_{CM}(s)$$

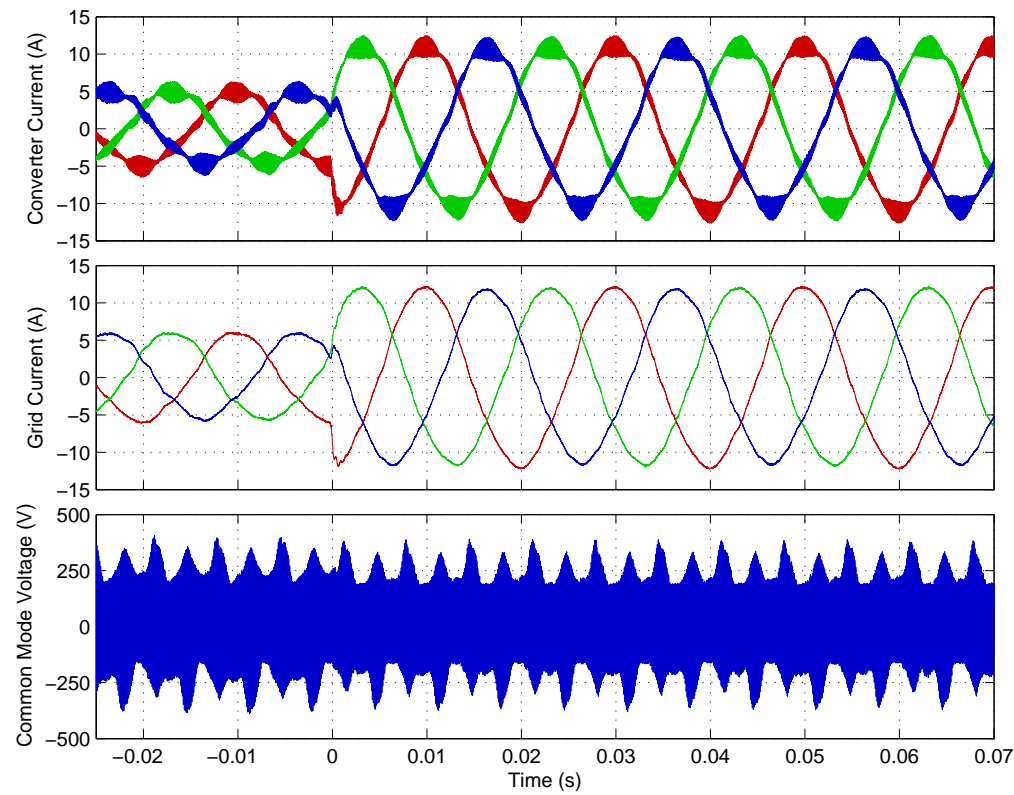
$$V_{CM}(s) = \left\{ s \left(\frac{L_1}{3} + L_{CM} \right) + \frac{3C_f + C_{CM}}{3sC_f C_{CM}} \right\} i_{CM}(s)$$

V_{CM}

- Equivalent common mode circuit

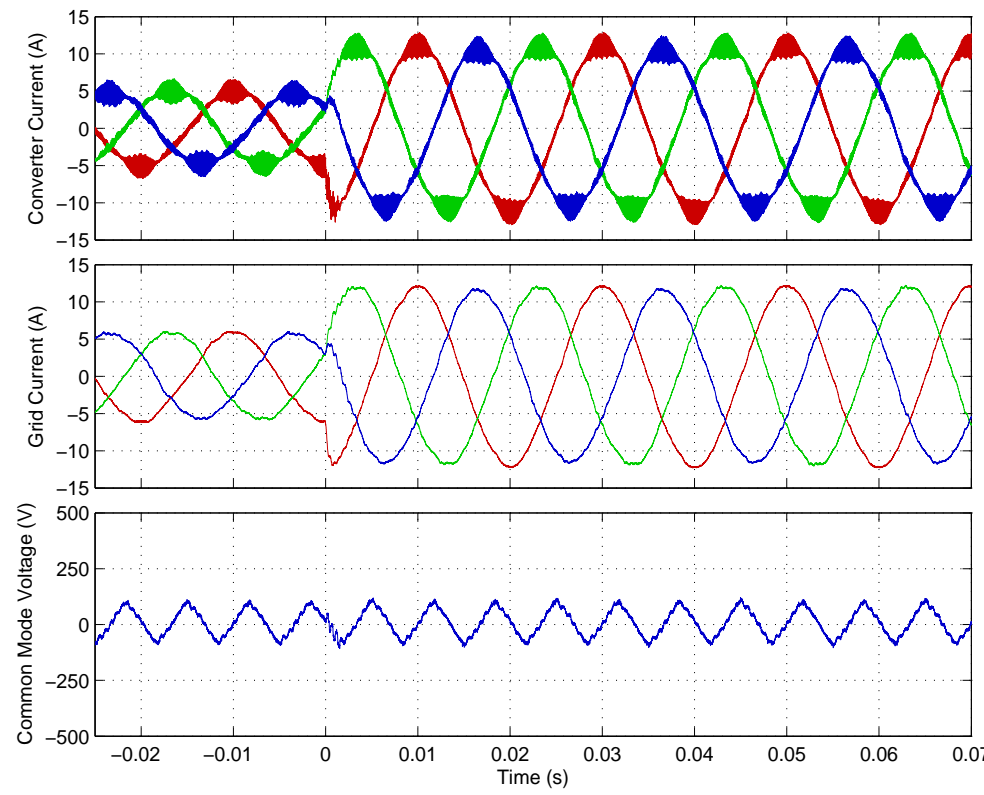


CM: Experimental Results



[7]

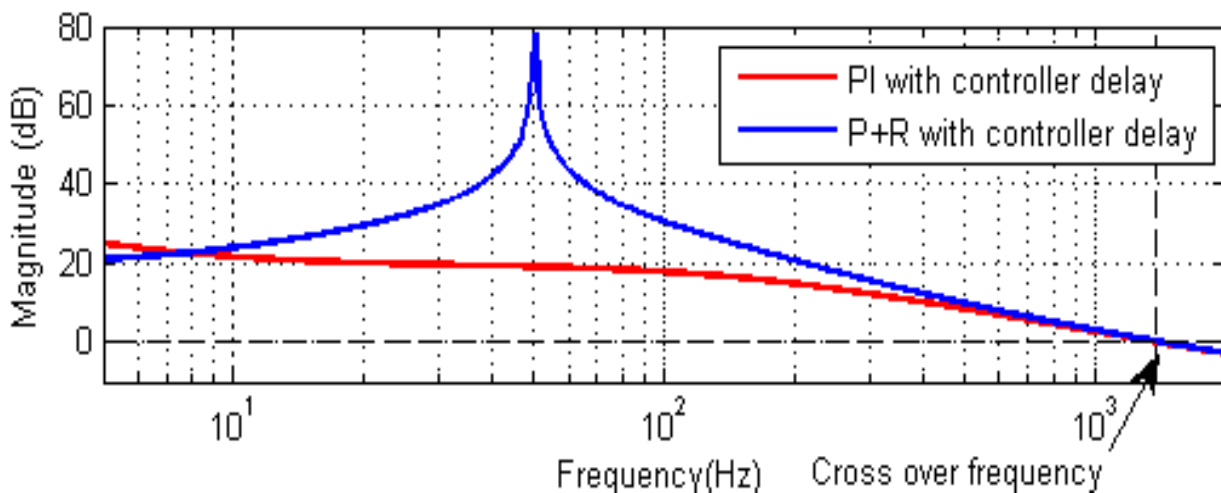
- No virtual neutral filter
- large DC bus common mode voltage \rightarrow EMI



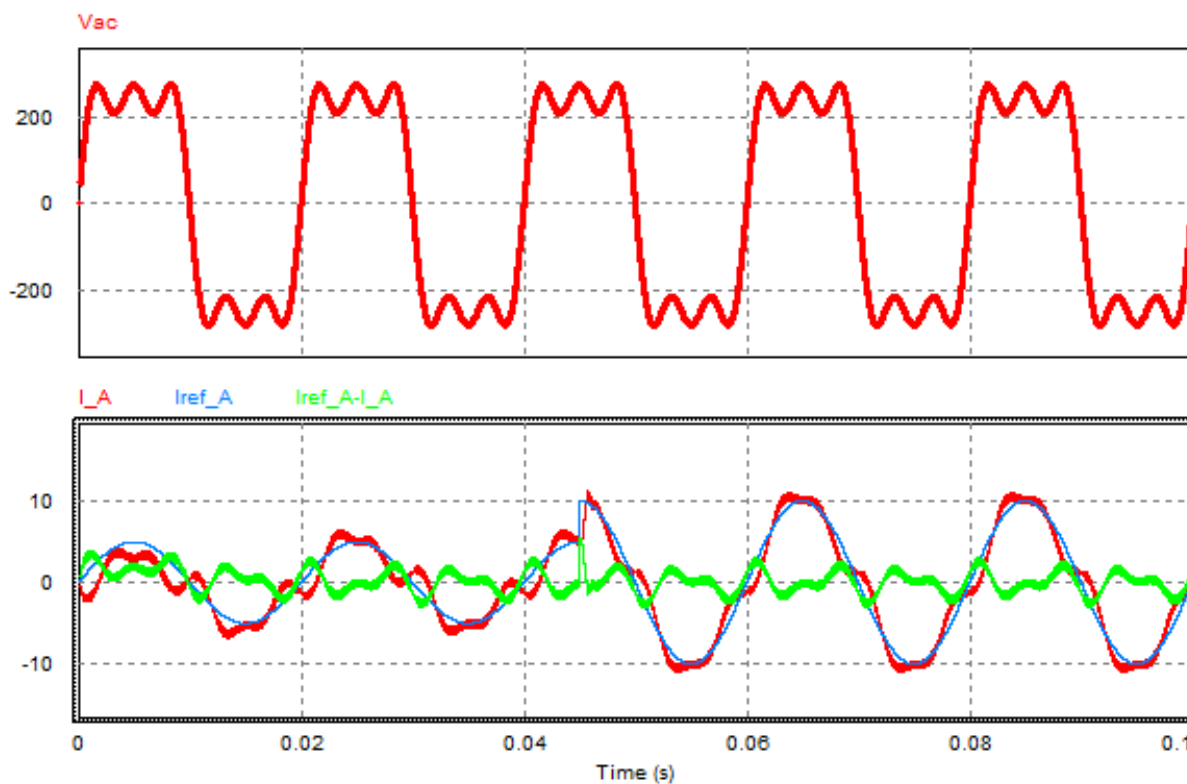
[7]

- virtual neutral filter
- LF DC bus common mode only

Part 3: Advanced Current Regulation: Distorted Grid



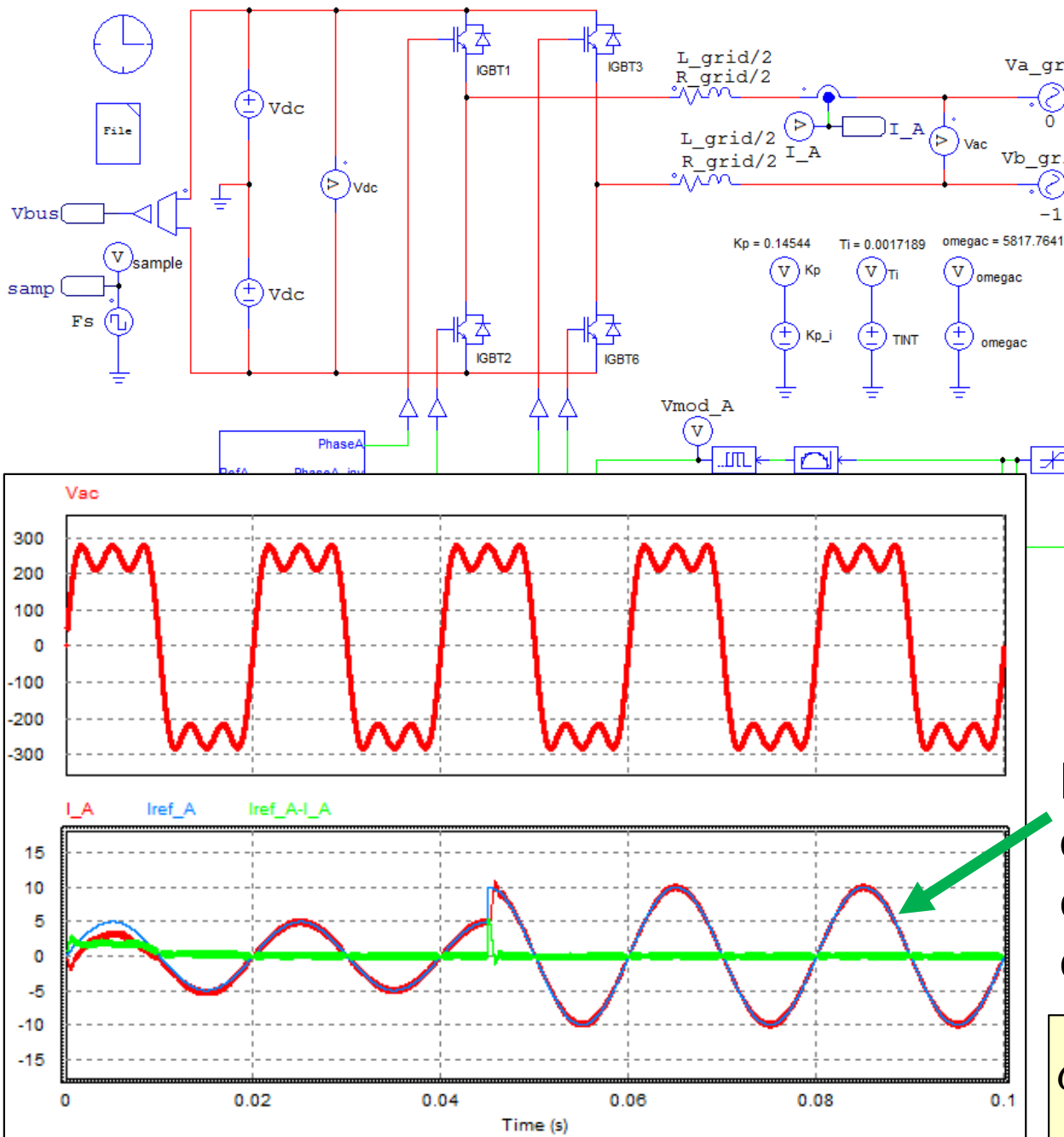
- Gain reduces with frequency
- Resonant gain is only at 50 Hz
- worse for LCL Filters



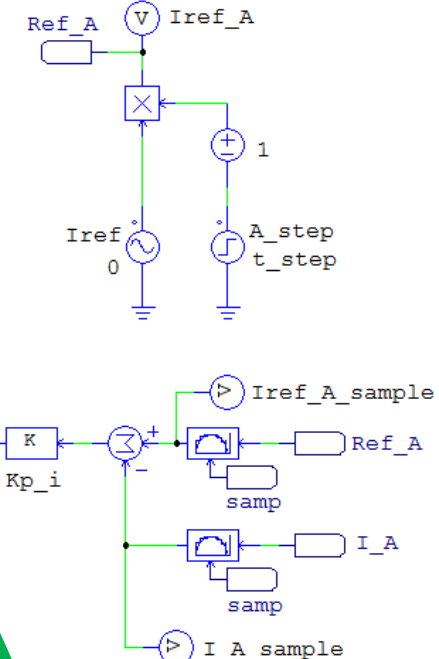
- 30% 3rd harmonic
- 20% 5th harmonic

Significant Current distortion even with PR controller

Regulation with Distorted Grid Voltages [8]



Current reference (pu)



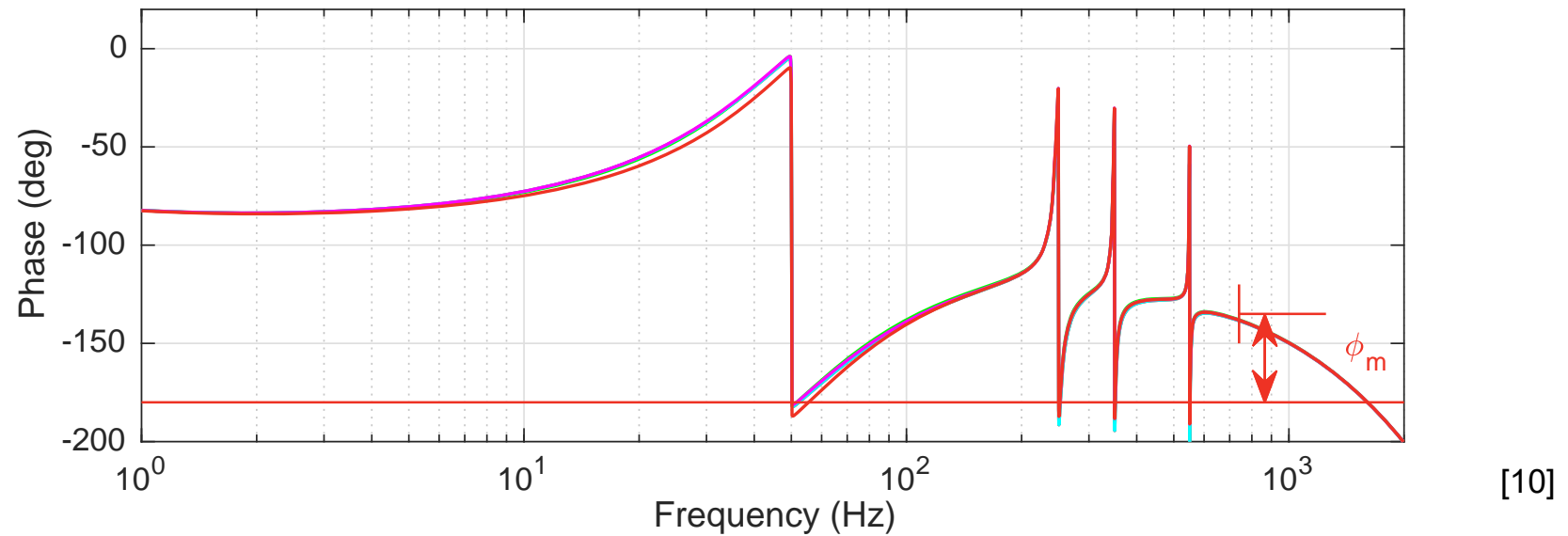
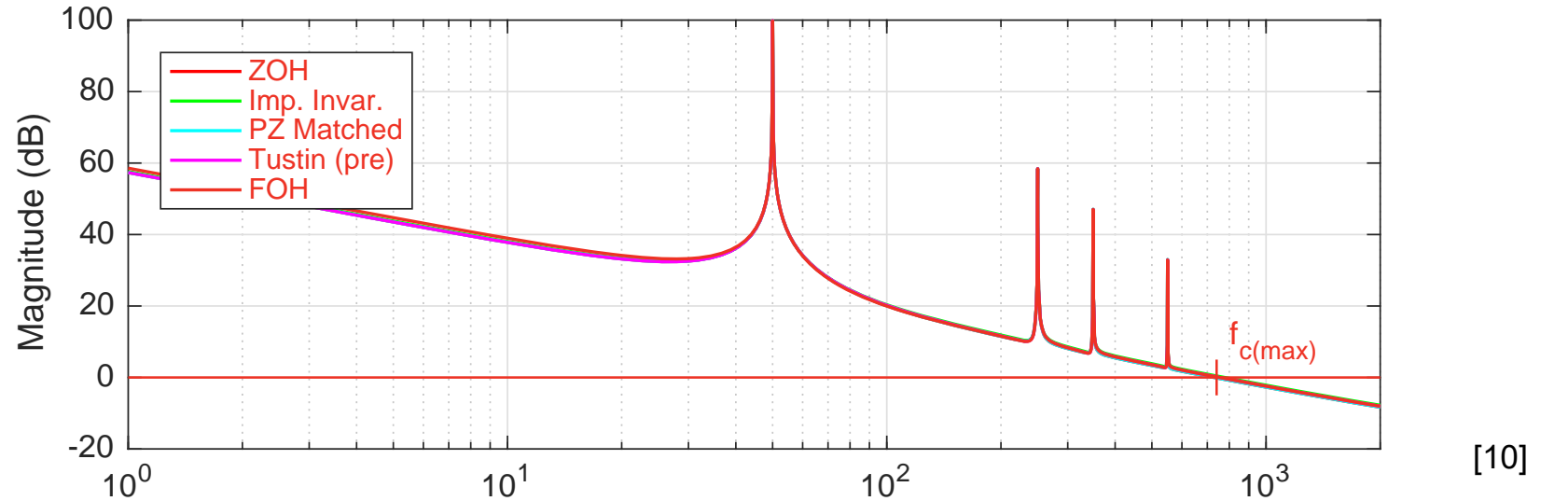
SOLUTION:
Cascade PR controllers at each harmonic frequency

No Current distortion with cascaded PR controllers

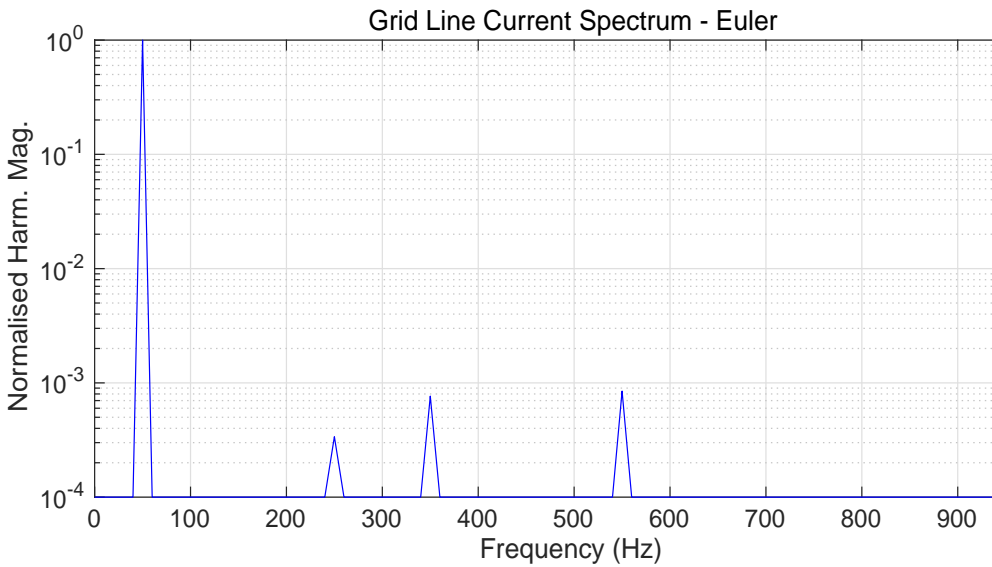
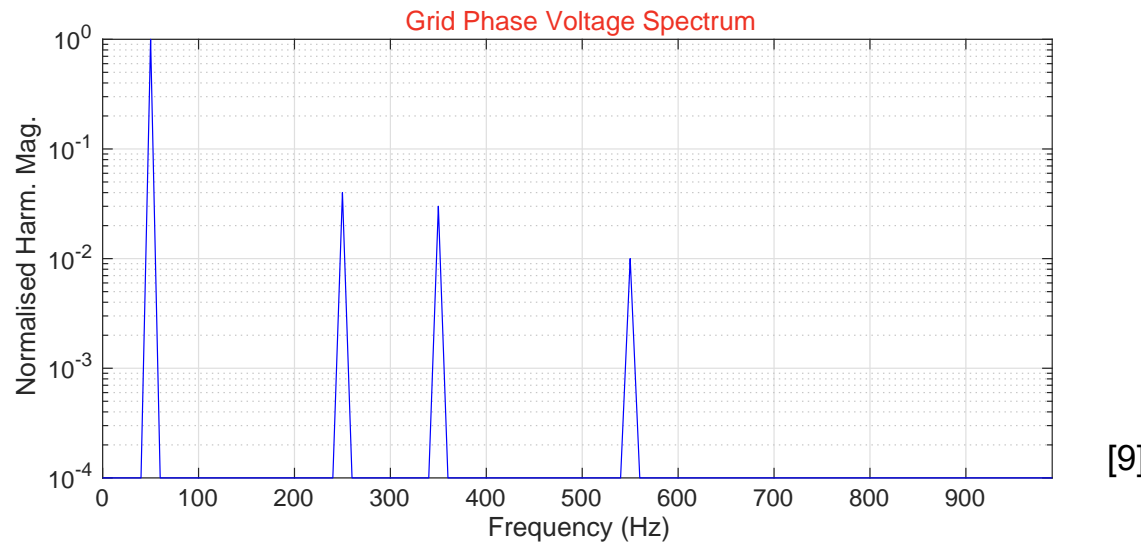
$$G_c(s) = k_p \left(1 + k_r \frac{s}{s^2 + \omega_o^2} + \sum_{h=2}^N k_{r,h} \frac{s}{s^2 + h^2 \omega_o^2} \right)$$

Current Regulator Frequency Response (N = 11)

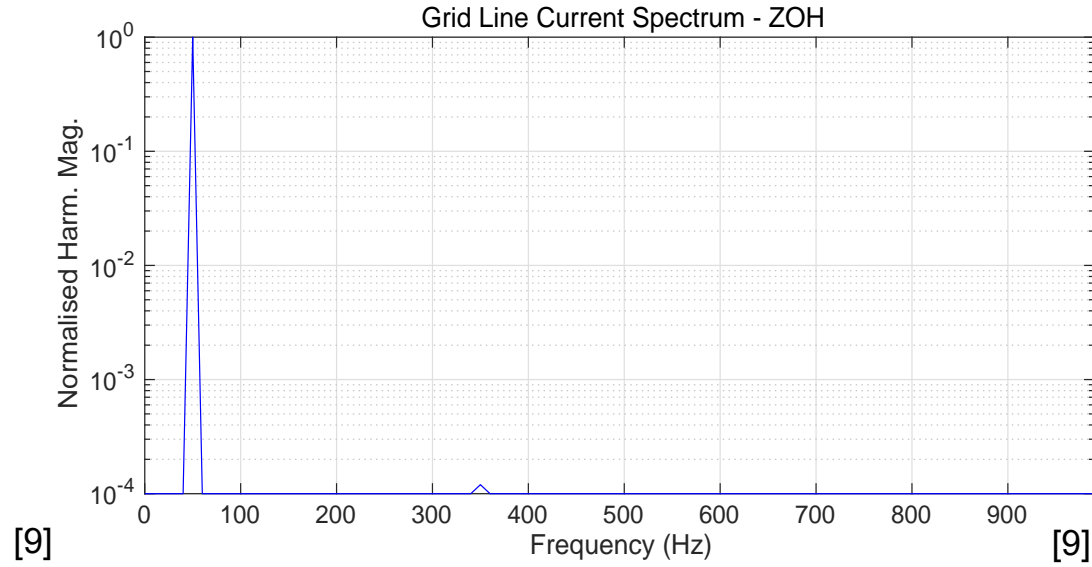
- For



Distorted Grid: Voltage and Current Spectrum



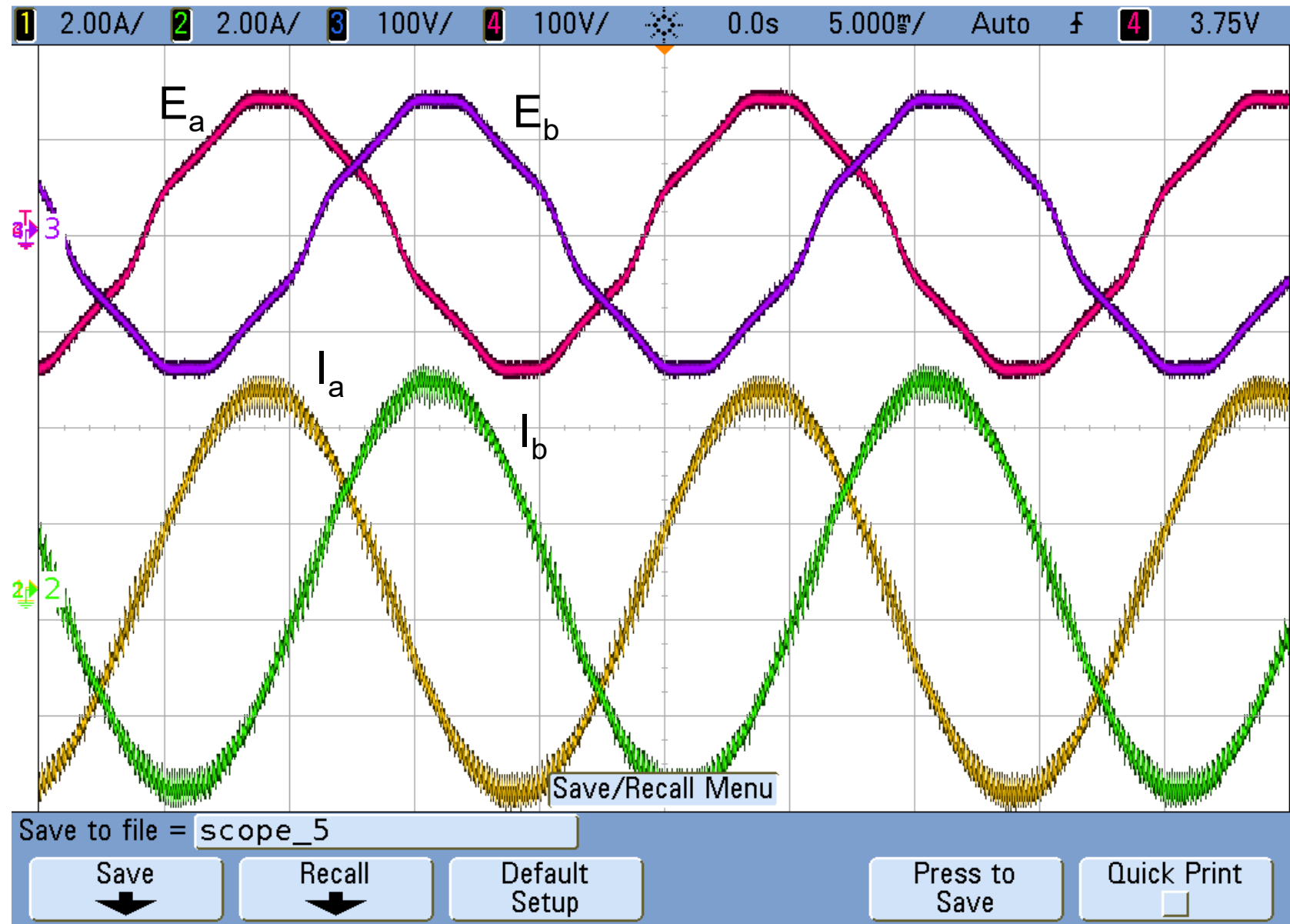
Conventional SOGI Regulator



State Space SOGI Regulator

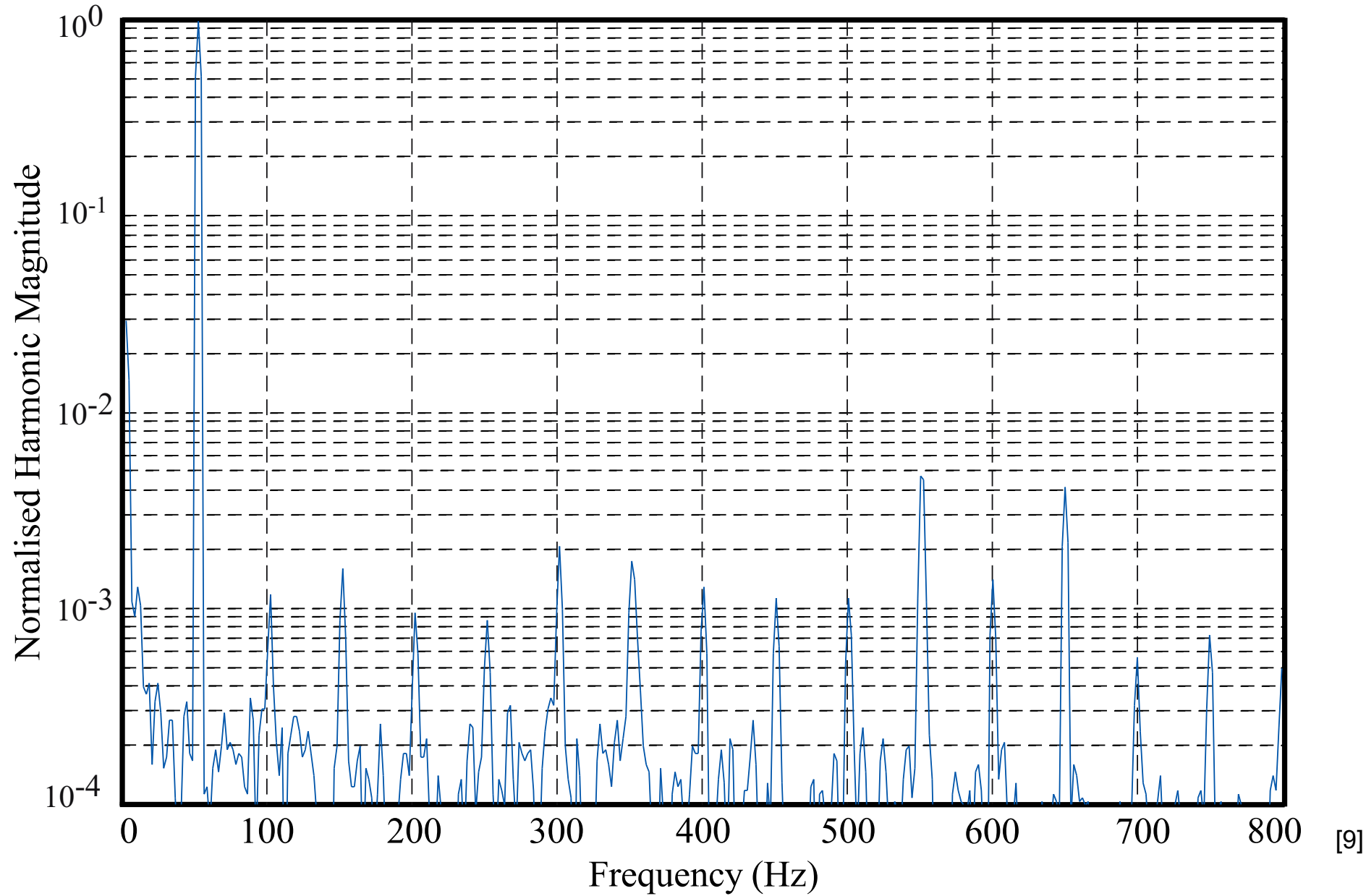
Distorted Grid: Time Domain Experimental

Experimental inverter response with ZOH SOGI structures



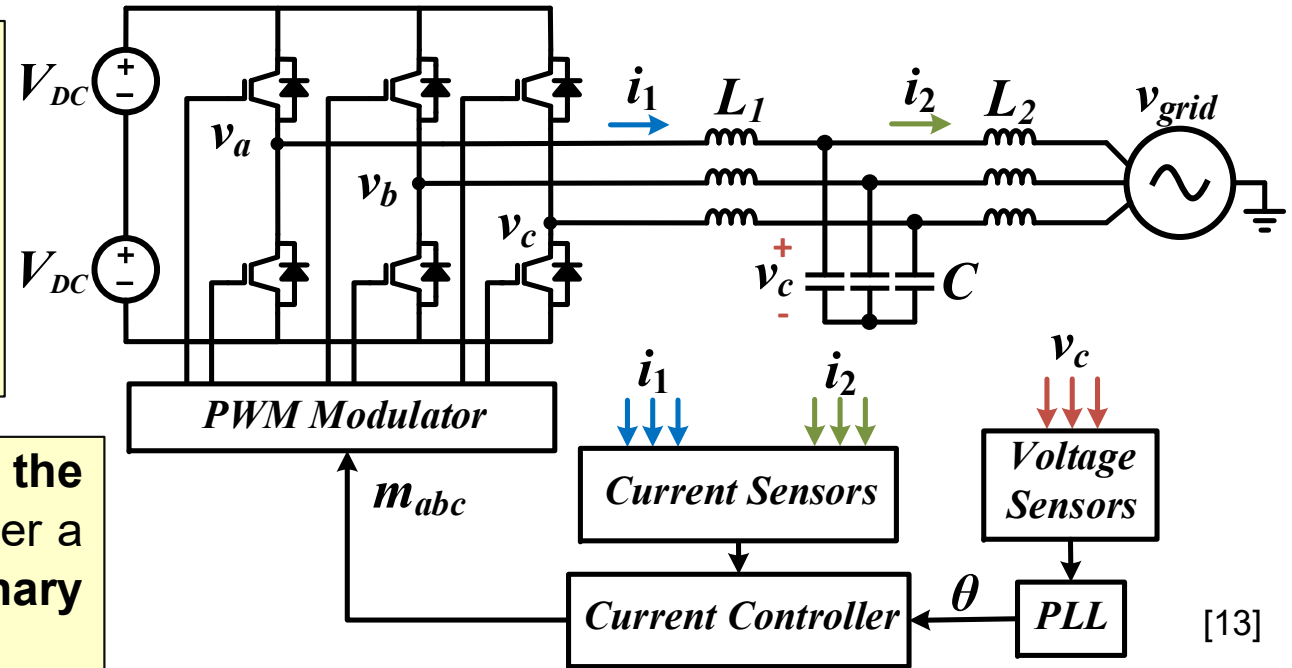
Distorted Grid: Spectrum Experimental

Experimental Current Spectrum – State Space SOGI ZOH



Advanced Current Regulation: Grid or Inverter Side?

- Renewable and distributed generation sources typically use **voltage source inverters** to supply **high quality power** to the grid.



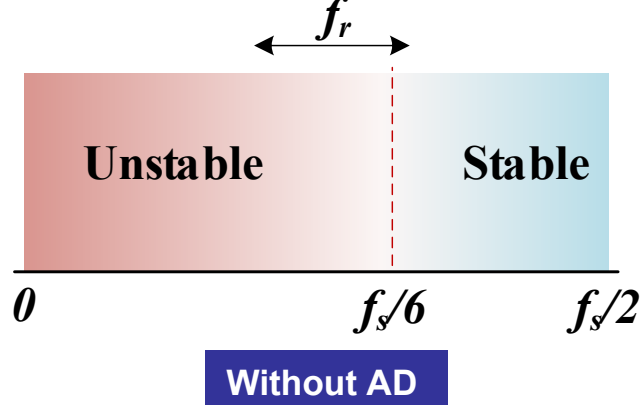
- Operates by **regulating the output currents** using either a **synchronous** or **stationary** frame strategy.
- Inductive (L)** or **inductive-capacitive-inductive (LCL) filters** are required for these inverters to attenuate the switching harmonics injected into the **grid**.
 - LCL filters** are preferred because of their **superior high frequency performance**.
- Can use **active** or **inherent damping strategies** as required for either **grid-current feedback (GCF)** or **inverter-current-feedback (ICF)**.

Grid Current Feedback (GCF) Regulation

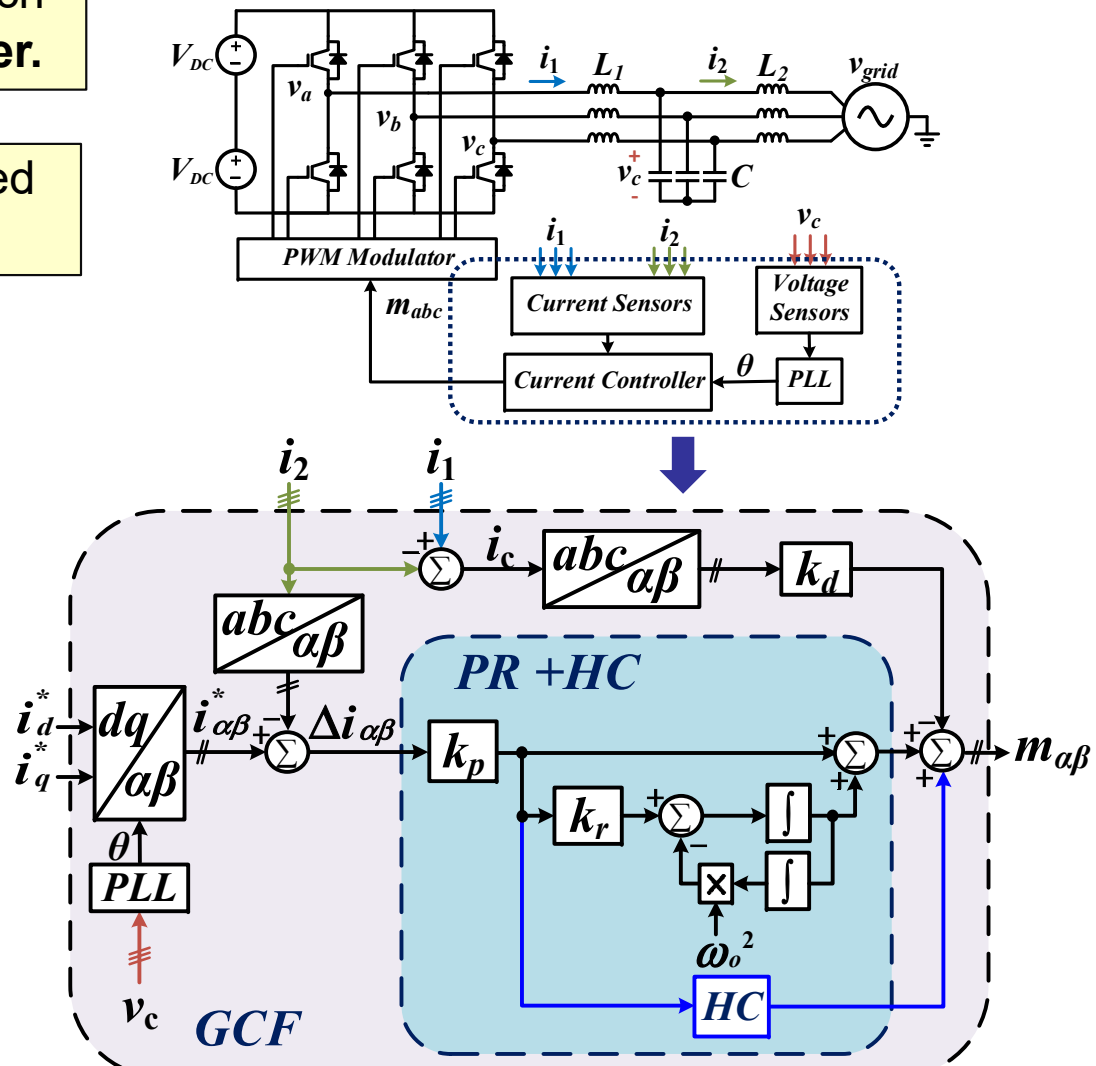
Grid current is directly controlled, which precisely regulates the exported power.

GCF is susceptible to instability caused by the LCL resonance.

Requires active damping (AD), using filter capacitor current feedback
requires inverter and grid side current sensors with an associated cost.



$$f_r = \frac{1}{2\pi} \sqrt{\frac{L_1 + L_2}{L_1 L_2 C}}$$



GCF control is stable if the LCL resonance is above the critical frequency due to its inherent damping

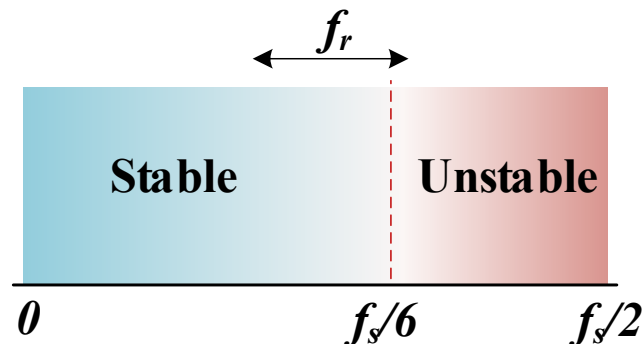
[13]

Inverter Current Feedback (ICF) Regulation

ICF control provides **inherent damping capability** and the need for only **inverter side current sensing**.

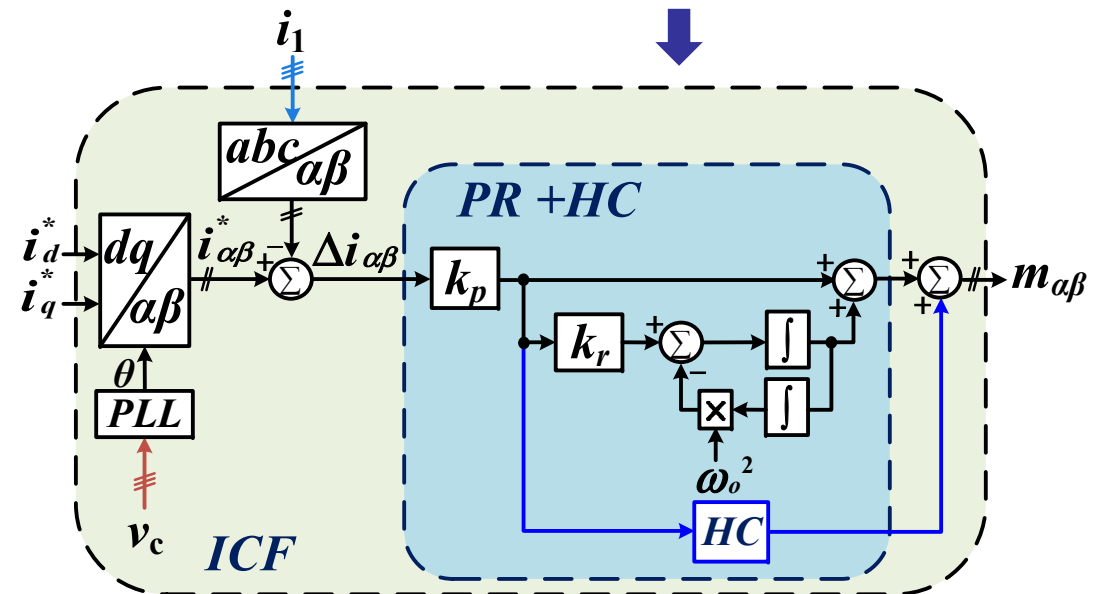
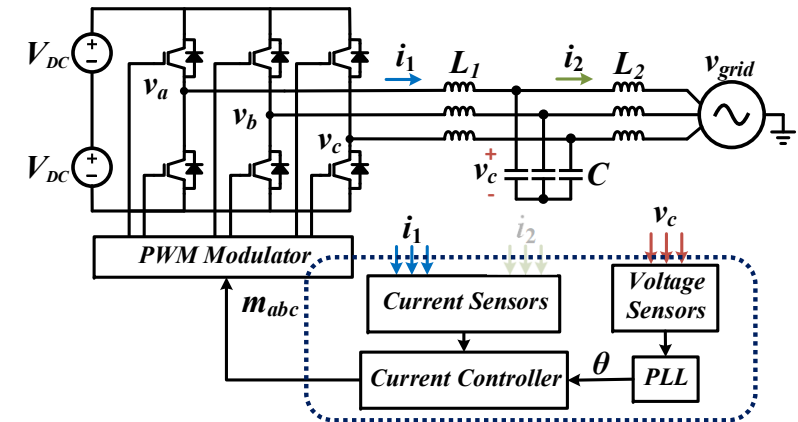
Some form of **capacitor current compensation** is required to achieve accurate grid current control .

ICF low frequency harmonic disturbance rejection properties are significantly **worse than GCF**.



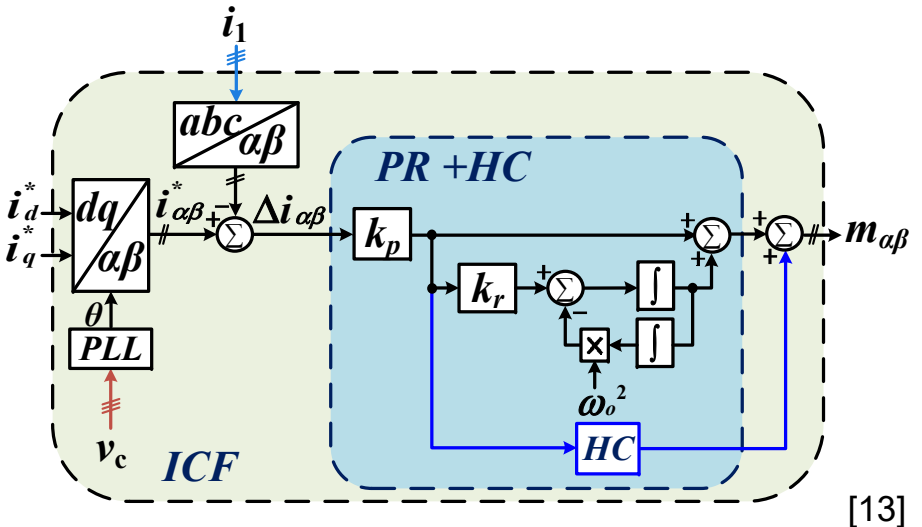
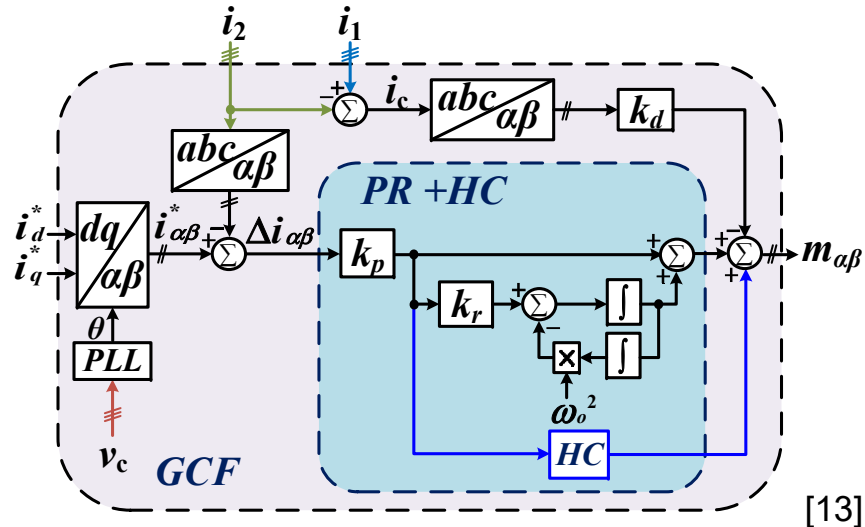
$$f_r = \frac{1}{2\pi} \sqrt{\frac{L_1 + L_2}{L_1 L_2 C}}$$

ICF control is stable if the LCL resonance is below the critical frequency due to its inherent damping



[13]

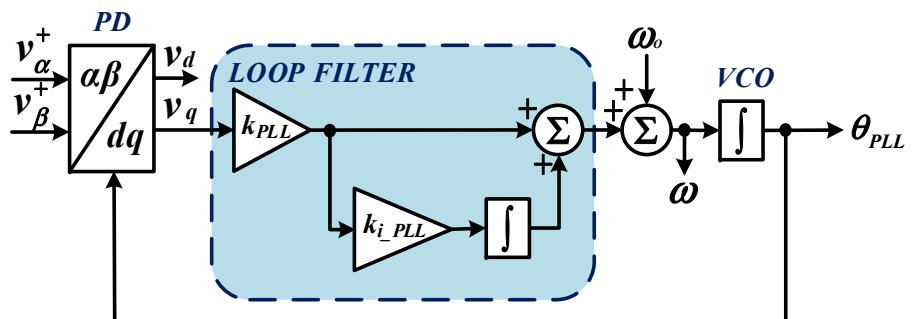
Comparison of GCF and ICF



GCF controller requires additional loop and current sensors for active damping and its tuning is not straightforward.

ICF controller although is cost effective poorly performs under distorted grid conditions due to lack of grid side current information.

In both cases, voltage sensors are required and the PLL bandwidth for both approaches is limited for a direct voltage fed PLL.



Voltage Measurement Synchronous Frame PLL

Self-Synchronising ICF Control (SSICF) [13] [14]

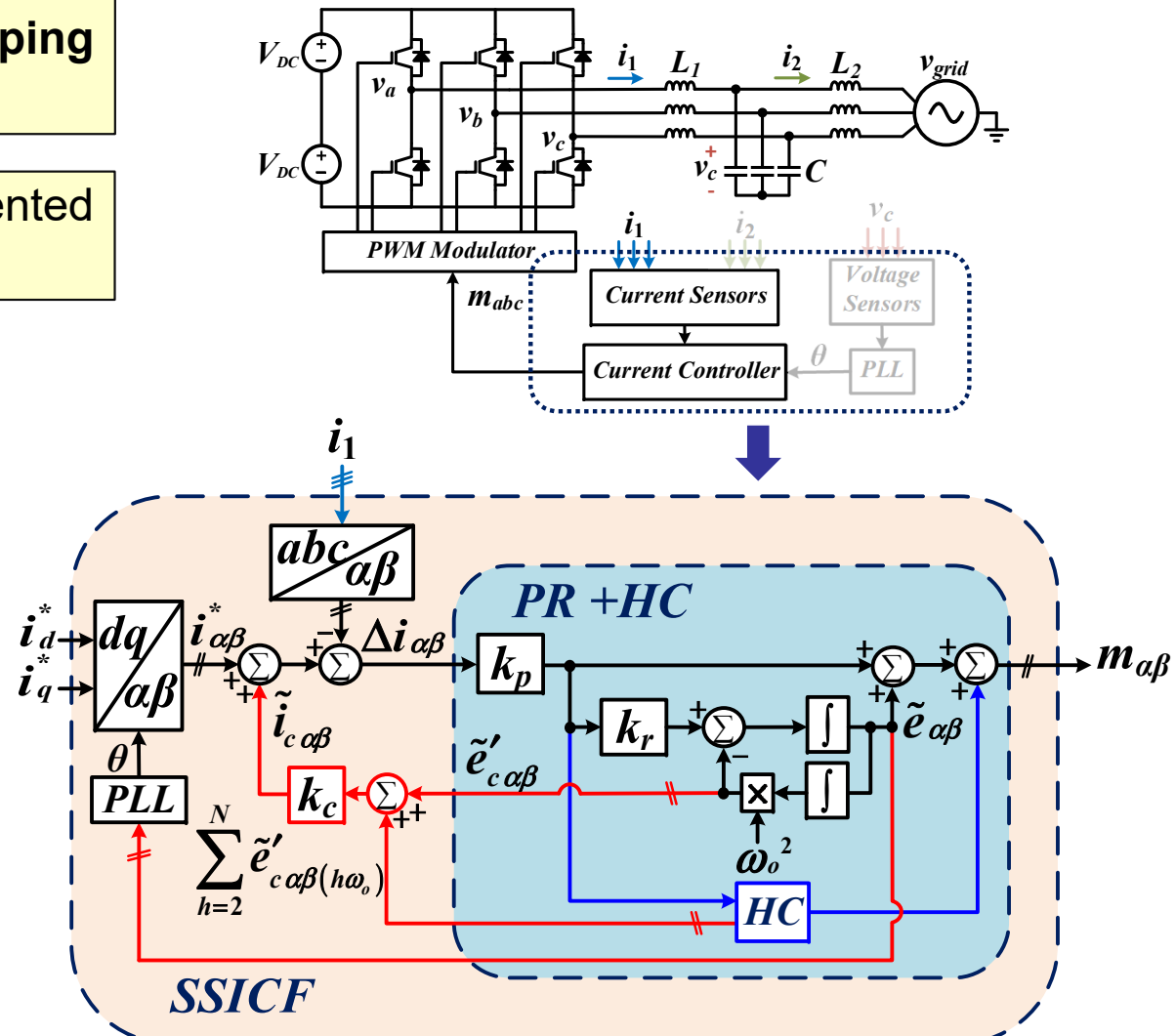
Strategy uses a **standard ICF control concept**, with its **inherent damping properties**.

The **PR + HC controller** is implemented using **SOGI resonator realisations**.

SOGI architecture is the key enabling element to self-synchronise.

Capacitor current and its harmonic contents can be estimated from the **PR SOGI**.

SSICF control requires only one current sensor per regulated phase with inherent damping, self-synchronising and immunity to disturbance effects of grid voltage harmonics.



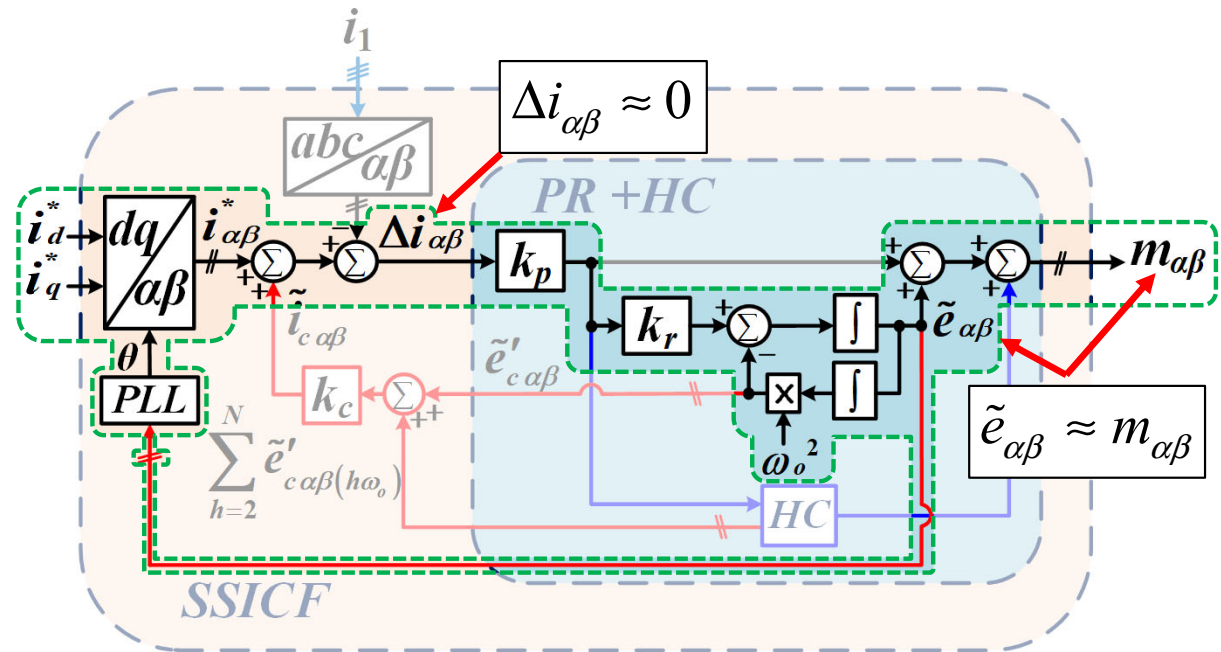
[13]

Self-Synchronising ICF Control (SSICF)

SSICF Principles

Under **steady state**, the **PR+HC controller eliminates all errors** between the **reference** and the **inverter side current**.

The **modulation command signals** is **equal** to the **resonators output**.



SOGI output will be *in-phase* with the inverter terminal voltage, and therefore approximately *in-phase* with the capacitor voltage and hence the grid voltage.

$$\angle \tilde{e}_{\alpha\beta} \approx \angle v_c \approx \angle v_{grid}$$

Feeding the SOGI output signals into a PLL will approximate the grid phase angle, θ .

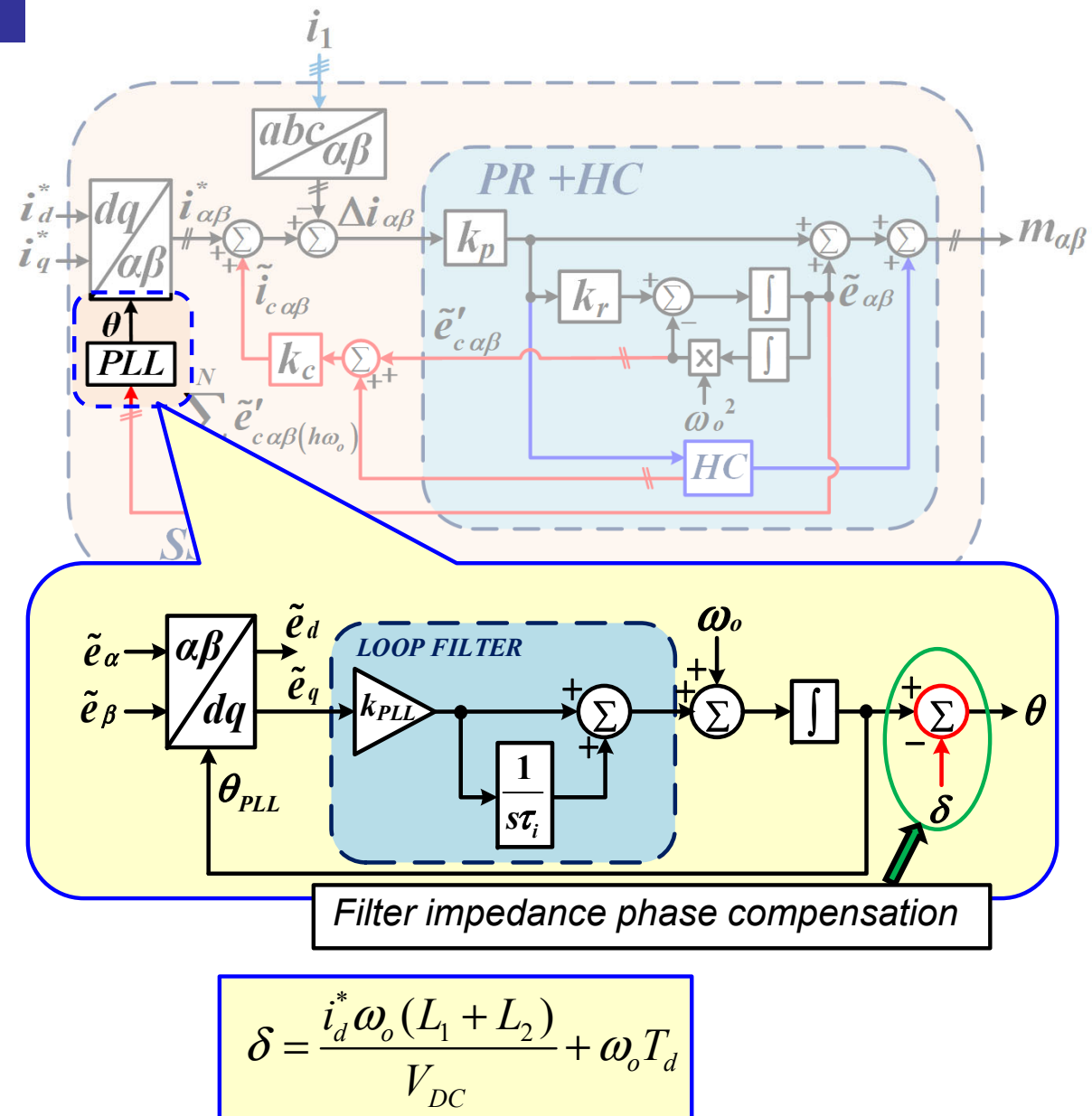
Self-Synchronising ICF Control (SSICF) - PLL

Filter Impedance Compensation

Voltage drop across the LCL inductors mostly introduces a small quadrature phase shift.

PLL without filter impedance compensation generates a phase reference that slightly leads the actual grid voltage phase.

Grid phase estimation can be improved by adding a compensation factor since the filter inductances are well defined.



Self-Synchronising ICF Control (SSICF)

LCL Capacitor Feedforward Compensation

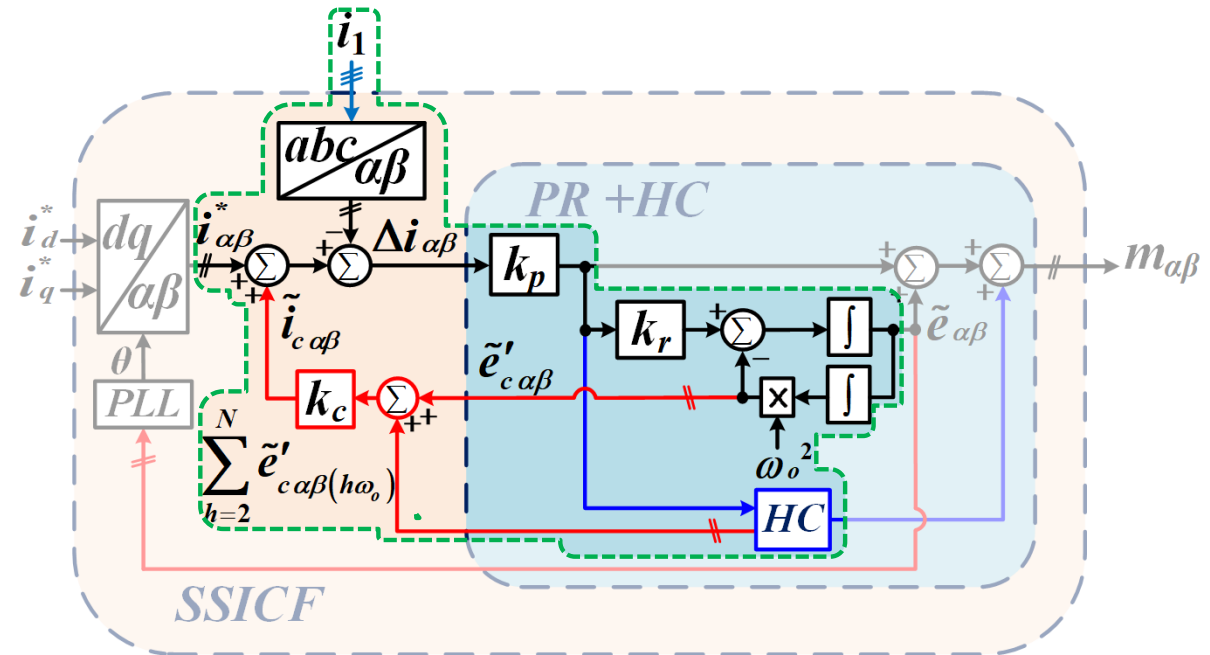
The LCL capacitor time domain voltage and current are

$$v_c(t) = V_c \sin(\omega_o t)$$

$$i_c(t) = C \frac{dv_c}{dt} = C \omega_o V_c \cos(\omega_o t)$$

Applying the relationship:

$$\angle \tilde{e}_{\alpha\beta} \approx \angle v_c \approx \angle v_{grid}$$



Time domain per phase output of the PR resonator can be defined in per unit terms as:

$$\tilde{e}(t) \approx \frac{V_c}{V_{DC}} \sin(\omega_o t)$$

Second integrator

$$\begin{aligned} \tilde{e}'(t) &= \omega_o^2 \int \frac{V_c}{V_{DC}} \sin(\omega_o t) dt \\ &= -\frac{\omega_o V_c}{V_{DC}} \cos(\omega_o t) \end{aligned}$$

Self-Synchronising ICF Control (SSICF)

LCL Capacitor Feedforward Compensation

Comparing:

$$i_c(t) = C\omega_o V_c \cos(\omega_o t)$$

$$\tilde{e}'_c(t) = -\frac{\omega_o V_c}{V_{DC}} \cos(\omega_o t)$$

The capacitor current can be estimated using:

$$i_c(t) = k_c \tilde{e}'_c(t) \quad \text{where} \quad k_c = -CV_{DC}$$

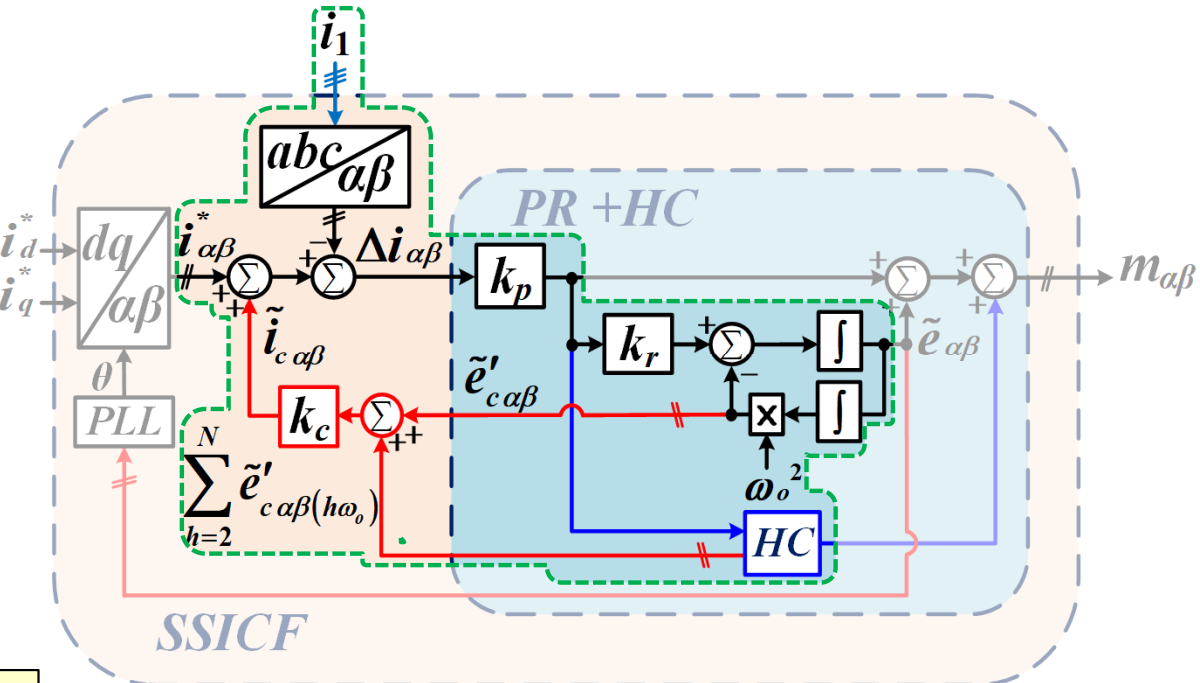
The estimated capacitor current can be subtracted from the reference currents to indirectly regulate the grid current since

$$i_2(t) = i_1(t) - i_c(t)$$

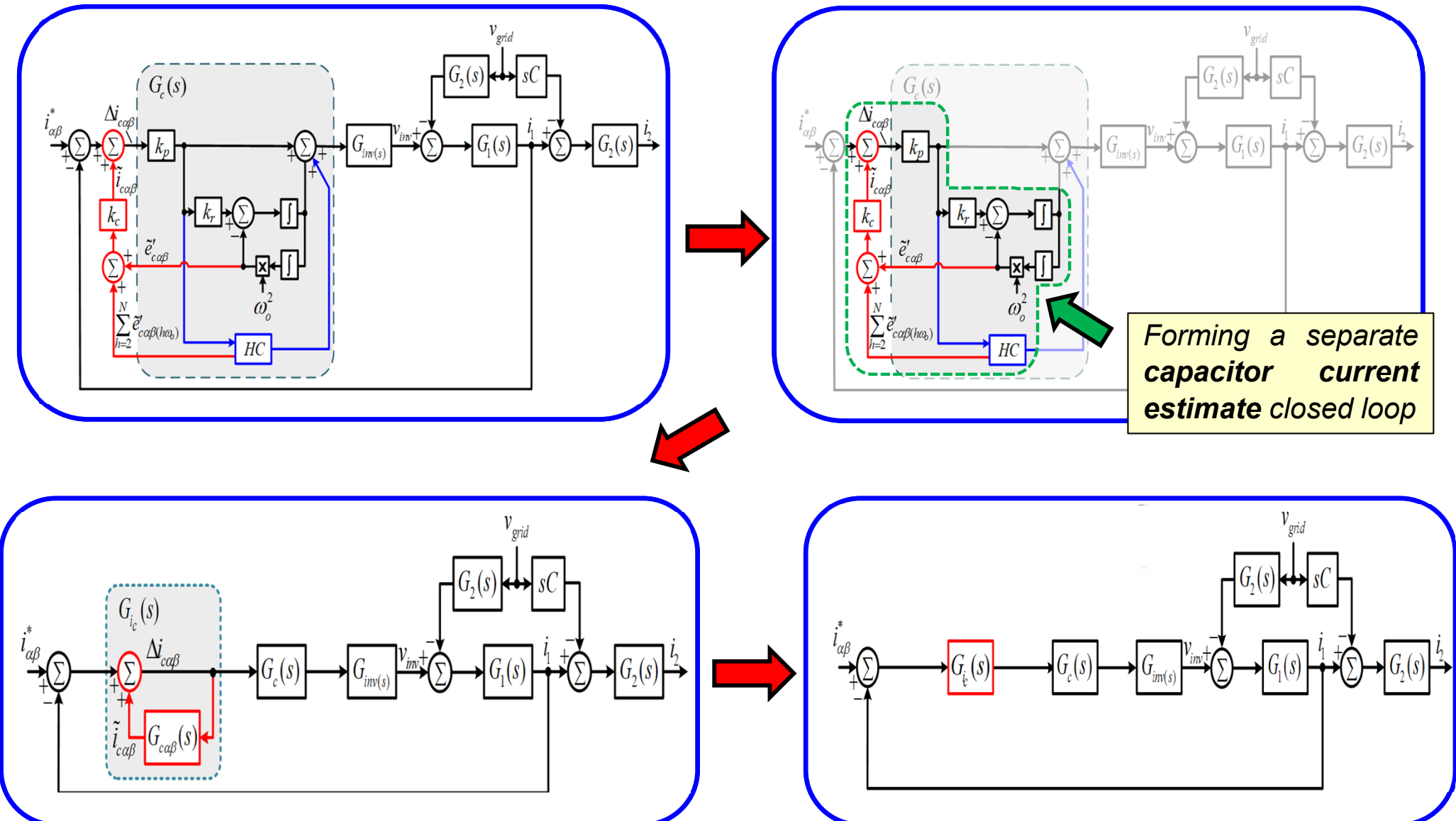
Each harmonic SOGI output is a pure sinusoid at the applicable frequency

Hence overall capacitor current estimation via superposition is:

$$\tilde{i}_{c\alpha\beta}(s) = k_c \left(\tilde{e}'_{c\alpha\beta}(s) + \sum_{h=2}^N \tilde{e}'_{c\alpha\beta(h\omega_o)}(s) \right)$$



Reduction of SSICF for Disturbance Rejection Analysis



SSICF - Disturbance Rejection Analysis

The objective is to indirectly regulate the grid- side current. Hence the controller transfer function must be developed as a function of grid-side current to evaluate its performance.

PR+ HC Current Controller:

$$G_c(s) = k_p \left(1 + k_r \frac{s}{s^2 + \omega_o^2} + \sum_{h=2}^N k_{r,h} \frac{s}{s^2 + h^2 \omega_o^2} \right)$$

Capacitor current estimate:

$$\begin{aligned} \tilde{i}_{c\alpha\beta}(s) &= k_c k_p \left(k_r \frac{\omega_o^2}{s^2 + \omega_o^2} + \sum_{h=2}^N k_{r,h} \frac{h^2 \omega_o^2}{s^2 + h^2 \omega_o^2} \right) \Delta i_{\alpha\beta}(s) \\ &= G_{c\alpha\beta}(s) \Delta i_{\alpha\beta}(s) \end{aligned}$$

Capacitor current estimate closed loop function:

$$G_{i_c}(s) = \frac{1}{1 - G_{c\alpha\beta}(s)}$$

Plant Transfer function:

$$G_1(s) = \frac{s^2 L_2 C + 1}{s^3 L_1 L_2 C + s(L_1 + L_2)}$$

$$G_2(s) = \frac{1}{s^2 L_2 C + 1}$$

$$G_{inv}(s) = V_{DC} e^{-sT_d}$$

The overall closed loop transfer function as a function of grid-side current is :

$$i_2(s) = i_{\alpha\beta}^* \frac{G_{i_c}(s) G_c(s) G_{inv}(s) G_1(s) G_2(s)}{1 + G_{i_c}(s) G_c(s) G_{inv}(s) G_1(s)} - v_{grid} \left(\frac{G_1(s) G_2(s) G_2(s)}{1 + G_{i_c}(s) G_c(s) G_{inv}(s) G_1(s)} + s C G_2(s) \right)$$

Grid-side current tracking error

Grid voltage disturbance rejection



$$Y_{g2} = \frac{i_2}{v_{grid}}$$

SSICF - Disturbance Rejection

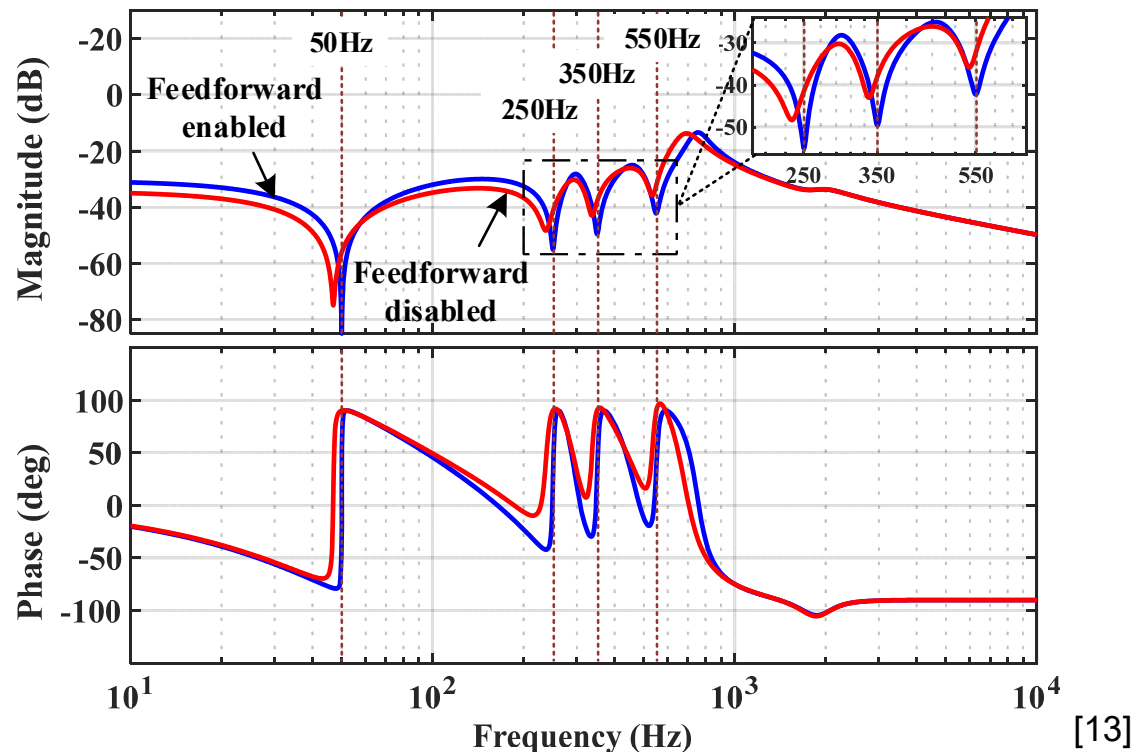
Without capacitor feedforward:

- Grid side disturbance rejection admittance resonant notches shift away from the grid fundamental and harmonic resonant frequencies.

With capacitor current feedforward compensation:

- Grid side disturbance rejection admittance notches return exactly to their target frequencies.

The feedforward capacitor current compensation of the SSICF controller substantially improves its grid-side harmonic disturbance rejection capability while still only requiring only one current sensor per regulated phase.



[13]

$$Y_{gICF}(s) = \left(sL_2 + \frac{1}{sC} \left(1 - \frac{1}{s^2 L_1 C + sCG_c(s)G_{inv}(s) + 1} \right) \right)^{-1}$$

$$Y_{gSSICF}(s) = \left(sL_2 + \frac{1}{sC} \left(1 - \frac{1}{s^2 L_1 C + sCG_{ic}(s)G_c(s)G_{inv}(s) + 1} \right) \right)^{-1}$$

SSICF - Stability Analysis

The discrete form characteristic equation is :

$$1 + G_{i_c}(z)G_c(z)G_{inv}(z)G_1(z)G_2(z) = 0$$

where

$$G_c(z) = k_p$$

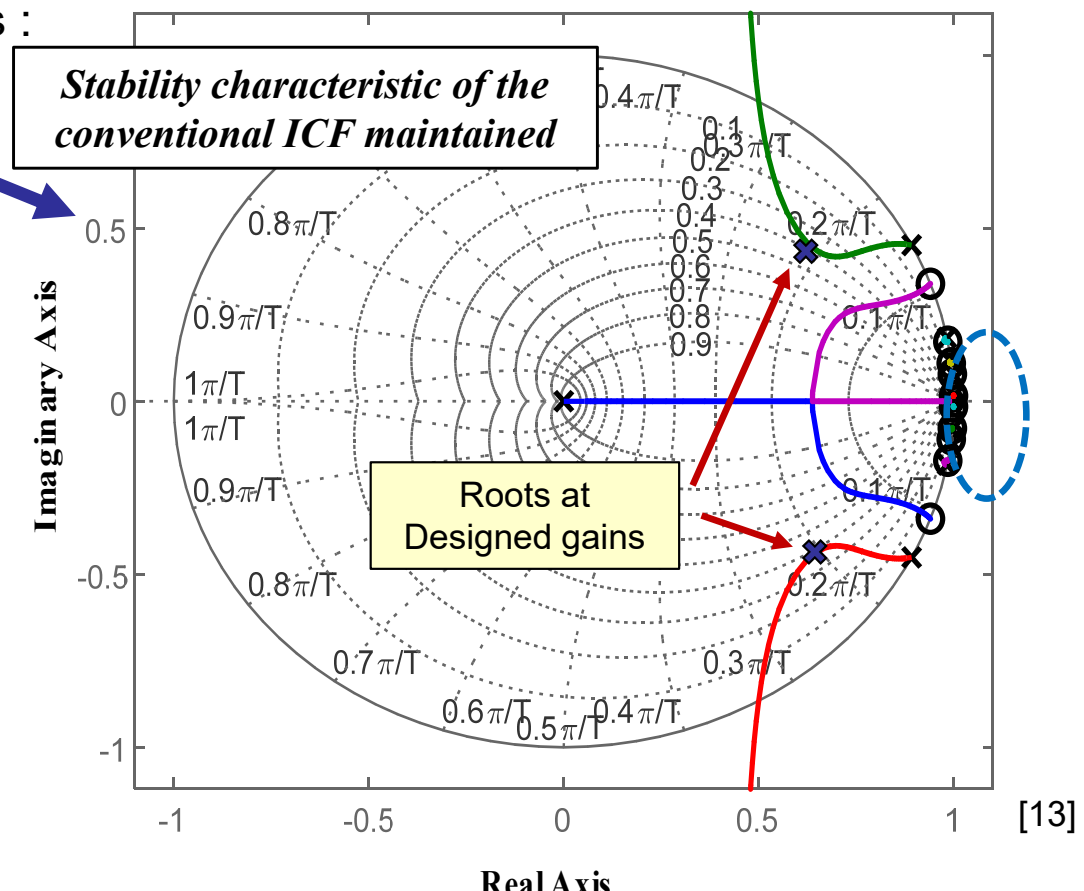
PR+HC current controller replaced with proportional gain.

$$G_{i_c}(z) = \frac{1}{1 - G_{co\beta}(z)}$$

PR SOGI capacitor current feedforward term

$$G_{co\beta}(z) = k_c k_p \left(k_r \sin\left(\frac{\omega_o T}{2}\right)^2 \frac{(z+1)^2}{z^2 - 2\cos(\omega_o T)z + 1} \right. \\ \left. + \sum_{h=2}^N k_{r,h} \sin\left(\frac{h\omega_o T}{2}\right)^2 \frac{(z+1)^2}{z^2 - 2\cos(h\omega_o T)z + 1} \right)$$

PR SOGI capacitor current feedforward in discrete time form using Tustin transformation with pre-warping.



The current controller gain can be calculated using :

$$\omega_{c(\max)} = \frac{\pi/2 - \phi_m}{1.5/T}$$

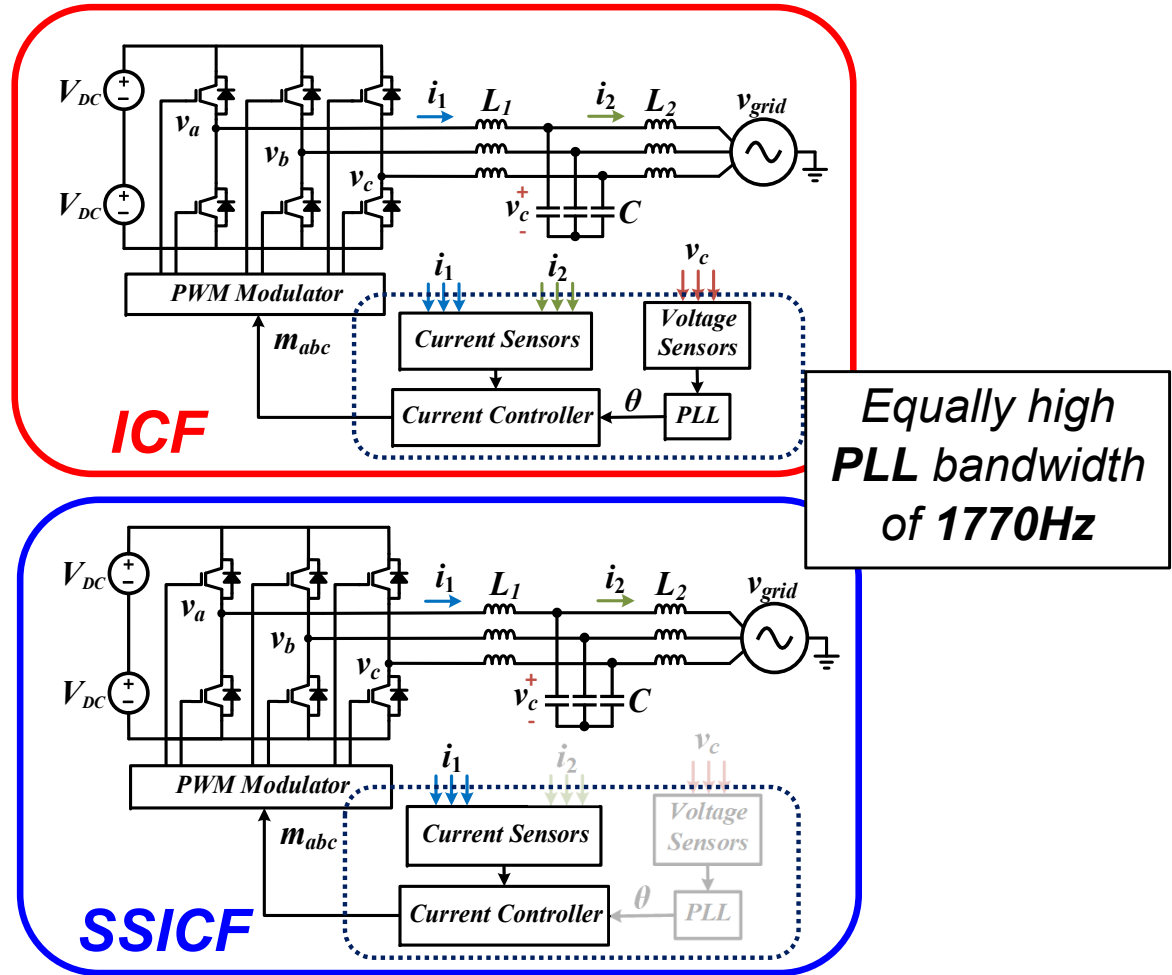
$$k_p = \frac{\omega_{c(\max)}(L_1 + L_2)}{V_{DC}}$$

$$k_r = \frac{\omega_{c(\max)}}{10}$$

SSICF - Simulation & Experimental Parameters

Parameters	Description	Values
V_{grid}	Grid Voltage	415Vrms
$2V_{\text{DC}}$	DC link voltage	650V
f_{nom}	Nominal frequency	50Hz
f_{sw}	Switching frequency	10kHz
f_s	Sampling frequency	20kHz
L_1	Inverter-side inductor	5mH
L_2	Grid-side inductor	4.2mH
C	Filter capacitor	5 μF

Simulation System:
PSIM software

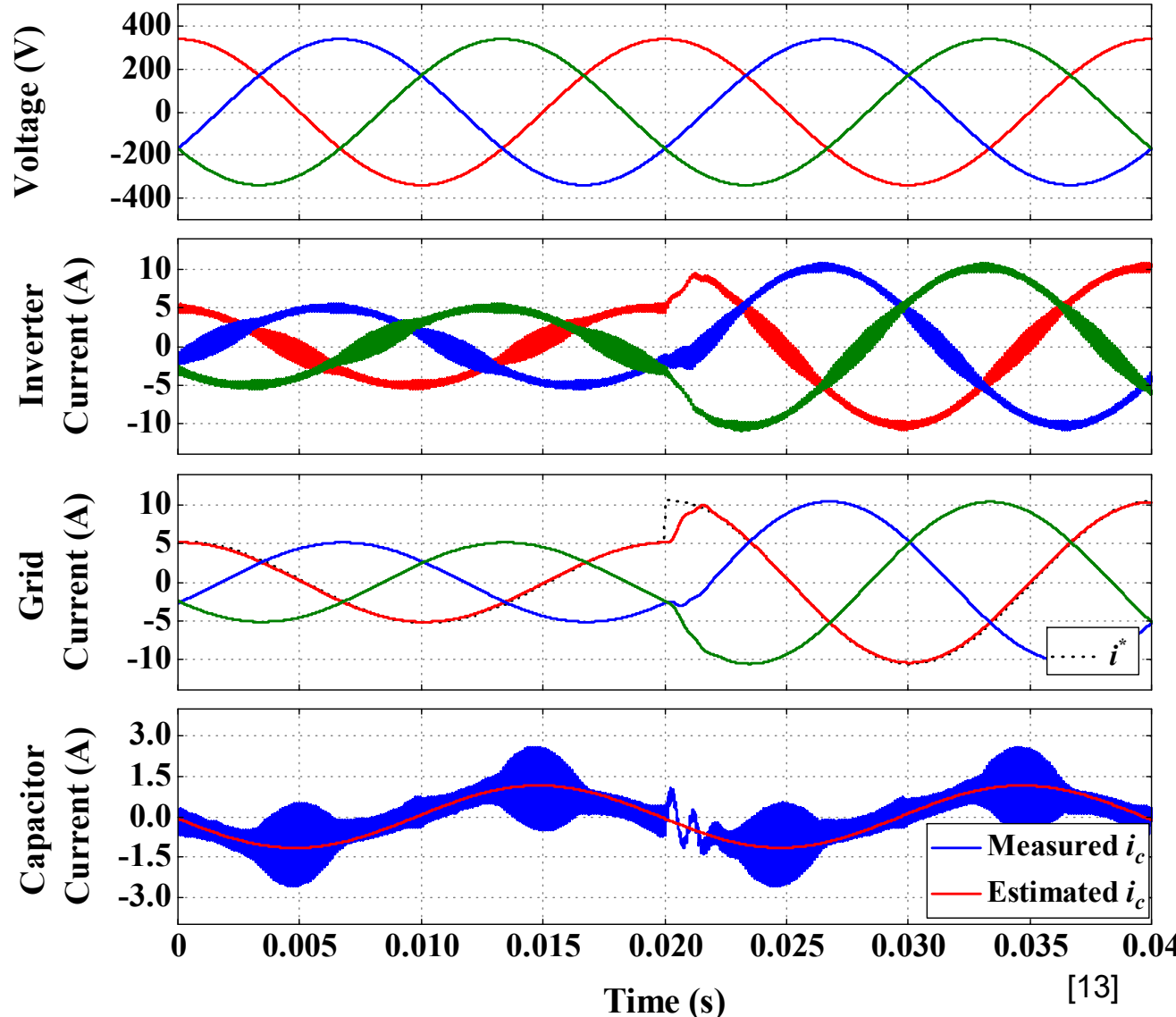


Experimental System:

- TMS320F2810 digital signal processor
- MX30 California Instrument grid emulator.

SSICF - Simulation Result

Transient response of SSICF control for a current step change

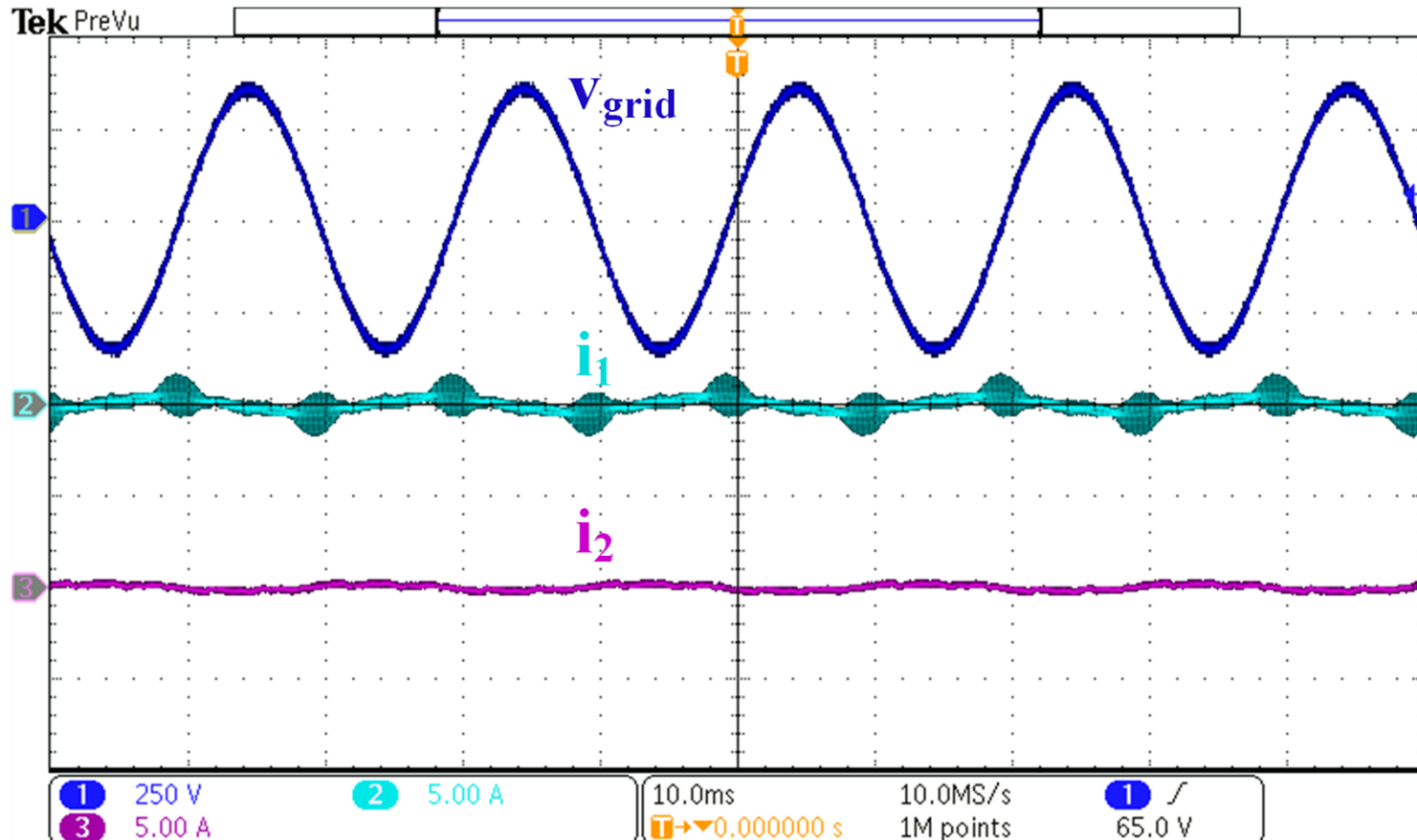


- Accurately estimates the capacitor current.
- Minimizes the fundamental phase error by subtracting the capacitor current estimate from the PLL derived current reference.
- Indirectly regulates the grid-side current very accurately.

Exhibits similar transient performance as conventional ICF

SSICF - Experimental Result

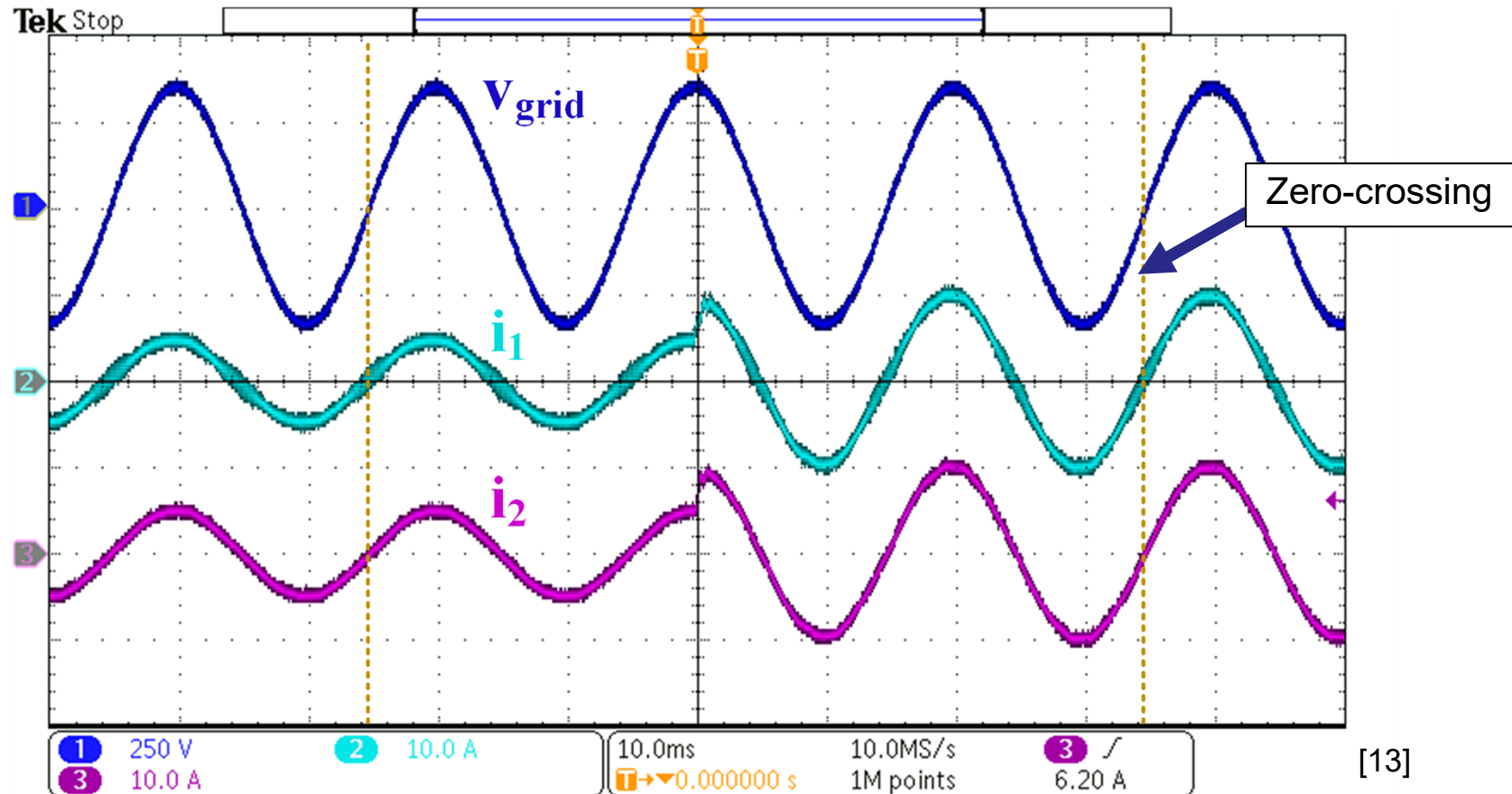
SSICF control regulating at 0A



- Indirectly regulates the grid current **to 0A** thanks to the PR SOGI capacitor current feedforward of the **SSICF control**.

SSICF - Experimental Result

Transient response of the SSICF control for a current step change

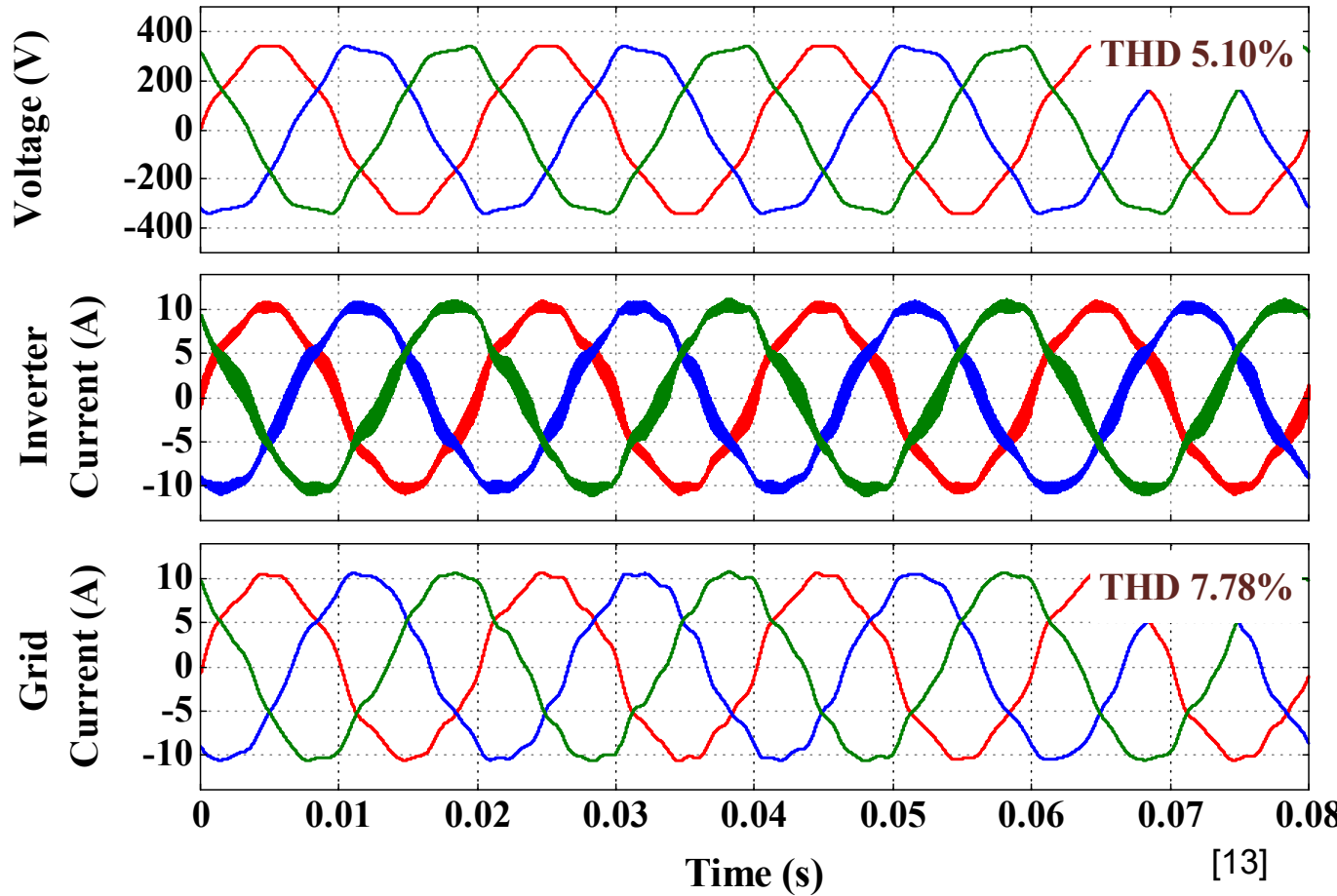


[13]

- Exhibits **the same transient response as in simulation** (thus confirming the practical viability of the controller).
- **Grid voltage and grid current are essentially in phase.**

ICF – Distorted Grid: Simulation Result

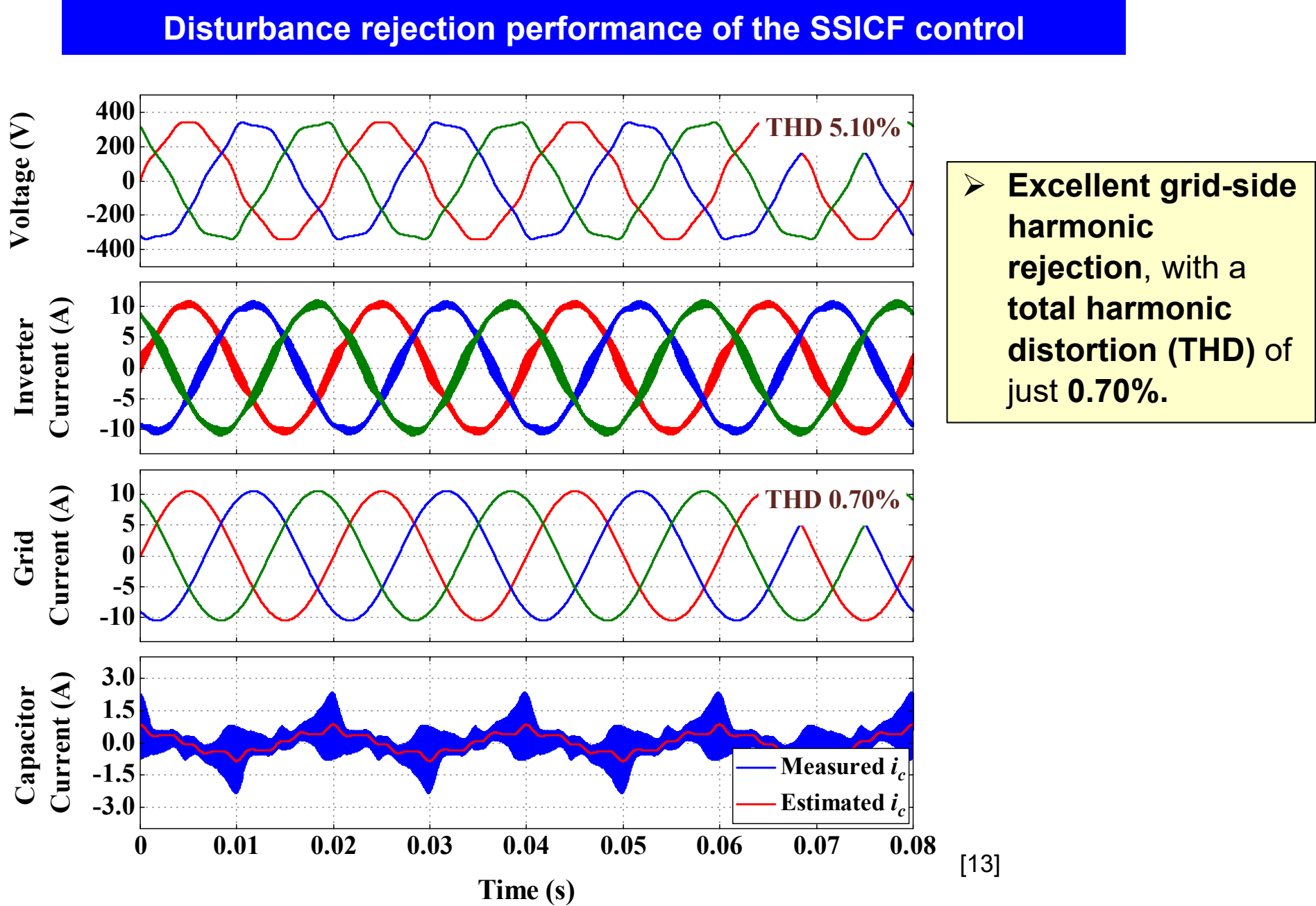
Disturbance rejection performance of the conventional ICF control



- Increased THD caused by the high bandwidth PLL allowing harmonics to flow through and create a **distorted current reference**.
- Conventional ICF is also unable to **reject grid-side current harmonics**.

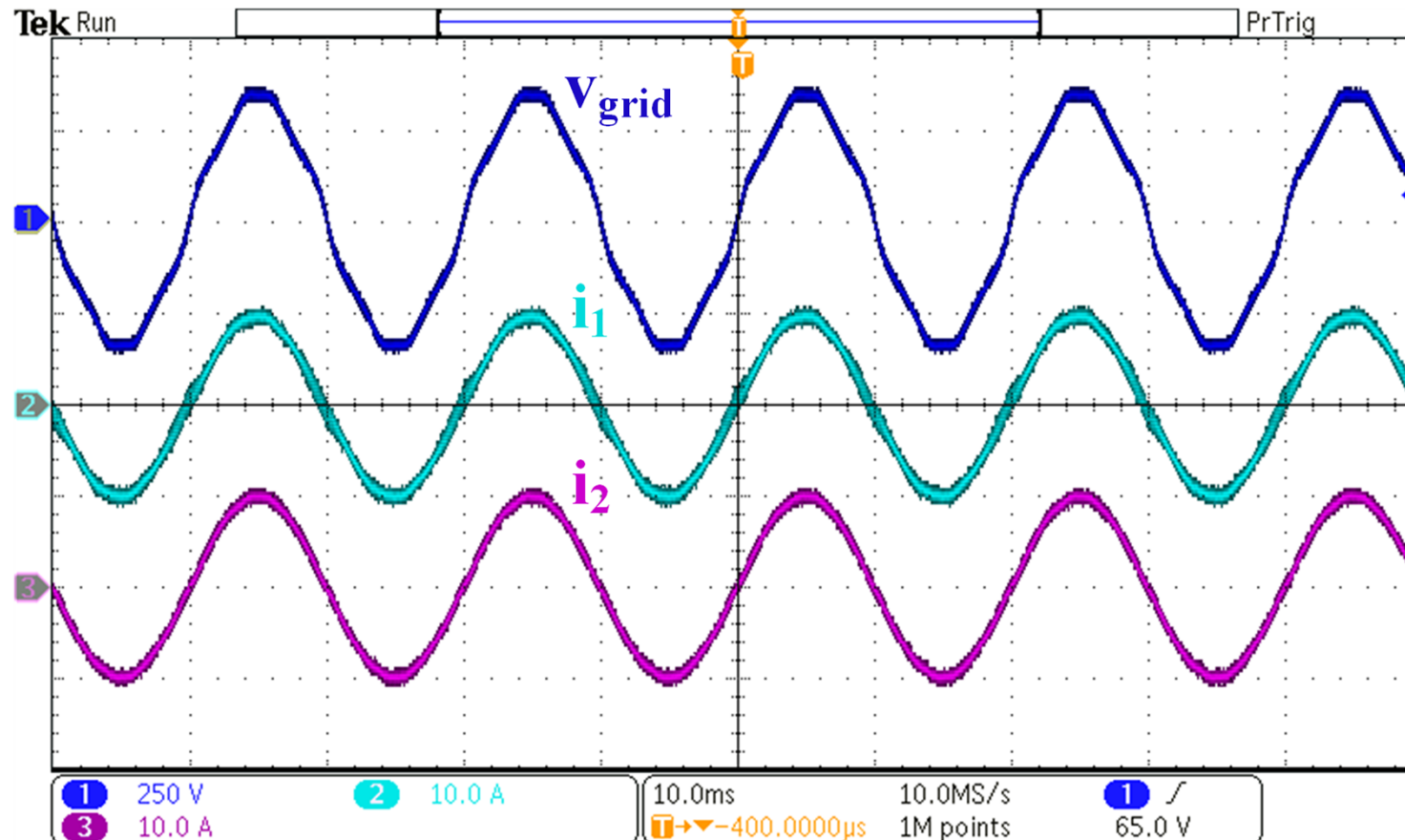
Harmonic distortion at the 5th (4%), 7th (3%) and 11th (1%) harmonic frequencies

SSICF – Distorted Grid: Simulation Result



SSICF – Distorted Grid: Experimental Result

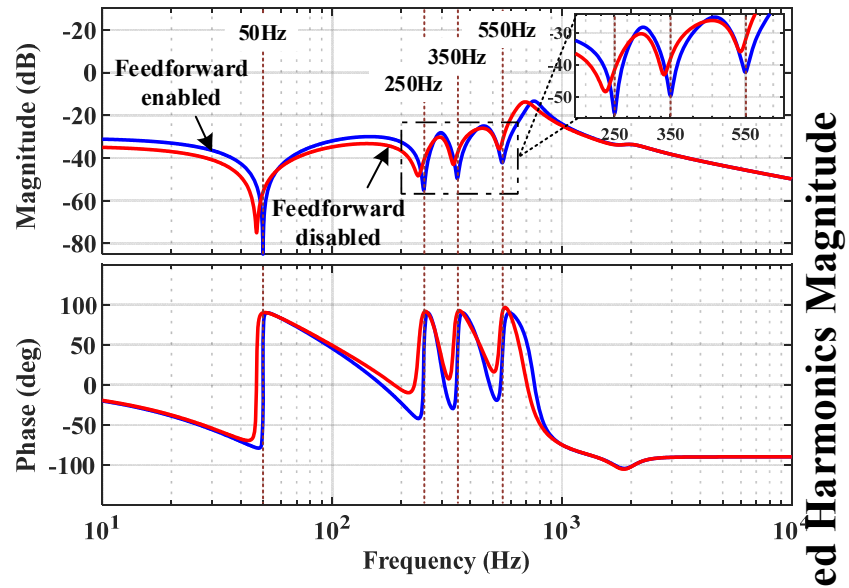
Disturbance rejection performance of the SSICF control
with capacitor current feedforward enabled



[13]

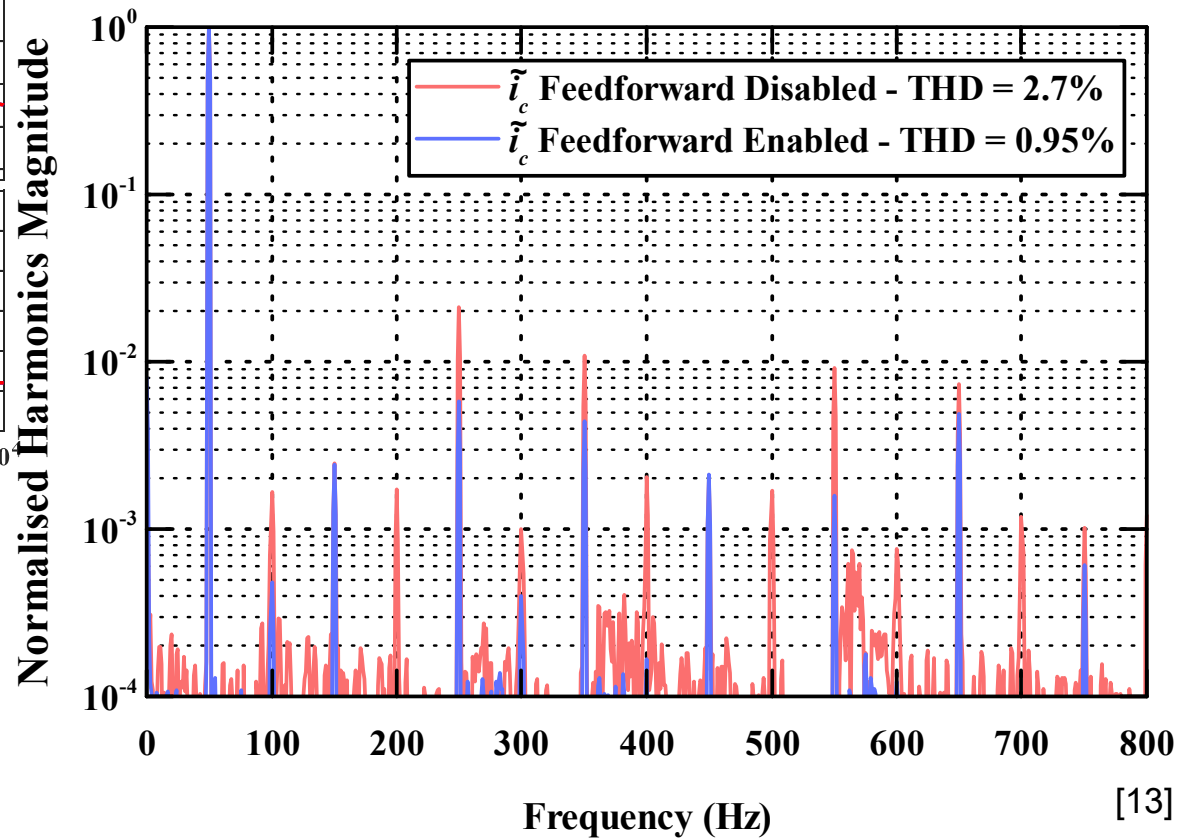
SSICF – Distorted Grid: Experimental Result

Harmonic Spectrum of SSICF Control with capacitor current feedforward enabled and disabled



With the capacitor current feed forward disabled, the attenuation occurs slightly away from the desired harmonic frequencies. This agrees with the disturbance rejection analysis.

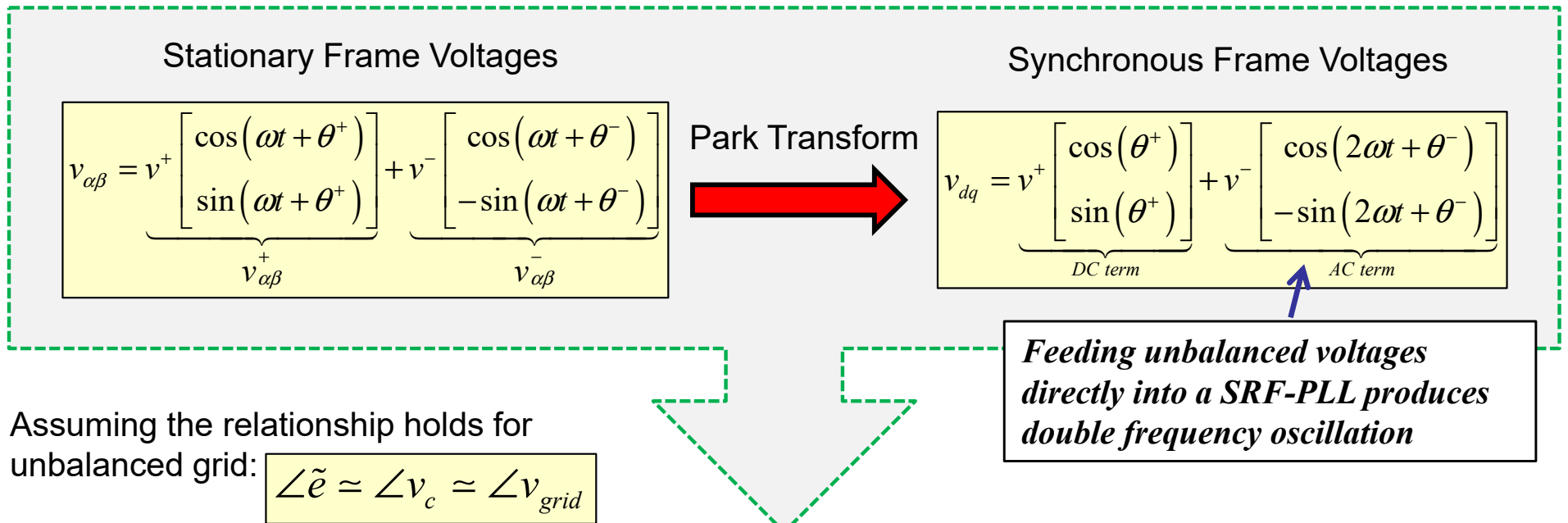
Disturbance rejection performance



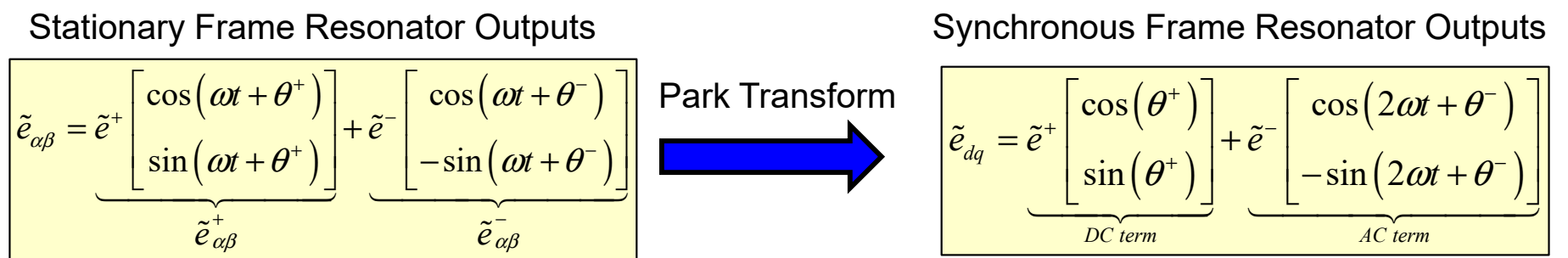
[13]

SSICF with Unbalanced Grid [15]

Voltage Double frequency Oscillation in Synchronous Frame:



Resonator Outputs Double frequency Oscillation in Synchronous Frame:



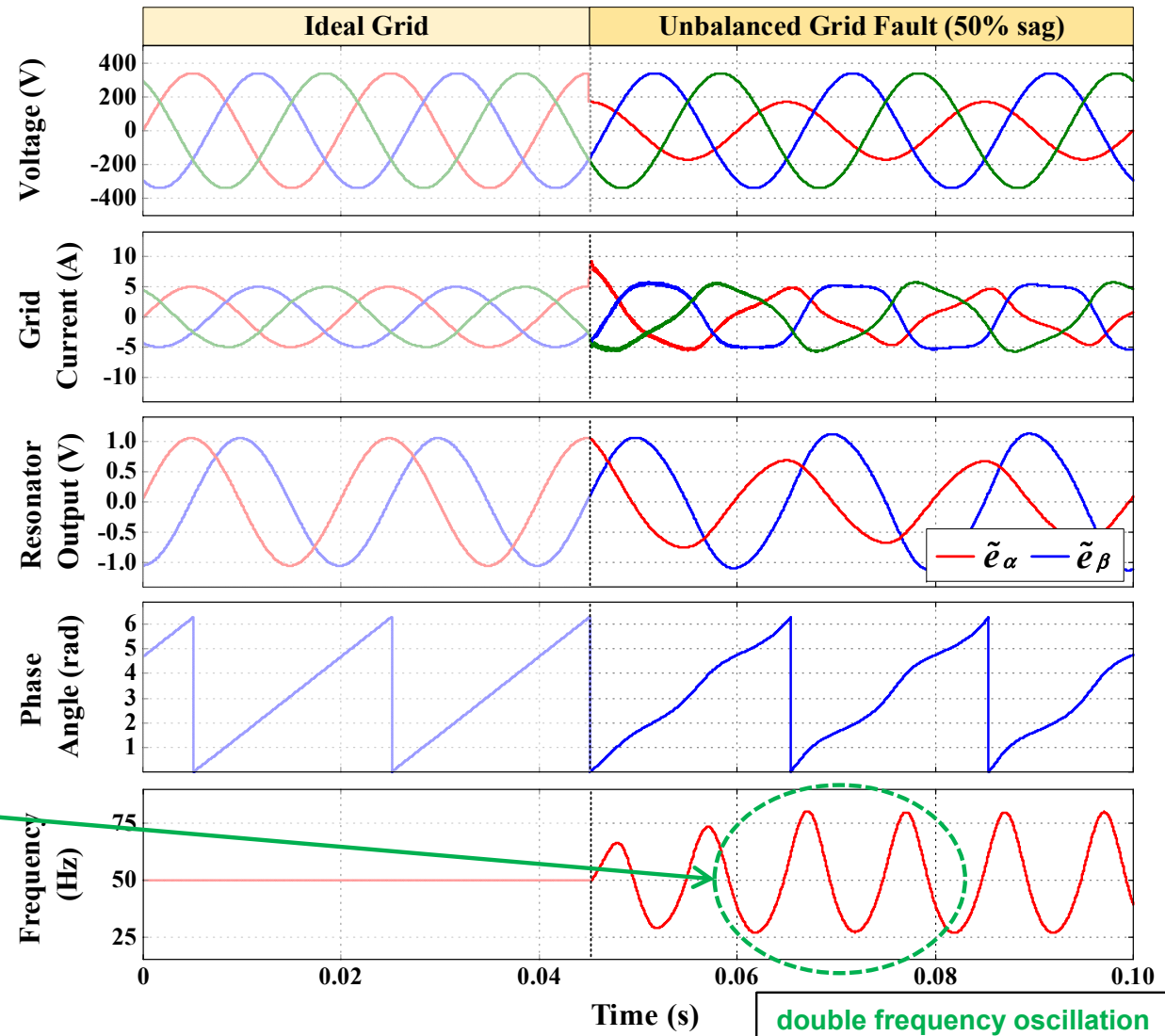
SSICF with Unbalanced Grid

Uncompensated Performance with Unbalanced Grid:

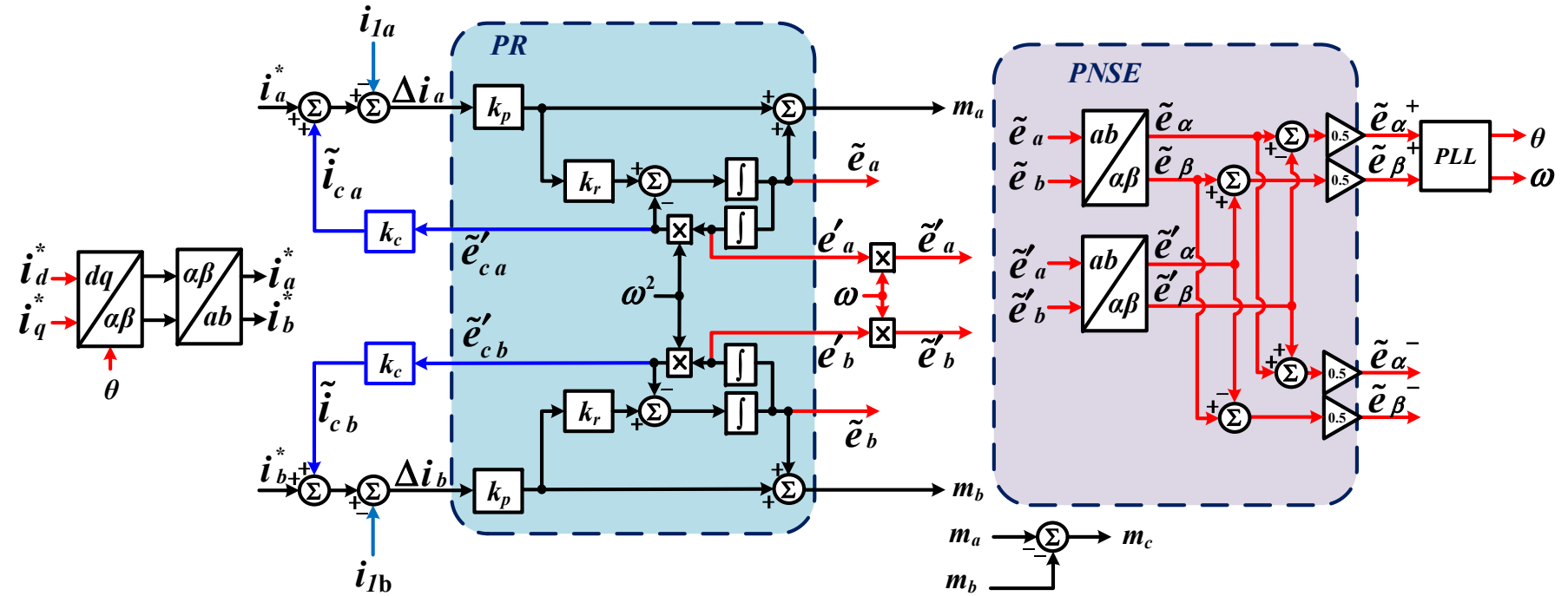
- **Unbalanced SOGI resonator output vector has the same double frequency oscillation AC term (in the synchronous frame) as the physical unbalanced grid voltages.**

- Adversely impacts the SRF-PLL performance.
- Injected currents become significantly distorted.

$$\tilde{e}_{dq} = \underbrace{\tilde{e}^+ \begin{bmatrix} \cos(\theta^+) \\ \sin(\theta^+) \end{bmatrix}}_{DC\ term} + \underbrace{\tilde{e}^- \begin{bmatrix} \cos(2\omega t + \theta^-) \\ -\sin(2\omega t + \theta^-) \end{bmatrix}}_{AC\ term}$$

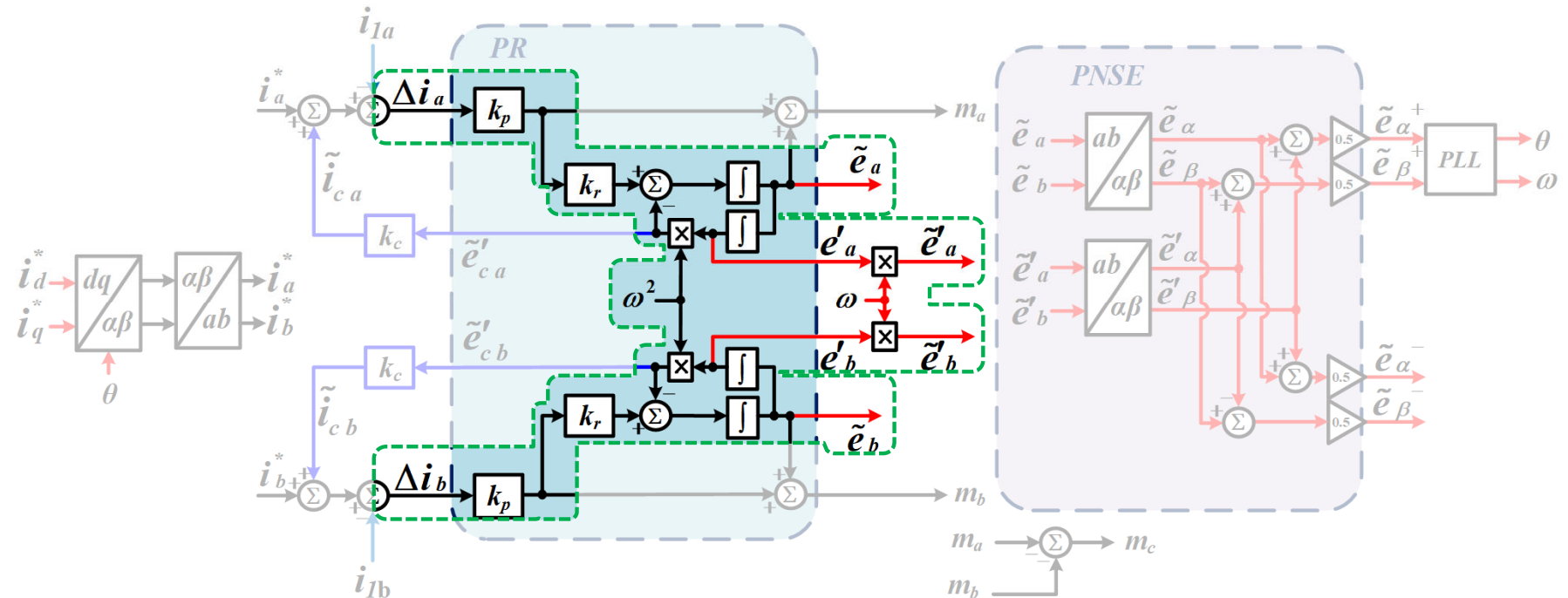


SSICF with Unbalanced Grid



- Strategy indirectly extracts the positive and negative sequence components of the unbalanced grid from the internal direct and quadrature terms of the current regulator resonator outputs.
- The PLL is synchronised to the positive sequence components of the resonator outputs – does not respond to unbalance ripple and still provides harmonic filtering.

SSICF - Sequence Extraction



SOGI implementation of the stationary frame PR current regulators intrinsically generates direct and quadrature terms for each regulator in the abc frame of reference.

Direct

$$\tilde{e}_x(s) = k_p k_r \left[\frac{s}{s^2 + \omega^2} \right] \Delta i_x(s)$$

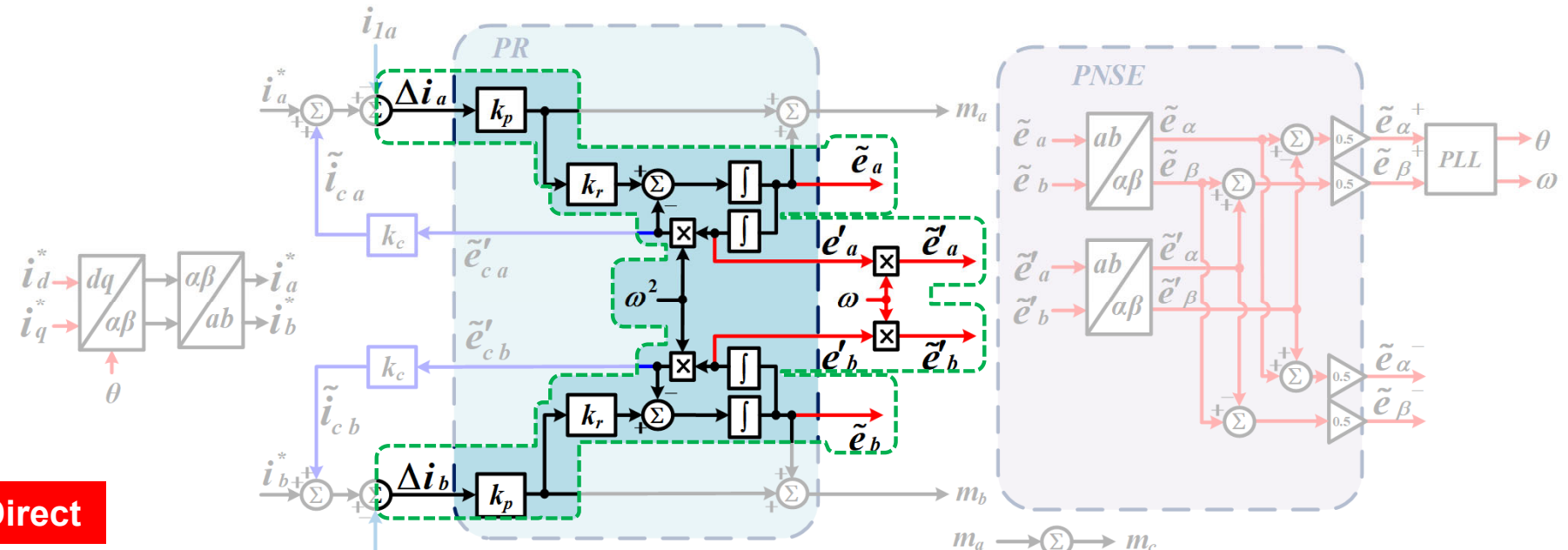
$x \in a, b$

Quadrature

$$\begin{aligned} e'_x(s) &= k_p k_r \frac{1}{s} \left[\frac{s}{s^2 + \omega^2} \right] \Delta i_x(s) \\ &= k_p k_r \left[\frac{1}{s^2 + \omega^2} \right] \Delta i_x(s) \end{aligned}$$

Shifts by a lagging 90° and a reduced magnitude factor of $|s|$

SSICF - Sequence Extraction



$$\tilde{e}_x(s) = k_p k_r \left[\frac{s}{s^2 + \omega^2} \right] \Delta i_x(s) \quad x \in a, b$$

Quadrature

$$\begin{aligned} e'_x(s) &= k_p k_r \frac{1}{s} \left[\frac{s}{s^2 + \omega^2} \right] \Delta i_x(s) \\ &= k_p k_r \left[\frac{1}{s^2 + \omega^2} \right] \Delta i_x(s) \end{aligned}$$

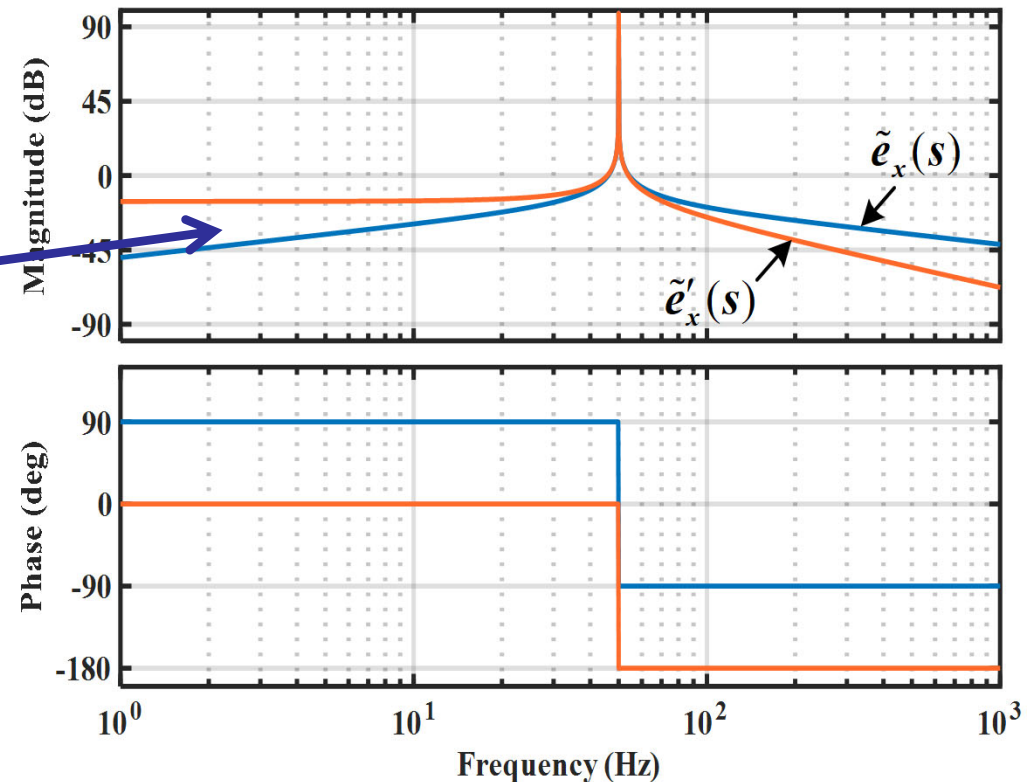
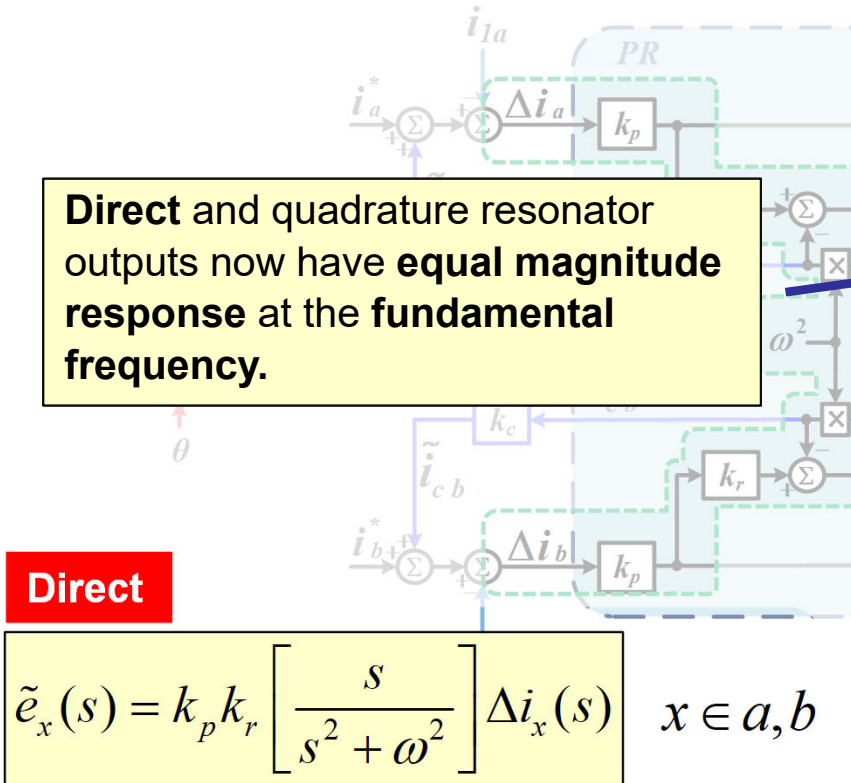
Scaled by ω

Scaled Quadrature

$$\tilde{e}'_x(s) = k_p k_r \left[\frac{\omega}{s^2 + \omega^2} \right] \Delta i_x$$

For sequence extraction from the resonator outputs, both direct and quadrature must have the same magnitude.

SSICF - Sequence Extraction



$$e'_x(s) = k_p k_r \frac{1}{s} \left[\frac{s}{s^2 + \omega^2} \right] \Delta i_x(s)$$

$$= k_p k_r \left[\frac{1}{s^2 + \omega^2} \right] \Delta i_x(s)$$

Scaled by ω

Scaled Quadrature

$$\tilde{e}'_x(s) = k_p k_r \left[\frac{\omega}{s^2 + \omega^2} \right] \Delta i_x$$

SSICF - Sequence Extraction

Transforming ab signals into $\alpha\beta$ signals:

$$\tilde{e}_y(s) = [T'_{\alpha\beta}] \tilde{e}_x(s)$$

$$\tilde{e}'_y(s) = [T'_{\alpha\beta}] \tilde{e}'_x(s)$$

where:

$$[T'_{\alpha\beta}] = \begin{bmatrix} 1 & 0 \\ \frac{1}{\sqrt{3}} & \frac{2}{\sqrt{3}} \end{bmatrix}$$

Reduced Clarke transformation can be used since

$$\tilde{e}_c = -(\tilde{e}_a + \tilde{e}_b)$$

Positive sequence components

$$\begin{bmatrix} \tilde{e}_\alpha^+(t) \\ \tilde{e}_\beta^+(t) \end{bmatrix} = \frac{1}{2} \begin{bmatrix} \tilde{e}_\alpha(t) - \tilde{e}_\beta(t) \\ \tilde{e}_\beta(t) + \tilde{e}_\alpha(t) \end{bmatrix}$$

Negative sequence components

$$\begin{bmatrix} \tilde{e}_\alpha^-(t) \\ \tilde{e}_\beta^-(t) \end{bmatrix} = \frac{1}{2} \begin{bmatrix} \tilde{e}_\alpha(t) + \tilde{e}_\beta(t) \\ \tilde{e}_\beta(t) - \tilde{e}_\alpha(t) \end{bmatrix}$$

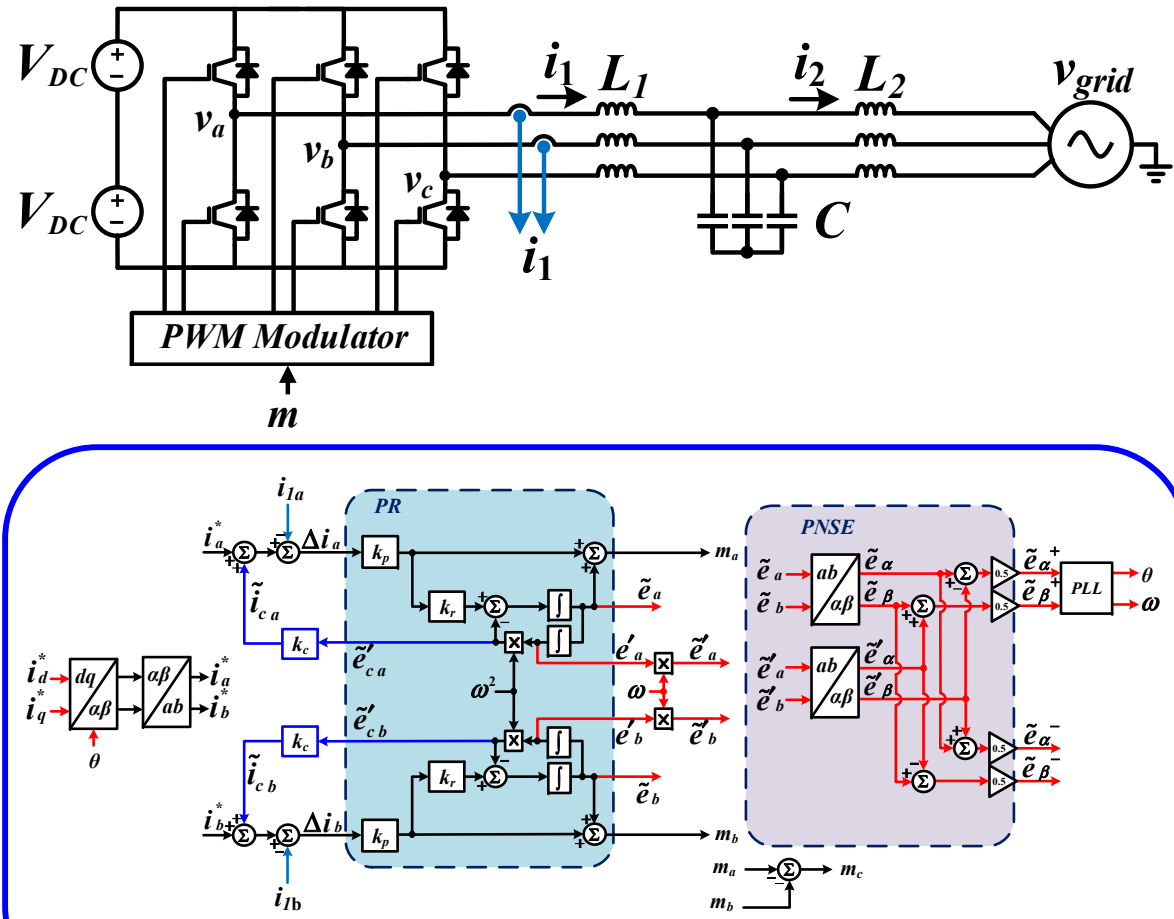
Recall: $\tilde{e} \approx m$

- Positive sequence components provides a set of **balanced synchronizing signals**.
- Feeds into PLL to create balanced three phase current references despite unbalance grid voltages.

SSICF - Simulation & Experimental Parameters

Parameters	Description	Values
V_{grid}	Grid Voltage	415Vrms
$2V_{DC}$	DC link voltage	650V
f_{nom}	Nominal frequency	50Hz
f_{sw}	Switching frequency	10kHz
f_s	Sampling frequency	20kHz
L_1	Inverter-side inductor	5mH
L_2	Grid-side inductor	4.2mH
C	Filter capacitor	5μF

Simulation System:
PSIM software

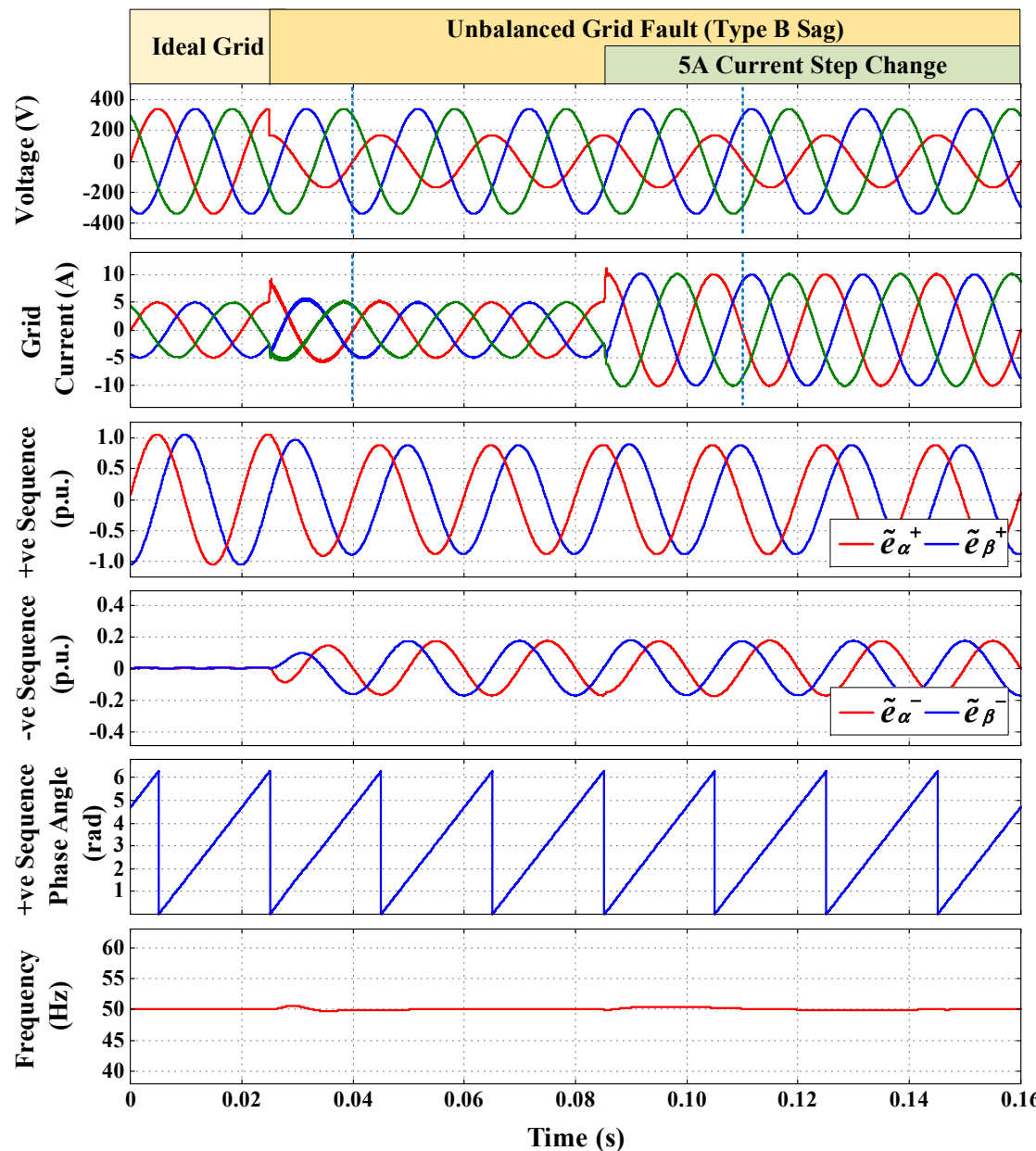


Proposed Control

Experimental System:

- TMS320F2810 digital signal processor
- MX30 California Instrument grid emulator.

SSICF - Simulation Result Type B Grid Fault



Type B Grid Fault

Transient response during type B grid fault transient and a **50% current step change** from $5A_{pk}$ to $10A_{pk}$.

Single line to ground fault is inflicted on phase a grid voltage at $t=0.025s$ to give a 50% voltage sag with a positive and negative sequence of:

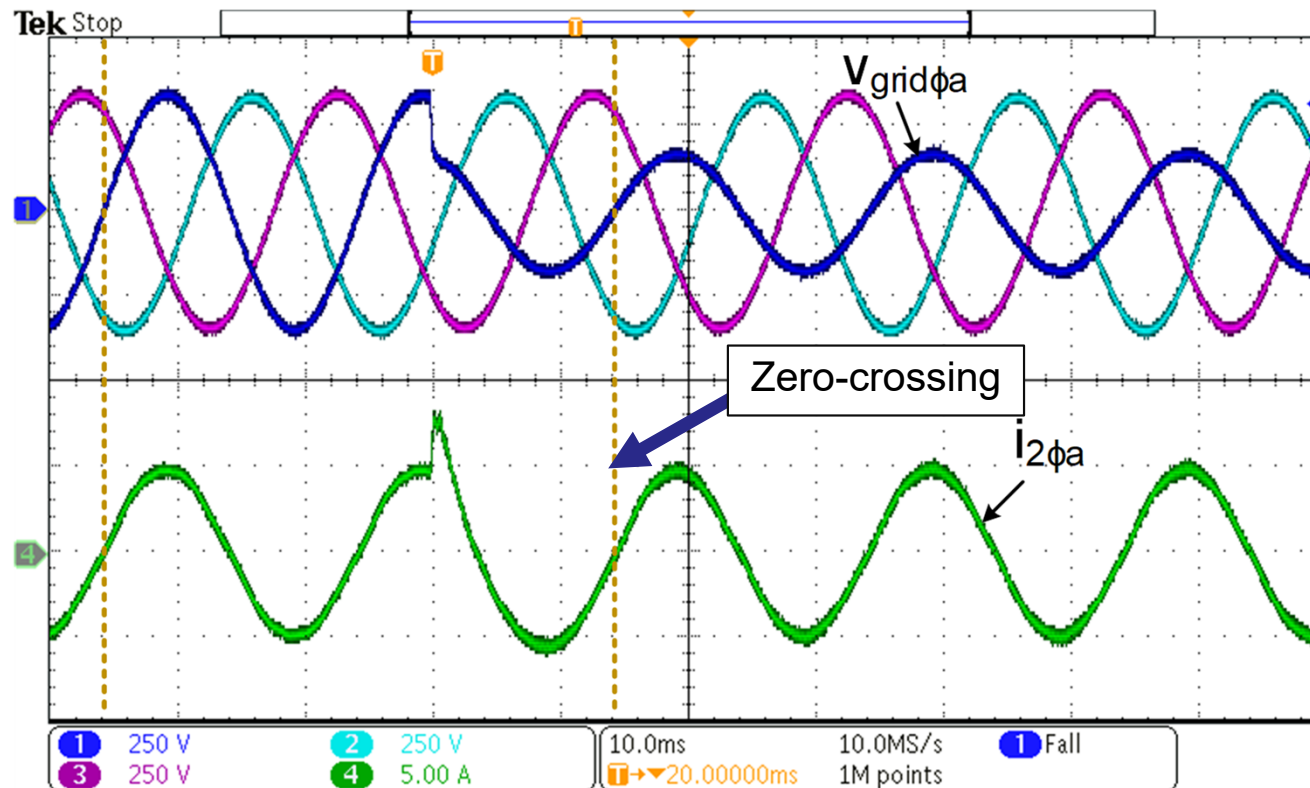
$$\vec{V}^+ = 0.833 \angle 0^\circ \text{ p.u.}$$

$$\vec{V}^- = 0.167 \angle 180^\circ \text{ p.u.}$$

SSICF - Experimental Result Type B Fault

Type B Grid
Fault

Transient response during type B grid fault transient

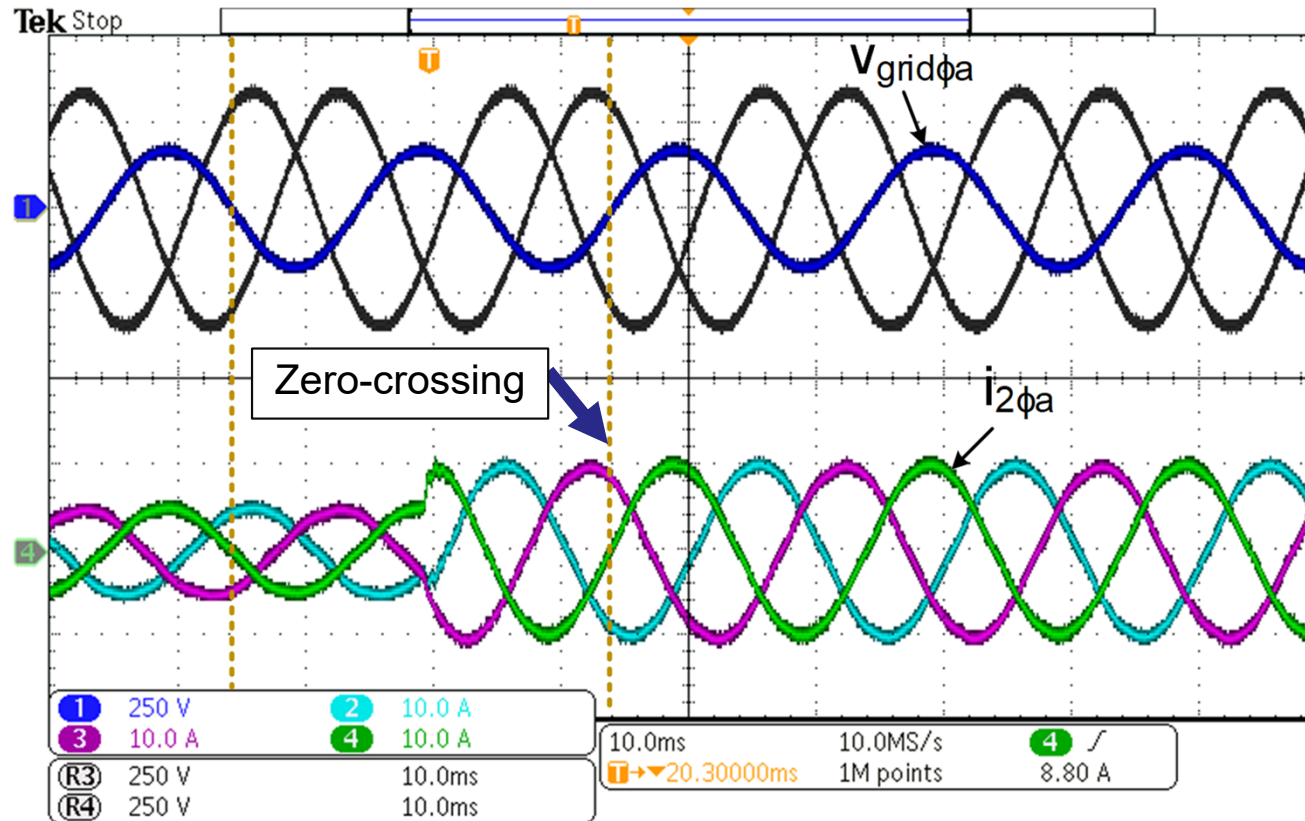


- Response matches simulation, **maintaining synchronisation** and **balanced sinusoidal current injection**.

SSICF - Experimental Result Type B Fault

Type B Grid Fault

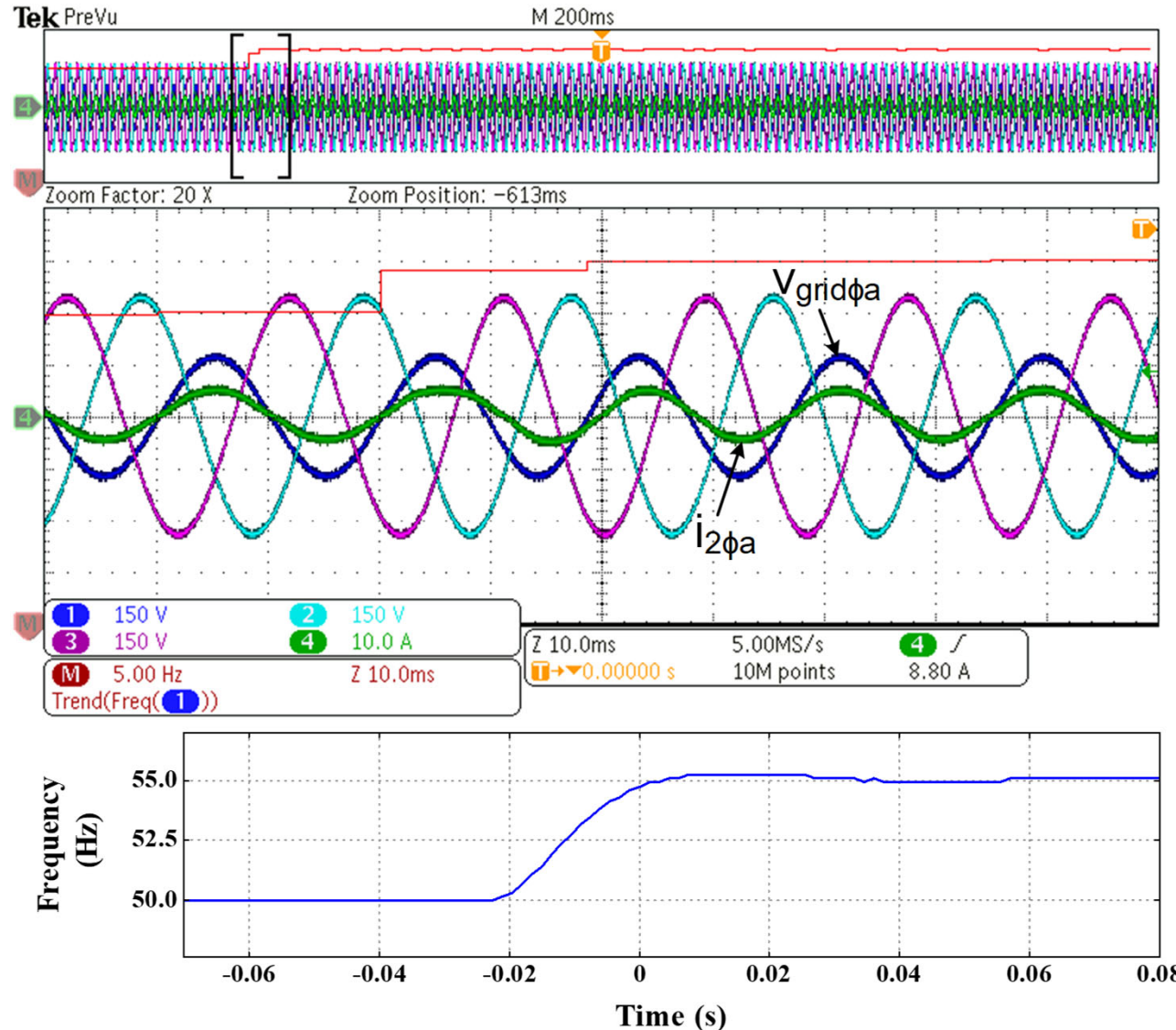
Transient response under a 50% current step change



- Response matches simulation, **maintaining synchronisation, balanced sinusoidal current injection and accurate grid-side current regulation.**

SSICF - Experimental Result Type B Fault

Performance of proposed strategy regulating at 5Apk under 5Hz frequency step change



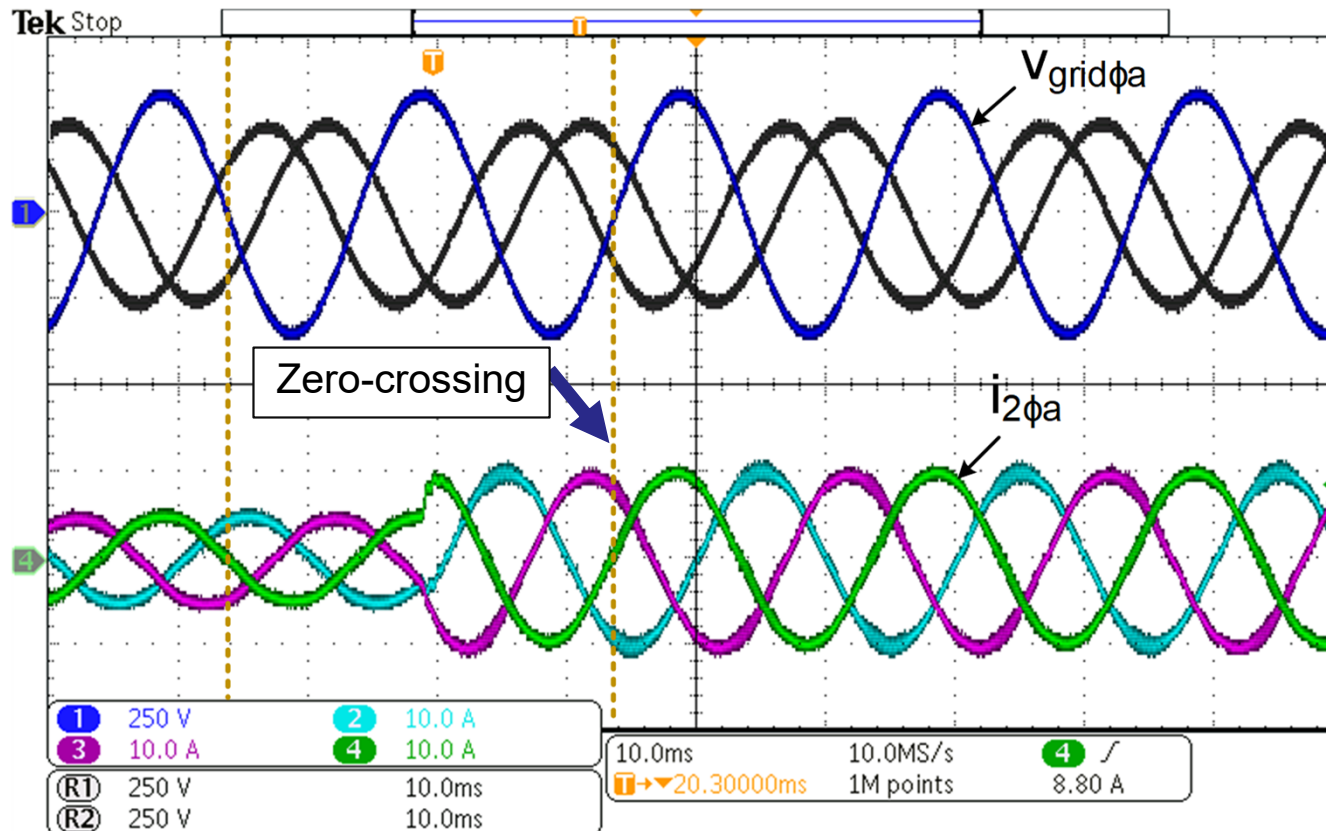
Type B Grid Fault

- PLL rapidly tracks frequency change to maintain accurate grid synchronisation and current regulation.

SSICF - Experimental Result Type C Fault

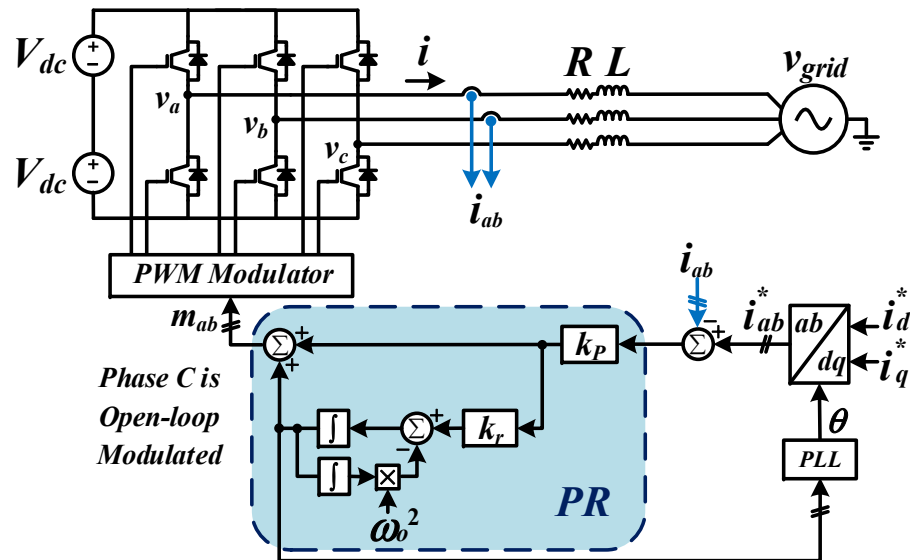
Type C Grid
Fault

Transient response under a 50% current step change



- Exhibits the same transient response as in simulation, maintains accurate sinusoidal grid-side current regulation and synchronisation despite extreme unbalanced voltages.

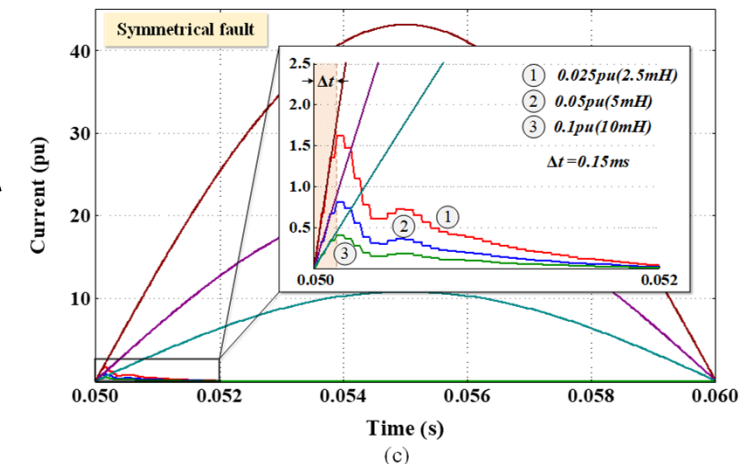
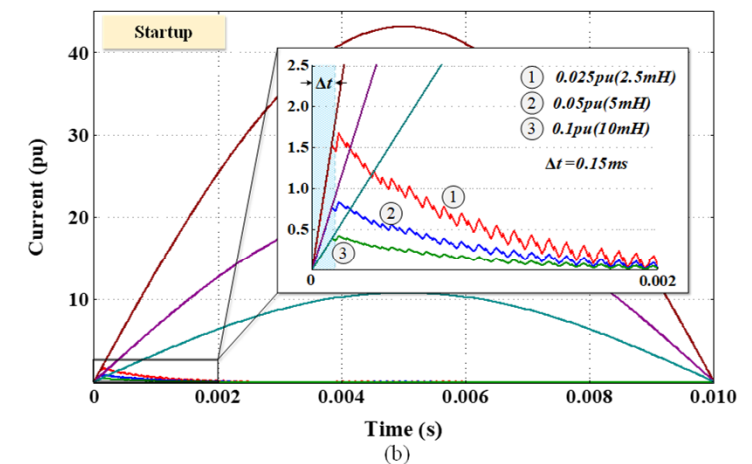
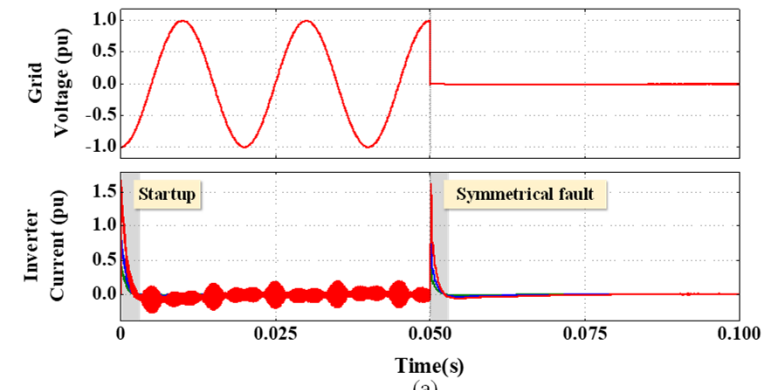
SSICF: StartUp and Fault Ride Through [16]



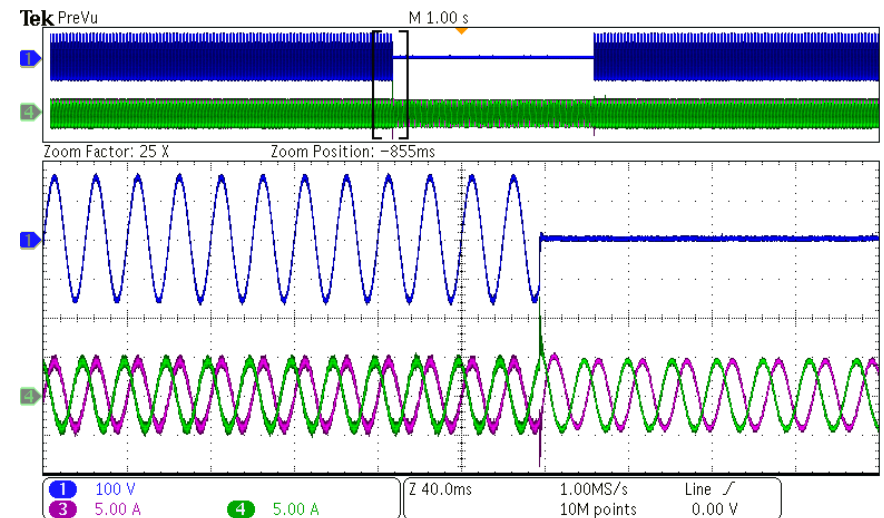
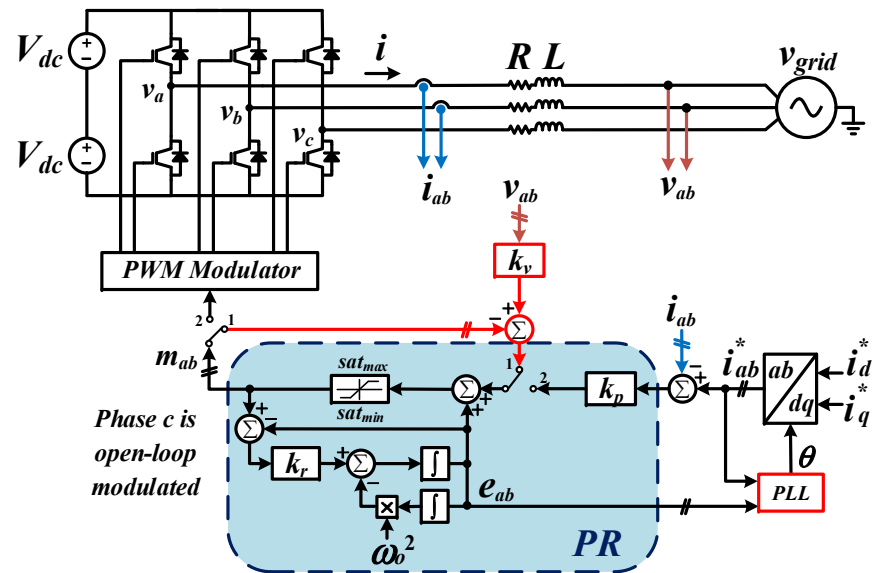
Grid Connected inverter controller by SSICF

Worst Case Startup and Fault Response determined by filter impedance until current regulator responds

Conclusion: Filter impedance less than 10% can lead to high fault current transients

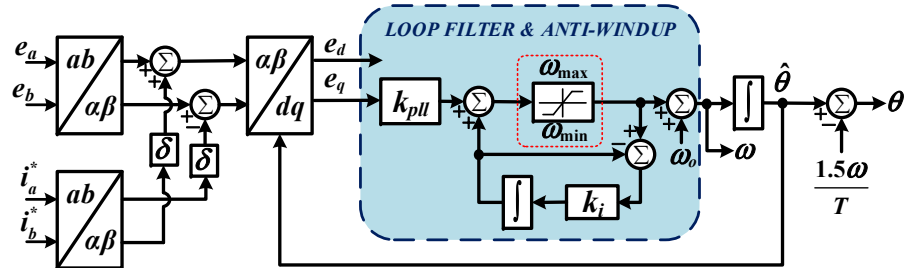


SSICF: StartUp and Fault Ride Through

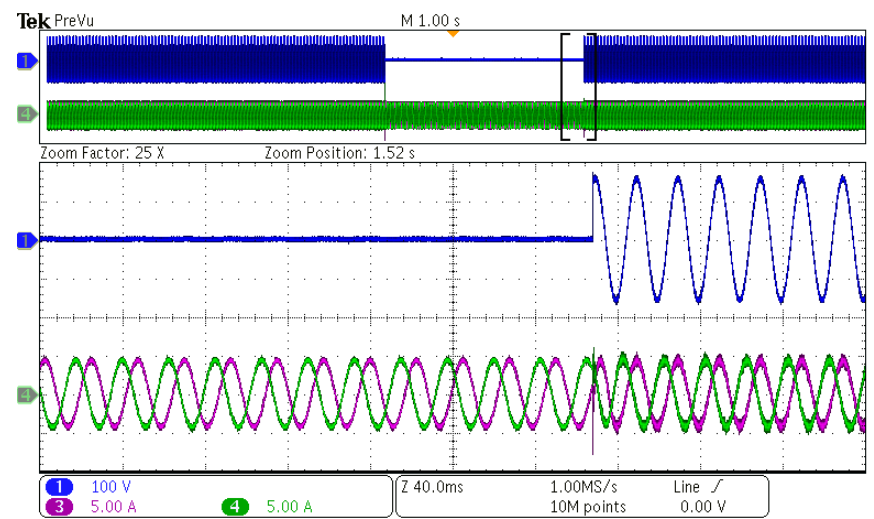


Experimental: 3phase fault starts

SSICF modified for startup (resonators match grid voltage before startup, PLL follows)



PLL response bounded by antiwindup structure (rides through severe fault)



Experimental: 3phase fault clears 10 sec later

Summary of SSICF

A new **SSICF control** strategy is presented for **LCL grid-connected inverters** using **only converter side current sensors**, that **self-synchronises to the grid** and achieves accurate indirect grid current regulation.

Uses the **resonant state variables** of a **stationary frame proportional resonant (PR) controller** with **harmonic compensators** to estimate the **capacitor voltage** and **current**, and adds a **feed-forward capacitor current compensation correction** to achieve accurate indirect grid current regulation.

A further **compensation term** is introduced into the **PLL** to **compensate** for the **voltage drop across the filter inductors** and better **synchronise** to the **grid**.

Improved performance is achieved with **minimal control complexity** using only a **stationary frame PR current controller** and **one converter side current measurement per phase**.

- The **strategy** is extendable to use **quadrature outputs** from the **stationary frame current controller resonator** to create **self-synchronised target current references**, and the **current errors** as **inputs** to a **frequency locked loop** to track grid frequency variations without external measurements.

Summary

This tutorial has covered the following principles:

- Closed loop current regulator bandwidth and gain selection based on PWM transport delay
- Improved current regulation via disturbance feed-forward compensation and delay reduction techniques
- Sampled digital current regulators
- Overmodulation, windup and signal conditioning
- Current regulation with high order LCL Filters including active damping techniques and gain design principles
- Current regulation with common mode DC bus ripple
- Self Synchronising Regulation and disturbance rejection
- Regulation with unbalanced and distorted (harmonics) grids

References

1. D.G. Holmes, and T. Lipo, *Pulse Width Modulation for Power Converters: Principles and Practice*, Wiley, 2003.
2. D.G. Holmes, T. A. Lipo, B.P. McGrath, W.Y. Kong, "Optimized Design of Stationary Frame Three Phase AC Current Regulators", IEEE Transactions on Power Electronics, Vol. 24, No. 1, Nov. 2009, pp2417– 2426.
3. W.Y. Kong, D.G. Holmes & B.P. McGrath, "Improved Stationary Frame AC Current Regulation using Feedforward Compensation of the Load EMF", IEEE Applied Power Electronic Conference (APEC), Washington, 2009, pp145-151.
4. D.N. Zmood, D.G. Holmes & G.H Bode, "Frequency Domain Analysis of Three Phase Linear Current Regulators", IEEE Trans. on Industry Applications, Vol. 37, No. 2, Mar. 2001, pp601-610..
5. B. P. McGrath, D. G. Holmes, "Accurate state space realisations of resonant filters for high performance inverter control applications", in Proc. IEEE 2nd Annual Southern Power Electronics Conference (SPEC), Auckland, 2016, pp1-6.
6. A.G. Yepes, F.D. Freijedo, J.Doval-Gandoy, O. Lopez, J. Malvar and P. Fernando-Comensana, "Effects of discretization methods on the performance of resonant controllers," *IEEE Trans. Power Electron.*, vol. 25, no. 7, pp. 1692 – 1712, Jul. 2010.
7. B.P. McGrath, D.G. Holmes, L. McNabb "A Signal Conditioning Anti-Windup Approach for Digital Stationary Frame Current Regulators", IEEE Trans. Industry Applications. Early Access, 2019
8. G.F. Franklin, J.D. Powell and M.L. Workman, *Digital Control of Dynamic Systems*, 3rd edn., Addison-Wesley, 1997.
9. S.G. Parker, B.P. McGrath, D.G. Holmes, "Managing Harmonic Current Distortion for Grid Connected Converters with Low Per-Unit Filter Impedances", in Proc. ECCE Asia DownUnder 5th IEEE Annual International Energy Conversion Congress and Exhibition, Melbourne, Australia, 2013, pp1150-1156.
10. S.G. Parker, B.P. McGrath, D.G. Holmes, "Regions of Active Damping Control for LCL Filters", IEEE Transactions on Industry Applications, Vol. 50, No. 1, Jan 2014, pp424 – 432.
11. S. G. Parker, D. S. Segaran, D. G. Holmes, B. P. McGrath , "DC Bus Voltage EMI Mitigation in Three-Phase Active Rectifiers Using a Virtual Neutral Filter", ECCEAsia ICPE, May 2014, Hiroshima, Japan.
12. J.W. Kolar, U. Drozenik, J. Minibock, H. Ertl, "A new concept for minimizing high-frequency common-mode EMI of three-phase PWM rectifier systems keeping high utilization of the output voltage", IEEE Applied Power Electronics Conference and Exposition (APEC), 2000
13. A. A. Nazib, D. G. Holmes, B. P. McGrath, "High Quality Grid Current Control For LCL Inverters Using Self-Synchronising Inverter Side Current Regulation", in Proc. ECCE Asia 2019 Conference, Busan, 2019.
14. A. A. Nazib, D. G. Holmes, B. P. McGrath, "A Self-Synchronising Stationary Frame Current Control Strategy for Grid-Connected Converters with Integrated Frequency Tracking ", in Proc. PEDG 2019 Conference, Xi'an, China, 2019.
15. A. A. Nazib, D. G. Holmes, B. P. McGrath, "Self-Synchronising Stationary Frame Current Regulation for Grid-Connected LCL Converters Under Unbalanced Grid Voltage Conditions", in Proc. ECCE 2019 Conference, Baltimore, USA, 2019.
16. A. A. Nazib, D. G. Holmes, B. P. McGrath, "Enhanced Transient Performance of a Self-Synchronising Inverter During Start Up and Severe Grid Fault Conditions", in Proc. ECCE Asia 2020 Conference, Nanjing, China, 2020.